DESIGN, SYNTHESIS AND BIOLOGICAL EVALUATION OF POTENTIAL ANTIBACTERIAL OLIGONUCLEOTIDES

ANDREW TRAUBE

Doctor of Philosophy

ASTON UNIVERSITY

December 2003

Aston University

Design, Synthesis and Biological Evaluation of Potential Antibacterial Oligonucleotides

Submitted by Andrew Traube for the degree of Doctor of Philosophy

December 2003

Thesis Summary

Purine and pyrimidine triplex-forming oligonucleotides (TFOs), as potential antibacterial agents, were designed to bind by Hoogsteen and reverse Hoogsteen hydrogen bonds in a sequence specific manner in the major groove of genomic DNA at specific polypurine sites within the *gyrA* gene of *E. coli* and *S. pneumoniae*. Sequences were prepared by automated synthesis, with purification and characterisation determined by high performance liquid chromatograpy, capillary electrophoresis and mass spectrometry.

Triplex stability was assessed using melting curves where the binding of the third strand to the duplex target, was assessed over a temperature range of 0-80 °C, and at pH 6.4 and 7.2. The most successful of the unmodified TFOs (**6**) showed a T_m value of 26 °C at both pH values with binding via reverse Hoogsteen bonds. Binding to genomic DNA was also demonstrated by spectrofluorimetry, using fluorescein-labelled TFOs, from which dissociation constants were determined.

Modifications in the form of 5mC, 5' acridine attachment, phosphorothioation, 2'-*O*-methylation and phosphoramidation, were made in order to increase T_m values. Phosphoramidate modification was the most with increased T_m values of 42 °C. However, the final purity of these sequences was poor due to their difficult syntheses. FACS (fluorescent activated cell sorting) analysis was used to determine the potential uptake of a fluorescently labelled analogue of **6** via passive, cold shock mediated, and anionic liposome aided, uptake. This was established at 20 °C and 37 °C. At both temperatures anionic lipid-mediated uptake produced unrivalled fluorescence, equivalent to 20 and 43% at 20 and 37 °C respectively.

Antibacterial activity of each oligonucleotide was assessed by viable count analysis relying on passive uptake, cold shocking techniques, chlorpromazine-mediated uptake, and, cationic and anionic lipid-aided uptake. All oligonucleotides were assessed for their ability to enhance uptake, which is a major barrier to the effectiveness of these agents. Compound **6** under cold shocking conditions produced the greatest consistent decline in colony forming units per ml. Results for this compound were sometimes variable indicating inconsistent uptake by this particular assay method.

Keywords: Triplex forming oligonucleotides; DNA synthesis; triplex stability; bacterial cell uptake; antibacterial activity.

Mum this is for you; without you none of this would have been possible.

Acknowledgements

I would firstly like to thank Micron for providing the opportunity for carrying out this research, which without their support would not have been possible.

My sincere thanks go to my supervisor Dr Bill Fraser generally for his overall help and guidance through the whole PhD process, and particularly with his input with the chemical side of the research. I would like to thank Dr Barbara Conway for her expertise regarding the delivery side of the project and her general support in pushing the project into new areas. I am also grateful to Dr Peter Lambert for his input regarding the microbiological side of the research, his general knowledge on everything, and also for providing me with laboratory working space.

I would like to thank Sue Lang for her practical knowledge and support in a number of aspects of the work, Alex Perry for her help with the DNA extraction work, Alex Foster and Karen Jones for their computer based assistance and everybody else in the microbiology laboratory for creating such a pleasurable working environment. I would also like to thank Lynda Birt, Rita Chohan and Roy McKenzie for their general laboratory support.

I would like to express my sincere thanks to Karen Farrow for her persistence in the MS analysis work, Roger Bird for his assistance with the FACS analysis and to Krista Fisher, Siobhan Dunbar and Katherine Chalmers for their aid in various aspects of the work, without which, the depth of the research would have been diminished.

A very big thank you must go to Simon Williams firstly for putting up with me throughout the 3 years, and secondly, for his enormous amount of support and advice throughout the course of the work, which all aided in retaining my sanity!

I would also like to say a big thank you to Mercia Spare for her continued friendship and support; we eventually got there!

I would finally (but by no means leastly) like to say huge thank you to Roy Traube for his continual support and input in my everlasting student career!

Figure Contents

Chapter 1

Chapter 2

Chapter 3

Table Contents

Abbreviations

5mC – 5-methyl Cytosine

A – Adenine

Acr – Acridine

ADP – Adenosine diphosphate

AML - Acute myeloid leukaemia

ATP – Adenosine triphosphate

BHI – Brain heart infusion

BNA – Bridged nucleic acids

BSA - Bovine serum albumin

C – Cytosine

CE – Capillary electrophoresis

Cellfectin® - TMTPS in association with DOPE

CFU – Colony forming units

CML - Chronic myeloid leukaemia

CPZ – Chlorpromazine

DMPG – Dimyristoylphosphatidylglycerol

DMRIE - 2 dimyristyloxypropyl-3-dimethyl-hydroxy ethyl ammonium bromide

DMRIE-C – DMRIE in association with choletsrol

DMT – Dimethyoxytrityl

DOPE – Dioleylphosphatidylethanolamine

DOSPA - 2,3-dioleyloxy-N-[2(sperminecarboxamido)ethyl]-N,N-dimethyl-1-propanaminium trifluoroacetate

DOTMA - N-[1-(2,3-dioleyloxy)propyl]-N,N,N-trimethylammonium Chloride

DPPC – Dipalmitoylphosphatidylcholine

DRV – Dehydration-rehydration vesicle method

E. coli – Escherichia coli

EDTA – Ethylene diamine tetra acetate

ENA – Ethylene nucleic acids

EtBr – Ethidium bromide

FACS – Fluorescence activated cell sorting

Fl – Fluorescein

G – Guanine

Gyr A – DNA gyrase A subunit

Gyr B – The B subunit of DNA gyrase

gyrA – The gene coding for A subunit of DNA gyrase

gyrB – Gene coding for the B subunit of DNA gyrase

HPLC – High performance liquid chromatography

K_d – Dissociation constant

LB – Luria Bertani

Lipofectamine™ - DOSPA in conjunction with DOPE

Lipofectin® - DOTMA in conjunction with DOPE

LPS – Lipopolysaccharide

$m^{5ox}C$ – 6-Keto derivatives of 2-deoxy-5mC

MIC – Minimum inhibitory concentration

MLV – Multilamellar vesicle

MMT – Monomethyoxytrityl

MP – Methylphosphonate

MPS – Mononuclear phagocyte system

MRSA – Methicillin resistant *Staphylococcus aureus*

MS – Mass spectrometry

NA – Nutrient agar

PAE – Post antibiotic effect

Par C – The Par C subunit of topoisomerase IV

Par E – The Par E subunit of topoisomerase IV

parC – The gene coding for the Par C subunit of topoisomerase IV

parE - The gene coding for the Par E subunit of topoisomerase IV

PBS Phosphate buffered saline

PC – Phosphatidylcholine

PE – Phosphatidylethanolamine

PEG – Polyethylene glycol

PFV – Programmable fusogenic vesicles

PG – Phosphatidylglycerol

PI – Phosphatidylinositol

PIT – Potential intrastrand triplex

PN – Phosphoramidate

PNA – Peptide Nucleic Acids

PO – Phosphodiester

PS – Phosphorothioate

QRDR – Quinolone resistance-determining region

RES – Reticuloendothelial system

RISC – RNA-induced silencing complexes

RNAi – RNA interference RNA

S. pneumoniae – Streptococcus pneumoniae

s.d.H_2O – Sterile distilled water

SDS – Sodium dodecyl sulphate

siRNAs – Small interfering RNAs

SUV – Small unilamellar vesicle

SVPD – Snake venom phosphodiesterase

T – Thymine

T_c – Liquid crystalline transition temperature of a given lipid

TE – Tris EDTA

TFO – Triplex forming oligonucleotide

THF – Tetrahydrofuran

T_m – The temperature at which half of the total oligonucleotide is dissociated

TMTPS - N,N^{I},N^{II},N^{III}-tetramethyl- N,N^{I},N^{II},N^{III}-tetrapalmitylspermine

TTBS – Tris Buffered saline containing Tween 20

UTI – Urinary tract infection

1.0 INTRODUCTION

The use of oligonucleotides as potential therapeutic agents has been the centre of a great deal of research during the past 25 years. Research is based around two different strategies, antisense and more recently, antigene strategies. These rely on the design and synthesis of oligonucleotides targeted to specific strands of mRNA (antisense) and DNA (antigene) in order to prevent protein synthesis. Although the two methods produce ultimately the same end goal, their modes of action are different (Hélène, *et al.*, 1992; Thuong and Hélène 1993).

The antigene approach potentially offers more powerful therapeutic agents as the gene is targeted specifically, preventing protein synthesis at its source. The antisense strategy relies on oligonucleotides that bind to single stranded mRNA by Watson-Crick base pairing. This requires binding of numerous oligonucleotides to the mRNA targets to cause full translationary blockade. This can result from steric blockade of ribosomal machinery, or the activation of cellular RNase H, P or L enzymes. The former mechanism relies on the ability of the antisense strand to form a sufficiently stable duplex, preventing binding of proteins at the same site, which in turn leads to RNA splicing, polyadenylation, and eventually degradation (Baker and Monia, 1999). In the latter process, activation of RNase enzymes results in the cleavage of the DNA/RNA hybrid into short chain oligonucleotides and hence the destruction of the mRNA message. The normal activity of these enzymes is associated with the replication and repair of genomic DNA (Zamaratski, *et al.*, 2001). The activation of the RNase enzymes, usually RNase H, is normally the favoured and most effective form for antisense activity. However, this creates problems in that in order to activate the enzyme, the oligonucleotide will need to be a recognisable substrate. Backbone modifications necessary to resist nuclease activity, renders the oligonucleotide unable to activate these enzymes, hence the antisense mechanisms are less effective. A recent, more advanced antisense technology has been developed that exploits the mechanism of RNA interference (RNAi) using small interfering RNAs (siRNAs) (Hutvágner and Zamore, 2002). Here, double stranded RNA molecules are introduced into cells that cause the degradation of specific mRNA molecules via a multistep process. The entry of the duplex RNA results in its cleavage into 21-25 bp double stranded fragments, with single nucleotide strands at the 3' end of each of the RNA strands, by the enzyme 'Dicer'; a member of the RNase III family of endonucleases.

The staggered ends of the duplex molecule enable recognition of the siRNA by protein components, which complex and form RNA-induced silencing complexes (RISC) upon ATP-dependent RNA unwinding. This reveals the active form of RISC that contains the single stranded RNA molecule, which in turn is able to target specific intracellular mRNA. Upon binding of the complex to the mRNA, the target is cleaved and hence the protein message destroyed. This latter process is brought about by a protein ribonuclease that is thought to form part of the RISC complex (Hutvágner and Zamore, 2002). Although not fully understood, these mechanisms operate in a wide range of organisms and as a result, this application of antisense technology holds very strong hope for future therapeutics.

In theory the antigene strategy by contrast, requires only one single oligonucleotide molecule to suspend protein synthesis in a given cell. However, the TFO concentration at the target site needs to be high due to the weak binding of unmodified oligonucleotides. These sites may also be inaccessible due supercoiling of the DNA itself or the result of secondary structure formation. Access to the target site may only be possible during transcription when the DNA is unwound. Such a phenomenon is true also of antisense technologies.

The effectiveness of antisense therapies has become clear during recent years with approval of 'Formivirsen' (Vitravene^{TM}), developed by Isis pharmaceuticals for the treatment of *Cytomegalovirus*-induced retinitis in AIDS patients (Hughes, *et al.*, 2001). Another promising antisense oligonucleotide, that has currently completed phase II clinical trials is Augmerosen, which inhibits BCL2 proteins. The protein is an apoptosis inhibitor and is associated with a number of cancers (Urban and Noe, 2003). In addition, there are also several other drugs that are under development and at various stages of clinical trial. These include antisense drugs that will target prostate, breast, pancreas, colon and lung cancers, acute and chronic myeloid leukaemia (A and CML), solid tumours, Crohn's disease, HIV and many more (Agrawal and Kandimalla, 2000). Antisense compounds are also successful analytical tools that have been used in the discovery of gene function. The antisense strategy has been under development for 25 years or more, nearly 10 years more than antigene technology. However, a lot of knowledge gained from antisense technology can be applied to antigene strategies, particularly when it comes to serum stability, cellular delivery and protection from nuclease degradation at target sites. The antigene

approach potentially provides a more powerful device both therapeutically and analytically, and this is why it is the focus of this research.

1.1 Triplex DNA

1.1.1 Triplexes and Their Discovery

Duplex formation relies on differing hydrogen bond numbers between nucleotides. Two hydrogen bonds allow the recognition of adenine (A) by thymine (T) or uracil (U), and three bonds allows recognition of guanine (G) by cytosine (C) (Figure 1.1).

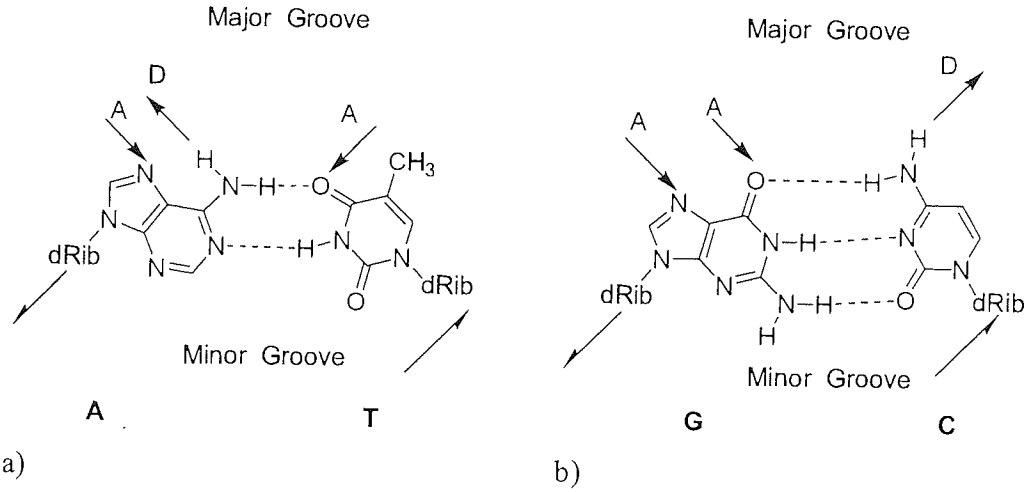

Figure 1.1 Hydrogen bond numbers that allow the recognition of A by T (a), and G by C (b). Diagram adapted from (Doronina and Behr, 1997).

It has been known for some time that oligonucleotides when bound in a duplex retain additional hydrogen bonding capabilities, known as Hoogsteen hydrogen bonds, in both the major and minor grooves of the double helix. Hoogsteen discovered these while studying cocrystals of adenine and thymine derivatives. He noticed that these demonstrated hydrogen bonding patterns dissimilar to those presented in Watson-Crick base pairs (Thuong and Hélène, 1993). Figure 1.1 shows the hydrogen bond donor (D) and acceptor (A) sites available on the four natural bases when in the Watson-Crick base paired conformation. These bonds allow binding of third strand oligonucleotide chains in a sequence specific manner in the major groove of a duplex molecule. These oligonucleotides have hence been termed triplex forming oligonucleotides (TFOs). Figure 1.2 shows the commonly occuring base triplets.

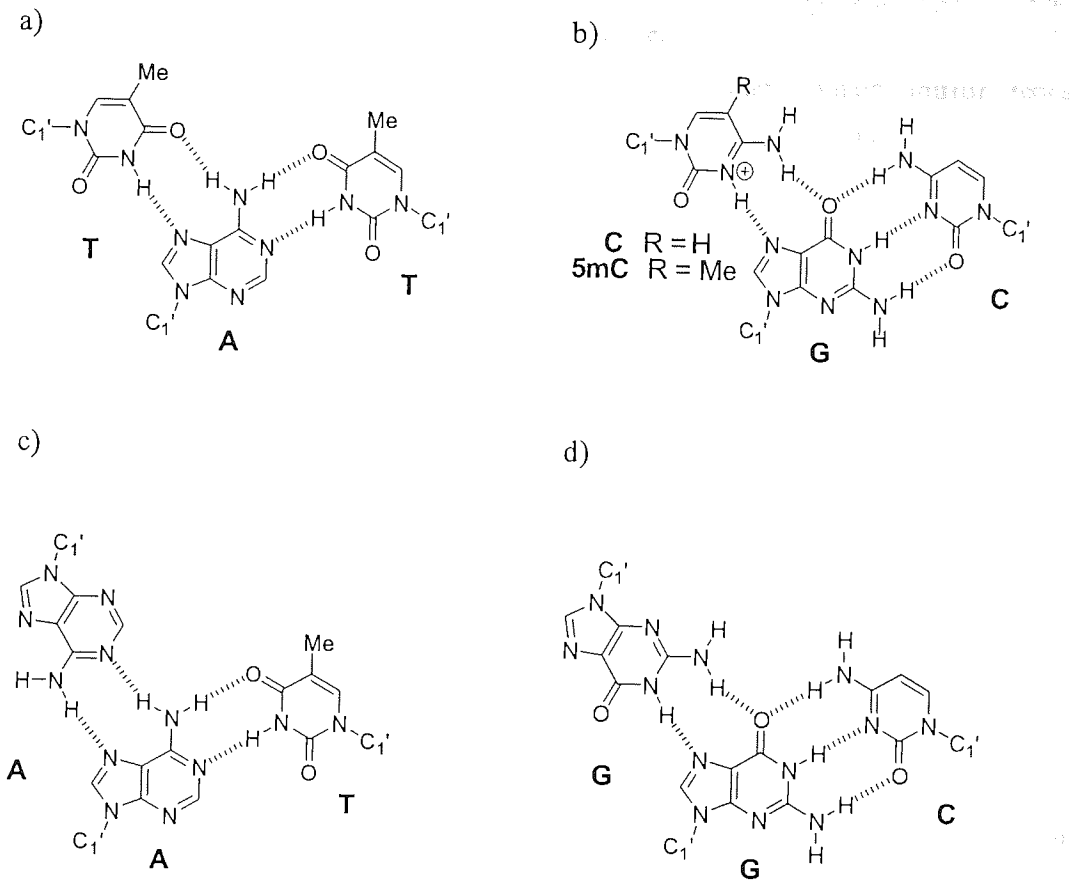

Figure 1.2 a) T*A-T triplex, b) C*G-C triplex showing a protonated C to produce the second Hoogsteen bond where the R group can be substituted for a methyl group to show the interaction of 5mC in a 5mC*C-G triplex. c) A*A-T triplex and d) G*G-C triplex with * indicating Hoogsteen hydrogen bonds and - indicating Watson-Crick base pairing. These symbols are applied throughout the thesis.

Although Hoogsteen bonds are retained in the minor groove, it is not wide enough to accommodate the oligonucleotide in a manner that would allow stable triplexation.

The model for triplex DNA was first demonstrated in 1957 by Felsenfield Davies and Rich, only a few years after the discovery of the duplex molecule (Felsenfeld, *et al.*, 1957). Although work was furthered during the following decades, real interest in triplex DNA did not really take off until the 1980s when intramolecular triplexes were discovered. These structures termed H-DNA, were found to form naturally within the

DNA of cells and to occur at homopurine-homopyrimidine sites. This terminology emanates from their structural stabilisation by hydrogen protons, elevated levels of which, are found in the media surrounding the triplex.

H-DNA forms only at purine-pyrimidine stretches that contain mirror repeat symmetry, and when one of the strands of the DNA is unwound. During unwinding one of the unpaired strands folds back on itself and forms Hoogsteen bonds with the purine strand. Either of the two strands is able to do this, but the conditions at the site of triplexation govern whether the polypurine or polypyrimidine strand forms the triplex. Hydrogen protons, present under acidic conditions, will cause the protonation of C residues in the pyrimidine strand enabling them to part take in a second Hoogsteen bond when in the triplex conformation. The pyrimidine triplex was discovered first and was so-called H-DNA. The purine form is pH-independent and hence does not require H ions, it is termed H*-DNA to distinguish between the two. Once in this triplex formation the remaining portion of the DNA remains unpaired.

Biological roles of such triplexes are still not fully understood, but would appear to be fundamental due to the prevalence of the necessary homopyrimidine-homopurine tracts found throughout eukaryotic and prokaryotic genomes. The occurrence of these mirror repeat sequences has been found to be as high as 1 in 50,000 base pairs in human DNA (Tiner Sr, *et al.*, 2001). In prokaryotes, particularly *Escherichia coli* (*E. coli*), 25 copies of these so-called PIT (Potential Intrastrand Triplex) sites occur per genome (Guntaka, *et al.*, 2003). These triplexes are currently thought to aid transcription, replication, recombination, and chromosomal organisation (Soyfer and Potaman, 1996). During transcription, the triplex DNA is thought to mediate binding of RNA polymerase at specific gene sites, either in the aiding of transcription or in inhibiting it. The polypyrimidine-polypurine sites are found at 5' flanking regions of a number of genes, where they are important in promoter function. These sites provide the initial binding sites for RNA polymerase.

Blockade of DNA replication is likely to arise from these intramolecular triplexes to halt DNA polymerase. The passage of the enzyme along the template strand of the duplex molecule will cause displacement of the non-template strand. At homopyrimidine-homopurine sites the displaced strand is able to fold back on itself, forming Hoogsteen interactions with the mirrored sequence further up the gene, which is found ahead of the replication fork. Subsequent displacement of the non-template strand is prevented due to triplexation, and the replication machinery is prevented

from further progression. Complete disruption of replication by this process has been observed but only during *in vitro* studies, where it has been demonstrated using single stranded DNA. This is not to say that the effect is not apparent in duplex DNA, but the effects have been less drastic. Here, the replicationary blockade was diminished but still detectable. It has since been proposed that the effect of triplexation on replication mechanisms is more transient and aids in the coordination of chromosomal replication as a part of cell growth (Hoyne, *et al.*, 2000).

Chromosomal organisation can result from triplex formation between two duplex sites on the same molecule. These sites can be quite distal and as a result, site specific folding of the molecule can occur, this in turn can aid condensation of the DNA into more compact structures within the cell. Studies using triplex-specific antibodies have shown that the formation of intrastrand triplexes takes place predominantly at the end of the S, and during the G_2 phase of the cell cycle. During these phases the genomic DNA is replicated and consequently a lot of DNA unwinding and recondensing will take place. It is therefore postulated that intrastrand triplexes have a role to play in the latter process (Agazie, *et al.*, 1996). Further studies have tried to illustrate this condensation process where triplex formation was carried out under ionically similar conditions to those presented intracellularly (Goobes, *et al.*, 2002). Condensation patterns were observed using circular dichroism and polarized light microscopy, and provided further evidence for this phenomenon. Similar mechanisms involved in the folding and condensing of DNA are also apparent for recombination processes. Here triplex formation between chromosomes or sites on the same DNA molecule can enable recombination processes to take place.

Interest was fuelled further by the demonstration of triplex formation by Hélène and Dervan in 1987, using short-chained oligonucleotides under suitable conditions (Le Doan, *et al.*, 1987).

1.1.2 Triplex Formation and Kinetics

Triplex formation takes place many times slower than duplex formation. It is strongly influenced by strand concentration (in the case of intermolecular triplexes), surrounding cation concentrations and temperature at the site of triplexation. It has been shown that association rates are as much as 3-fold slower, and there is a marked increase in the dissociation rates during triple helix formation compared with duplex

formation (Hélène, *et al.*, 1992; Thuong and Hélène, 1993). The actual rates of formation have been found to be 10^3 $M^{-1}\cdot s^{-1}$ for triplex formation and 10^6 $M^{-1}\cdot s^{-1}$ for duplex formation, a rate that will vary according to TFO sequence (Fox, 1995).

The first stage of triplex formation must overcome the electrostatic repulsion of the three strands caused by the polyanionic nature of the backbone of these oligonucleotides. Although encountered in duplex formation, repulsion is greater in triplexation due to the presence of three adjacent DNA strands. The repulsion experienced is diminished by cations that form so-called 'cationic clouds' around the negative phosphates, which also bind to these groups, hence they aid both triplex and duplex formation. However, the cations surrounding these triplexes will be of differing valency states and are comprised of metal ions and polyamines. This is particularly true of intracellular conditions where typical intracellular cation components are 140 mM K^+, 1 mM Mg^{2+}, and 1 mM (or 5 mM in the nucleus) Spermine (Sp^{4+}). The concentration and charge state will actually determine the extent of the binding to the backbone. Monocations stabilise triplexes if present in sufficient concentrations but to a lesser extent than di- or polycations at similar concentrations. Monocation concentrations of 0.1-1.0 M are necessary for stable triplexation (Felsenfeld and Rich, 1957), whereas divalent cation concentrations between 1-10 mM are required. In fact Sp^{4+} is actually the most triplex-stabilising of all intracellular ions and is so at 0.1 to 5.0 μM concentrations (Singleton and Dervan, 1993). The concentration of the cation will determine its ability to compete for binding sites; hence those at a higher concentration will generally out compete those at lower concentrations. Therefore, the competition that prevails for backbone binding sites can actually destabilise the triplex.

The effect of ionic conditions on the overall stability of the triplex is determined by the nature of the sequence, as some triplets are more affected by salts than others. James *et al* (James, *et al.*, 2003), showed that T*A-T triplets were more sensitive to cations than C^+*G-C triplets; also, T*A-T containing triplexes with increasing C^+*G-C inserts were less sensitive to ionic conditions. This is perhaps not surprising due to the nature of the protonated third strand C residues, which will exert a stabilising effect on the triplex due to the partial neutralisation of the anionic charges of the backbone.

The actual process of third strand binding is thought to take place in a similar manner to that of duplex DNA, and results from the initial binding of 3 to 5 bases, which induces a zipping effect whereby the following bases bind in sequence. This is known as nucleation, which has a high negative activation energy; higher than that which enables duplex formation (Protozanova and Macgregor, 1996), and takes place at the 5' end of the target purine strand upon binding of the TFO. The initially bound nucleotides are stabilised via stacking interactions that in turn induce conformational changes in the underlying duplex, allowing the other bases to bind more readily. These changes in the duplex DNA are essential in order for the third strand to bind successfully and with reasonable stability. However, this is a limiting step in triplexation because the target duplex molecule is relatively rigid. A similar conformation change occurs during the formation of the duplex molecule, but because the single strands are much more flexible, the strands more readily associate. This is why the nucleation process during duplexation only requires the binding of 2-3 bases before the zipping process can take place (Rougée, *et al.*, 1992).

The zipping process that follows nucleation during triplexation, is thought to occur specifically in the 5'-3' direction in relation to the target purines. This is due to nucleic acids demonstrating a right-handed conformation. Binding in the 5'-3' direction allows binding of subsequent nucleotides without effect to the previously bound base. If binding were to take place in the 3'-5' direction, the binding conformation of previously bound nucleotide would have to be altered to incorporate the next base in sequence, a process which is clearly unfavourable (Alberti, *et al.*, 2002).

The effect of increased temperature on triplex formation appears to be detrimental to the nucleation phase. At lower temperature the rate of triplexation is thought to increase due to greater stabilisation of the initial 3 to 5 nucleotides that bind enabling the zipping mechanism to take place (Rougée, *et al.*, 1992; Protozanova and Macgregor, 1996; James, *et al.*, 2003).

Hoogsteen hydrogen bonds allow base triplets to recognise and bind to target purine residues of the duplex molecule. However, these are by no means the only forces that maintain triplexation upon binding of the third strand. There is a number of other forces whereby the third strand and the duplex interact that determine the stability of the triplex. These include base stacking, van der Waals' forces, electrostatic interactions and interactions between the sugar phosphate backbone (Walberer, *et al.*, 2003). Base stacking interactions take place between the neighbouring bases in the

third strand once in the triplex conformation. Although these are not fully understood, it is thought that there are two contacts made between consecutive bases that aid triplex stability significantly. Where these are not maintained, stability is hindered greatly, as would be the case if a mismatched base was introduced into the third strand. All these forces are however not independent and will all combine to maintain stable triplexes.

Triplex stability can be measured in a number of ways such as through association and dissociation constants. A way that is widely used, is by the T_m value (Soyfer and Potaman, 1996). This is based on thermal melting studies of the triplex and is defined as the temperature at which half of all the bound third strand molecules are dissociated from the duplex target. This value is used in this study to estimate the stability of a given TFO.

1.1.3 The Effects of Triplex DNA on Transcription and Replication

Since triplex binding occurs in the major groove, the TFO has the potential to block or effect transcription and hence the manufacture of fundamental protein products. This occurs in a number of ways:

1. The triplex when formed can overlap binding sites for regulatory proteins and 'machinery' such as transcription factors and hence prevent transcription initiation.
2. Triplex binding can perturb the usual structure of the duplex molecule resulting in conformational changes, which in turn can alter rates and efficiency of RNA polymerase initiation, or even prevent binding of proteins at these sites. The change in structure can extend outside the site of triplex binding and can be medium or even long range.
3. Binding of the TFO within specific genes can cause a halt to the transcriptional 'machinery' and hence prevent gene transcription through steric hindrance.
4. Blockade of repair mechanisms that are responsible for rectifying errors produced during replication and hence are inevitably, cytotoxic.
5. Activation of genes that code for negative regulation protein factors that act to control transcription (Frank-Kamenetskii and Mirkin, 1995; Neidle, 1997).

The binding of the TFO can therefore cause a number of effects, however, they are generally associated with protein synthesis at the transcriptional level. One of the major problematic areas associated with this technology, and the focus of great

research, is the poor stability of triplexes. In order for a TFO to be successful it must out compete replicational and transcriptional proteins for genetic binding sites. It is unlikely that binding of a natural oligonucleotide, in a triplex manner, will be sufficient to stop enzymatic machinery once it has been launched (Thuong and Hélène, 1993). Such a problem is evident from antisense technology. Through antisense technology it was found that ribosomes during translation remove oligonucleotides when bound to mRNA in much the same way as they unwind secondary structures. Only irreversible reactions such as the cleavage of mRNA by RNase H, or intercalation of the oligonucleotides with chemical reagents that produce very strong binding are found to produce the desired effect. Also the binding of the TFO will be transient due to susceptibility of oligonucleotide to nucleases, that is if it is not degraded before it binds, and therefore its ability to exert the desired effect will be minimal.

1.2 Triplex Stability

Both pyrimidine and purine bases are able to form stable triplexes, the orientation of which and the conditions under which they do so are variable. In order for a stable triplet to be formed, the third strand base must make two Hoogsteen bonds with the purine base involved in Watson-Crick base pairing in the duplex molecule. The pyrimidine strand of duplex DNA is unable to bind the third strand properly as these bases only present one hydrogen bonding capability compared with the two exhibited by the purine bases (Figure 1.1). As a result, a current restriction at the centre of the antigene strategy is the requirement for oligopurine tracts within the duplex DNA target. Hence a great deal of research is under way into extending the recognition system in triplex DNA.

The third strand can take one of two orientations; parallel triplexation where Hoogsteen bonding is involved, or antiparallel triplex formation where the base undergoes a full 180° rotation to form reverse Hoogsteen bonds. Bases T, C and G are able to take on either of the orientations, whereas A is only able to adopt the reverse Hoogsteen conformation. As a rule polypurine TFOs will generally form reverse Hoogsteen structures, whereas polypyrimidine-containing TFOs will tend to adopt Hoogsteen structures. These binding orientations can be seen in Figure 1.2 (Pg 18) where bases T and C adopt parallel bonds, and, A and G form antiparallel Hoogsteen interactions. The latter has the advantage due to Hoogsteen bonding oligonucleotides forming more stable triplexes because of increased isomorphism (Hélène, *et al.*, 1992). The importance in conserving isomorphism is paramount to the prevention of backbone distortion and to enhance neighbouring base interactions. Even though attempts have been made to maintain isomorphism through base substitutions, only two base triads are truly isomorphous, T*A-T and C^+*G-C where the cytosine (C^+) is protonated. Base isomorphism means that when the C1' atoms (the C atom of the sugar unit attached to the base) of the two bases involved in Watson-Crick base pairing are fixed, the C1' of the third strand nucleotides, positioned in the major groove, are superimposable (Thuong and Hélène, 1993; Soyfer and Potaman, 1996; Doronina and Behr, 1997). As a result the backbone of the third strand retains a regular conformation. Figure 1.3 highlights this point and shows the positioning of the C1' atom of the third strand nucleotides in the major groove when bound by Hoogsteen and reverse Hoogsteen hydrogen bonds. The diagram clearly illustrates C

and T to be isomorphous when bound by Hoogsteen bonds as the C1' atoms are in close proximity. Other bases bound in the same manner and by reverse Hoosteen interactions do not mirror this similar proximity. Also illustrated is the fact that binding via reverse Hoogsteen bonds implies a lack of isomorphism.

Figure 1.3 The proximity of C1' atoms of consecutive nucleotides in third strand oligonucleotides when bound via Hoogsteen and reverse Hoogsteen interactions. Where the C1' atoms are in close proximity isomorphism is implied and a more stable triplex formed (Soyfer and Potaman, 1996).

Whenever TFOs bind to the duplex target there is a stability penalty. The more non-isomorphous steps in a third strand the less stable the triplex due to increased backbone distortion. Triplex stability is generally governed by stacking interactions, van der Waals forces and dipolar interactions between neighbouring bases. Where bases are not isomorphous these interactions are weakened, and hence so to is the overall stability of the triplex.

Approaches to increasing triplex stability include, strand switching, substitution of alternate natural bases, addition of synthetic base analogues or modified bases, attachment of intercalating agents at various sites on the third strand, and lastly, backbone modification. Each of these is discussed below.

1.2.1 Alternate Strand Strategy

The technique of strand switching is one attempt to overcome the necessity for homopurine-homopyrimidine target tracts in order to extend the TFO target site. The mechanism relies on the design of two distinct TFOs that are connected by a linker group. This strategy provides greater target variability because although tracts of purines are still required, they do not need to be continuous as the TFO is able to cross the major groove of the duplex, and bind to the alternate strand.

The TFO conjugate can be made up in any combination of polypurine or polypyrimidine sequences. For example;

1. 3' – purine – linker – purine – 3'
2. 5' – pyrimidine – linker – pyrimidine – 5'
3. 3' – purine – linker – pyrimidine – 5'
4. 5' – pyrimidine – linker – purine – 3'

The linkers used to connect the two TFOs vary, and are either nucleotide or artificial in nature. Some examples of non-nucleotide linkers include hexaethylene glycol, propane-1,3-diol and xylose derivatives (Doronina and Behr, 1997). The choice of which will depend on the type of junction to be crossed and the length of linker required to bridge the interstrand gap. Artificial linkers are only required where the two triplex motifs bind via the same orientation, either via a parallel orientation utilising Hoogsteen hydrogen bonds, or in an antiparallel manner using reverse Hoogsteen bonds. This is necessary due to the change in orientation of the alternate strand in the target duplex, the two strands of which have opposing orientations. In order to form a continuous TFO conjugate, a 3'-3' or a 5'-5' linker is required, as is the case in 1 and 2 above. Unmodified nucleotides are unable to bridge this gap due to the switch in sequence orientation, and hence an artificial linker is required. Giancola *et al* (Giancola, *et al.*, 2001), produced such TFOs using 1,2,3-propanetriol as a successful 3'-3' linker. A 15mer TFO, comprising two interlinked third strands that bound via Hoogsteen bonds in a parallel orientation in relation to the target purine strands demonstrated a T_m of 45 °C.

In the case of 3 and 4, where the two interlinked TFOs are of different orientations, one long TFO can be produced. The type of motif switch affects the ease and success of this strategy.

Figure 1.4 Alternate strand triplex binding where R indicates purine residues and Y pyrimidine residues. The dotted lines illustrate the tilt of Watson-Crick base pairs along the major groove, whereas the solid lines highlight Hoogsteen hydrogen bonds. a) Represents the binding across a purine-pyrimidine junction depicting a two base overlap between the two triplex binding domains, and b) represents the binding across a pyrimidine-purine junction and illustrates a two base gap between the two third strands (Gowers and Fox, 1999).

An initial antiparallel motif linked to a parallel motif TFO will be more successful than the reverse. This was highlighted in work carried out by Marchand *et al* (Marchand, *et al.*, 1998). An increase in triplex stability of 3 to 5 fold was demonstrated using an alternate strand TFO with a purine-pyrimidine switch region. This is apparent due to the tilt of the third strand backbone in relation to the duplex axis (Figure 1.4a). Where a purine-pyrimidine junction is presented, two bases overlap as a result of this tilt, and hence it is thought that no linker is needed additional to the phosphodiester unit in the backbone. It is also possible that the two

nucleotides in the third strand will not actually form specific triads and as a result will protrude into the major groove and provide enhanced flexibility at this junction. This helps to maintain the continuity of the helices (Beal and Dervan, 1992). However, work carried out by Brodin *et al* (Brodin, *et al.*, 1999) partly contradicted these findings. They produced a number of purine-pyrimidine alternate strand TFOs in order to optimise triplex formation. Oligonucleotides containing head to tail TFO regions were compared, with TFOs containing the same regions but interlinked by nucleotides. It was actually established that the TFOs with the linked regions produced more stable triplexes.

Where a pyrimidine-purine junction is presented (Figure 1.4b), TFO backbones are tilted in opposite directions producing a two base gap, as a result the distance between alternate purine binding sites is greater and linkers are required to promote successful triplex formation (Gowers and Fox, 1999). Hence the former strategy is the more successful. A similar phenomenon is apparent with linked TFOs of the same orientation (1 and 2 above). It is clear here that the distance represented by a 5'-5' linker (17-23 Å) is far greater than that of 3'-3' linker (5-8 Å) (Ono, *et al.*, 1991).

Crossing the major groove of the duplex provides its own set of problems and in order to be successful, entropy must be kept to a minimum. The great problem is the backbone distortion associated with this strategy and hence a loss of isomorphism leading to a loss of base stacking interactions. These will be particular true at the junction site and will result from the structural strain imposed by crossing the major groove.

An alternative to the strand switching strategy, but one that still utilises linked TFOs in order to increase the TFO recognition repertoire, but prevents triplex destabilisation due to backbone distortion, is the use of linked TFOs that form triplexes on the same strand, but at separate sites. Again this approach can utilise third strands containing triplex motifs of any and variable orientation. This strategy can be employed where two polypurine sites are separated by a number of mismatched inversion sites, which would prevent stable triplexation in the case of a continuous single TFO. McGuffie and Catapano (McGuffie and Catapano, 2002) used such a strategy, and produced a 23mer made up of a 12mer parallel (C,T)-containing sequence that was linked to an 11mer (G,T)-containing antiparallel sequence via a 3'-3' phosphodiester linkage. The sequence actually relies on the weak binding T in the third strand to a C in the target strand at the 3'-3' junction to provide the flexibility for the switch of the orientation of

the strand. This was targeted to a polypurine-polypyrimidine tract within the P2 promoter region of the *c-myc* gene. This is an important target as it is the over- or non-regulated expression of this gene that drives cell proliferation in many cancers. The study showed that in comparison to the single G,T and C,T oligonucleotides, the linked TFO showed increased triplex stability at lower concentrations and improved in *vitro* blocking of nuclear binding proteins at the target site.

A further adaptation of the strand switching strategy, and ultimately the answer to the need for polypurine target sequences, is the ability of nucleotides to switch from purine residues in one strand to purine residues in the other, while maintaining isomorphism and stacking interactions. One particular attempt to do this utilised αN^7 or αN^9, and βN^7 or βN^9 2-aminopurine nucleotides in a switching model for alternate strand recognition schemes. Two switching models were identified, one containing αN^7 and βN^7, and the other containing βN^7 and βN^9 residues, which bind in an antiparallel manner and consecutive C1' atoms remain almost central within the major groove of the duplex molecule (Parel and Leumann, 2001). This is perhaps the ultimate solution to the need for polypurine target sequences and implies that TFOs will be able to bind anywhere within genomic DNA. Initial research was not as promising as hoped and further development of this strategy is needed.

1.2.2 Base Modification and Substitution

1.2.2.1 Base Substitution

Third strand oligonucleotides will usually contain what are termed mismatches due to the target sequence rarely being solely homopurine in nature. What is usual is that the polypurine target sequence contains C-G, or T-A interrupts that generally serve to destabilise the triplex, and can actually prevent triplexation altogether (Huang, *et al.*, 1996). These problems emanate from the fact that these bases have only one available hydrogen bond for TFO targeting. The effect on triplex stability produced by the mismatch will be dependent on surrounding conditions.

- The base itself has an effect because some bases are more inhibitory than others, such as C*T-A triplets that are the most destabilising, particularly at neutral pH and above.
- Neighbouring bases will have an effect also. For example two neighbouring C^+s will repel one another and hence have an overall destabilising effect on the triplex.
- The pH at the site of triplexation will determine C protonation, so where the mismatch is represented by C, triplexation under more neutral pHs will be weaker than presented at acidic pH due to the addition of a second Hoogsteen bond available for third strand binding.
- Position of the mismatch within the third strand sequences is problematic. Central mismatches are more detrimental to triplex stability than terminal counterparts.

Mismatches generate a structural burden on the triplex causing marked decreases in T_m values. The binding of the third strand is such that the mismatch will be either completely or partially expelled from the natural third strand position, which will in turn result in a loss of stacking interactions between it and neighbouring bases. This in addition to the loss of Hoogsteen bonding, causes a drastic decrease in triplex stability. As a result of these findings, when a TFO is being designed, it is essential to isolate target sequences where such bases are minimal. As a rule target sequences should contain no more than 3 mismatch bases. Further discussion of this design process in relation to the design of the TFOs produced for the purpose of this study, is given in Chapter 2. To increase the recognition scheme and stability of triplex DNA where these mismatches are present, natural bases have been used in order to target the C-G, or T-A interrupts.

The T, C and G bases are able to bind parallel or antiparallel to the duplex target and as a result have the potential to compensate any mismatch within that target sequence. The use of C in such a strategy would however be disadvantageous due to its pH dependency, therefore (G,T)-containing oligonucleotides have been widely investigated as alternatives. Numerous studies have shown G and T to be the most successful third stand residues for T-A and C-G inversion sites respectively (Fossella, *et al.*, 1993). In this recognition scheme, however, G is only successful in the parallel

orientation, whereas T is successful in both the parallel and antiparallel TFO orientation. Where a T-A inversion is presented and third strand binding is antiparallel in nature, the least destabilising base substitution has been found to be C, but again, this is restricted by the pH conditions surrounding the triplex.

In these (G,T)-containing sequences, T favours the parallel orientation and G favours the anti-parallel conformation, but when mixed, the binding orientation is generally thought to be antiparallel (McGuffie and Catapano, 2002). This has been found to be dependent upon the number of TpG and GpT steps (Hélène, *et al.*, 1992; Neidle. S, 1997). Where the number is high and there are few contiguous runs of Gs, or Ts, then the oligonucleotide will favour the antiparallel orientation due to the high energy penalty caused by binding in a parallel manner. This emanates from backbone distortion that is associated with each step due to the involvement of non-isomorphous triplets (Giovannangéli, *et al.*, 1992). However, when the TpG and GpT steps are low the parallel orientation is preferred. In addition to this, further consideration is required to the length of G and T stretches, which plays a role in the overall alignment of the TFO (Faucon, *et al.*, 1996).

(G,T)-containing TFOs however, are not really the ultimate answer. NMR and molecular dynamics studies showed that (G,T)-containing oligonucleotides are non-isomorphous and hence lead to backbone distortion which in turn causes problems with base stacking and inevitably weakened triplex stability (Xodo, 1995). As a result, current research centres on identifying and producing base analogues, which have a high affinity for these inversion sites. While the numbers of analogues available for C-G inversions is high, there is a lack of analogues for the recognition of T-A inversion sites. This is due to the C5 methyl group, which sterically hinders base recognition (Guianvarc'h, *et al.*, 2003).

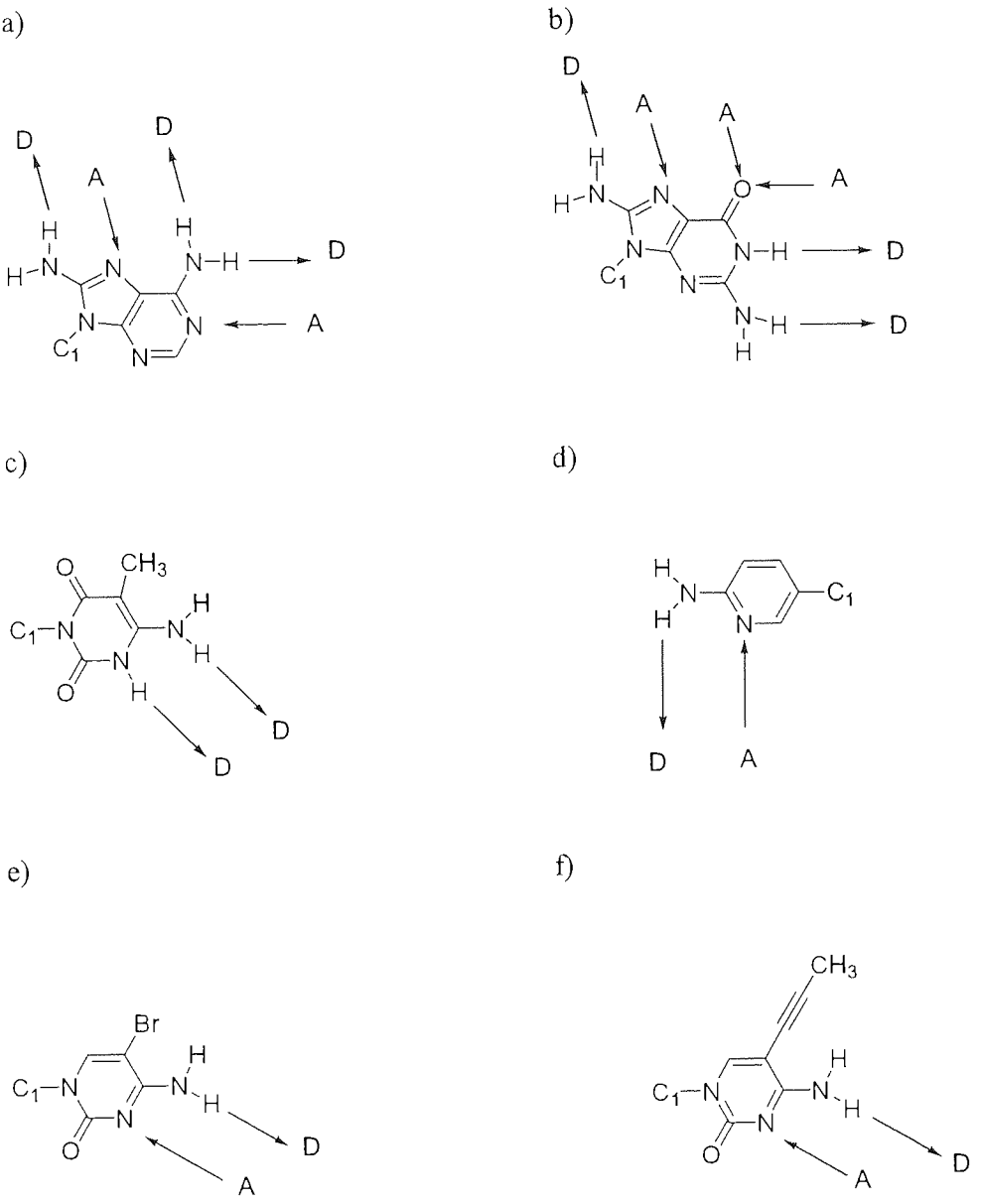

Figure 1.5 Structures of a number of base analogues used to enhance triplex stabilities; a) 8-aminoadenine and b) 8-aminoguanine c) 6-keto derivatives of 5-methyl cytosine, d) 2-aminopyridine, e) 5-bromocytosine, f) 5-propynylcytosine. A and D represent hydrogen bond acceptor and donor sites respectively, under triplex forming conditions.

g)

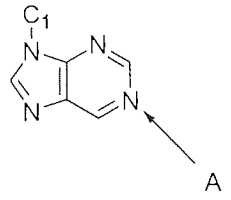

h)

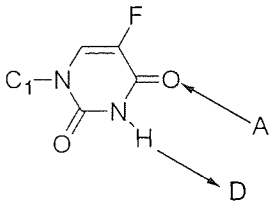

i)

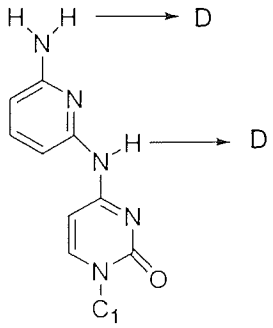

j)

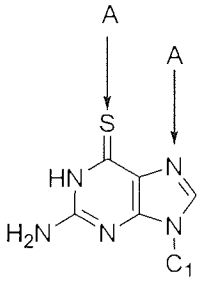

k)

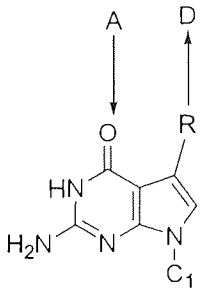

l)

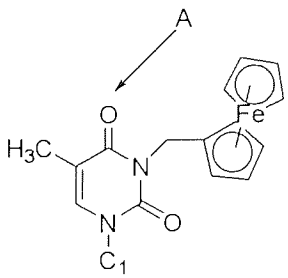

Figure 1.5 Continued g) 2'-deoxynebularine, h) 5-fluoro-2'-deoxyuridine, i) N^4-(6-amino-2-pyridinyl)deoxycytidine, j) 6-thioguanosine k) 7-deazaguanosine R = H, 9 deazaguanosine R = NH, 7-chloro-deazaguanosine R = Cl and l) ferrocenemethyl-thymidine. A and D represent hydrogen bond acceptor and donor sites respectively, under triplex forming conditions.

1.2.2.1.1 Analogues of Adenine

The need for adenine analogues is not a prerequisite as these bases are successful in triplex formation, participating in two Hoogsteen interactions with target purines whilst being pH independent.

Aminopurine analogues such as 8-aminoadenine and 8-aminoguanine (Figure 1.5a and b), have been used to enhance triplex stability. Their use is only apparent in hairpin DNA where the aminopurine undergoes Watson-Crick interactions with thymine and cytosine respectively, as well as interacting with third strand oligonucleotides. Here the introduction of an amino group at the 8 position of the nucleotide enhances triplex stability by enabling a further Hoogsteen bond interaction, and therefore these bases can form three Hoogsteen H bonds as opposed to the usual two. 8-Aminoadenine and 8-aminoguanine cannot, however, be used in conventional triplex formation due to the necessity for participation in Watson-Crick interactions (Aviñó, *et al.*, 2002).

1.2.2.1.2 Analogues of Cytosine

The pH dependency of C residues is one of the major limiting factors associated with pyrimidine motif triplexes. Under acidic pH, C becomes protonated (C^+), the protons acquired by N3 of third strand C residues, are able to interact with the N7 of duplex guanines, forming an additional Hoogsteen interaction totalling the two necessary for stable triplex formation (Figure 1.2b). Stability is also enhanced by electrostatic interactions that are formed between the positive charge of the C^+ and the negative charge of phosphate-sugar backbone. Hence at acidic pH the triplex is more stable. This protonation can create complications where there are two or more adjacent protonated cytosines, which will electrostatically repel one another due to their overall positive charge leading to triplex destabilisation.

The degree of protonation will also vary due to the position of the C in the third strand relating to its exposure to the surrounding media. Those residues in direct contact with the media, as would be the case with terminal residues, will be more effected by pH fluctuations, whereas those less exposed, as would be the case with more central residues, will maintain protonation at perhaps higher pH values.

At neutral pH, protonation is not apparent and as a result, triplex stability is compromised due to the availability of a single Hoogsteen bond. This is a phenomenon associated with intracellular triplex formation, where pH conditions at

and around genomic DNA are strictly maintained between pH 7.2 to 7.3. A further complication of C-rich TFOs is their ability to self-associate forming i-DNA under acidic pH (Figure 1.6) (Praseuth, *et al.*, 1999). This results from H-interactions that form between C and C^+ residues forming C^+-C duplexes.

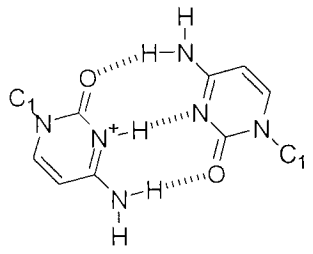

C^+ C

Figure 1.6 The structure of I-DNA formed between to C residues.

As a consequence third strand C residues are non-advantageous and should therefore be avoided.

Numerous studies have investigated C analogues in an attempt to solve the problems associated with third strand C residues. The triplex stabilising properties of the 6-keto derivatives of 2-deoxy-5mC ($m^{5ox}C$) have been studied (Figure 1.5c) (Xiang, *et al.*, 1996). Although good at increasing triplex stability *in vitro*, the base fails by being difficult to synthesis and hence has not been used in biological studies. 2-Aminopyridine (Figure 1.5d) is more basic than C and has the advantage of being able to form stable triplexes at neutral pH (Neidle, 1997).

Analogues such as 5-bromocytosine, and 5-propynylcytosine (Figure 1.5e and 1.5f) support stable triplex formation when opposite G in the target strand (Amosova and Fresco, 1999). Although TFOs containing these demonstrate lower T_m than those containing C at acidic pH, they do have the advantage of forming pH independent triplexes.

2'-deoxynebularine and 5-fluoro-2'-deoxyuridine (Figure 1.5g and 1.5h) show G-C interrupt recognition capabilities (Stilz and Dervan, 1993). These both bind through third strand hydrogen bonds in the same way as natural nucleotides (Huang, *et al.*, 1996). Another base mimetic, N^4-(6-amino-2-pyridinyl)deoxycytidine (Figure 1.5i), is able to actually cross the major groove of the duplex at C-G inversions and undergo hydrogen bonding with the duplexed G. The pyridine ring spans the major groove of the duplex and places the 6-amino group attached to the ring in hydrogen bonding

proximity to the N7 or O6 of the G. Such positioning of the pyridine ring would also allow it to undergo favourable stacking interactions to maintain triplex stability. This analogue was also shown in the same study to form stable triplexes with T-A interrupts.

Specificity of these analogues provides potential problems for this strategy, as substituted bases may be able to bind at non-specific sites. For these analogues to be truly successful the need to be sequence or base specific is fundamental, unless they are to serve merely as intercalating agents, (discussed later). The development of bridged nucleic acids (BNAs) is one possible solution (Figure 1.7 a)).

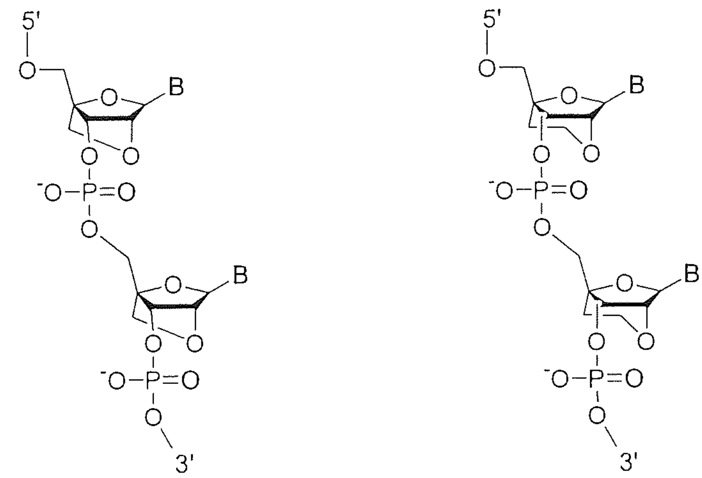

a) b)

Figure 1.7 The structure of a) BNAs and b) ENAs.

These have a fixed N-type sugar (C3'-*endo*) conformation and a particular example that has been developed is 2'-*O*,4'-*C*-methlyeneribonucleic acid (2',4'-BNA) (Hari, *et al.*, 2003). These types of nucleotide have strong triplex-forming ability particularly toward C-G inversions sites but also to A-T mismatches. This creates the problem in that they are not truly sequence-specific. However, with 1-isoquinolone as the nucleobase C-G specificity of the nucleotide is achieved. This is because the 2-carbonyl oxygen of the isoquinolone binds strongly to the 4-amino hydrogen of C, but the H4 of the isoquinolone and the C5 methyl group of T repel one another, favouring BNA*C-G triads. T_m values assessed through melting studies under near physiological conditions proved this and were enhanced for C-G targets over any other target duplex by a minimum of 9 °C.

A separate study showed that an increase in triplex stability of 10 to 20 times was achievable in the case of BNA-modified 15mers containing 5 and 7 modifications, respectively. Interestingly where all nucleotides are BNAs, the TFO does not bind to its target (Torigoe, *et al.*, 2001). This is believed to be because the BNA bases are too rigid being held in the C3'-*endo* conformation, which does not provide sufficient flexibility to support triplexation. On the other hand, NMR studies of triplexes containing natural bases have shown that the sugar rings are flexible and can shift from C3'-*endo* to C2'-*endo* puckering conformation (Gotfredsen, *et al.*, 1998; Asensio, *et al.*, 1999).

Further modifications using 2'-*O*, 4'-*C*-ethylene nucleosides (ENAs) (Figure 1.7b)), which are held in the same C3'-*endo* conformation, have been evaluated for their ability to increase triplex stability with single, multiple, or complete substitutions, compared with the same BNA modifications. The T_m studies of homopyrimidine TFOs show vast improvements in triplex stability with ENAs over natural TFOs as well as marginal improvement over BNA-containing TFOs (Koizumi, *et al.*, 2003). Of particular interest is that fully ENA-modified TFOs were able to form stable triplexes where BNA counterparts failed. The future use of these agents is promising, particularly as they show good levels of nuclease resistance.

As discussed, numerous modifications have been made to increase the pH range over which C-containing triplexes are stable. The most successful of these would appear to be the use of 5'-methyl cytosine (5mC) (Figure 1.2 b) Pg 18). There are strong literature precedents for 5mC as a successful stabiliser (Soyfer and Potaman, 1996; Amosova and Fresco, 1999; Leitner, *et al.*, 2000). For example, Leitner *et al* studied the effect of C protonation and methylation of intramolecular triplex stability. After establishing a T_m for the triplex containing natural C at pH 5.0 and 7.0, they then substituted 1 and then 3 of the C bases for 5mC, and measured T_m values. The results illustrated that the greater the number of substitutions the greater the increase in T_m. A single 5mC for C substitution, improves this value by 2.1 °C.

The increase in triplex stability by 5mC is still not fully understood but is thought to result from a number of factors. One factor is that 5mC has a higher pK_a than C, which as a result increases the pH range over which the base is protonated. The substitution of the methyl group causes a shift in protonation equilibrium; as a consequence $5mC^+$ is stable at neutral pH and above. Binding of the third strand 5mC also produces a spine of hydrophobic methyl groups that disrupt water molecules and

hence cause entropic stabilisation of the triplex. The overall effect is increased hydrogen bonding, base-stacking interactions, and, in particular, base stacking energies.

There is however a problem that is associated with the incorporation of all third strand C analogues in the polypyrimidine TFOs. C*G-C and T*A-T are the only truly isomorphous TFOs. Whichever combination of bases form the third strand the C1' atom remains constant and backbone distortion is avoided. However, introducing C analogues potentially disrupts this isomorphism, and as a result, causing decreased triplex stability. The use of 5mC maintains this isomorphism while decreasing the pH sensitivity of the C residue.

1.2.2.1.3 Analogues of Guanine

Polypurine TFOs containing contiguous runs of G residues will have a natural tendency to self-associate forming G quartets in the presence of certain cations including; K^+, Na^+, Ca^{2+} and Mg^{2+}. Of these ions G interactions with K ions is the most widely understood and documented. This is perhaps due to K being the predominant intracellular ion, where the formation of these quartets and intrastrand structures will severely diminish triplex forming capabilities, and even prevent triplexation completely by G-rich TFOs.

The interaction occurs when the K^+ forms the centre of the quartet by forming electrostatic interactions with the four O6 atoms of the G residues (Figure 1.8). These quartets are then able to stack and hence form quadruplexes.

Figure 1.8 G quartet formation mediated by K^+, which can lead to the formation of quadruplexes, a particular problem associated with G-rich oligonucleotides (Doronina and Behr, 1997).

These structures are not just artificial phenomena associated with G-rich TFOs, evidence for their formation as part of natural biological processes is mounting. Functions associated with telomerases, immunoglobulin switch regions and other biological systems have been proposed. There is growing interest in the use of these structures as potential drug candidates where they have been successfully used as thrombin-binding aptamers and HIV integrase inhibitors during *in vitro* studies (Miyoshi, *et al.*, 2003). This culminates from indications that these quadruplexes are able to bind directly to proteins and inhibit their function. Such inhibition was implicated by G-rich antisense oligonucleotides used as cellular antiproliferative agents. Inhibitory effects were found not to emanate from binding to mRNA molecules and the subsequent inhibition of target protein production, but from the formation of quadruplexes (Agrawal, *et al.*, 1996; Đapić, *et al.*, 2003). A similar occurrence is therefore possible with the use of TFOs. As a result numerous attempts have been made to overcome this tetrad formation, the majority of which centre around the replacement of G with analogues. Examples include 6 thioguanosine (Figure 1.5j) where the O6 atom is replaced by a sulphur atom. This reduces electronegativity while maintaining Hoogsteen bonding capability. The approach was

successful in weakening tetrad formation but triplet-binding stability was also weakened by as much as 100-fold in some cases (Neidle, 1997).

7- and 9-Deazaguanosine, whose N7 H-bond acceptors were replaced with a C-H and N-H group respectively, have also been tested (Figure 1.5k). The basis of these modifications was to remove the Hoogsteen bonds between the 2-amino and N7 groups so as to disrupt tetrad formation but to retain triplex binding donor and acceptor patterns for G*G-C triplets. The modified N7 group becomes an H-bond donor as opposed to an acceptor and therefore prevents H-bonding interactions with the 2-amino group of the adjacent G residue. Again, although successful in preventing tetrad formation they failed to maintain or improve triplex stability.

A further modification to the 7-deazaguanosine (Figure 1.5k), was the attachment of a chlorine atom at the N7 position to produce 7-chloro-7-deaza-2'-deoxyguanosine. This was first developed in 1995 and originally showed promise in duplex formation where stability was increased (Ramzaeva and Seela, 1995; Ramzaeva and Seela, 1996). Aubert *et al* (Aubert, *et al.*, 2001). This was incorporated into a 15mer TFO targeted to a 16 bp oligopurine-oligopyrimidine tract in proviral HIV-1 DNA. *In vitro* melting studies showed an increase of 5 °C in the T_m value of the TFO with multiple incorporations of the G analogue compared with the unmodifed oligonucleotide. However, multiple incorporations were not additive. The same T_m increase was observed whether 2, 3 or 5 substitutions were made. Melting observations were confirmed by gel shift analysis.

The prevention of tetrad formation was made apparent with the melting studies carried out in two differing triplex buffers, one containing NaCl and the other more representative of physiological conditions containing KCl. Triplex transitions were present under both conditions in the case of the modified TFO, but only in NaCl containing buffer in the case of the unmodified TFO. These results show the substitution of G with the 7-chloro-7-deaza-2'-deoxyguanosine to be successful.

A further complication of G-rich oligonucleotides is their ability to form homoduplexes when interspersed with A residues. These occur at G, A repeat sites within polypurine TFOs under favourable conditions, and can be parallel or antiparallel in nature. The formation of such structures is temperature-dependent, being favoured at lower temperatures, which then dissociate to form triplexes with the target duplex molecule as the temperature increases (Noonberg, *et al.*, 1995a; Noonberg, *et al.*, 1995b; Arimondo, *et al.*, 2001). The temperature at which the

homoduplex dissociates and triplex formation takes place is not clear. Arimondo *et al* demonstrated a transition midpoint of 25 °C for a particular 13mer parallel homoduplex, but this would presumably be sequence dependent. (G,A)-Homoduplexes can, however, be avoided by using so called 'zipper' oligonucleotides (Fox, 2000). In this strategy the TFO is bound to a shorter complementary oligonucleotide to form a duplex molecule with a single stranded overhang in the TFO strand. The overhang region can be as short as 3 nucleotides at the 3' end, or 6 at the 5' end. Although not fully understood, it is thought that when in proximity to the target duplex site, the overhang region recognises the target and binds, presumably initiating the nucleation process involved in binding of the third strand, and consequent expulsion of the complementary oligonucleotide (Svinarchuk, *et al.*, 1996). Svinarchuk *et al* actually demonstrated successful triplexation of a 20mer 'zipper' oligonucleotide via DMS footprinting assays that was more successful than its 'non-zipper' counterpart. This provides another approach to rectifying the problems of self-association related to G-rich oligonucleotides and one that does not require base modifications.

1.2.2.1.4 Analogues of Thymine

Analogues of thymine have been produced in an attempt to overcome A-T inversion sites in the target duplex strand that cause triplex destabilisation due to T presenting a single Hoogsteen bond.

Analogues include ferrocenemethyl-T (Figure 1.5l), which has a ferrocene group attached at the N3 position of the T. Research, particularly in the area of anti-cancer drugs, has shown that ferrocene compounds interact with nucleic acids in a non-covalent manner, which has sparked interest in the production of non-platinum based anti-cancer therapeutics. Its ability to interact with nucleic acids fuelled interest in its triplex-stabilising potential. However, a recent study has shown increased T_m values with modified oligonucleotides compared with unmodified TFO, but only at pH 5.5 (Petraccone, *et al.*, 2003). At pH 6.0-7.0 this stabilisation is absent due to reasons that are thought to be two-fold, arising from the fact that the ferrocenemethyl-T causes enthalpic disruption of the triplex. The ferrocenemethyl-T pulls the T base out of its natural plane, which creates a 'cavity' exposing the adjacent C bases involved in third strand binding to the surrounding solvent. The over exposure of these neighbouring C residues to the solvent created by the 'cavity' favours deprotonation toward neutral

pH, hence the decreased stability in comparison to the non-modified triplex. At pH 5.5 the C neighbours would appear to be fully protonated (C^+) and as a result hold the ferrocenemethyl-T in the major groove and enable it to participate in interactions with duplex bases. Consequently stability is enhanced at this pH. However, this effect is likely to be sequence dependent and as a result would not be expected for other sequences where there are no neighbouring C residues to the ferrocenemethyl-T.

1.2.2.2 Triplex Binding Ligands and Intercalating Agents

Another means of increasing triplex stability is by using triplex binding ligands or intercalating agents. These are designed to bind to the triplex DNA more favourably than to duplex molecules. These can be used either free in solution, where a number will bind to the formed triplex once produced, interacting with the triplex at various sites if available, or by covalent C5'and/or C3' attachment of the agent to the TFO during synthesis. The former method provides an analytical tool for increasing triplex stability but is of little therapeutic use *in vivo* or for therapeutic means.

Many of these agents exert their stabilising effect by intercalating at T*A-T sites within the triplex rather than at C^+*G-C sites, this is due the cationic nature of a lot of the agents that are electrostatically repulsed by C^+*G-C triplets.

The first agent to be investigated was ethidium bromide (EtBr) as it is a well known intercalator of DNA particularly duplex DNA. It has been found that EtBr actually intercalates more strongly into triplex than duplex DNA, for reasons that are not fully clear but may be due conformational differences that are apparent between the duplexes and the triplexes. EtBr like many intercalating agents will bind at T*A-T triplets due to its cationic nature, and will hence avoid C^+*G-C triplets due to electrostatic repulsion. Binding at the same A-T site within the duplex molecule is also apparent, but the difference in duplex conformation is such that it poses less affinity for EtBr binding (Sun and Hélène, 1993).

While the list of intercalating agents is long it was found that agents that were polycyclic in nature tended to be more triplex-specific. Reasons for this are thought to emanate from the sheer size of such molecules, which are too large to permit efficient stacking with duplex DNA (Fox, 2000). Triplex-specific agents include benzo[e]pyridoindole (BePI), naphthylquinolines, anthocyanins and amidoanthraquinones.

BePI was the first polycyclic triplex specific intercalator to be described (Neidle, 1997). This agent has been shown to increase T_m values by greater than 20 °C (Thuong and Hélène, 1993). It exerts it effect due to its cationic nature and intercalates between T*A-T triplets resulting in increased base stacking interactions via stabilisation of both polypyrimidine and polypurine TFOs.

Naphthyloquinolines are polycyclic agents in which the aromatic rings are not fused. They are able to maintain stacking interactions with base triplets, but due to their non-fused nature, they retain flexibility and can accommodate the propellor twist of the triplets (Keppler, *et al.*, 1999). Keppler *et al* demonstrated increased triplex stability of a TFO incorporating a naphthyloquinoline dimer compared with that incorporating a single subunit. Both, however, have shown increased stability over unmodified TFOs, but this agent is more effective at stabilising parallel rather than antiparallel third strands. Other members of the quinoline family in the form of bis-4-aminoquinolines have shown triplex-stabilising properties (Strekowski, *et al.*, 2003). These compounds are again T*A-T specific, but found to be superior to the afore mentioned compound in enhancing triplex stability.

Anthocyanins are a group of water-soluble plant pigments and their use as triplex binding ligands emanates from structural similarities to potent triplex stabilisers. They have only been used recently in their natural form, but studies have shown mild increases in triplex stability (Mas, *et al.*, 2000). However, with structural modifications, these agents potentially hold promise as successful triplex stabilising agents.

The amidoanthraquinones are an interesting group of interacalators, in that they contain many isomers that exhibit varying properties that enable them to interact more favourably with specific duplex and triplex DNA. Two particular families are the 1,4- and the 2,6-disubstituted amidoanthraquinones, which intercalate more strongly with duplex and triplex DNA respectively (Fox, *et al.*, 1995). Studies have shown the former to intercalate more strongly with duplex DNA due to enhanced base stacking interactions compared to triplex DNA, where such interactions lead to structural perturbation causing triplex destabilisation. Binding of 1,4-disubstituted amidoanthraquinones takes place in the major groove and as a result competes with the TFO. The triplex binding of the 2,6-amidoanthraquinone is brought about by its ability to bridge all three bases of the triplet and stack between the 6 bases of

consecutive triplets. However, the stabilisation of triplexes would appear to be sequence specific (Keppler, *et al.*, 2001). Research carried out by Keppler *et al* showed that the relative stabilising properties of this compound were more pronounced in an (A,G)-containing TFO compared to a (G,T)-containing third strand. Interestingly other isomers such as 1,8- and 2,7-disubstituted compounds demonstrated the reverse trend.

Polyamines have also been extensively investigated as triplex-stabilising agents where they are predominantly used in triplex melting studies to enhance triplex formation. Examples include putrescine, spermidine and spermine, which are all found intracellularly, where they play important roles in cell proliferation and differentiation (Thomas and Thomas, 1993). Triplex stabilisation is favoured over duplex because of an increased charge density produced from the polyanionic nature of the three DNA strands, as opposed to the two presented by the duplex molecule. Although these polyamines are present intracellularly at concentrations sufficient to promote triplexation, a large portion will already be involved in interactions with cellular macromolecules, causing diminished levels available for triplex formation. As a result researchers have attempted to incorporate polyamines, particularly spermine, into TFOs to enhance their triplex binding capabilities. Studies have been successful, with the attachment of a spermine moiety at the 5' end increasing triplex stability compared with unlinked counterparts (Tung and Stein, 1993). Stability results from diminished backbone repulsion between the three strands of the triplex, which enhances association and hinders dissociation. A further adaptation of this was the attachment of the spermine to residues within the TFO. One particular research group attached spermine to 5mC residues, producing 5mC-(N^4-spermine) residues, to determine the effect on triplex stability (Barawkar, *et al.*, 1994; Barawkar, *et al.*, 1996). It was shown that TFO containing these residues produced more stable triplexes, but increasing numbers of residues caused melting temperatures to fall respectively, perhaps due to the repulsion between spermine chains, or between spermine chains and C^+ residues at lower pH.

Chemically reactive moieties can also be tethered to the end of oligonucleotides as a slightly more advanced type of intercalating agent. Psoralen is an example (Figure 1.9 b)); it is a photoreactive intercalator that when bound at the 5' end of a TFO, after near UV light activation (320-400 nm), forms covalent crosslinks with the target duplex at T-A sites. The psoralen moiety has two photoreactive double bonds that crosslink to

the T residue at 5'-TpA-3' steps in the duplex molecule upon activation. In this case the TFO is used to deliver site-specific mutagenesis, which causes irreversible inactivation of the host gene via steric blockade of RNA polymerase. This mechanism has been shown to be successful both in *in vitro* experiments using plasmid DNA and in living cells where triplexes have been found to be stable for 72 hours (Grigoriev, *et al.*, 1993; Macaulay, *et al.*, 1995). The success of this method will, however, depend on the cell's ability to rectify the DNA damage by nucleotide-excision and recombination repair pathways; systems that are ubiquitous to bacterial and mammalian cells (Duval -Valentin, *et al.*, 1998). In particular, *E. coli* produces UvrA, B and C excinuclease enzymes that initiate repair of DNA damage caused by photoreactive compounds such as psoralens. Duval-Valentin *et al* showed recognition of the damaged site via these enzymes, but cleavage was diminished. This, it was proposed, was due to the binding of the TFO itself which prevented the usual cleavage pattern that originates on the 5' side of the psoralen induced damage (the site of triplex formation). This was supported by work carried out by Guieysse *et al* who showed further that the triplex actually inhibits the incision step carried out by the repair enzymes (Guieysse, *et al.*, 2000). While covalently bound, psoralen linked TFOs provide strong evidence for triplex stabilisation, their therapeutic use appears unlikely to be effective due to the necessity of photoactivation. Such activation would not be possible in the case of diseases caused by TB, HIV or inaccessible tumours.

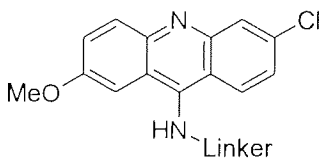

a)

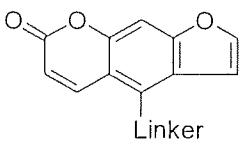

b)

Figure 1.9 The structure of a) the acridine and b) the psoralen labels that can be tethered to TFOs.

Acridine as a triplex stabiliser has strong literature precedents, and was first used due to its duplex intercalating properties, but its triplex binding capabilities are superior (Figure 1.9 a)). It has been shown (Aubert, *et al.*, 2001) to increase T_m by 15 °C when

incorporated at the 5' end of a TFO containing 7-chloro-7-deaza-2'-deoxyguanosine (Figure 1.5k). This T_m increase was not shown by the unmodified oligonucleotide.

TFO binding avidity is increased with the intercalation of the acridine simply because the tethered acridine moiety provides a greater number of contacts between the third strand oligonucleotide, and the duplex target, and hence provides additional binding energy when in the triplex formation (Barawkar, *et al.*, 1996). The acridine will intercalate at the junction between the duplex-triplex domain, raising the T_m of olgonucleotide by as much as 16 °C in some cases (Kukreti, *et al.*, 1997). This junction is visible as it represents a form of structural discontinuity in the underlying duplex, which results from conformational changes in the duplex molecule that occur upon binding of the third strand. These are necessary for successful triplexation. It has been shown, through a number of molecular modelling and fluorescence studies, that attachment at the 5' end of the third strand oligonucleotide has a greater stabilising effect than at the 3'. It has in fact been shown to increase the stability of the triplex by up to 500 times when bound at this position (Klysik, *et al.*, 1997). Klysik *et al* showed that the binding of acridine enhanced this stability by reducing the K_d value of a specific TFO from 2.5 μM to 5 nM. As well as decreasing the dissociation constant the acridine moiety has also been shown to increase association rates of third strand oligonucleotides, a factor particularly important when considering the therapeutic properties of such TFOs (Lacoste, *et al.*, 1997). Lacoste *et al* demonstrated binding of acridine-conjugated TFOs where triplex formation had been absent in non-conjugated counterparts. However, intercalation elsewhere in the oligonucleotide has also been shown to enhance stability. Kukreti *et al* (Kukreti, *et al.*, 1997) incorporated an acridine moiety centrally in a 14mer at an inversion site. The acridine was tethered via a linker group to prevent distortion of neighbouring Hoogsteen interactions. The study showed increased T_m values of 16 °C. Multiple acridine attachments have also been tested for their ability to enhance stability, but were found to be non-additive. This is probably due to the selective binding of the acridine moiety at the triplex-duplex junction.

1.2.3 Backbone Modification

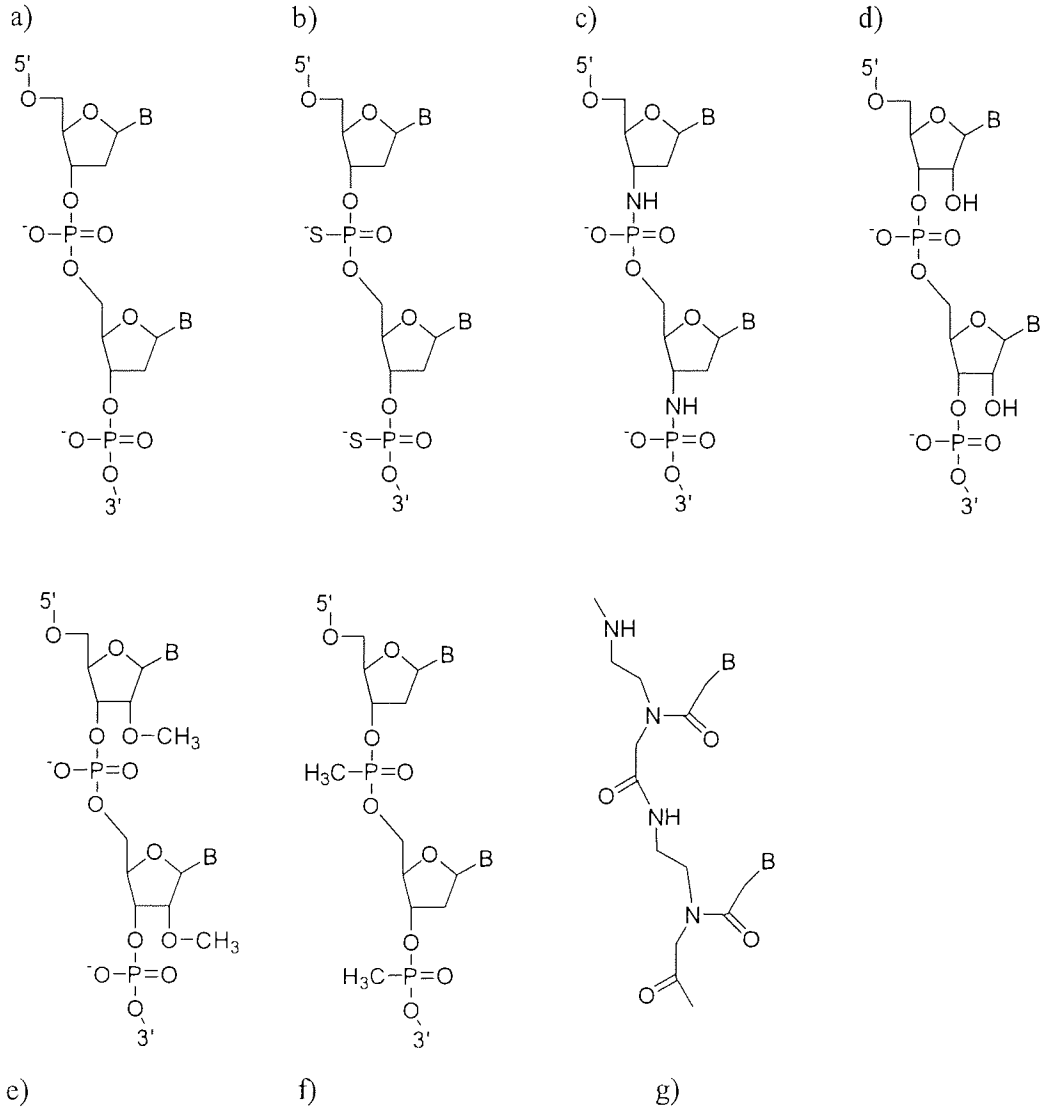

Figure 1.10 Different backbone modifications used to enhance triplex stability and to confer nuclease resistance, where B implies the base of the nucleotide and a) phosphodiester, b) phosphorothioate, c) N3'-P5'phosphoramidate, d) RNA, e) 2'-*O*-methyl RNA, f) methylphosphonate, g) PNA backbones.

1.2.3.1 Phosphodiester (PO) Backbone

The normal phosphodiester backbone of oligonucleotides (Figure 1.10 a)) poses two major problems for the antigene strategy; the first of these is the polyanionic nature of the backbone that emanates from the phosphate groups associated with this structure,

and the second is their non-modified nature implies exonuclease susceptibility. The former creates stability issues due to backbone repulsion, which as discussed is encountered when the three DNA chains come together to form the triplex. This repulsion is the major rate-limiting step of triplex formation and is not only a problem during formation, but is also key in the dissociation of the third strand.

The degradation of the oligonucleotides is problematic when targeting intracellular sites; a necessity if this strategy is to be used for therapeutic means. Nuclease enzymes are present within cells for the sole purpose of degrading unwanted DNA such as mismatched, mutated or exogenous DNA. Specifically, exonucleases are responsible for the degradation of single stranded DNA and will actually digest single stranded DNA in the 3'-5' direction via the sole recognition of the 3'-hydroxyl groups (Lehman and Nussbaum, 1964). Consequently the phosphodiester backbone has been modified in a number of ways to produce TFOs that evade nuclease activity and that form more stable triplexes.

1.2.3.2 Phophorothioate (PS) Backbone

Phosphorothioate modification (Figure 1.10 b)) results in the replacement of one of the non-bridging O atoms in the PO-backbone for a S atom, rendering the oligonucleotide resistant to nuclease degradation. While the latter is produced, the oligonucleotide still maintains sequence specificity and will form triplexes with stability similar to that of unmodified counterparts. Triplex formation is affected by the binding motif of the third strand however, where it has been found that polypurine TFOs will form triplexes with stability similar to PO-based oligonucleotides, whereas pyrimidine motif TFOs fail to produce stable triplexes (Fox, 2000). Studies have highlighted a degree of non-specific activity by TFOs modified in this way. In such cases cell growth, proliferation and enzyme activity have been affected, usually due to the TFOs ability to interact with cellular proteins (Brown, *et al.*, 1994). The degree of non-specific binding has been found to correlate with the number of PS-modifications in a given sequence, hence a fully modified oligonucleotide will have a greater affinity for non-specific sites than a TFO with less modifications. The degree of phosphorothioation does not affect the degradation rate of the oligonucleotides and as a result modification at the 3' end of the TFO is sufficient to evade nuclease activity. However, pharmacokinetic studies of PS-oligonucleotides have shown further complications exhibited by these compounds. In a number of animal models, PS-

oligonucleotides will interact with serum proteins including fibrinogen, γ-globulins and albumin, as well as causing decreases in arterial blood pressure, transient decreases in white blood cell counts, and complement activation (Agrawal and Iyer, 1997). Effects result solely from backbone modifications and are subsequently sequence-independent (Shaw, *et al.*, 1997; Levin, 1999).

1.2.3.3 Phosphoramidate (PN) Backbone

Phosphoramidate modification involves replacement of O3 with an NH group (Figure 1.10 c)), which confers nuclease resistance along with enhanced triplex-forming capabilities. PN oligomers are resistant to snake venom phosphodiesterases (SVPD), mammalian cell nucleases and nuclease activity associated with human plasma (Gryaznov, *et al.*, 1996). In studies using mobility shift assays, PN oligomers have been shown to bind with increased affinity to the target duplex by up to two orders of magnitude. Here the K_d decreases from 10^{-6} to 10^{-8} at neutral pH (Torigoe, 2001). T_m studies from the same study illustrated an increase of 35 °C and supported pyrimidine motif triplex formation at physiological pH. A number of other studies have demonstrated triplex T_m values in excess of 45 °C, and as high as 62 °C for PN oligonucleotides.

The increased triplex stability is thought to emanate from a slightly different backbone conformation compared with PO-TFOs. The backbone conformation adopted by PNs during triplexation is the BI conformation as opposed to BII adopted by the PO-third strands. The sugar rings consequently form an *N*-conformation (C3'-*endo* conformation) similar to that depicted in RNA, which stabilises this conformation to produce a more rigid structure (Micklefield, 2001). These structural variations favour Hoogsteen bonding more strongly than that of phosphodiester TFOs, and result in more stable triplexes (Escudé, *et al.*, 1996). Interestingly, such a conformation does not favour reverse Hoogsteen interactions, and decreased triplex stability is expected with this binding orientation. In contrast (G,T)-containing PNs have been shown to present even stronger triplex-stabilising capabilities. PN-TFOs must, however, present additional interactions to those produced simply by the conformational variation, otherwise RNA TFOs would be expected to exhibit the same stability, which is not the case. Further stabilising factors are thought to originate from altered hydration properties of the triplex produced by the substituted NH group, and enhanced rigidity that this modification confers (Gryaznov, 1999). The

latter is thought to facilitate Hoogsteen bond formation due to reduced entropy resulting in a decrease in dissociation rates of the third strand.

The advantage PN-modifications have over PS, apart from the apparent increases in triplex stability, is that they do not participate in non-specific interactions with cellular proteins. Therefore undesirable effects should not result (Micklefield, 2001). Pharmacokinetic analysis of these relatively new compounds is absent currently, perhaps due to the recent development of these agents.

1.2.3.4 RNA Backbone

RNA (Figure 1.10 d)) is able to form stable triplexes with duplex DNA but only in a parallel manner in relation to the purine strand of the DNA duplex. Stability is knnown to be sequence-, TFO-length, pH- and salt-dependent. The versatility of these RNA-TFOs is, however, limited due to recognition by intracellular nucleases. Methylation to produce 2'-*O*-methyl RNA (Figure 1.10 e)) reveals TFOs that are not only more triplex-stable in comparison to DNA and RNA counterparts, but that are also nuclease resistant (Fox, 2000). Studies have shown modification of this kind resulted in 24 times greater nuclease resistance than for unmodified counterparts. This was apparent after exposure to SVPD and DNase I endonucleases (Ito, *et al.*, 2003). The reasons for this increased stability is not fully clear but it is predicted from NMR and X-ray crystallographic studies that the structure of these 2'-*O*-methyl RNA TFOs is more preorganised and therefore more rigid than phosphodiester oligonucleotides. Because of the structural similarities with PN-TFOs these are thought to exert increased triplex stability in much the same way. It is thought that this pre-organised state more closely resembles the final triplex structure and, as a result, third strand binding by these TFOs is more favourable (Cassidy, *et al.*, 2003).

1.2.3.5 Methylphosphonate (MP) Backbone

Methylphosphonates were produced as non-ionic compounds by substituting one of the non-bridging O atoms in the PO-backbone for a methyl group (Figure 1.10 f)). They were produced in an attempt to increase cellular uptake (either passively or via absorptive endocytosis due to increased lipophilicity), to increase nuclease resistance and to reduce electrostatic negativity to improve triplex binding affinity. In addition it was hoped that the neutral nature of these oligonucleotides would also decrease affinity for plasma and intracellular proteins. Although nuclease resistance is conferred, uptake is not enhanced and affinities for nucleic acid targets are only

improved if the MP-linkages are pre-organised into the correct binding conformation (Micklefield, 2001). Although pyrimidine-containing oligonucleotides, with C substituted by 5mC and targeted to the envelope gene of HIV proviral DNA, have shown improved target affinity (Guntaka, *et al.*, 2003). However, work in this field seems quite contradictory. Some research groups have shown diminshed T_m values in comparison to PO-TFOs where triplexation was not detectable at all, and others have shown similar or improved binding affinities. It has been reported that purine-motif MPs have shown increased stability when bound to single- or double-stranded DNA but polypyrimidine TFOs comprised of T residues, do not form stable triplexes (Praseuth, *et al.*, 1999). Attempts have been made to improve the binding affinity of MP-oligonucleotides by hybridisation with phosphoramidate residues producing methanephosphonamidates, which are currently under further investigation.

1.2.3.6 Peptide Nucleic Acids (PNA)

A further adaptation to non-ionic oligonucleotides comes in the form of peptide nucleic acids. PNAs are DNA mimetics in which the nucleotide bases are retained but the PO-backbone is replaced by a polyamide structure made up of N-(2-aminoethyl)glycine units (Figure 1.10 g)) (Dean, 2000). Consequently PNAs do not have a 5'-3' orientation but instead have an amino (NH_2) to carboxyl (CO_2H) orientation. Due to the altered backbone composition PNAs are nuclease-, protease- and peptidase-resistant and serum stable, so avoid degradation (Lundemose, 2001). The neutral charge also prevents non-specific interactions that have been associated with the polyanionic nature of PO- and PS-oligonucleotides. Such a phenomenon was shown in a study where (C,G)-containing PNAs were designed and delivered to pulmonary epithelium systemically. PO-counterparts containing CpG motifs were shown to induce a proinflammatory cytokine response that was not triggered by the PNAs of the same sequence (Yuan, *et al.*, 2003).

Recognition mechanisms asserted by PNAs for single- and double-stranded DNA are the same as those demonstrated by unmodified DNA molecules, but PNAs would appear to be more sensitive to mismatches (Good and Nielsen, 1998). PNAs are able to form duplexes and triplexes via Watson-Crick and Hoogsteen interactions, due to the retention of the standard DNA nucleobases.

Figure 1.11 The four types of interaction depicted by PNAs and double stranded DNA (Koppelhus and Nielsen, 2003).

Single strand binding mirrors DNA-DNA interactions, but binding to duplex DNA can take one of four binding modes (Figure 1.11) (Nielsen, 2001). The first of these involves standard triplexation via Hoogsteen bonds as discussed throughout this chapter. The second is represented by triplex formation involving two PNA molecules and a single DNA strand. The binding of the first PNA via Watson-Crick interactions to the polypurine target results in the displacement of the alternate duplex strand, and the subsequent binding of a second PNA via Hoogsteen interactions, forming P-loop structures. Binding of the third strand can take place in an antiparallel manner, where the carboxyl terminus aligns itself with the 5' end of the purine target, or in a parallel manner where the amino terminus aligns with the 5' end of the purine target. The triplexes formed by PNAs are very stable and exhibit T_m values of between 50 and 90 °C, which, when formed, do not dissociate even in the presence of 100-1000 fold excess of charged, and neutral lipids, proteins, competitor DNA, and polyamines (Dean, 2000). However, higher triplex stabilities are usually associated with polypyrimidine PNAs as opposed to polypurine counterparts when triplexes are formed via invasive mechanisms (Nielsen and Egholm, 2001). Co-joining two targeted PNA strands to form so-called bis-PNA has enhanced this mode of invasive binding.

The third mechanism of binding is duplex invasion. It is similar to triplex formation and results in the displacement of the non-target duplex strand and binding of the

PNA to the target strand via Watson-Crick bonding. In this case there is an absence of third strand binding and hence the duplex molecule is retained.

The final mode of binding is similar to the third mode except that a second PNA binds to the displaced non-target strand, and hence two duplexes are formed (double duplex invasion). However, for this to take place the A and T residues need to be substituted for 2,6-diaminopurine and thiouracil residues respectively. Due to the neutral charge of these molecules, duplex and triplex formation via these invasive mechanisms, are ionically-independent. In fact, rates of formation of the different structures are actually hindered under ionically rich conditions. Levels of Na and K ions greater than 50 mM are sufficient to hinder this formation; levels lower than those exhibited physiologically.

Research groups such as that led by Nielsen have shown effective use of PNAs against peritonitis in mice and rats along with effective antibacterial action against a range of pathogens via antisense mechanisms (Schou, *et al.*, 2000). The use of PNAs as effective antigene agents has also been demonstrated both *in vitro* and *in* vivo. McMahon *et al* (McMahon, *et al.*, 2002), produced PNAs targeted to the angiotensinogen gene of mice. This protein is responsible for the development and establishment of hypertension, where it acts to raise blood pressures. Intraperitoneal injections of the designed PNA into hypertensive rats, produced decreases in blood pressure, along with diminished serum levels of angiotensin, and decreased levels of mRNA coding for the protein in the brain and liver, the two organs associated with high levels of angiotensinogen production.

The activities of PNAs do not just end at antisense- and antigene-mediated inhibition of transcription, PNAs can also act as mutagens as well as inducers of gene expression. The former results from PNA triplexes inducing DNA repair pathways, which repair sites of triplexation as they would normal lesions. The latter results from the P-loop structure being recognised as a transcription bubble and the subsequent transcription by RNA polymerases leading to up-regulation of protein synthesis.

However, the PNA construct is not completely optimal. The altered backbone means the molecule is electrostatically neutral, and as a result, is relatively insoluble, producing poor bioavailability (Senior, 2000). Cells, particularly bacterial cells, do not admit neutral compounds, so the need for modifications, in order to enhance uptake, is profound. Modification of these molecules is relatively straight forward owing to the neutrality of the PNA, and attachment of cationic detergents, conjugation

to peptides or lipophilic cations, and binding to cell-specific receptor ligands have successfully enhanced uptake (Muratovska, *et al.*, 2001; Koppelhus and Nielsen, 2003). In the latter case the attachment of a phosphonium cation to a PNA enabled delivery to the mitochondria of the cell, a particularly difficult task in itself. However, by far the best method reported for enhanced delivery is via the conjugation to peptides. These peptides are degradents of specific proteins that harbour cell-penetrating properties. These peptides maintain such properties and are able to cross the plasma membrane in an energy-independent manner (Pooga, *et al.*, 2001).

Recently it has been demonstrated that PNAs may not be sequence-specific as originally thought. In a particular study, PNAs were designed to investigate the enzyme-DNA interactions of bacteriophage T4 Dda helicase (Tackett, *et al.*, 2002). It was found that although the PNA inhibited ATPase activity of the enzyme, interactions between the PNA and the helicase were absent. Further investigation revealed that the inhibition of the enzyme resulted from non-specific interactions of the PNA with the single stranded DNA substrate of the enzyme and self-aggregation. Therefore ATPase activity was inhibited due to depletion of substrate. A number of sequences of varying length and base composition were assessed yielding similar results. Although the mechanisms of these non-specific interactions are not fully understood, they are thought to emanate from the enhanced hydrophobic nature of PNAs compared with DNA or RNA molecules. The tendency to aggregate in this way, to the point of precipitation, is a major drawback to the success of this strategy.

1.2.4 TFO Design

To date, numerous ways of increasing triplex stability using modified TFOs have been documented. However, binding motifs of the third strand as well as the target site itself have also been implicated as sources of triplex instability. One of the biggest debates is between pyrimidine- and purine-containing TFOs and their relative triplex-mediating stabilities. Pyrimidine motif triplexes have been widely explored due to their isomorphous nature but are of course pH-dependent. Purine TFOs on the other hand are advantageously pH-independent, but are non-isomorphous and as a result would perhaps tend to imply a weaker binding motif. Studies have however, shown that polypurine TFOs are actually more effective for *in vivo* inhibition of transcription and these TFOs have been shown to be stable under intracellular

conditions for 3 days (Debin, *et al.*, 1997). Reasons for this enhanced stability are not fully understood. It is thought that the triplex stability of purine containing oligonucleotides is actually governed by G residues, which are stabilised by Mg^{2+} ions; one of the predominant intracellular cations. These actually stabilise consecutive runs of G residues more so than single G molecules. They do this by binding to the N7 atom of the G, which presents a lone pair of electrons. The proximity of the O6 atom on the same residue enhances this negative potential. Where consecutive runs of G molecules are present, this negative potential is deepened further due to the presence of the same atoms on neighbouring molecules. As a result the binding potential of the Mg^{2+} is enhanced in this situation (Debin, *et al.*, 1999). From this it has been shown that the G content is the determining factor in the stability of polypurine TFO for this reason, and for high affinity binding, a G content of 54% is required (Perkins, *et al.*, 1998). Further explanation of the stability of (G,A)-containing TFOs led to the discovery of these triplexes having an enthalpy value of approximately 0, indicating them to be temperature independent and as a result dissociation of the third strand occurs along with the duplex target in one step (Pilch, *et al.*, 1991; Arimondo, *et al.*, 2001). Association rates of these purine-containing TFOs have also been shown to be greater than their polypyrimidine counterparts when directly compared. The formation of triplexes containing the former were shown to take minutes, whereas third strand binding in the case of the latter, under the same conditions, was shown to take hours (Faucon, *et al.*, 1996).

Within purine containing TFOs there is the added question; which motifs form more stable triplexes, either (G,A)- or (G,T)-containing TFOs? The latter, although not strictly polypurine in the manner previously discussed, are able to bind via the same antiparallel mechanisms and therefore need consideration here. The literature is however slightly contradictory on the different stabilities of these two types of oligonucleotide. (G,A)-Containing TFOs have been shown to form more stable triplexes, potentially due to the increased backbone distortions, compared with (G,T)-containing TFOs (Perkins, *et al.*, 1998). However, other studies have shown the opposite. The formation rates of (G,T)-containing third strands have been demonstrated to be greater than for (G,A)-containing TFOs (Paes and Fox, 1997), which is advantageous therapeutically, as these TFOs have to compete with DNA binding proteins, which have very rapid binding kinetics.

Mismatches have, however, been shown to be more detrimental to the binding of (G,T)-containing TFOs in comparison to their (G,A)-counterparts, implying greater affinity of the latter to a wider spectrum of potential target sites.

The target site will also play a key role to the success of triplex design, and as stated, currently requires purine residues on the target strand. However, another consideration that is necessary is the content of A residues present at the target site, as A-tracts disfavour triplex formation (Sandström, *et al.*, 2002). These tracts characteristically have a narrow minor groove, a shallow and wide major groove, and highly 'propeller-twisted' base pairs. Because of this structure they tend to be rigid in nature and have higher melting behaviours than strands containing other base pairs. Triplex formation is affected by the rigidity due to the inability of the duplex to alter its structural conformation on the binding of the third strand, a necessary process to promote successful triplexation. Interruption with a single G-C base pair into these tracts causes structural relaxation, which is more favourable to third strand hybridisation. This is thought to result from the introduction of the N2 amino group of the G residue into the minor groove of the duplex molecule, which hinders the propellor-twist associated with the A-tracts, hence more flexibility in the target strand. When designing TFOs all these factors need to be taken into consideration.

1.3 TFO Uptake

The second major problematic area of antigene therapeutics is the uptake of the TFO into a given cell type. Problems here centre on the anionic nature of the oligonucleotide due to the phosphate backbone, and the cell wall, which results in electrostatic repulsion of the two. The degree of repulsion is affected by the chain length of the oligonucleotide. Longer sequences exhibit a greater overall negative charge as a result of a greater number of phosphate groups in the backbone. This is one of the rate-limiting steps to uptake and needs to be overcome before delivery processes can begin. The basis of the research is to mask the charge of the oligonucleotide in order to cross the cell wall and carry the oligonucleotide to its target. Although passive diffusion is possible, it is both inefficient, requiring far higher concentrations of the TFO than carrier-mediated alternatives, and, *in vivo* and intracellular trafficking usually results in degradation (El-Aneed, 2004). However, surface binding interactions between the cell and the oligonucleotide have been demonstrated to facilitate passive uptake, particularly in mammalian cells. Binding to heparin proteins on the cellular surface is a known phenomenon, and results in the internalisation of the oligonucleotide via endocytosis (Stein, 1999). This process has however been found to be calcium-dependent and is markedly affected by decreased temperature.

The structure of the bacterial cell wall, and the one that we are more interested in for the purpose of this study, is simpler than the eukaryotic cell membrane. It is subdivided into Gram-positive and Gram-negative entities (a major characterisation scheme for bacteria), which have different components and overall structures (Figure 1.12).

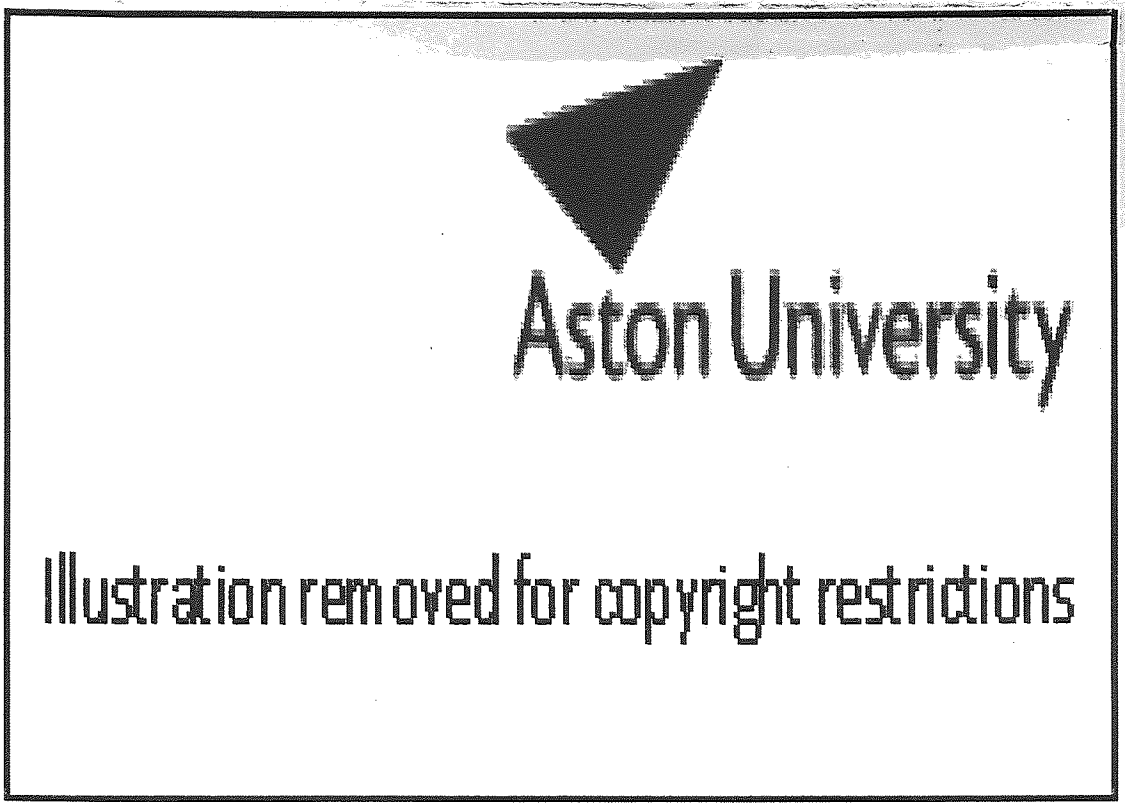

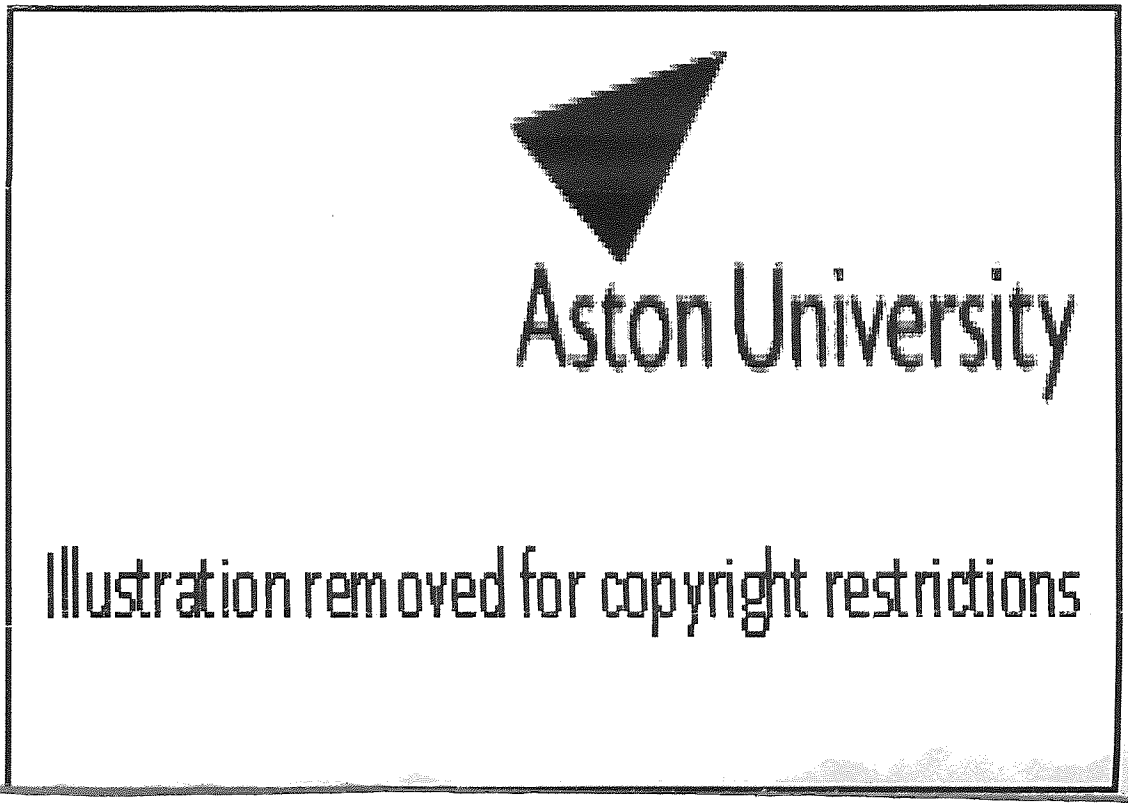

Figure 1.12 The structures of the bacterial cell wall where a) represents the Gram-positive cell wall and b) represents the Gram-negative cell wall (Prescott, *et al.*, 2002).

The cytoplasm and cell contents are encased in a phospholipid bilayer interspersed with proteins necessary to maintain the integrity of the cytoplasmic or plasma membrane. Surrounding this is the periplasm, which is gel-like in nature and contains enzymes and proteins that are responsible for nutrient acquisition, peptidoglycan synthesis and the modification of potentially toxic compounds. The periplasmic space associated with Gram-negative bacteria is larger than that found in Gram-positive bacteria and as a result contains more of these periplasmic proteins. The periplasm is surrounded by a layer of peptidoglycan that is important in maintaining the rigidity of the cell wall particularly in Gram-positive bacteria where this layer is significantly larger (20-80 nm) (Figure 1.12). This is where the similarities between the two cell walls ends. The more porous nature that the Gram-positive cell wall structure implies, means that barriers to entry of exogenous agents are limited and as a result these bacterial can take up relatively large compounds.

In addition to those structures already described, the Gram-positive cell wall also contains teichoic acid residues. These are polymers of glycerol or ribitol joined by phosphate groups that are attached to subunits of the peptidoglycan layer or to plasma membrane lipids. The latter are hence called lipoteichoic acids. It is the teichoic acids that produce the negative charge of the cell wall.

The Gram-negative cell has an additional membrane located outside the peptidoglycan layer forming the outer membrane. This is tethered to the peptidoglycan layer by Braun's lipoproteins, which hold the membrane in place. Further such integrity is produced by adhesion sites caused by the fusion of the two membranes at a number of sites throughout the cell wall. These have been suggested to also act as direct paths for the uptake of certain substances such as growth factors that can pass directly into the cytoplasm avoiding the periplasm. Lipopolysaccharide (LPS) units protrude from the cell membrane and consist of three units; lipid A, the core polysaccharide and the O side chain. The LPS portions of the membrane create a very hydrophobic environment and as a result, generate low fluidity in the membrane. They are responsible for preventing antibody damage to the cell (the O side chain interacts with the antibodies before they reach the cell), for the negative charge of the cell wall (emanating from the polysaccharide unit), for stabilising the outer membrane and also for some of the toxic effects associated with bacterial infections. Also inter-dispersed through this layer are non-specific porin channels that allow the uptake of essential molecules into the cell. The outer membrane serves as a strong permeability

barrier to many chemotherapeutic agents slowing passage across the wall (Nikaido, 1994). The porin channels, although numerous (approximately 50,000 on the surface of *E. coli*), aid exclusion also. They are proteins that contain charged amino acid residues that orient water molecules within the channels. This makes it difficult for hydrophobic compounds to pass through. In *E. coli*, the organism used in this research, these channels are quite restrictive in diameter with a minimum opening of 7 by 10 Å allowing the passage of substances no larger than 600-700 Daltons. This makes the influx of current antibiotics therapies very difficult and slow (Nikaido, 1994).

Bacteria do not just have passive barriers to foreign agents but also have active pump mechanisms in place to drive agents from the cell. This has become all too apparent with the emergence of resistant organisms. These pumps are very effective in pumping out antibiotic agents before they have a chance to exert an antibacterial effect. One particular group known as translocases has a diverse range of substrates and is known to efflux a number of antibiotics in a number of drug-resistant bacteria (Good, *et al.*, 2000). As there is such a wide substrate range a potential ability to pump oligonucleotides out of the cells is implied and this needs consideration in the future if the agents in this study are to be successful antibacterials.

Due to the poor permeability of the Gram-negative cell wall, and *E. coli* being the organism upon which the majority of this research was carried out, a number of mechanisms and carrier agents was assessed for their ability to aid uptake of designed TFOs.

1.3.1 Cold Shocking

One method used for the purpose of this study to enhance oligonucleotide uptake *in vitro*, is to employ cold $CaCl_2$ solution. Bacterial cells are exposed to the oligonucleotide in the presence of ice-cold $CaCl_2$ solution over a set time period; this is followed by a short heat shock period where the sample is placed at 37-42 °C, and is finally placed back on ice (Chapter 8). Such a technique is generally used in plasmid transfection for the purpose of cloning experiments. The process is not fully understood but the cycle of events that occur is; the $CaCl_2$ interacts with the bacterial cells making them competent and able to take up exogenous DNA, which in turn allows the binding of the oligonucleotide to the surface of the cell. This is perhaps possible due to the masking of the anionic backbone charges by the Ca^{2+} ions, which

then facilitate this binding. The DNA is then internalised during the heat shock process (Brown, 1996). It is possible that binding of the Ca^{2+} to receptor sites on the cellular surface induces the opening of ion-gated channels, consequently the oligonucleotide is able to pass into the cell.

Another theory is that the bacterial membrane is permeable to the chloride ions but not the Ca^{2+} ions, and hence these passively diffuse into the cell. Because of the osmotic pressures created by this, water is drawn into the cell causing it to swell, this in turn draws in the extracellular DNA. Again Ca^{2+} ions potentially diminish backbone charge allowing the initial interaction of the oligionucleotide and the cell before it is internalised. This, however fails, to explain the uptake mechanism that is responsible for this internalisation. Whichever mechanism prevails, the process is successful yielding transfection rates in excess of 60% during cloning experiments. However, while this technique enhances uptake *in vitro*, its use *in vivo* is clearly not feasible. A potential answer to this is co-administration of the oligonucleotide with agents that would permeate the membrane to allow uptake of the TFO.

1.3.2 Chemical-Mediated Uptake

Chlorpromazine (CPZ) is a phenothiazine, a group of drugs that are used as neuroleptics but that have been shown to possess antibacterial, as well as antiviral, antifungal, antimycobacterial and antiprotozoal properties (Amaral and Kristiansen, 2000). Its use solely as an antimicrobial agent since the 1950s has been overlooked due to its neuroleptic effects and the development of overwhelming alternative antimicrobial agents during this time.

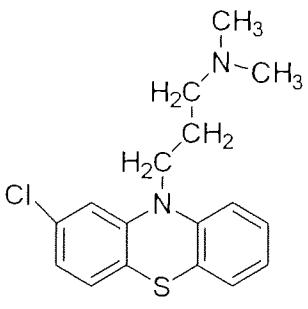

Figure 1.13 The structure of Chlorpromazine.

The antibacterial mode of action is still not clear but its interaction with cell membranes has been shown to increase permeability of the cell to exogenous agents. The hydrophobicity of the tricyclic ring structure (Figure 1.13) is thought to allow partitioning into the hydrocarbon tail portion of the phospholipid bilayer, while the hydrophilic tail groups are able to interact with the polar head groups of the phospholipids (Chen, *et al.*, 2003). Interaction between CPZ and bacterial cell envelope proteins is also thought to ensue (Amaral and Lorian, 1991). Interaction of CPZ with DNA is also possible (De Mola and Posthumaa, 1983), either by the intercalation in the minor groove of the duplex molecule between base pairs (Amaral, *et al.*, 2001), or by preventing incorporation of thymidine residues into the DNA (Amaral, *et al.*, 1992). However, it is unlikely that the CPZ will penetrate the bacterium to this extent, and therefore exerts it effect at the cell wall. Studies by Chattopadhyay *et al* (Chattopadhyay, *et al.*, 1998) showed CPZ to disrupt and cause damage to the cytoplasmic membrane. This membrane contains proteins that are responsible for production of the proton-motive force that enables membrane transport and hence the viability of the cell. A lack of cell lysis, after prolonged incubation with CPZ, and the uncontrolled influx of glucose, followed quickly by its efflux, led to this conclusion. What is perhaps more interesting, currently and for the purpose of this study, is the ability of CPZ to work synergistically with current antibiotics, reversing bacterial drug resistance. This has been shown in a number of bacteria including methicillin-resistant *Staphylococcus aureus* (MRSA), where resistance to oxacillin was markedly reduced by CPZ (Kristiansen, *et al.*, 2003). Other cases have shown increased activity of gentamicin in association with CPZ in children presenting with recurrent pylonephritis. The enhanced activity was attributed to the increased permeability of the infecting *E. coli* to the gentamicin caused by the CPZ (Amaral, *et al.*, 2001). Such a case is important here because it provides possibilities for the enhanced uptake of TFOs in order to produce an increased antigene effect and therefore provides an alternative strategy for uptake. Co-administration of the two components is possible as indicated in the case described above. However, doses of CPZ would have to be sub-clinical to prevent unwanted neuroleptic side effects. Nonetheless, numerous other systems have been developed in order to optimise oligonucleotide delivery.

1.3.3 Lipofection

There are presently two major candidates for the *in vivo* delivery of DNA particles, which are viral vectors and lipids. Viral vectors, although target specific and with high delivery efficiency, are limited by the size of the DNA that they can deliver. They also have high immunogenicity risks, are complex to construct and have the potential to form an infectious agent. Liposomes on the other hand demonstrate low toxicity, are capable of transfecting DNA particles of any size and although delivery efficiency is diminished, they are a safe alternative to viral vectors (Rädler, *et al.*, 1997; Oberie, *et al.*, 2000; Almofti, *et al.*, 2003). It was for these reasons that they are used in this present study as transfecting agents in order to aid uptake of the designed TFOs.

The number of agents available in this area is vast, but can be categorised by physico-chemical properties into three main groups; those that are cationic, anionic, or neutral, all of which are discussed below. The success of a delivery system is measured not just by its ability to carry an agent across the cell wall and membrane but its effectiveness at getting that agent to its target site, and maintaining levels of the agent at the target in order for it to produce the desired effect. For *in vivo* use there is the problem of serum stability and the ability of the agent to remain biologically available throughout the systems of the body. In the case of antigene agents, effective levels will have to be maintained for at least the half-life of the target protein and probably longer until the desired level of gene knockout is achieved. Liposomes are particularly good at this due to the ease at which their properties can be manipulated, which in turn can alter bio-distribution of drugs to target organs whilst masking their toxicity and improving their therapeutic index (Campanhã, *et al.*, 1999).

1.3.3.1 Cationic Liposomes

The rationale for the use of cationic liposomes is that by their nature they interact with the anionic phosphate groups of the oligonucleotide backbone and self-complex. They were first proposed as a vehicle for DNA uptake in 1987 by Felgner *et al* (Felgner, *et al.*, 1987). The liposomes are made up of a polar head and non-polar hydrocarbon chain, which assemble into bilayers with the head in the water phase and the hydrocarbon chains congregating together in the centre. Cationisation of the lipids, by creating a positively charged head group, enables the interaction of the lipid with DNA due to the negative charges of the phosphate backbone and hence neutralisation of the charge. The interaction of the two causes condensation of the DNA into a more

compact structure, a process that has been visualised via metal-shadowed, negative staining and freeze-fracture electron microscopy (Eastman, *et al.*, 1997). However, the final structure of these complexes is unclear, and there is great dispute as to whether the interaction results in the internalisation of the DNA (internal model), or whether the DNA and lipid merely aggregate, where the DNA binds to the surface of the lipid (external model) (Eastman, *et al.*, 1997). Understanding this is fundamental to understanding initial lipid-DNA complexation to cell interactions, that promote the uptake of these structures.

Cationic lipids are normally coupled to a neutral or zwitterionic co-lipid that serves to stabilise the liposome. This also serves to destabilise the endosome that is produced on uptake into eukaryotic cells (see below), hence these agents were designed for delivery of oligonucleotide into mammalian cells, more so than bacterial cells, where endosome formation is not apparent. The co-lipid usually takes the form of either dioleylphosphatidylethanolamine (DOPE) or cholesterol. DOPE, has been confirmed by numerous research groups to be the most efficient *in vitro* transfection agent when associated with cationic lipids, due to the ability of the lipid to facilitate membrane fusion between the lipid-DNA complex, and the cell membrane, expelling the DNA into the cytoplasm (Hong, *et al.*, 1997). However, this is not apparent *in vivo*, where cholesterol was found to be more effective, probably due to increased stability demonstrated by cholesterol-containing lipid complexes under these conditions.

The cationic head can take a number of forms but tertiary or quaternary ammonium, or protonatable polyamines are preferred. The valency state of this head will usually determine its efficiency in binding DNA, for example polyamines such as spermine or spermidine are favoured because they will bind to DNA more strongly than their singly charged counterparts (Blau, *et al.*, 2000).

The hydrocarbon chain is usually made up of a pair of aliphatic chains or a cholesterol ring structure. The chain length is important for the transfecting property of the lipid, not only in its ability to fuse with the cell membrane, but for toxicity issues. The chains are normally made up of monounsaturated fatty chains 18 carbons in length, or of saturated C12, C14 fatty chains. The reduction in chain length of these has been shown to reduce transfectability due to increased rigidity of the liposome and reduced fusability (Felgner, *et al.*, 1994). Cholesterol acts by compacting the lipids in the liposome, which enhances transfection more so than lipids containing the aliphatic

chains for reasons, which are not fully understood, although the latter aliphatic chains are generally more commonly used.

Linker structures also play a role in the efficiency of transfection produced by the lipid, in that certain linkers promote stability and decrease biodegradability of the lipid, and *vice versa*. These may also affect the cytotoxicity of the lipid.

1.3.3.1.1 Mammalian Cell Delivery

The positively charged lipid-DNA complex (lipoplex) that is produced is electrostatically attracted to the negatively charged glycoproteins of the cell wall. This interaction enables the internalisation of the complex.

The internalisation of the oligonucleotide is made possible by the process of fusion and endocytosis, the latter of which is triggered by extracellular signals resulting from the adherence of the liposome to the outer cell wall. The mechanisms of this are not fully understood and there is great debate over whether or not the process of fusion actually takes place at all. Its involvement in the process of successful uptake is questionable due to the fusion of lipids with the cell membrane resulting potentially in the release of the DNA to the extracellular fluid. This was postulated after fusion experiments that showed poor gene delivery (Pedrosa de Lima, *et al.*, 2001). As a result, the process of internalisation in mammalian cells is now generally thought to arise from a process of adsorptive endocytosis in which the oligonucleotide is compartmentalised into an endosome. However, a recent study has highlighted fusion as a necessary mechanism to allow entry and compartmentalisation of large lipoplexes (Almofti, *et al.*, 2003). The endosome will fuse with intracellular lysosomes, exposing the oligonucleotide to hydrolytic enzymes, which will act to degrade the DNA; a protective mechanism adopted by cells to eradicate macromolecules upon entry. The role of the co-lipid is, however, to release the DNA before lysosomal fusion and therefore must take place in the early stages of endosomal uptake (Miller, 1998). This DOPE or cholesterol-aided release, results in free movement throughout the cytosol and usually in an accumulation within the nucleus of the cell (Noguchi, *et al.*, 1998; Hughes, *et al.*, 2001). The mechanism of endosomal release is not clear, but one proposal is that the oligonucleotides are released as a result of fusion of the cationic liposome with anionic liposomes in the cytoplasmic membrane. The DOPE undergoes polymorphic changes under physiological conditions, resulting in the formation of an inverted hexagonal phase, which is thought to disrupt the liposome membrane (Miller,

1998; Pedrosa de Lima, *et al.*, 2001). It may be this structural change that promotes the fusion of the cationic lipids with the membrane anionic lipids, which in turn form charge neutral pairs. This disrupts the interaction between the cationic lipids and the DNA, and hence the oligonucleotide is released (Zelphati and Szoka Jr, 1996; Xu and Szoka Jr, 1996). Levels of release are generally low and the level of liposomal internalisation does not correlate with the subsequent gene expression or suppression. Hence this form of DNA delivery is well documented as being very inefficient. The liposomes also have a tendency to aggregate forming macromolecular lipoplexes.

The nucleotide chain may then pass to the nucleus, either via binding to newly synthesised nuclear proteins found in the cytoplasm, or passively during cell division (Blau, *et al.*, 2000). The latter is possible with oligonucleotide chains, which due to their small size are able to pass quite freely through nuclear pores, found throughout the nuclear membrane. Another possibility is that residual lipid remains after endosomal release enabling fusion of the lipid with the nuclear membrane. In turn this enables release of the free DNA into the nucleus and allowing it to interact with its target. Passage to the nucleus has to be relatively swift to avoid endonuclease activity, which degrades the oligonucleotide chains in the cytoplasm. However, little is known about the detail of intracellular trafficking and nuclear penetration.

1.3.3.1.2 Bacterial Cell Delivery

The method of interaction and internalisation by bacterial cells is much simpler than that by mammalian cells. The production of endosomes and fusion with lysosomes is not apparent and uptake is more a case of lipid fusion resulting in the release of the oligonucleotide into the cytosol of the cell. The initial interaction is thought to take place due to ionic forces that exist between the cationic lipid and the anionic teichoic acids (Gram positive bacteria) or LPS (Gram negative bacteria) residues that are located on the surface of the bacterial cell (Jones and Kaszuba 1994). Bacteria do have mechanisms in place to deal with the uptake of exogenous macromolecules and those that destroy foreign DNA take the form of endonucleases. These are numerous within the cell, hence a large amount of effort has been put into the modification of backbones to render them 'invisible' to such action, as discussed earlier. Also there is the absence of a nuclear membrane to penetrate, as the genome of bacteria lies naked in the cytoplasm of the cell.

The effectiveness of cationic lipid-mediated delivery of oligonucleotides is dependent upon the ability of the lipid to adsorb onto the cell wall of the bacteria and its subsequent ability to diffuse into the cell; something that is determined by the lipid content of the liposome and hence requires a great deal of work to optimise (Kim, *et al.*, 1999). Aspects such as lipid size, charge and cytotoxicity are key to this process and will vary according to the target cell line. This is clear from a number of *in vitro* studies carried out to assess liposomal encapsulation of bactericidal compounds. While liposomally-encapsulated chloramphenicol and streptomycin were shown to be inactive against *E. coli*, other studies demonstrated enhanced antibacterial activity of neomycin and penicillins when liposomally encapsulated (Bakker-Woudenberg, *et al.*, 1986; Omri, *et al.*, 1995). The difference would appear to be due to the different liposomal preparations used.

The cytotoxicity of the lipid emanates from the necessity of the electronegative state of the wall to allow for efficient functioning of membrane proteins, receptors and ion channels. Therefore the concentration of lipid should be low enough not to produce cytotoxic effects. Gram-negative bacterial cells have been shown to be more resistant to higher concentrations of lipid than Gram-positive counterparts (Campanhã, *et al.*, 1999). Here it was also shown that positively charged bacteria were unable to survive due to damage to surface proteins where the cationic vesicles actually adhere. Interestingly no fusion between the vesicles and the bacterial membranes was demonstrated coupled with a lack of lysis, indicating mere adherence as the source of cellular death. In addition to this, it was made clear that larger liposomes have a more detrimental effect at lower concentrations due to an increased affinity for the cell surface resulting from a greater positive charge density.

Fusion depends on the physical state of the two lipids which is determined by the liquid-crystalline transition state of the lipid, which is more fluid-like and hence more fusogenic at a specific temperature (T_c). If the T_c values of the lipid and cell membrane do not correlate then fusion will be hampered because below these temperatures the lipids are more rigid. Cationic liposomes seem thus far to be in this more rigid state, and as a result, their effectiveness against bacterial targets has only really been apparent in the case of intracellular pathogens such as *Brucella*, *Listeria*, *Salmonella* or *Mycobacterium* species (Desiderio and Campbell, 1983). Effects are generally not seen in extracellular bacteria due to the rigid nature of these liposomes preventing fusion. The effectiveness against intracellular pathogens emanates from

the endosomal uptake mechanics of the infected mammalian cell, causing the internalisation of the liposome containing the antibiotic and hence the enhanced antibacterial activity (Beaulac, *et al.*, 1998).

1.3.3.2 Anionic Liposomes

Liposomes made of anionic lipids or phospholipids have also been found to be effective delivery agents. The reasons for the success of this strategy is unclear and perhaps unexpected due to the electrostatic repulsion that would normally occur between the two electronegative entities. However, interactions are clear and these liposomes have been imaged, using electron microscopy, clustering around bacterial cells (Kaszuba, *et al.*, 1997). Such anionic interactions can be enhanced by the incorporation of phosphatidylinositol (PI), which has been found to interact strongly with the bacterial surface through hydrogen-bonding interactions (Jones and Kaszuba, 1994). These interactions appear strong enough to overcome the electronegative repulsion. However, non-PI containing anionic lipsomes have also been successful in bacterial delivery and have also been found to discriminate against mammalian cells. Anionic liposomes made up of dimiristoylphosphatidylglycerine (DMPG) and dipalmitoyl phosphatidylcholine (DPPC), so called fluidosomes due to a non-cholesterol content, have shown an inability to fuse with epithelial cells (Desjardins, *et al.*, 2002). The addition of cholesterol to these membranes results in increased rigidity of the liposome, which markedly affects the fusion process. Enhanced delivery of antibacterials in *in vivo* studies, via fluidosomes, has been demonstrated in comparison to more rigid, cholesterol-containing liposomes (Schiffelers, *et al.*, 2001). DPPC and DMPG in combination confer a low T_c value ($\leq$ 37 °C), which implies great fusability at this temperature; an important issue when considering the therapeutic use of such agents. The discrimination emanates from the differing lipid composition of the cell membranes of bacterial and epithelial cells. The phospholipid content of the *E. coli* outer membrane is composed of 85% phosphatidyl ethanolamine (PE) and 15% phosphatidylglycerol (PG), comprising phosphatidyl glycerol and diphosphatidylglycerol (Lugtenberg and Peters, 1976). This content varies slightly between different bacterial species, but PE is the major constituent of these membranes. The phospholipid content of epithelial cells, on the other hand, comprises 53% phosphatidylcholine (PC), 27% PE, 7% phospatidylinositol (PI) and 8% sphingomyelin (Desjardins, *et al.*, 2002). Of these constituents, the PE is the

component that accounts for the fusogenic nature of the membrane and as a result will be responsible for liposome fusion. In epithelial cells the 27% PE is located on the inner leaflet of the membrane, which is inaccessible to external particles such as liposomes, whereas in bacteria, it is located on the external membrane. It is for this reason that anionic liposomes are unable to fuse with epithelial cell membranes. This differentiation provides an inadvertent targeting strategy against bacterial infections and as a result has sparked interest in these agents as carriers of bactericides. One important area of research is in the targeting of *Pseudomonas aeroginosa* infections associated with cystic fibrosis patients. These infections occur in pools of mucus within the lungs of these patients, resulting from dehydrated pulmonary secretions and decreases in mucocillary clearance from the lungs. Premature death is usually due to the level of lung tissue degradation caused by the organism. The drug-resistant strains of the organism have developed thick cellular membranes that serve to prevent uptake of current therapeutics. Delivery of bactericides via this liposome method has the potential to bypass these impermeable membrane barriers, due to fusion between the two membranes. Delivery of liposome-encapsulated antibiotics to such infections would have to be via the lungs and would relying on aerosolisation. Because of the non-systemic nature of this delivery system, it means that larger doses of the antibiotics can be administered to the patient without toxicity. These organisms have a thickened outer membrane, which serves as one of their antibiotic resistance barriers. Administration of tobramycin encapsulated in DPPC and DMPG liposomes demonstrated almost complete eradication of *Pseudomonas* infections in rat models, whereas treatment with free tobramycin left a large infective pool of the organism (Beaulac, *et al.*, 1996). Furthermore the administration of the drug in this manner resulted in an increased release of the tobramycin compared with other liposomes, as well as a sustained level of the antibiotic in the lung with reduced systemic drug absorption (Beaulac, *et al.*, 1997). Extension of this study to other organisms such as *Stenotrophomonas maltophilia*, *Burkholderia cepacia*, *E. coli* and *Staphylococcus aureus* has harvested similar results showing increased antibiotic activities when liposomally encapsulated at sub-MIC concentrations (Beaulac, *et al.*, 1998).

The other area of bacterial targeting is to biofilms that are associated with Gram-positive bacteria such as Staphylococcal species. These again provide a barrier to current antibiotics. Particular species include *Staphylococcus epidermidis*, which is renowned for its ability to adhere to prosthetic devices potentially resulting in

septicaemia. Other species of this genera include MRSA of which there are fully drug-resistant strains. Jones *et al* (Jones, *et al.*, 1994; Jones, *et al.*, 1997) have shown successful fusion of anionic liposomes, containing bactericides such as triclosan, with biofilms and the subsequent release of the contents. Marked growth inhibition was demonstrated.

The success of these agents in bactericide delivery to both Gram-positive and Gram-negative cells, as depicted in the cases outlined above, prompted interest for the use of such agents in this current research.

1.3.3.3 Neutral Liposomes

Neutral liposomes were developed to counter problems associated with cationic lipids in *in vivo* models, due to their inherent ability to interact with serum proteins. This is particularly problematic if they are to be used as therapeutic agents. Cellular delivery of DNA has been successful using neutral liposomes where fluorescein-labelled oligonucleotides have been imaged in the nuclei of mammalian cells with formulations demonstrating serum stability (Sasaki, *et al.*, 2001). The formulation of these liposomes incorporating oligonucleotide or plasmid DNA, relies on their hydrophilic properties meaning they can be encapsulated into the aqueous space inside the liposome. However, because there are no charge interactions, encapsulation efficiencies are low with 3% and 10% reported in separate studies (Stuart and Allen, 2000). Encapsulation can be improved by the attachment of polyethylene glycol (PEG) to the liposome surface, which has been shown to double this efficiency. Novel formulation protocols have also been developed increasing liposomal DNA content to 50-70%. However, generally low encapsulation efficiencies and aggregate forming properties of these liposomes (Beaulac, *et al.*, 1997), which result from their neutral nature, makes these liposomes unfavourable currently as oligonucleotide delivery agents. Charged phospholipids avoid aggregation to a degree due to repulsive mechanisms.

It is clear that in order to make neutral liposomes strong candidates for oligonucleotide delivery, these problems need to be addressed. Currently, cationic and anionic delivery systems provide more favourable tools for TFO uptake.

1.3.3.4 Pharmacokinetics of Liposomes

Liposomal encapsulation of TFOs not only enhances cellular delivery, but also provides protection from degradation and clearance during circulation *in vivo*.

Systemic injections of naked oligonucleotides result in rapid degradation and removal of the TFO by the reticuloendothelial system (RES) or the mononuclear phagocyte system (MPS). Studies have shown after 5 minutes post drug administration, only 0.01% of the oligonucleotide remained, which became undetectable after 15 minutes. By comparison, liposomally-encapsulated oligonucleotides were found at concentrations of 71% and 11%, 5 minutes and 2 hours post-injection, respectively. Intact oligonucleotides were found in the liver, spleen, lungs and kidneys (De Oliveira, *et al.*, 2000). Other studies have shown similar residence times with 13% of the administered concentration of encapsulated DNA still in circulation 2 hours after injection. Interestingly, during this study, gene expression in the lung, spleen, heart, liver and kidney increased with increasing cationic lipid used in formulation. Under high cationic lipid to DNA concentrations, free liposomes have been found to co-exist, and it is these that are thought to enhance gene delivery by increasing retention times of lipid-DNA complexes, and mediating gene delivery (Song and Liu, 1998). However, the ease of removal and degradation of unmodified liposomes from circulation is still a problem. Cationic lipids are more problematic due to their electropositivity enabling them to bind electronegative serum proteins (Fujii, 1999). Incubation of cationic lipids in plasma resulted in increased turbidity and the formation of clot-like structures, with the eventual release of liposomal contents. Specific factors responsible for these effects are bovine serum albumin (BSA), lipoproteins and macroglobulins. These act via different mechanisms to destabilise the liposome and the uptake process. BSA decreases cell association, immunoglobulin G (IgG) alters charge potential by almost neutralising the cationic charge, and other factors such as heparin displace the oligonucleotide from the liposome (Garcia-Chaumont, *et al.*, 2000). IgG is an opsonin and therefore its binding to the liposomal surface will also cause activation of phagocytic processes and hence the digestion of the liposome. The binding of this antibody can also lead to the binding of complement factors, which in turn can induce the complement cascade, a further consequence of the use of these cationic liposomes. These liposomes are therefore cleared in a similar fashion to naked oligonucleotide by the RES and MPS.

There is debate over whether cationic liposomes are more immunogenic than neutral or anionic liposomes. As a result studies carried out by Sachetelli *et al* (Sachetelli, *et al.*, 1999) set about answering this. A process of immunisation was set up with a population of mice and clearly demonstrated that no antibodies were raised against

anionic fluidosomes (DPPC and DMPG containing liposomes). Such an immune response would be unexpected due to the negative nature of these liposomes and hence an inability to interact with serum proteins. Anionic lipids were also found to provide greater protection than cationic lipids *in vivo*. Here 50% of an oligonucleotide encapsulated in cationic liposomes was degraded in 40 min, whereas oligonulceotide encased in anionic liposome remained intact for a minimum of one hour.

The immunogenicity of a given liposome is based on a number of factors including its size and T_c value. The larger the lipid size the greater the chance it has at invoking an immune response. T_c causes an immune response at both its extremes; if a liposome has a T_c that is particularly high or low then it has more potential to produce an immune response. The reasons for this are unclear.

Efforts have been made to overcome the immunogenicity of liposomes by a number of approaches. One of these is through the production of more rigid lipids, which prevent association of serum proteins. Such liposomes would be ineffectual, however, in the delivery of therapeutics to bacterial cells, where fusion is the means of uptake. Another adaptation is the use of lipid-DNA complexes with high charge ratios. One of the problems associated with the interaction of serum proteins is that they are able to form bridges between liposomes and hence induce aggregation. However, with highly charged complexes, the proteins are unable to overcome the increased repulsion between the lipoplexes, and the bridges are not formed (Pedrosa de Lima, *et al.*, 2001).

Liposomal modification via the incorporation of polymers such as PEG, has been shown to increase liposomal circulation times by preventing interactions with serum proteins. Grafting PEG to the surface of the liposome does not just prevent liposomal recognition by RES, but has also been demonstrated to target specific sites, particularly in the case of bacterial infections. The liposomes preferentially localise at the site of infection potentially due to increased capillary permeability at these sites, whereas unmodified liposomes do not (Schiffelers, *et al.*, 2001). The main foci of infection or haemorrhagic zone will contain the greatest bacterial numbers resulting in a very pronounced inflammatory response. One of the responses of which is to increase permeability of surrounding capillaries in order to flood the site with cells and components of the immune system in an attempt to eradicate the infection. This however is not only associated with bacterial infections, but will occur at any disease site that causes in an inflammatory response. As a result these liposomes have also

been successful in the delivery of drugs to combat other disease states such as arthritis (Corvo, *et al.*, 2002). Programmable fusogenic vesicles (PFV) are a further adaptation to the grafting of PEG moieties to the surface of liposomes. These vesicles contain cholesterol, dioleyldimethylammonium chloride, DOPE and are stabilised by PEG-lipid conjugates. PFVs are stable in circulation and go unrecognised by the RES due to the hydrophilic polymer coating so accumulation at disease sites is possible. However, the real advancement comes in the ability of these liposomes to shed the PEG coating and become fusogenic, something that can be programmed to take place after minutes or hours have elapsed. This latter process is made possible by varying the hydrophobic anchoring domain of the PEG subunit. The coat desorbs and interacts with other hydrophobic binding sites liberating the liposome, upon which it is able to fuse with target cells. Cells can be targeted via the use of a cationic lipid in the liposome formulation, thereby preventing leakage of the liposome content into the surroundings of the target cells (a possibility if the liposomes remain stagnant for any length of time), which in the case of oligonucleotides would be of little gain due to the inability of these to enter cells via passive means. The success of this strategy has been shown through the delivery of anticancer agents in a number of studies (Hu, *et al.*, 2001). The ability of PEG-conjugated liposomes to target infectious sites, to produce sustained drug concentrations, is a major advantage particularly when considering leukopenic patients. The difficulty in treating such patients with infections is renowned and prone to failure. Targeted drug delivery, as is the case with PEG-conjugated and other long circulating liposomes, could benefit these patients greatly (Bakker-Woudenberg, 2002). Experiments using leukopenic rats demonstrated increased antibacterial activity of liposome-encapsulated antibiotics compared with free antibiotics, targeted to *Klebsiella pneumoniae* in normal rats (Schiffelers, *et al.*, 2001). However, antibacterial effects of the same drug-lipid formulation were markedly diminished in rats with impaired defences. The problem here was the rapid systemic spread of the infection, which would be controlled more in a normal individual by normal host defences. Co-administration of free and encapsulated antibiotic eradicated the infection due to targeted drug delivery produced by the liposomes, and systemic clearance of the pathogen due to the free antibiotic. However, liposomes used here were rigid and contained cholesterol, and investigation under the same study of PEG-conjugated fluidosomes showed increased drug efficacy and complete survival of the rats. This was apparent due to the slightly more leaky

nature of these liposomes that allows seepage of the drug during systemic circulation, but sufficient targeted drug concentration at the haemorrhagic zone of infection was maintained.

This strategy highlights the second major problem associated with liposomes in that they are generally non-site specific and as a result the liver is always an involuntary target at which the liposomes tend to accumulate. Although conjugation of PEG moieties imparts site specificity, it does not confer cell specificity. Attempts to improve this centre on the attachment of further ligands to the liposomal surface. Liposomes have been grafted with ligands or antibodies in order to enhance target site specificity and internalisation. Various chemical modifications have been made including conjugation of the liposomes to transferrin (large populations of transferrin receptors are found on tumour cells) (Tros de Ilarduya, *et al.*, 2002), poly(L-lysine) derivatives, folate (targeted to tumour cells), heme (targeted to hepatocytes) and antibodies (Garcia-Chaumont, *et al.*, 2000; Lebedeva, *et al.*, 2000). A successful example of the latter was the encapsulation of oligonucleotides with cationic lipids coated with the anti-GD_2 antibody in order to control cell proliferation in the case of cancerous cells. GD_2 is an antigen found on the surface of neuroblastoma cells and targeting of liposomes to this site enhanced uptake as well as causing replicatory inhibition. Pharmacokinetic studies showed increased serum stability and long circulation times with over 40% still present in the blood and spleen 24 hours post-injection (Brignole, *et al.*, 2003). Although studies have shown improved targeting of such liposomes, attachment of cell-specific antibodies has also shown increased clearance by the RES (Fujii, 1999).

Although liposomes do not have the same DNA transfection ability of viruses, their non-hazardous nature and the continual advances made in this technology make them prime candidates as future gene delivery vehicles. The high levels of encapsulation and transfection efficiency with cationic and anionic lipids, and particularly the latter in DNA delivery to bacterial cells, made these agents prime advocates for TFO delivery during this current research project.

1.4 The Current Research Project

1.4.1 Aims and Objectives

The aim of the research illustrated here was to assess the antibacterial, antigene potential of TFOs targeted to the *gyrA* gene of *E. coli* and *S. pneumoniae*. Unmodified oligonucleotides and modified oligonucleotides, targeted towards an oligopurine tract in the DNA gyrase gene, were synthesised in accordance with literature precedents for binding affinity, and triplex stability under intracellular conditions. A number of uptake strategies have also been applied in order to improve TFO delivery to bacterial cells by mechanisms that have been widely explored by other research groups and have shown a good level of success. The gyrase gene was the target gene of choice due to the fundamental activity of the gyrase enzyme within the bacterial cell crucial for survival. The enzyme is also the target of the fluoroquinolone agents, a group of very potent antibacterials to which, bacterial resistance is strongly emerging.

1.4.2 DNA Gyrase

DNA gyrase is one of four topoisomerase enzymes found in the bacterial cell, all of which are responsible for the maintenance of DNA structure, via cutting and resealing, during transcription and replication. Topoisomerase I and III form type I enzymes and are able to cut single stranded DNA, whereas II and IV are both type II enzymes, which are responsible for cutting double strands. It is the latter two that are of more interest here as their functioning is inhibited by fluoroquinolones, the primary target of which is organism-dependent.

DNA gyrase (topoisomerase II) is a tetramer made up of four subunits; two A and two B subunits, which are in turn transcribed by the genes *gyrA* and *gyrB*, respectively. The role of the enzyme is fundamental to bacterial survival due to its ability to catalyse a number of topological changes in DNA. The gyrase enzyme binds to the DNA at the point where two double stranded regions cross, where it either induces negative supercoiling and relaxation of linked structures and knotting (Hugo and Russell, 1998), or it acts to promote supercoiling (McEachern and Fisher, 1989; Travers, *et al.*, 2001; Stuger, *et al.*, 2002). However, the process of unknotting in *E. coli*, has since been proven to be controlled solely by topoisomerase IV (Olavarrieta, *et al.*, 2002). These processes are essential during DNA replication and transcription where the gyrase enzyme will bind ahead of the replication fork in order to induce negative supercoiling, and hence enable unwinding of genes for replication or

transcription. The gyrase enzyme is also able to bind behind the replication fork in order to induce supercoiling and condensation of the DNA post-replication or transcritption.

The process of supercoiling is the preferred reaction of the enzyme. In this process the GyrA dimer of the enzyme binds to the double stranded DNA via the C-terminal of the molecule. The subsequent binding of ATP to GyrB clamps the DNA in place for supercoiling. The N-terminal of the A subunit, cuts one of the double strands with a 4 base stagger (the so-called 'gate' segment), the intact double helix is then pulled through the cut ends, which are then ligated, again via the N-terminal. In the reaction, the transported helix is clamped by the B subunit, which post cleaving of the other helix by the A subunit, is passed to the A subunit through the gated segment. The hydrolysis of ATP to ADP by the B subunit of the enzyme, and its subsequent release, results in the release of the clamp and the freeing of the helices. During the process of negative supercoiling ATP is not required, and it takes place via the binding of the GyrA to the transported segment after cleavage of the second helix, where it is then passed to GyrB (Hocking and Maxwell, 2002).

One of the major groups of antimicrobial agents that target the topoisomerase enzymes is the fluoroquinolones. There are numerous other groups including coumarins, cyclothialidines, flavones and terpenoids but these have little clinical relevance due to toxicity and diminished antibacterial activity. Fluoroquinoloes have a broad spectrum of activity in a range of infections such as urinary tract infections, sexually transmitted diseases, gastrointestinal infections, respiratory tract infections, bone and joint infections, and skin and soft tissue infections (Hooper, 1998). Their potency is slightly greater in Gram-negative bacteria as opposed to Gram-positive but they are successful for the treatment of infections caused by either group of organisms. They are a useful group of agents particularly in the treatment of infections where the causative organism is resistant to other antibiotics, as the resistance mechanisms exhibited by these bacteria are generally not effective against this group of compounds. The fluoroquinolones have slightly different primary targets in Gram-positive compared with Gram-negative bacteria, however, in both cases the drug is able to form complexes with the GyrA subunit of the gyrase enzyme. While the binding has been clearly demonstrated (Hooper 1998), the means by which they exert their antibacterial action is less clear. It has been shown that they bind to the enzyme during the cleavage-resealing phase of the supercoiling process, resulting in

an inability of the enzyme to ligate the single strands of DNA, and hence the DNA becomes fragmented. This occurs at each region of supercoiling within the DNA at the site of gyrase binding (Hooper, 2002). However, actual cellular death is thought to emanate from other mechanisms and not from the prevention of supercoiling directly. This is apparent from the fact that cell growth is inhibited by concentrations of fluoroquinolones far less than those concentrations necessary to completely inhibit DNA supercoiling. It is thought that these lethal events arise from the blocking of the replication fork that is produced during DNA replication and transcription, and hence the enzyme-quinolone complex produces a blockade against DNA or RNA polymerase (Willmott, *et al.*, 1994; Hooper, 2002). While the killing mechanisms are still not clear, induction of error-prone or 'SOS' DNA repair, has been found to be a characteristic response of *E. coli* to fluoroquinolone administration. These will serve to correct lesions at the site of quinolone-gyrase interaction, however, it is not clear whether these mechanisms are favoured, or whether it is these that actually cause cell death. Three mechanisms have been implied in the killing process depicted by fluoroquinolones. The first requires both RNA and protein synthesis and hence cells need to be dividing, and the second involves killing in the absence of cell division as well as RNA and protein synthesis. The third occurs when RNA and protein synthesis are active, but cell division is not (Wickens and Pinney, 2001). Research carried out by Wickens and Pinney showed a 70-fold increased survival rate of *E. coli* (post antibiotic effect (PAE)) when protein and RNA synthesis were inhibited, with a 20-fold increase in survival when cell division was inhibited. This would indicate that quinolones require protein and RNA synthesis as well as cell division to take place in order to exert their full lethal effect, and that cellular death is associated with the drug's disruption of these processes.

1.4.3 Bacterial Resistance to Quinolone Antibiotics

The occurrence of quinolone-resistance in 1990 in enterobacteriaceae was as low as 1% in Europe and the USA (Gales, *et al.*, 2000), but increased use of the drug due to resistance to other antibiotics such as trimethoprim, which is prescribed in the case of uncomplicated urinary tract infections (UTI), has lead to the emergence of increased resistance. A 5 year study between 1995-2000 in the Netherlands, illustrated quinolone-resistant bacteria in 1995 to be an exception both in cases where the

infection was community or hospital acquired. By 1999 such resistance was commonplace in both situations (Hoogkamp-Korstanje, *et al.*, 2003).

1.4.3.1 Resistance among *Escherichia coli*

Quinolone resistance in *E. coli* arises from a number of mechanisms, but most commonly and detrimentally from chromosomal mutations in the genes that code the A subunit, as it is the GyrA subunit of the enzyme that is the primary target for these antibiotics in this organism. It can be a result of single or multiple mutations within the quinolone resistance-determining region (QRDR) of *gyrA* (residues 67-106), most commonly leading to the substitution of amino acid ser-83 to leu causing high-level resistance. Substitutions involving val and ala have also been observed. Such mutations cause the production of gyrase enzymes with an altered quinolone binding site, hence antibiotic binding affinity is markedly diminshed (Martínez, *et al.*, 1998; del Mar Tavío, *et al.*, 1999). Mutations within the gene coding for topoisomerase IV (*parC* and *parE*), as well as in *gyrB*, have also been demonstrated, but confer much lower levels of resistance in this organism. However, highly resistant strains of *E. coli* contain multiple mutations that arise in a stepwise manner, usually originating in *gyrA* or *parC* with second and third step mutations occurring in *parC* or *gyrA* respectively. Mutations in *gyrB* and *parE* can also be involved but are rarer (Gales, *et al.*, 2000). Other mechanisms identified include active efflux pumps and the down-regulation of OmpF, one of the major porin channels found on the surface of *E. coli*. These act by preventing accumulation of the antibiotic in the cell due to an increased permeability barrier and the enhanced efflux of the drug out of the cell.

1.4.3.2 Resistance among *Streptococcus pneumoniae*

S. pneumoniae is a particularly important pathogen as it is a cause of mortality worldwide, producing diseases such as bacterial pneumonia (of which it is the most common cause) and otitis media. It is one of the major three causative organisms associated with meningitis and has become the most common cause of meningitis in children (Tarasi, *et al.*, 1999). Resistance of the organism to β-lactam antibiotics has lead to treatment of *S. pneumoniae* with more potent antibiotics such as fluoroquinolones, which in turn has conveyed further resistance. They are the antibiotics currently in the UK that show the greatest increase in usage (Cubbon, *et al.*, 2000). However, increasing rates of resistance are not only thought to emanate from drug overuse, but also from genetic transfer between organisms. Viridans group

streptococci occupy the same oropharyngeal space as *S. pneumoniae* and as a result horizontal transfer of resistance genes is possible due to genetic similarities of the organisms. Such a phenomenon has actually been illustrated *in vitro* (Ferrándiz, *et al.*, 2000).

Quinolone resistance in *S. pneumoniae* is two-fold and although mutations in *gyrA* play a role, *parC* is the initial mutational site, particularly in the QRDR, owing to it being the primary target of the fluoroquinolones. The *parC* and *parE* genes code for topoisomerase IV, again a tetramer, where ParC and ParE are homologous to GyrA and GyrB respectively. Like the gyrase enzyme it is responsible for maintaining DNA topology, but this enzyme is involved chromosomal partitioning. GyrA is thought to be the secondary target for these antibiotics in this organism. Substitution of ser-79 to tyr or phe is generally the origin of ParC-mediated resistance. However, in highly resistant strains substitution of ser-83 with tyr or phe in GyrA is also observed and is found to be necessary to achieve this level of resistance (Muñoz and De La Campa, 1996; Stewart, *et al.*, 1999). Mutations in *parE* have also been demonstrated in bacterium exposed to quinolone antibiotics, but no link between this and resistance to the antibiotic could be made (Zhanel, *et al.*, 2003). Efflux pumps have also been found to be active in resistant strains of *S. pneumoniae*, interestingly these pumps have been found active, albeit at a low levels, in highly quinolone susceptible strains. But again the major contributing factor to resistance is mutations within *parC* (Broskey, *et al.*, 2000). Attempts to remedy the situation of increasing resistance currently centre at the production of new fluoroquinolones analogues. While many have been produced, gemifloxacin shows the greatest promise, particularly against *S. pneumoniae* where it has superior antibacterial activity compared with other fluoroquinolones (Kim, *et al.*, 2001). It also has a less ability to produce resistance in the organism due to the necessity for additional mutations in the topisomerase IV and gyrase enzymes to increase MIC values of the antibiotic (Jones, 2002). However, infections caused by resistant isolates, resulting from prior exposure to earlier less effectual fluoroquinolones, have been shown to affect the susceptibility of these organisms to the newer more potent agents. One case reported a nosocomial outbreak of ciprofloxacin-resistant bronchitis and lower respiratory tract infections. The isolation of the causative organism revealed mutations in *parC* and *gyrA*, and non-susceptibility to more potent quinolones (Critchley, *et al.*, 2002). Fully resistant

strains of *S. pneumoniae* provide a further complication in that they have been shown to confer resistance to other groups of antibiotics (Hooper, 2002).

As mutations in the gyrase A gene play such a key role in the resistance to the quinolones, it seemed an ideal target for the purpose of this research. The success of the antigene strategy in an antibacterial context, would provide a very powerful tool for combating resistance among the two afore mentioned organisms. In addition to this, the use of this strategy provides a potentially more versatile drug candidates in that genetic mutations conferring resistance to the TFOs, can be quickly identified through genomic sequencing, and subsequently, an altered TFO produced that is once again able to bind at the target site.

The use of the antigene strategy is not restricted to *E. coli* and *S. pneumoniae* but can be applied to any organism containing homopurine tracts, which are ubiquitous to prokaryotes, as discussed. As a result this technology has the potential to combat some of the most severe cases of bacterial resistance such as is the case with some strains of MRSA. Cases of infections caused by these MRSA strains have been on the increasing for sometime (Gottlieb, 1999). Results from the Department of Health's mandatory surveillance scheme for England and Wales illustrated resistance rates of 42% among all reported cases of *S. aureus*-based bacteraemias (Anon, 2002). The prevalence of these so-called 'superbugs' is now all too apparent with recent government initiatives to introduce increased hygiene measures into NHS hospitals in an attempt to stem the rising rates of nosocomial infections. Infection control directors will employed in a bid to improve hygiene practises to prevent the spread of resistant organisms among patients, incidences of which are higher in the UK than anywhere else in Europe (Times, 2003).

2.0 OLIGONUCLEOTIDE DESIGN, SYNTHESIS, PURIFICATION AND CHARACTERISATION

2.1 Introduction

This chapter highlights the sequences that have been synthesised for the basis of the entire study and illustrates their purity and characterisation. Discussion as to the choice and design of the sequences is also included. Synthesis, purification and characterisation protocols, along with sequence composition, are detailed in chapter 8 and are referred to throughout this chapter. Sequences were synthesised using the Beckmann Oligo 1000 synthesiser using an automated synthesis protocol, this process is demonstrated below.

2.1.1 Automated Solid-Supported Oligonucleotide Synthesis

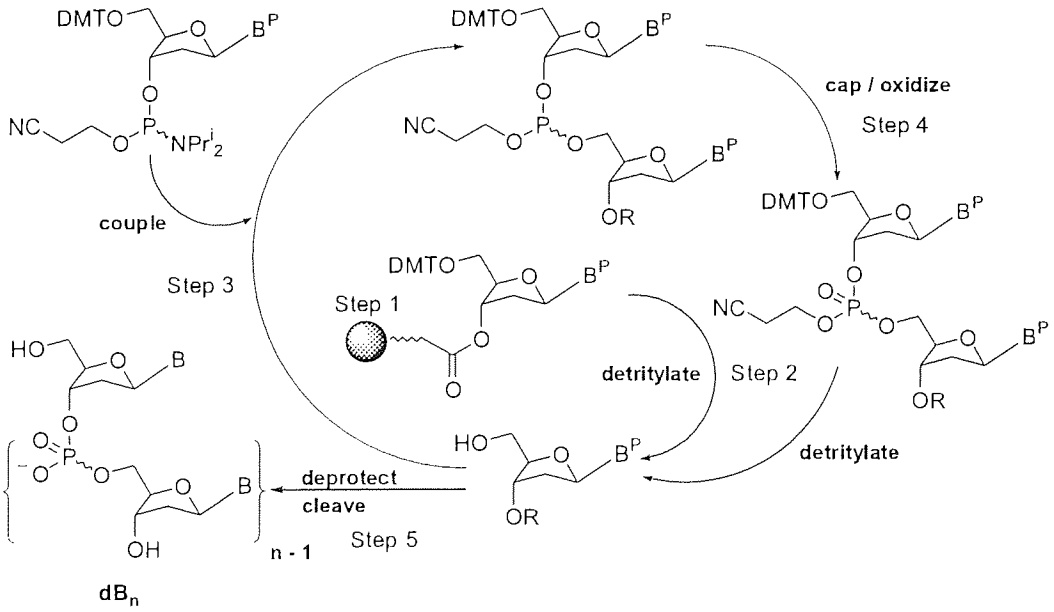

Figure 2.1 – The automated DNA synthesis cycle carried out on a Beckman Oligo 1000 synthesiser.

Figure 2.1 shows the stepwise synthesis reactions that are carried out in order to synthesis the designated oligonucleotides. The five synthesis steps are summarised as follows (McMurry, 2004):

Step 1 - The 3' protected nucleoside is attached to the solid silica support, the base (B) varies according to the initial nucleotide in the desired sequence to be synthesised. There are two positions on the nucleoside that are protected, the 5' hydroxyl group and the free NH_2 attached to the base. The protective group attached to the free NH_2 varies according to the base, in the case of A and C there is a benzoyl group, G is protected by an isobutyryl group and T is unprotected. The 5' hydroxyl group is protected in all cases by a *p*-dimethoxytrityl (DMT) group. The necessity of these groups is to prevent non-specific and uncontrolled reactions, and to ensure bases are attached in the correct order.

Step 2 – The DMT group is removed from the bound nucleoside using 'Deblock' solution (Beckman Coultier). The reagent consists of 3% trichloracetic acid in dichloromethane. This acts to cleave the DMT group revealing the 5'-OH group, liberating a dimethoxytrityl cation that produces an orange colouration, a clear indication to the operator that this process is taking place.

Step 3 – The second nucleoside in the sequence is bound, which has a phosphoramidite group at the 3' position. The 5' hydroxyl group of the support forms a covalent bond with the phosphite group of the free nucleoside in the first stage of the coupling process. This reaction requires the addition of 'Activate' solution (Beckman Coultier), which comprises 0.5 M tetrazole in CH_3CN. The tetrazole reacts with the 3' NPr^i_2 group of the nucleoside producing a reactive triazole intermediate. This is able to react with the 5' hydroxyl of the subsequent nucleotide forming a phosphite ($P(OR)_3$) group and consequently a dinucleotide.

Step 4 – The dinucleotide undergoes oxidation via the addition of iodine using Oxidize solution (Beckman Coultier), which reacts with the phosphite to produce a phosphate. This reagent consists of 3% iodine in tetrahydrofuran (THF) in the presence of 20% pyridine and 2% water.

Capping also takes place at this step, which involves the blocking of any unreacted 5'-OH groups in order to prevent later coupling with subsequent nucleosides, a process

necessary to prevent the synthesis of unwanted sequences. Cap 1 and Cap 2 (Beckman Coultier) are used in combination and consist of 10% Acetic Anhydride in THF and 2,6-lutidine, and 17% N-methylimidozole/THF respectively.
This concludes the first coupling cycle. This cycle (steps 1 to 4) that is repeated until the desired sequence is produced.

Step 5 – The final step involves the cleavage of the ester bond attaching the sequence to the silica support, and the deprotection of the free NH_2 groups attached to the bases. This is achieved using aqueous ammonia (Chapter 8).

2.2 Results

2.2.1 The Synthesised Sequences

Table 2.1 The sequences produced for this research. Sequences with base pair (bp) numbers depict target sequences and their location within the *gyrA* gene. Oligonucleotides 1-33 pertain to *E. coli* sequences and 34-39 to *S. pneumoniae* sequences where Acr and Fl indicate acridine and fluorescein labels respectively. Bold bases = base substitutions, underscored bases = 5mC residues.

Oligo	Sequence	B/Bone
1	1026bp 1052bp	
	3'-TTTTCTTTTTGCGCACCTTCCGTAGTC-5'	PO
2	1026bp 1052bp	
	5'-AAAAGAAAAACGCGTGGAAGGCATCAG-3'	PO
3	5'-AAAAGAAAAACGCGTGGAAGG-3'	PO
4	3'-AAAAGAAAAACGCGTGTAAGG-Acr-5'	PO
5	3'-CGGAGAAAAGTGAAGAAGAAC-Acr-5'	PO
6	3'-AAAAGAAAAACGCGTGGAAGG-5'	PO
7	3'-Fl-AAAAGAAAAACGCGTGGAAGG-5'	PO
8	3'-AAAAGAAAAACGCGTGGAAGG-5'	PS
9	3'-CGGAGAAAAGTGAAGAAGAAC-5'	PO
10	3'-Fl-CGGAGAAAAGTGAAGAAGAAC-5'	PO
11	5'-TTTTGTTTTTGGGGGGGTTGG-3'	PO
12	5'-TTTTGTTTTTGGGGGGGTTGG-Fl-3'	PO
13	3'-TTTTGTTTTTGGGGGGGTTGG-5'	PO
14	3'-Fl-TTTTGTTTTTGGGGGGGTTGG-5'	PO
15	5'-UUUUGUUUUUGGGGGGGUUGG-3'	RNA
16	3'-AAAAGAAAAACGCGTGGAAGG-5'	PN
17	5'-AAAAGAAAAACGCGTGGAAGG-3'	PN
18	5'-TTTTGTTTTTGGGGGGGTTGG-3'	PN
19	3'-TTTTGTTTTTGGGGGGGTTGG-5'	PN
20	5'-TTTTGTTTTTGGGGGGGTTGG-Fl-3'	PN
21	3'-TTTTGTTTTTGGGGGGGTTGG-Fl-5'	PN
22	5'-TTGGTGTGGGTTGGTGTGTTT-3'	PN

Table 2.1 Continued from previous page.

Oligo	Sequence	Back-Bone
23	1020bp 1044bp	
	5'-ACTGGTAAAAGAAAAACGCGTGGA-3'	PO
24	1020bp 1044bp	
	3'-TGACCATTTTCTTTTTGCGCACCT-5'	PO
25	5'-TTTTCTTTTTGCGCACCT-3'	PO
26	5'-TTTTCTTTTTGCGCACCT-3'	PO
27	5'-Acr-TTTTCTTTTTGCGCACCT-3'	PO
28	1021bp 1051bp	
	3'-GACCATTTTCTTTTTGCGCACCTTCCGTAGT-5'	PO
29	1021bp 1051bp	
	5'-CTGGTAAAAGAAAAACGCGTGGAAGGCATCA-3'	PO
30	5'-TTTTGTTTTTTGTGGGGTTGG-3'	PO
31	5'-Acr-TTTTGTTTTTTGTGGGGTTGG-3'	PO
32	3'-TTTTGTTTTTTGTGGGGTTGG-5'	PO
33	3'-TTTTGTTTTTTGTGGGGTTGG-Acr-5'	PO
34	1231bp 1248bp	
	5'-AAGGAAAAAGCGGAAGCG-3'	PO
35	1231bp 1248bp	
	3'-TTCCTTTTTCGCCTTCGC-5'	PO
36	3'-AAGGAAAAAGTGGAAGTG-5'	PO
37	2553bp 2572bp	PO
	5'-AGAAAAAGAAGAAGTTGGGA-3'	
38	2553bp 2572bp	PO
	3'-TCTTTTTCTTCTTCAACCCT-5'	
39	3'-AGAAAAAGAAGAAGCCGGGA-5'	PO

2.2.2 High Performance Liquid Chromatography (HPLC) and Capillary Electrophoresis (CE) Traces

6 HPLC and CE Traces

a) (i)

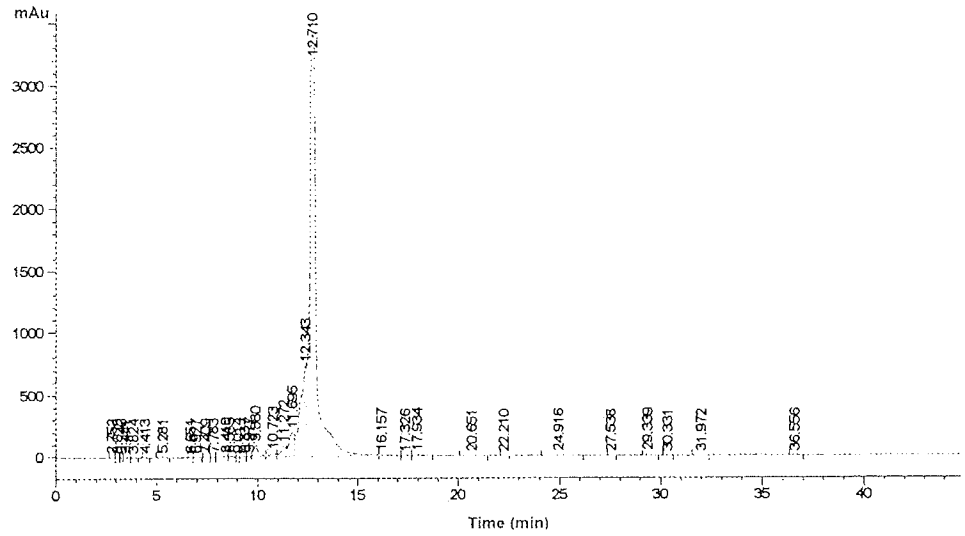

(ii)

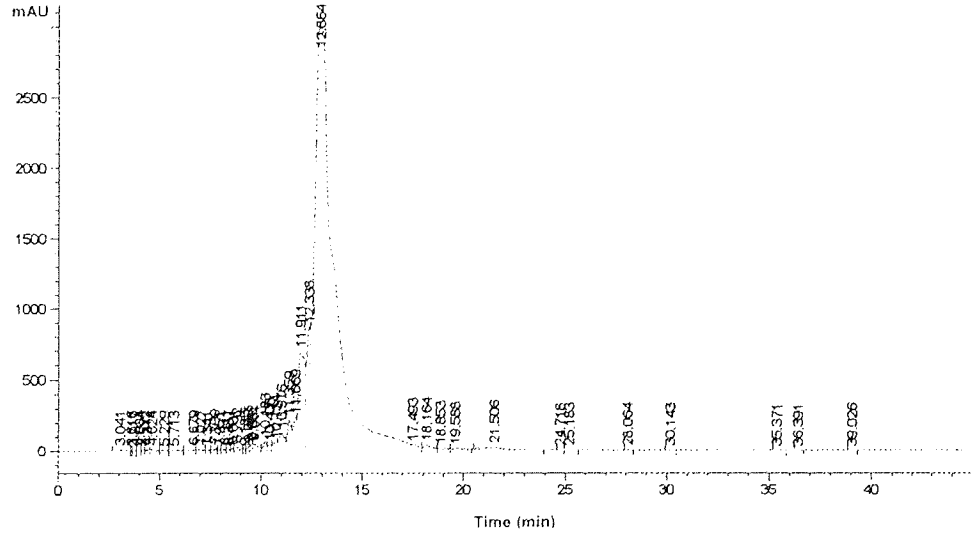

Figure 2.2 Continued over the page.

(iii)

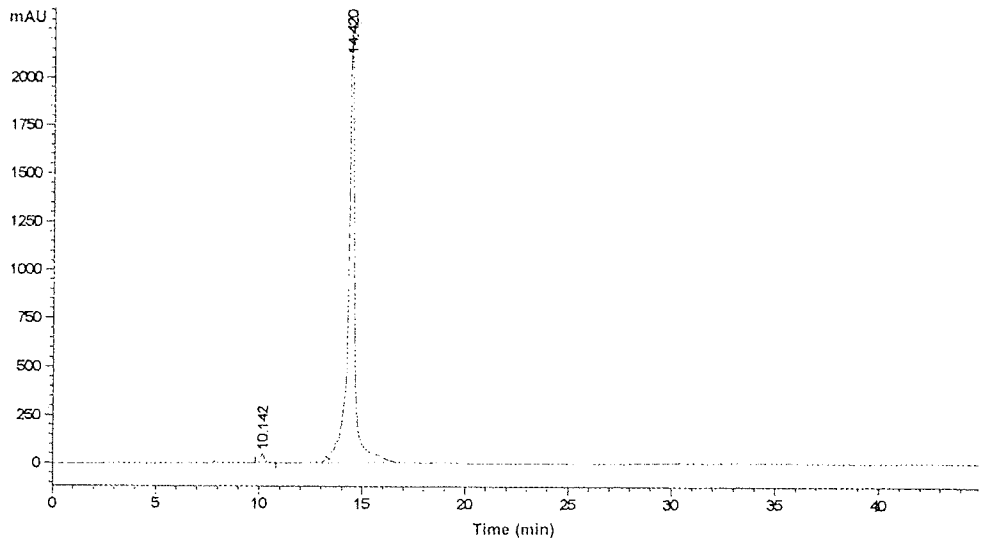

b)

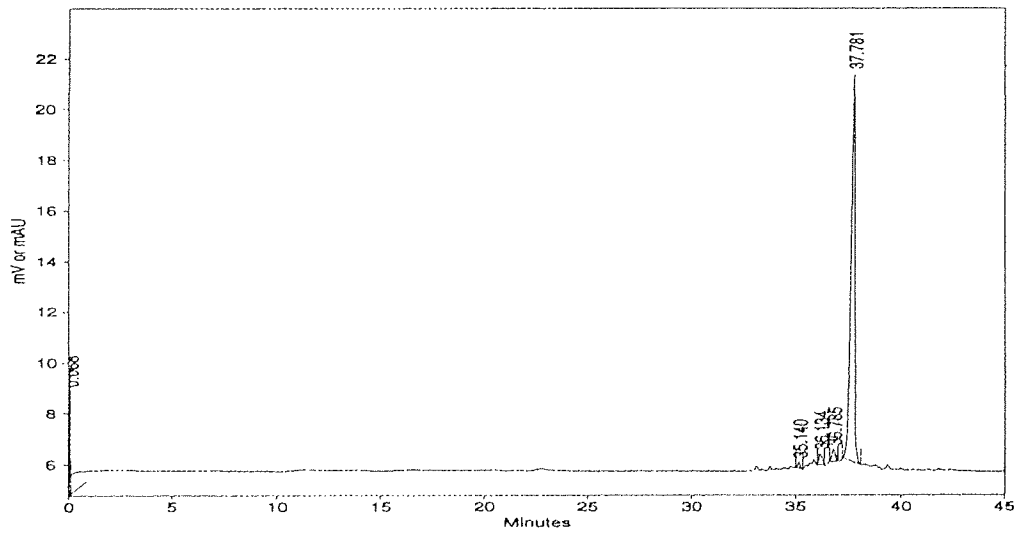

Figure 2.2 Characterisation of the oligonucleotide **6** where a) (i) represents an analytical run of the crude oligonucleotide sample, (ii) represents a purification run of the crude oligonucleotide sample, (iii) represents an analytical run of the purified oligonucleotide sample and b) a CE trace of purified **6**.

Figure 2.2 illustrates; the purification process of **6** from the crude oligonucleotide produced straight from deprotection after automated synthesis (Figure 2.2 a) (i)); HPLC purification (Figure 2.2 a) (ii)) where the major peak, with a retention time of 12.664 minutes, was collected to give the purified oligonucleotide, (Figure 2.2 a) (iii)) post-desalting and filtration. In the latter the purity of the samples is illustrated by the presence of an abundant single peak. Figure 2.2 b) shows the results obtained when the purified oligonucleotide was exposed to CE. Here again the purity of the sample is demonstrated by a major single peak. All sequences were similarly prepared and analysed for purity.

11 HPLC and CE Traces

a) (i)

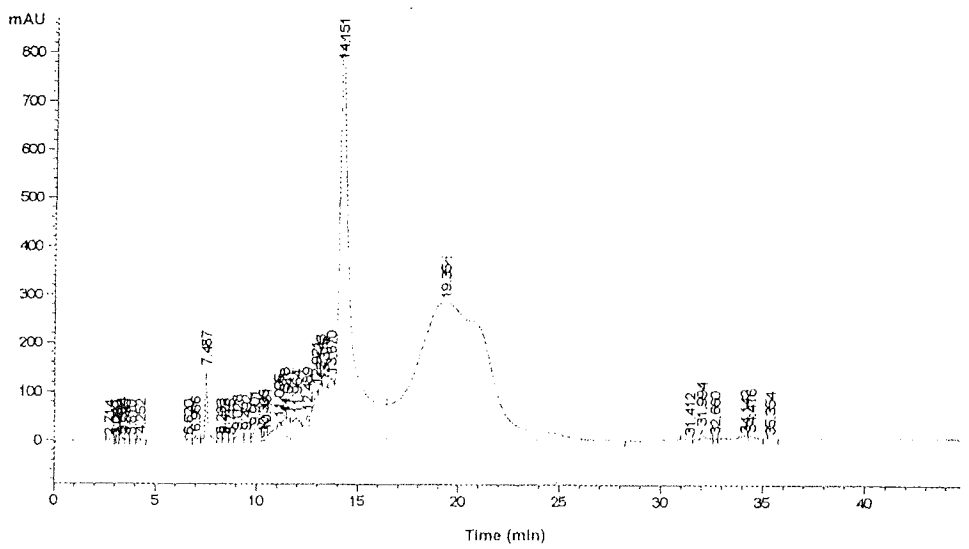

Figure 2.3 Continued over the page.

(ii)

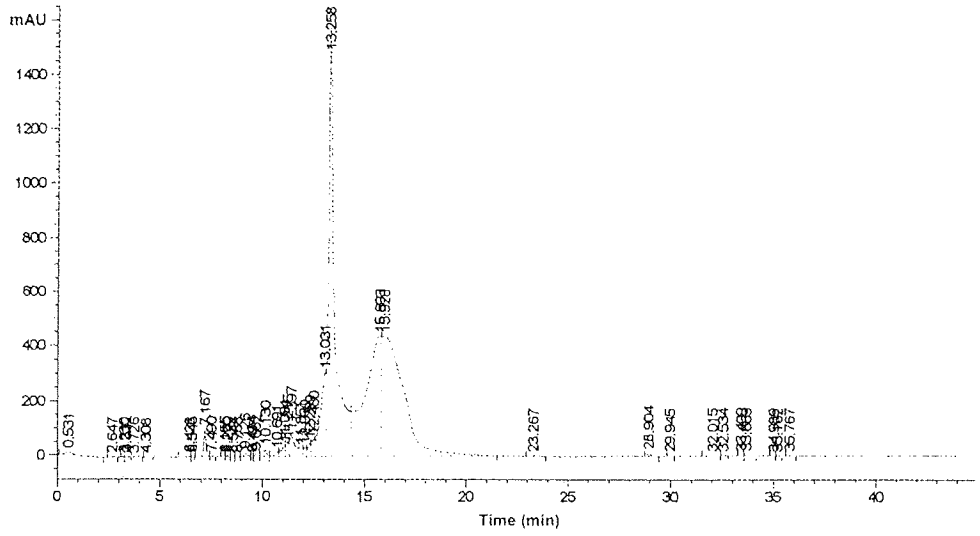

(iii)

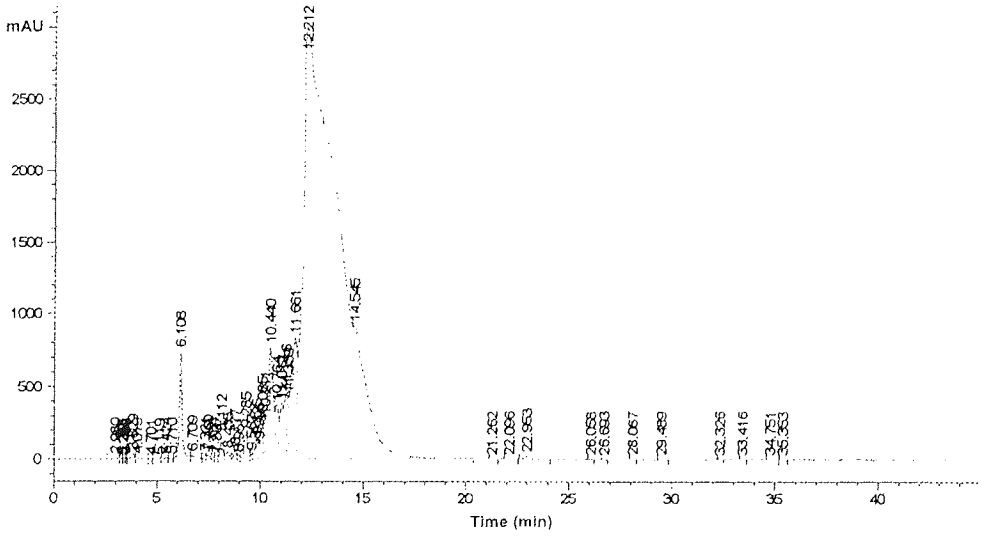

Figure 2.3 Continued over the page.

(iv)

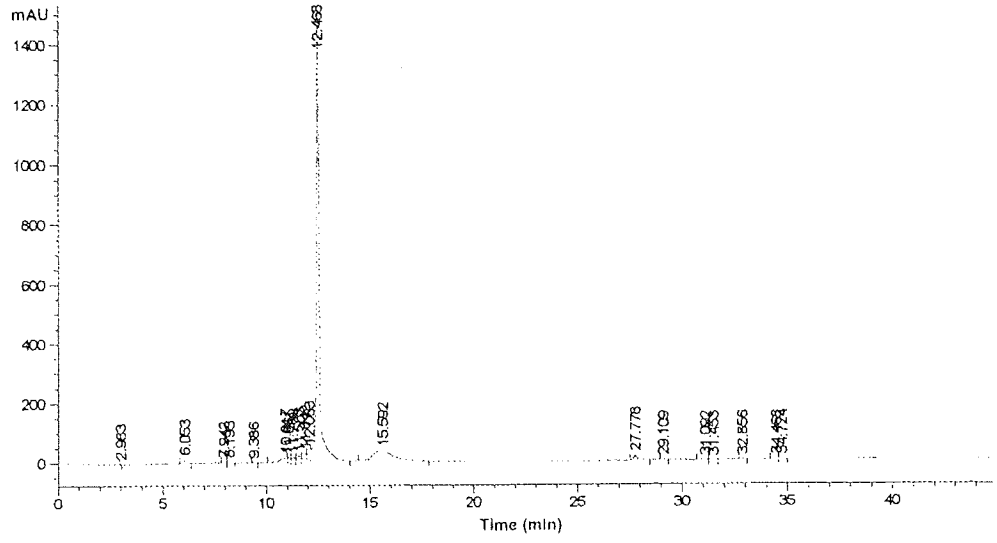

b)

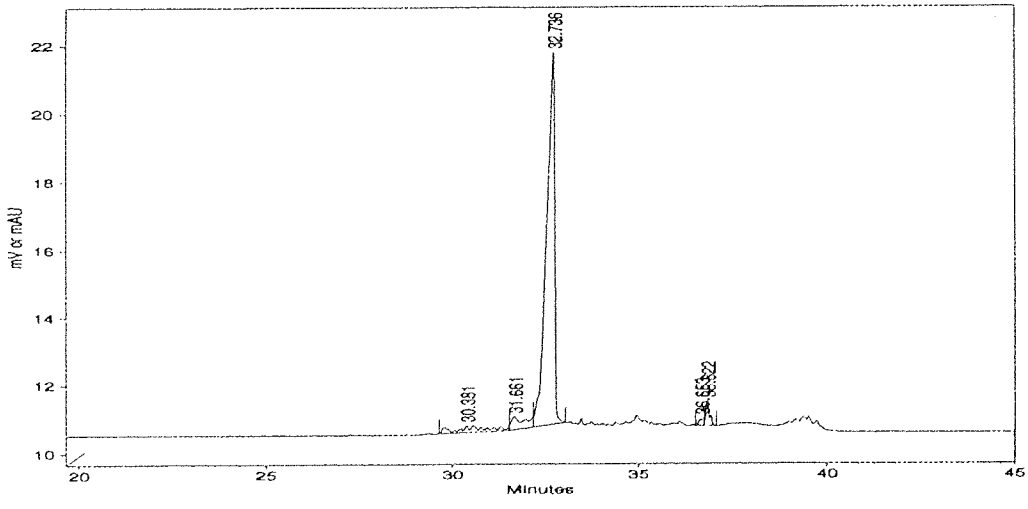

Figure 2.3 Characterisation of the oligonucleotide **11** where a) (i) represents an analytical run of the crude oligonucleotide sample, (ii) represents a purification run of the crude oligonucleotide sample at ambient temperature, (iii) represents a purification run of the crude oligonucleotide at 50 °C, (iv) represents an analytical run of the purified oligonucleotide sample at 50 °C and b) a CE trace of purified **11**.

Figure 2.3 illustrates the HPLC and CE traces produced during the purification and characterisation process of **11**. Although PO in nature, this sequence produced atypical HPLC traces with an abundant peaks produced at around 14 minutes and 13 minutes in a) (i) and (ii) respectively. However, the results also illustrate another smaller but broader peak around 19 minutes in (i), and 15 minutes in (ii). It was postulated that these had emanated from hyperstructure formation, and as a result, during the purification run the column temperature was increased to 50 °C in order to disseminate these structures. This was proved successful as indicated in (iii), where purification carried out at this temperature yielded a very large abundant peak and the absence of a broad second peak. This is mirrored in (iv), where the analytical run of the purified sequence at 50 °C indicates a sample containing a single abundant species of sequence. Figure 2.3 b) highlights the purity of this sequence after CE application and again depicts a single abundant peak.

8 HPLC and CE Traces

a i)

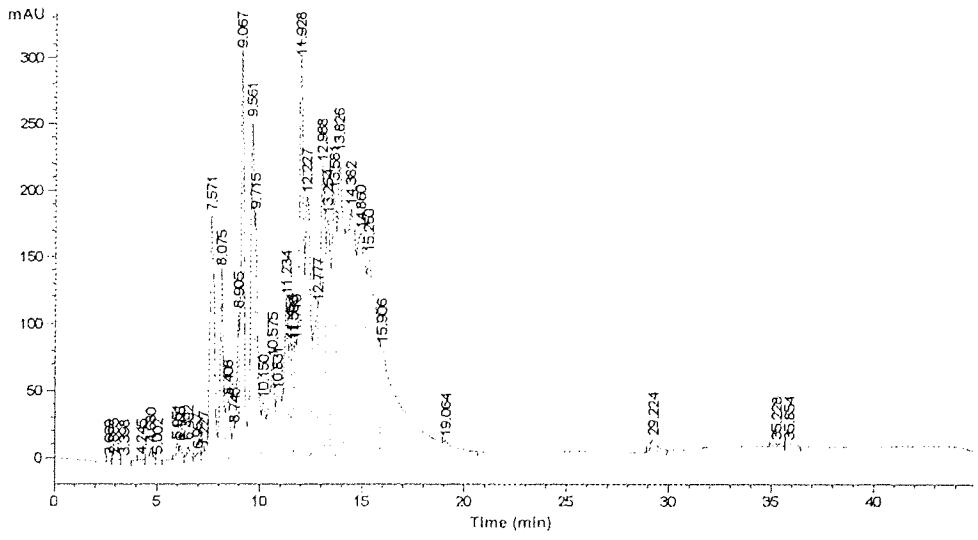

Figure 2.4 Continued over the page.

ii)

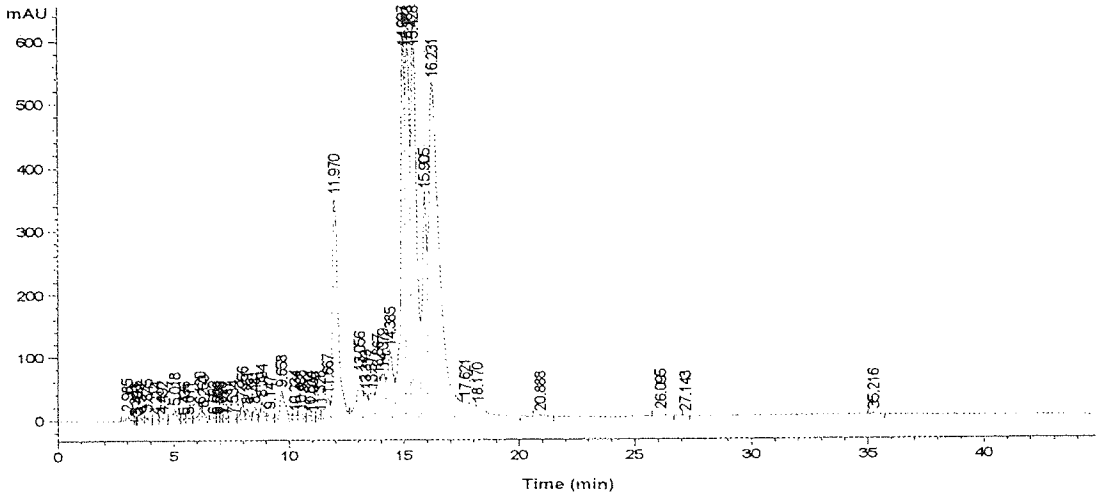

iii)

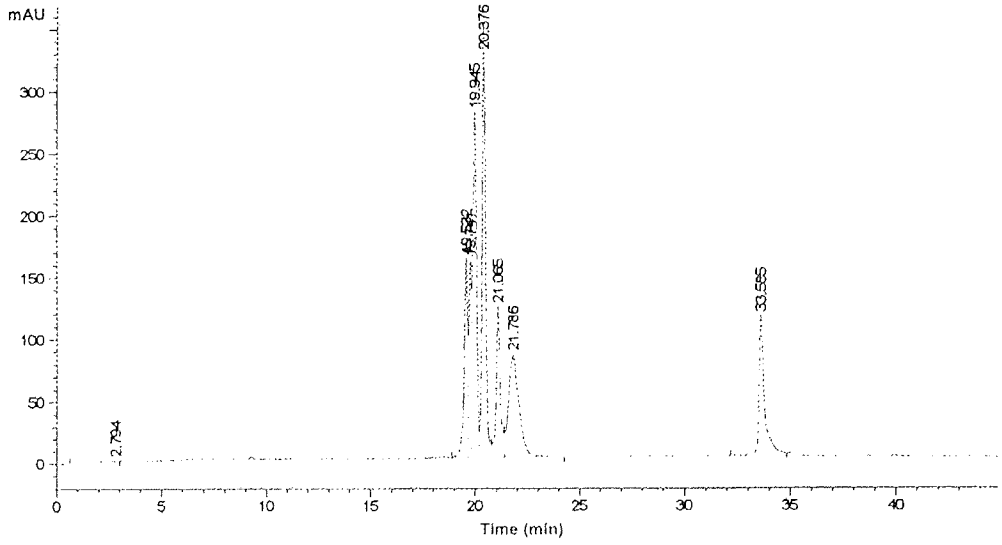

Figure 2.4 Continued over the page.

b)

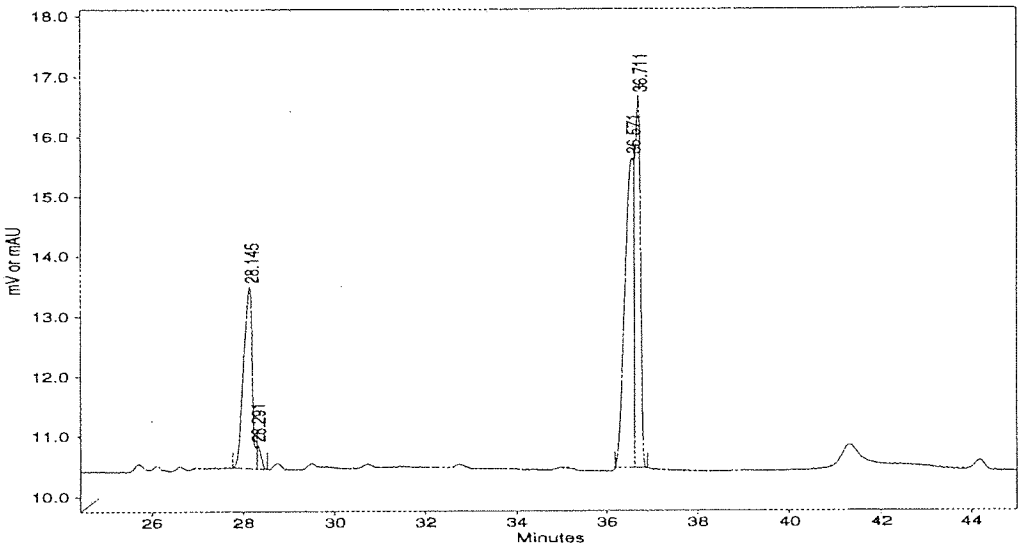

Figure 2.4 Characterisation of the oligonucleotide **8** where a) (i) represents an analytical run of the crude oligonucleotide sample, (ii) represents a purification run of the crude oligonucleotide sample, (iii) represents an analytical run of the purified oligonucleotide sample and b) a CE trace of purified **8**.

Figure 2.4 illustrates the purification and characterisation of the phosphorothioate sequence **8**. The HPLC and CE traces indicate an impure sample due to the production of multiple peaks indicating a range of sequences of varying sequence length produced from a degree of failed synthesis. After HPLC purification, the number of these peaks is slightly diminished but they are still apparent, which is further illustrated in the CE trace. Hyperstructure formation was ruled out due to increased column temperatures producing no trace variation (data not shown).

16 HPLC and CE Traces

a i)

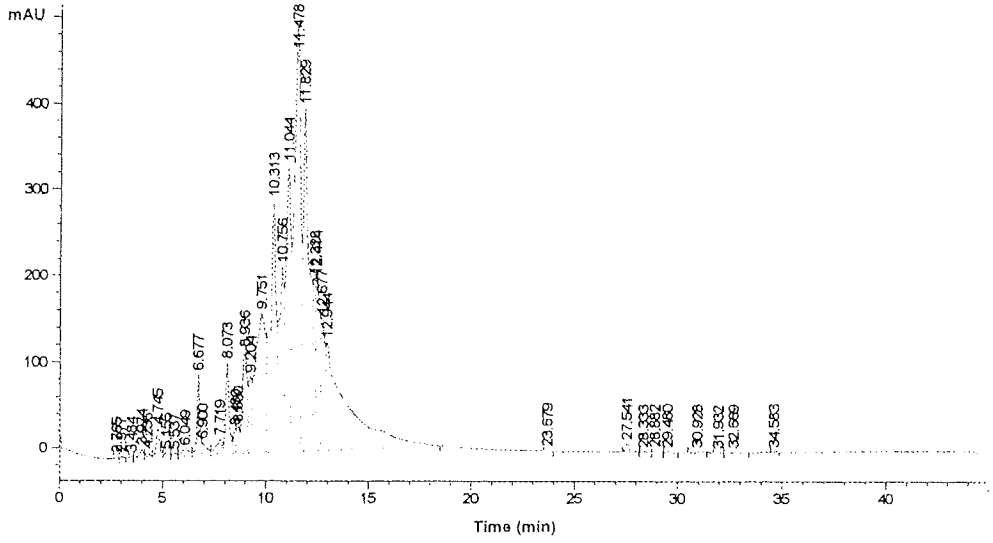

ii)

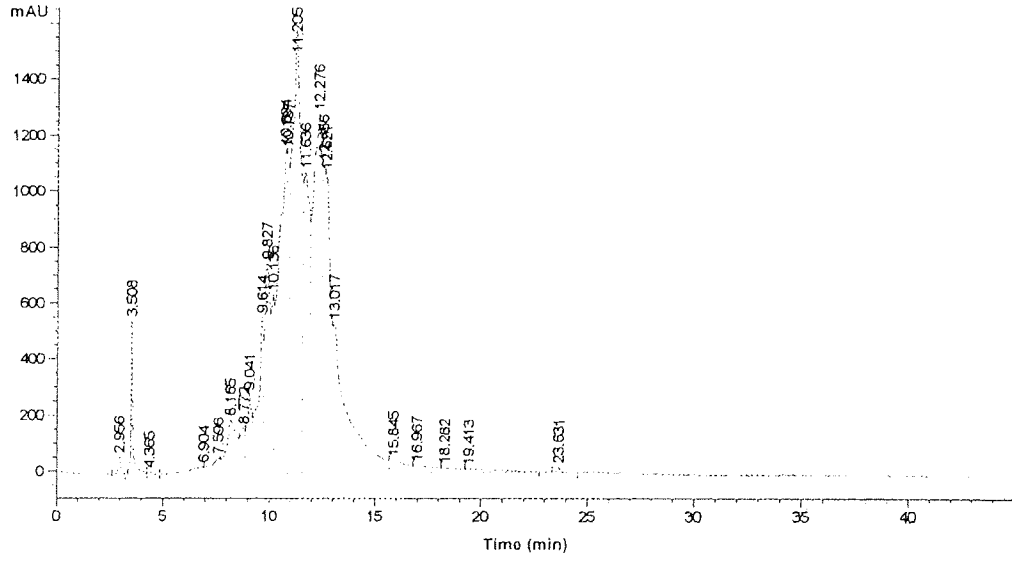

Figure 2.5 Continued over the page.

iii)

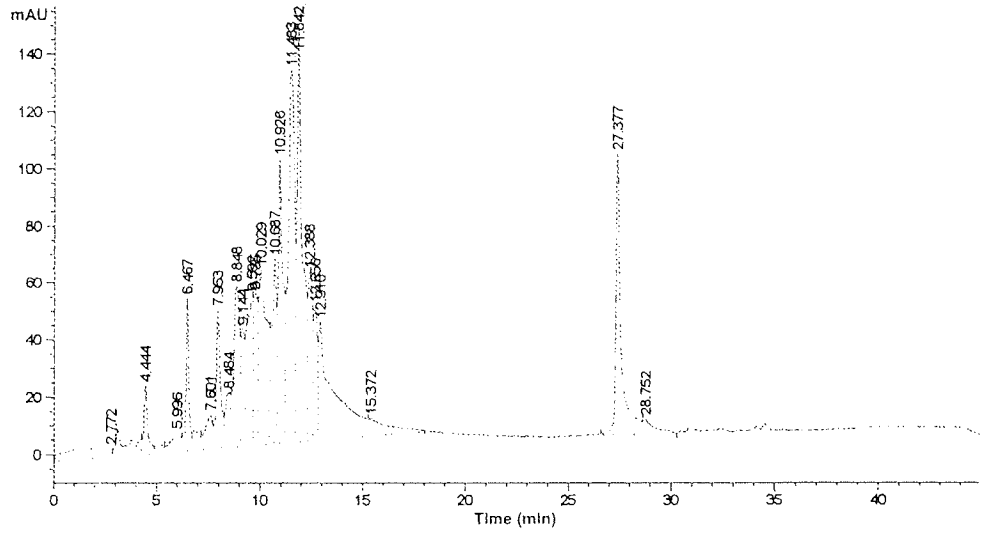

b)

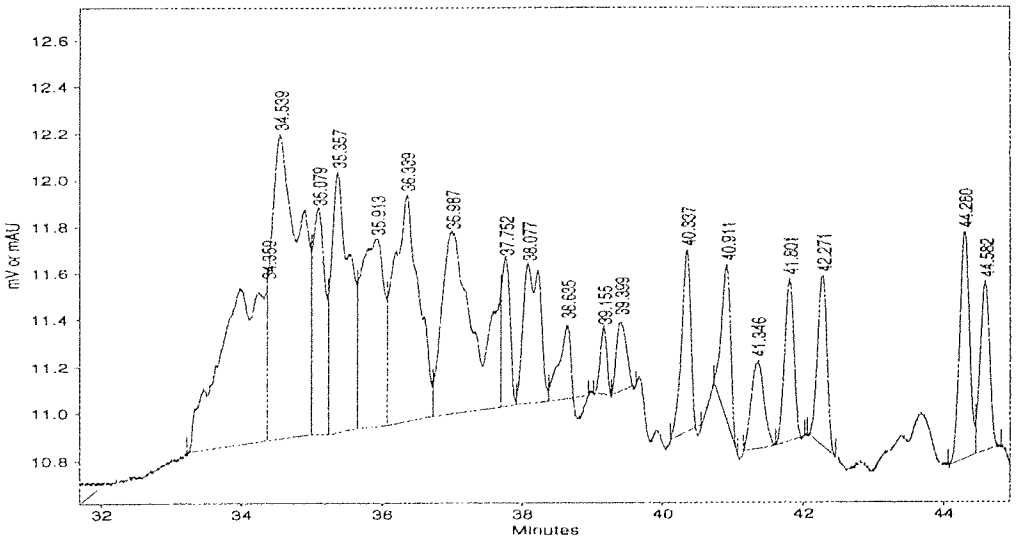

Figure 2.5 Characterisation of the oligonucleotide **16** where a) (i) represents an analytical run of the crude oligonucleotide sample, (ii) represents a purification run of the crude oligonucleotide sample, (iii) represents an analytical run of the purified oligonucleotide sample and b) a CE trace of purified **16**. All HPLC runs were performed at 50 °C.

Figure 2.5 illustrates representative HPLC and CE traces of the phosphoramidate sequences, where the results of the purification and characterisation process for **16** are shown. Similar to the phosphorthioate sequences, multiple peaks are represented, indicating sequences of varying chain length produced from an inefficient synthesis process.

2.2.3 Mass Spectrometry Analysis of Oligonucleotides Synthesised

Table 2.2 Data compiled from MS analysis of all synthesised sequences where, ND = Non-detectable, IS = Insufficient sample.

Sequences	Calculated Mass	Found Mass
1	8149.2652	8148.12
2	8408.5313	ND
3	6570.3466	IS
4	7151.1613	IS
5	7151.1613	IS
6	6570.3466	6570.64
7	7165.2964	7167.66
8	6891.6866	ND
9	6570.3466	IS
10	7165.2964	7168.37
11	6576.2446	6577.35
12	7174.8109	ND
13	6576.2466	ND
14	7174.8109	ND
15	6576.2446	ND
16	6550.6522	ND
17	6550.6522	ND
18	6556.6582	ND
19	6556.6582	ND
20	7093.2604	ND
21	7093.2604	ND
22	6556.6582	ND
23	7467.9000	7465.79
24	7235.8000	7235.75
25	5397.5113	5397.66
26	5467.6453	5467.28
27	6048.4600	5677.97
28	9992.6397	IS
29	10233.8756	IS
30	7124.7827	IS
31	7705.5974	IS
32	7124.7827	IS

Table 2.2 Continued from over the page.

Sequences	Calculated Mass	Found Mass
33	7705.5974	IS
34	5638.8600	5638.70
35	5357.4400	5357.13
36	5668.8700	5668.64
37	6296.1747	IS
38	5934.8638	5935.20
39	6266.1529	6265.83

Table 2.2 illustrates the result obtained from mass spectrometry analysis of all the sequences synthesised in this research project. MS analysis was carried out as a method for characterisation to determine whether the calculated molecular masses matched the actual masses. Where molecular ions were produced, theoretical and actual masses tended to correlate and were in agreement to at least 0.1%.

2.3 Discussion

2.3.1 Sequence Design

The homopurine-homopyrimidine target sites for potential triplexation were identified using criteria set out in Chapter 1. As stated oligopurine tracts were identified within the *gyrA* gene of *E. coli* and *S. pneumoniae* as potential targets simply by manual screening of the *gyrA* genes. This is a fundamental gene to ensure viability of the organism, and with the prevalence of mutations within the coding region leading to resistance to antibiotics, particularly fluoroquinolones, this would appear to be an ideal target for potential antibacterial TFOs.

Various potential targets were found in *E. coli* to be suitable in that they contained runs of contiguous purines with no more than 3 mismatched base pairs. These were found throughout the *gyrA* gene and were common to a number of strains of *E. coli* including both quinolone-resistant and non-resistant strains.

A number of target sites was identified and synthesised (Table 2.1), each between base pairs 1020-1052 (Table 2.1). The target sequences were extended compared with the TFOs in order to accomodate the binding of acridine for triplex melting studies (Chapter 3).

TFOs designed to target sites within in *E. coli*, were designed as a comparative model. Four sets of sequences were designed; those of a polypurine nature designed to bind in an antiparallel manner via reverse Hoogsteen bonds (**4**, **6**, **7**, **9**, **10**), those designed of a polypyrimidine nature to bind in a parallel conformation via Hoogsteen bonds (**25-27**,), and finally two sets of (T,G)-containing oligonucleotides of differing orientations (**11-14**, and **30-32**,). This latter set (**11-14** and **30-32**), have potential to bind in either a parallel or antiparallel motif (Chapter 1). Their purpose was to assess which orientation, parallel or antiparallel, is more favourable, and ultimately to determine whether or not these purine-pyrimidine mixed sequences have a stronger binding affinity to the duplex target than their polypurine or polypyrimidine counterparts.

The base substitution of 5mC for C in **26** and **27**, was made in accordance with strong literature precedents for enhanced, pH-independent triplex stability. The 5mC group increases the pK_a of the base when in the 5mC*G-C triad formation, and hence the pH range over which the base is stable. Although numerous other modifications are

possible 5mC is very well studied and understood with the necessary phosphoramidite being commercially available (Chapter 1).

Acridine-tagged oligonucleotides (**4**, **27**, **31**, **33**) were produced in order to assess intercalation as means of triplex stabilisation. Again numerous agents are available but acridine has strong literature precedents for its ability to greatly enhance triplex stability (Chapter 1). Commercial availability of the phosphoramidite form made it the intercalator of choice here.

Fluorescein labelled oligonucleotides (**7**, **10**, **12**, **14**, **20**, **21**), were produced for fluorescence studies to assess the triplex binding ability of TFOs with extracted genomic DNA (Chapter 4).

Backbone modifications were made again in accordance with the literature. The phosphorothioate, **8**, was produced in order to evade nuclease degradation (Chapter 1).

The 2'-*O*-methyl modification (**15**) was produced in order to improve triplex stability again based on literature precedents whilst having a suitable modification to help avoid nuclease degradation (Chapter 1).

Phosphoramidate oligonucleotides (**16-19**, **22**) were again produced for their nuclease resistance but more over for their ability to enhance triplex stability. Many studies have shown their ability to raise T_m values greatly (Chapter 1).

After studying the *gyrA* gene sequence of *S. pneumoniae*, strain R6 (a ciprofloxacin sensitive, wild type strain), two polypurine tracts were identified as potential targets for triplex formation. Analysis of the same gene in a number of other strains revealed the presence of the same polypurine targets. These targets were completely conserved in all but one of the strains. This strain contained a 3' end A residue as opposed to a G in the purine rich target strand (sequence **34**, Table 2.1). The potential problem regarding triplex stability was assumed to be relatively minor, the reasons being two fold; a) the target strand as it stands contains only two mismatches, with the addition of the A substitution totalling three. Three mismatches is within the tolerable limit for successful triplexation; b) this base mismatch falls at the very terminal base of the target. This position for such a mismatch is well documented as being less destabilising than one positioned more centrally (Soyfer and Potaman, 1996).

The first target site was identified between base pairs 1231 to 1248. This site was a strong site for triplex formation due to the polypurine site containing only two C-G inversion sites and being 18 base pairs in length.

The second site was found up-stream of the first site between base pairs 2553 to 2572, and slightly longer at 20 base pairs. This site again contained only 2 mismatches; two A-T inversions.

In Table 2.1 substituted bases are indicated by bold lettering, highlight the placing of mismatch sites within the *S. pneumoniae* TFOs (**36**, **39**). In the case of **36** and **39** the mismatches have been replaced with natural bases that the literature states to be the most stable substitution for that triad. In these cases, C has been replaced with T, and T has been replaced with C. It is stated that T is the most stable base to oppose a C-G inversion site within the target purine strand, and is so whether the TFO is to bind in a parallel or antiparallel manner. In the case of the A-T inversion there actually is no natural base that will specifically recognise this site. However, C is the least triplex destabilising (Gowers and Fox, 1999).

Once the target sites were chosen in both organisms, and the TFOs designed, each TFO was screened for its targets within other organisms using Genbank databases, this included other bacteria and microorganisms, as well as the human genome. The former was to ascertain whether the target site was conserved in other microorganisms to assess the potential of the designed TFOs as broad spectrum agents. The latter is important for potential later use of the TFO as therapeutic agents. The TFO will need to bind specifically within the genome of the target organism as binding within the host DNA could lead to undesirable side effects of drugs using this technology. While the database searches revealed little in the way of consevation within in other microorganisms, human genome searches illustrated no exact sequence matches (data not shown).

2.3.1 DNA Synthesis

All sequences were produced using a standard Beckman Oligo1000 synthesiser and standard method, except for the phosphorthioate and phosphoramidate sequences. In the former the synthesis methodology remained unaltered, but the 'Oxidise' reagent was replaced with the sulphurising reagent. The introduction of this at Step 4 of the

synthesis cycle results in the substitution of one non-bridging O for S in the phosphate group of the oligonucleotide backbone (Chapter 1).

During phosphoramidate synthesis, the process is notoriously less efficient owing to a switched direction of synthesis (5'-3' as opposed to 3'-5'). There is also the added complication that unlike standard amidites, the phosphoramidate amidites are reported to have half-lives of typically 5 days once in solution, with G having a half-life of 1 to 2 days. As a result, several methods have been developed of which a phosphoramidite amine-exchange reaction seems to be the best (McCurdy, *et al.*, 1997; Fearon, *et al.*, 1998). The changes in methodology are discussed here in relation to the synthesis cycle shown (Figure 2.1), and to the methodology outlined in Chapter 8.

In relation to step 1, universal support columns were used for the phosphoramidate synthesis (Figure 8.2). Detritylation of the support, to reveal the free OH group to enable coupling of the first nucleoside monomer, occurred under normal reagent conditions. The flushing of the system with 'Deblock' solution, in order to remove the protective groups to enable coupling to commence in step 2, was unaltered. For the purposes of the phosphoramidate synthesis the 'Deblock' solution consisted of a 3% dichloracetic acid in dichloromethane, instead of trichloroacetic acid (as in phosphodiester synthesis). The reason for this is due to the phosphoramidate amidites being N-protected by a monomethyoxytrityl (MMT) group instead of a DMT group. This N-MMT group is more acid labile than a DMT-protected oxygen atom due to the weaker bonding between the N and the MMT group, hence a weaker acidic solution was used.

Instead of protecting the 5'-OH, the MMT protects the 3'-NH group. Its removal allows the coupling of the subsequent nucleoside. It is for this reason that synthesis has to take place in the 5'-3' direction. The detritylation reaction consequently yields a trityl cation that produces a yellow colouration again indicating the removal of the protective group.

For the purpose of this synthesis the addition of the 3% dichloracetic acid enabled the removal of the DMT group attached to the universal support providing a free OH group for the addition of the first base. Steps 3 and 4 proceeded as set out in Figure 2.1 with the attachment of the nucleosides, and, oxidation and capping of the sequence. Capping was performed using 1:1:8 ratio of isobutyric anhydride - 2,6-lutidine – THF prepared under argon. This time capping was necessary to block any unreacted 3'-NH groups again to prevent synthesis of unspecified sequences.

In step 5, deprotection took place as before using concentrated ammonia.

Initial synthesis protocols utilised a prolonged coupling phase where the standard coupling step was increased from 1 to 10 min. Analysis of sequences produced revealed samples with a very low yield of a mixture of compounds that were non-characterisable; HPLC traces showed numerous peaks at a very low abundance which could not be separated for purification purposes, (data not shown). After further investigation a second method of synthesis was produced after successful synthesis of two, T8-phosphoramidate sequences.

Utilising the prolonged coupling synthesis method, the orange colouration produced by the removal of the DMT group from the universal support was apparent even in the second and third coupling cycles. This indicated that the support had not been fully deprotected by a single flush of Deblock solution. Also apparent during this cycle was the lack of yellow colouration produced as a result of MMT removal. It was proposed that the cause of this was due to insufficient deprotection of the support in step 2. Consequently, in the second and third coupling cycles, sites within the support were still being deprotected, and hence the orange colouration witnessed. Due to the lack of this deprotection, coupling yield for the first base was immediately diminished. The addition of normal coupling inefficiencies at each stage of the synthesis cycle gives some idea to the low yield of the initial round of synthesis.

The two synthesis cycles used to produce the T8-phosphoramidates were the standard Beckman oligonucleotide synthesis method and the phosphoramidate synthesis protocol set out above. However, in both cases the initial detritylation step was repeated until the DMT groups had been completely removed, i.e. until the orange colouration was no longer apparent. The two methods were compared to ascertain whether or not one produced a greater yield. This was determined after synthesis, post-deprotection by HPLC analysis of crude samples (Chapter 8). Yields were equal and as a result the prolonged coupling method was discarded due to time restrictions and replaced with the standard Beckman protocol.

2.3.2 HPLC and CE Results

Impurities evidenced by HPLC and CE analysis usually take the form of n-1, n-2 and other failed sequences, where n implies the desired nucleotide length. Impurities of

this sort result from synthesis cycles that are less than 100% efficient. However, impurities can also arise from reaction by-products and excess reagents.

At each step of the coupling cycle any inefficiency is accumulative. This is not such a problem for short sequences (8-10mers) synthesised on a small scale (30 nmole). For longer sequences (20-30mers) synthesised on a larger scale such as 1μmole, as is the case with the synthesis here, the efficiency of coupling overall is strongly diminished. Hence the purity and abundance of the required oligonucleotide is lower.

2.3.2.1 Phosphodiester Synthesis

The phosphodiester sequences produced for the purpose of the research generally show a good level of purity in that they are represented by single peaks by both HPLC and CE analysis. Representative traces of **6** can be seen in Figure 2.2. However, Figure 2.3 illustrates atypical traces represented by the HPLC analysis of **11**. In Figure 2.3 a) (i) and (ii) a large abundant peak is depicted followed by a smaller broader peak. Sequence **11** had a high G content so it was postulated that this secondary peak resulted from hyperstructure formation caused by G-quartet and quadruplex formation. As a result, the HPLC column temperature was increased to 50 °C to discourage these interactions and to produce a single sample peak for collection. Figure 2.3 a) (iii) and (iv) indicate the success of the raised column temperature where a large single peak is depicted.

The efficiency for this phosphodiester synthesis chemistry is greater than 99% per synthesis cycle resulting in an overall product purity of 80-85% for an oligonucleotide of 25 bases (Gilar and Bouvier, 2000). The remaining impurities will result from failed sequences that have arisen from incomplete reactions that have occurred throughout the synthesis cycle. These impurities were not present in the final product as they would have been discarded during the purification runs of the HPLC process. As a result the samples indicated above used for the purpose of this study were of high purity.

CE is a more powerful analytical tool than HPLC as it has a higher separating power and can as a result differentiate between oligonucleotide samples that have only one base difference in length. The results for the phosphodiester sequences, represented here are indicative of samples containing an abundance of a single oligonucleotide.

2.3.2.2 Phosphorthioate Synthesis

Phosphorothioate synthesis was clearly less efficient than phosphodiester synthesis (Figure 2.4). The synthesis of **8** showed multiple peaks on both HPLC and CE analysis.

CE analysis showed four separate peaks, one at ~28 min approx 2.5 mAU with a shoulder at ~28.5 min. The third peak was represented by a large single peak at ~36.7 min and 6.5 mAU units in height, with the final peak forming a shoulder to this peak at ~36.5 min with a height of 5.5 mAU. MS analysis failed to detect a molecular ion making it difficult to determine whether any one of the peaks was produced by the desired sequence. However, for the purpose of the biological evaluation, it was assumed that if the sequence was present, it would have a stronger binding affinity to the target than any of the other sequences (n-1, n-2 and so on), that compromise the sample solution.

Phosphorothioate synthesis was less efficient than phosphoramidite synthesis with the sulfurising reagent having an efficiency of 96%. That is, at every coupling step 96% of the linkages will be phosphorothioate with the rest remaining as phosphite groups. These will form sample impurities, after capping, in the form of n-1, n-2 and so on sequences. A 96% efficiency rate implies an overall yield of;

$$100\ (0.96^{n})$$ where n = the number of couplings.

Therefore in the case of **8**, where there are 20 couplings, the overall theoretical yield of the designed TFO will be 44% assuming every other chemical process is 100% efficient. This implies a greater abundance of other oligonucleotides.

2.3.2.3 Phosphoramidate Synthesis

The HPLC and CE traces for the phosphoramidate sequences synthesised show numerous peaks; typical representative traces depicting **16** can be seen in Figure 2.5. The multiplicity of peaks produced by these agents would imply them to be highly impure containing phosphoramidate oligonucleotides of a range of lengths.

The HPLC traces show a broad span of peaks between ~5 to ~15 min retention time, and then a single peak with a longer retention time of ~25-30 min (this is only apparent in the analytical run of purified **16** in the results presented), which varied slightly from one sequence to the next. The latter is quite unusual in that during the

purification process, such a peak was observed but was discarded as an impurity (data not shown here), due to its low abundance. As a result, it is unexpected that it would be present here. Taking this into consideration would imply that these peaks are not produced be an oligonucleotide of different length and hence a longer retention time, but rather that it is produced by some form of hyperstructure created by the oligonucleotide self-associating. This form of self-association is particularly common where there are high numbers of contiguous G residues. Guanine bases are able to form G quartets and other structures, which will have different retention times to the single stranded oligonucleotides. These structures are very likely with the phosphoramidate sequences as they contain a high percentage of G residues. As a result, purification and analytical HPLC runs were performed at 50 °C to minimise hyperstructure formation, but this was not fully successful. Phosphoramidates are also notorious for being 'sticky', that is they have a greater tendency to self-associate than other oligonucleotides. Alternative methods such as ion exchange or denaturing conditions (pH 12) were considered but neither was readily available nor accessible.

The HPLC behaviour was mirrored by CE analysis, which showed a multitude of peaks after 34 min migration time. The CE used here separates oligonucleotides according to their size. The capillary column is filled with polyacrylamide and bisacrylamide, which cross link to form a sieve. As charged particles pass through the capillary they are sieved out in accordance with their size, i.e. the smaller the particle the easier it can pass through, hence the smaller the migration time, and vice versa. In the case of the phosphoramidates hyperstructures would have meant longer migration times due to an increase in overall particle size, particularly in the case of multi-strand association.

Phosphoramidate synthesis is well known for being less efficient using the same processes that are successful in phosphodiester synthesis. McCurdy *et al* (McCurdy, *et al.*, 1997) have shown yields of pure phosphoramidates ranging from 37.8% to 62% produced via the amine-exchange reaction. These yields varied according to the length and composition of the phosphoramidate sequence, the greater yield depicted by the shortest oligonucleotide (11mer) and the lowest yield by the longest (15mer). In this study carried out by McCurdy, it was also predicted that the cycle efficiency, using the amine-exchange reaction, was between 92-95%. As a result yields of the phosphoramidates synthesised here would be expected to be between 17-34%

(calculated using the formula stated above for phosphorthioate coupling, where n = 21 due to the use of a universal column (Figure 8.2)).

There are two main areas that impurities can be manifest as a result of the synthesis cycle directly, producing short incomplete sequences. The first can occur during the detritylation step, prior to coupling, and happens when reactive sites remain unreacted. This can occur anywhere in the cycle and as a result is a cause of n-1, n-2, n-3.....n-(n-1) sequences. These sequences are capped but will still remain in the end product before purification. Sequences made up of small numbers of bases will be discarded during HPLC purification due to small retention times and low abundance. However, those sequences n-1 and n-2 in length if in high enough abundance are hard to decipher by the operator, that is assuming the HPLC has the resolution to separate these sequences.

The second area of failure can occur following on from that illustrated above. If the sequence fails to 'deblock' properly and is not 'capped' efficiently then these sequences continue into the next coupling step as a reactive entity. However, the oligonucleotide will be missing a base. These are quite common areas of sequence failure (Gilar and Bouvier, 2000) and explain the poor synthesis of the phosphoramidate sequences here.

Potential means to improve the efficiency have been explored by other research groups. One example includes the use of a double couple/oxidise procedure where steps 3 and 4 are repeated. The basis behind the improved efficiency is based on the equilibrium theory for an amine-exchange reaction (McCurdy, *et al.*, 1997). This states the double couple/oxidise process to be more efficient than a single coupling and oxidation step. The reason for this is perhaps due to the fact that the initial coupling step followed by the oxidising step leaves unreacted NH groups which are able to bind subsequent nucleotides during the second coupling step. The addition of the bases during the first step produces an equilibrium concentration of binding, which leaves free binding sites. The oxidation then fixes those nucleotides that are bound. The following coupling step allows further equilibration to take place, but again not entirely saturating the free sites. However, binding efficiency is greatly increased compared with the single couple/oxidise procedure. The application of this method could be explored here.

2.3.3 MS Analysis

The molecular weights (MW) that were produced by ionising negative electrospray MS, correlated, where available, with the majority of those calculated theoretically (Table 2.2). All comparisons made between theoretical and actual weights were within a maximum of three MW units, with the majority falling within one.

The only one that was an exception was **27**, which exhibited an actual MW of 5677.97 in comparison to a theoretical MW of 6048.46. The difference represented by **27** (a MW difference of 370.59), may have been a result either due to some form of oligonucleotide degradation or a lack of ionisation by the sequence. The former may have resulted from the cleavage of the acridine moiety, although the MW of acridine is 558.1509, which does not tally with the MW difference. The latter is perhaps more reasonable and for some reason the sequence failed to ionise fully, the acridine may have been proactive in causing this.

This reason is also the only one that can be assigned to those oligonucleotides that showed no MW via MS. Its difficult to explain why some of the samples ionised well and some not at all. The only possible explanation could be that the concentration of these was so low and in such a low abundance that once ionised they were undetectable.

None of the samples (except **6**) were detected when samples were analysed in H_2O alone. The reason for this was probably due to the masking of the sample signal by ubiquitous Na and K ions that can be picked up by the sample at any number of steps along the synthesis/purification cycle. One particular place is through the desorption from glassware used in the preparation of reagents that are used in the synthesis or analysis process. Highly purified water, such as that used as a resuspension medium after desalting, can adduct these cations to the oligonucleotides electrostatically (Grieg, *et al.*, 1995). Sensitivity to MS analysis is markedly reduced as a result of these ions masking the oligonucleotide signal, hence no spectra is produced.

Suspension of the oligonucleotides in 50mM piperidine counteracts this problem because the volatile piperidinium ion displaces and replaces the Na ions. Because the piperidine is volatile it is lost in the heating of the sample during the ionisation process and as a result pure samples are available for ionisation and detection.

The results illustrated show the purity of the synthesised sequences used in the following studies outlined in the following chapters.

3.0 *IN VITRO* TRIPLEXATION

3.1 Introduction

The work outlined in this chapter examines the ability of all TFOs designed for the purpose of this study to form triplexes during *in vitro* studies. The first section uses a well documented method of studying these triplexes using melting curves with measurements via UV-spectrophotometry. This method enables the measurement of a T_m value to be made, which is the temperature at which 50% of the TFO dissociates from the duplex target. This is a straightforward method of directly ascertaining the stability of a given TFO.

The second section of the chapter looks at the ability of given TFO to find and bind to its target within genomic DNA. This method is more closely representative of the situation in *in vivo* studies, as the TFO will have to find its target in amongst mega bases of DNA (instead of a 26mer as is the case in the triplexation curve studies), as well as manoeuvring its way around various other intramolecular DNA structures. The use of these methods was essential to gain insight into the duplex-targeting properties of the various TFOs so that subsequent antibacterial experiments could be designed and validated effectively.

3.2 Results

3.2.1 Triplexation Curves

Figures 3.1 and 3.2 demonstrate representative triplexation curves produced during triplex melting and annealing assays, carried out at pH 6.4 and 7.2. Where triplexation is present, a biphasic curve is presented with a triplex (T) and duplex (D) transition, where triplex formation is not apparent a single duplex transition is usually presented. The transition denoted T, highlights the dissociation of the third strand oligonucleotide from the duplex molecule. The duplex transition indicates the dissociation of the two target strands that form the duplex molecule. The temperature halfway between the triplex transition (T) is the T_m value of the TFO, utilised as a measure of stability of a given TFO for the purpose of this research.

a)

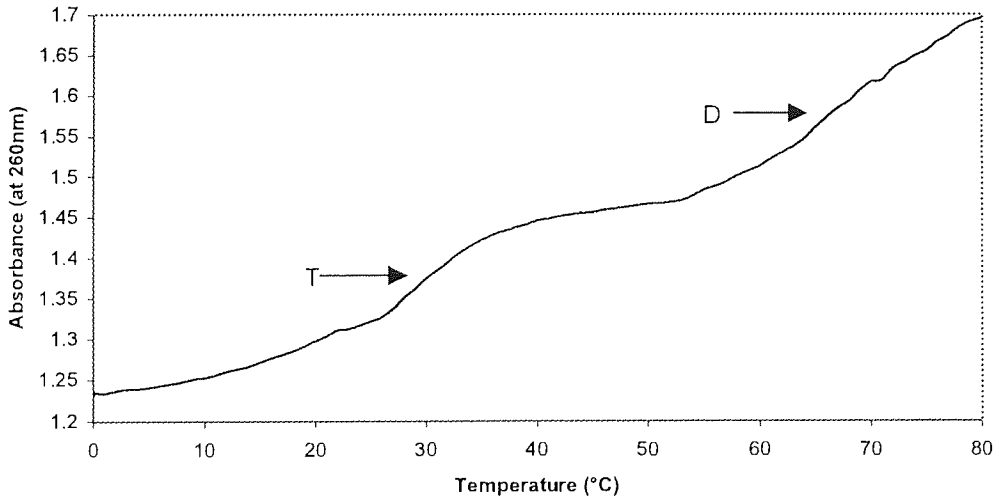

Figure 3.1 Continued over the page.

b)

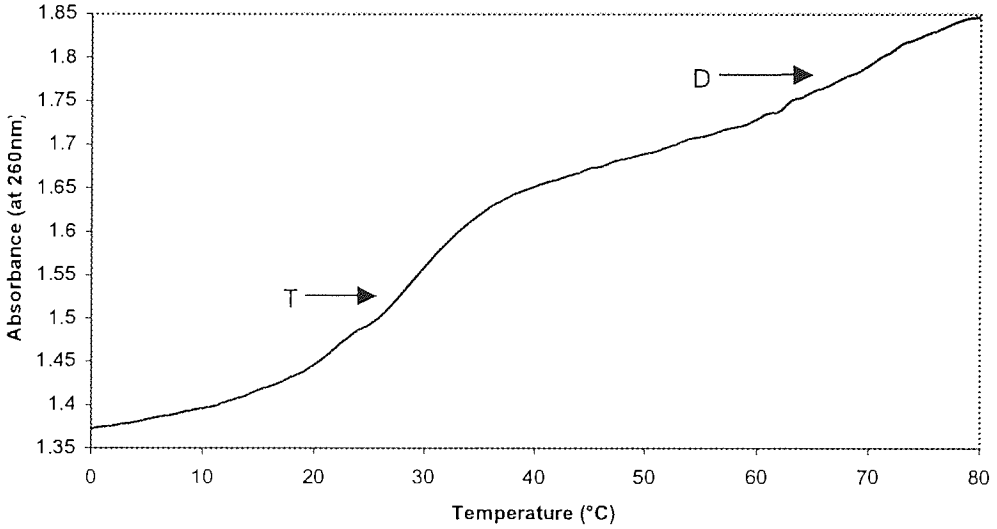

Figure 3.1 Triplexation curves representing **6** in association with the target duplex (**1** and **2**), at a) pH 6.4, and b) pH 7.2 where D and T represent duplex and triplex transitions respectively.

Figure 3.1 illustrates the triplex binding of **6** to its duplex target molecule comprised of **1** and **2**, in relation to temperature at pH 6.4 and 7.2. The curves in Figure 3.1 a) and b) demonstrate typical biphasic triplex melting characteristics.

a)

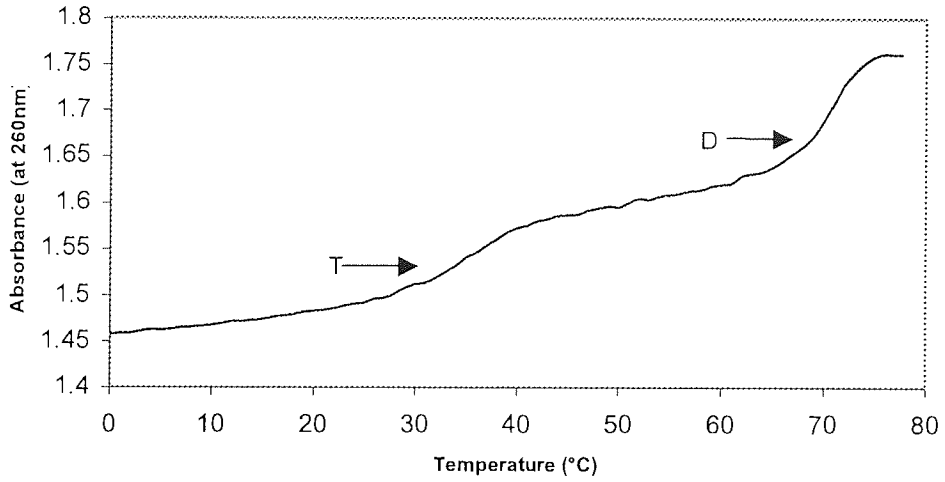

b)

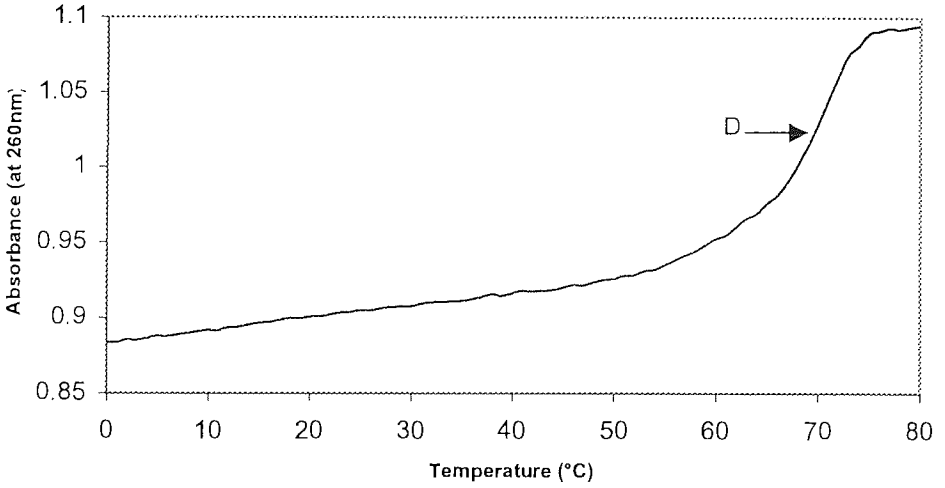

Figure 3.2 Triplexation curves depicting the pH dependency of **25** in association with the target duplex (**23** and **24**) where a) represents triplexation at pH 6.4 and b) triplexation at pH 7.2. D and T indicate duplex and triplex transitions respectively.

Figure 3.2 illustrates the melting behaviour of the TFO **25** in association with **23** and **24**, the target duplex and is representative of situations where third strand binding fails. Here in Figure 3.2 a) at pH 6.4, a biphasic curve is represented with a duplex and triplex transition. However in Figure 3.2 b) only a single transition is present

pertaining to the dissociation of the duplex strands indicating a lack of triplex formation by the TFO **25**. Such results indicate this TFO to be pH-dependent.

Table 3.1 Triplex T_m values for all designed TFOs where NT indicates no triplex transition and NM indicates the absence of measurement.

		T_m (°C)	
TFO	**Sequence**	**pH 6.4**	**pH 7.2**
Target	5'-AAAAGAAAAACGCGTGGAAGGCATCAG-3'		
	3'-TTTTCTTTTTGCGCACCTTCCGTAGTC-5'	n/a	n/a
4 (PO)	3'-AAAAGAAAAACGCGTGTAAGG-Acr-5'	NM	30 +/-1
6 (PO)	3'-AAAAGAAAAACGCGTGGAAGG-5'	26 +/-1	26 +/-1
8 (PS)	3'-AAAAGAAAAACGCGTGGAAGG-5'	NT	NT
11 (PO)	5'-TTTTGTTTTTGGGGGGGTTGG-3'	NT	NT
13 (PO)	3'-TTTTGTTTTTGGGGGGGTTGG-5'	NT	NT
15 (RNA)	5'-UUUUGUUUUUGGGGGGGUUGG-3'	NT	NT
16 (PN)	3'-AAAAGAAAAACGCGTGGAAGG-5'	42 +/-0.8	NT
17 (PN)	5'-AAAAGAAAAACGCGTGGAAGG-3'	NT	NT
18 (PN)	5'-TTTTGTTTTTGGGGGGGTTGG-3'	NT	45 +/-1
19 (PN)	3'-TTTTGTTTTTGGGGGGGTTGG-5'	42 +/-1.7	42 +/-1
20 (PN)	5'-TTTTGTTTTTGGGGGGGTTGG-Fl-3'	NT	48 +/-1
21 (PN)	3'-Fl-TTTTGTTTTTGGGGGGGTTGG-5'	NT	NT
22 (PN)	5'-TTGGTGTGGGTTGGTGTGTTT-3'	NT	NT
Target	5'-ACTGGTAAAAGAAAAACGCGTGGA-3'		
	3'-TGACCATTTTCTTTTTGCGCACCT-5'	n/a	n/a
25 (PO)	5'-TTTTCTTTTTGCGCACCT-3'	35 +/-1	NT
26 (PO)	5'-TTTTCTTTTTGCGCACCT-3'	38 +/-1	NT
27 (PO)	5'-Acr-TTTTCTTTTTGCGCACCT-3'	39 +/-1	NT

Table 3.1 Continued from over the page.

		T_m (°C)	
TFO	**Sequence**	**pH 6.4**	**pH 7.2**
Target	5'-CTGGTAAAAGAAAAACGCGTGGAAGGCATCA-3'		
	3'-GACCATTTTCTTTTTGCGCACCTTCCGTAGT-5'	n/a	n/a
30 (PO)	5'-TTTTGTTTTTTGTGGGGTTGG-3'	NT	NT
31 (PO)	5'-Acr-TTTTGTTTTTTGTGGGGTTGG-3'	NT	NT
32 (PO)	3'-TTTTGTTTTTTGTGGGGTTGG-5'	NT	NT
33 (PO)	3'-TTTTGTTTTTTGTGGGGTTGG-Acr-5'	NT	NT
Target	5'-AAGGAAAAAGCGGAAGCG-3'		
	3'-TTCCTTTTTCGCCTTCGC-5'	n/a	n/a
36 (PO)	3'-AAGGAAAAAG**T**GGAAG**T**G-5'	21 +/-0.5	20 +/-0.25
Target	5'-AGAAAAAGAAGAAGTTGGGA-3'		
	3'-TCTTTTTCTTCTTCAACCCT-5'	n/a	n/a
39 (PO)	3'-AGAAAAAGAAGAAG**CC**GGGA-5'	NT	NT

Table 3.1 illustrates the triplex T_m values obtained for all the TFOs synthesised during the study, by triplex melting and annealing assays. The table highlights the sequence composition of the TFOs along with the duplex targets to which they were to bind.

Figure 3.3 shows the result of triplex melting curves produced by the phosphoramidate sequence **20**. Although two transitions are seen at pH 6.4 (Figure 3.3 a)), only one is seen at pH 7.2 (Figure 3.3 b)). In the case of the latter, the transition is represented by a large change in absorbance, larger than the change in absorbance demonstrated by the combination of the triplex and duplex transition in Figure 3.3 a) and also larger than the single transition represented in Figure 3.2 b). This indicates potential for the joint dissociation of duplex and triplex strands producing the single transition. In this case the T_m value of the triplex would be close to that of the duplex and hence clear dissociation of the different strands is not visible. This implies the potential for triplex formation by other sequences that did not produce the standard biphasic curves during the melting studies.

a)

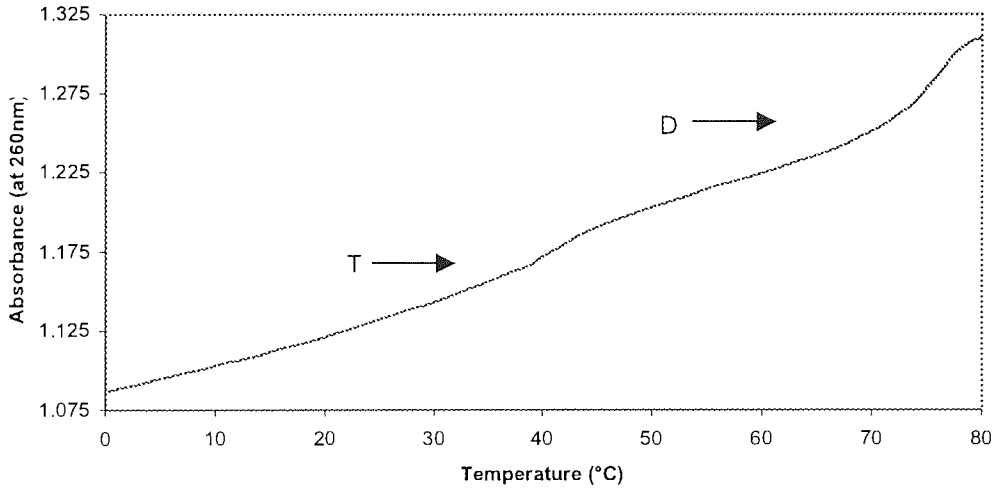

b)

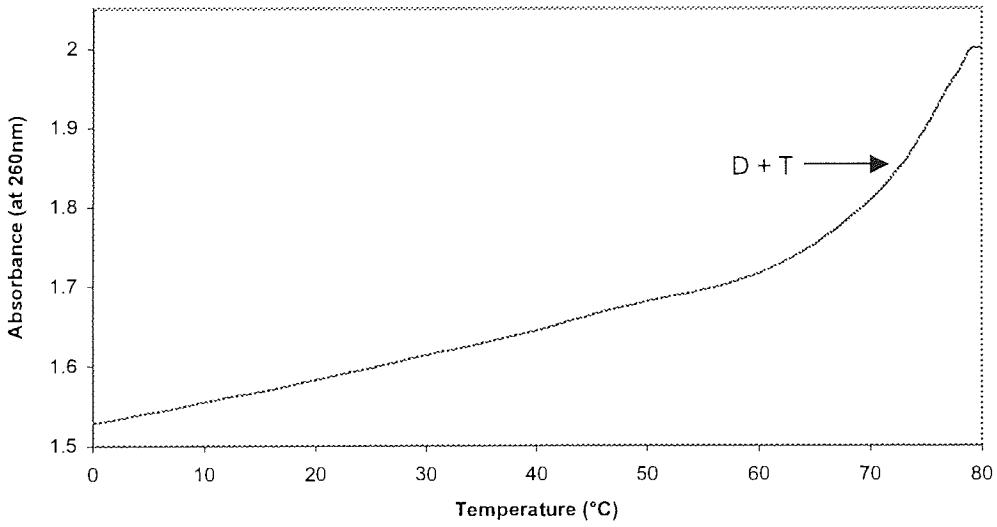

Figure 3.3 Triplex curve representing the annealing behaviour of **20**, where D and T represent duplex and triplex transition respectively. a) illustrates the standard biphasic curve with the two transitional phases, b) illustrates a single transition that possibly pertains to total strand dissociation.

3.2.2 Fluorescence Spectrophotometry

3.2.2.1 DNA Extraction

Table 3.2 Quality and quantity of genomic DNA extracted from *E. coli.*

Extraction	DNA Quantity (μg/ml)	DNA Quality
1	558	1.61
2	443	1.33

Here the quality and quantity of the DNA extracted from *E. coli* for the purpose of the fluorescence plate assays is shown, see Chapter 8 for a full explanation. Pure DNA has a value = 1.8.

3.2.2.2 Plate Assay

Figures 3.4, 3.6 and 3.8 demonstrate the fluorescence emitted by fluorescein-labelled oligonucleotides, when bound to genomic DNA extracted from *E. coli.* The fluorescence produced by the designed TFOs is compared to control sequences in order to ascertain the specificity of binding.

Figures 3.5, 3.7 and 3.9 highlight the association curves produced by the designed TFOs during the plate assays and these along with the dissociation constants (K_d) were calculated using GraphPad Prism®.

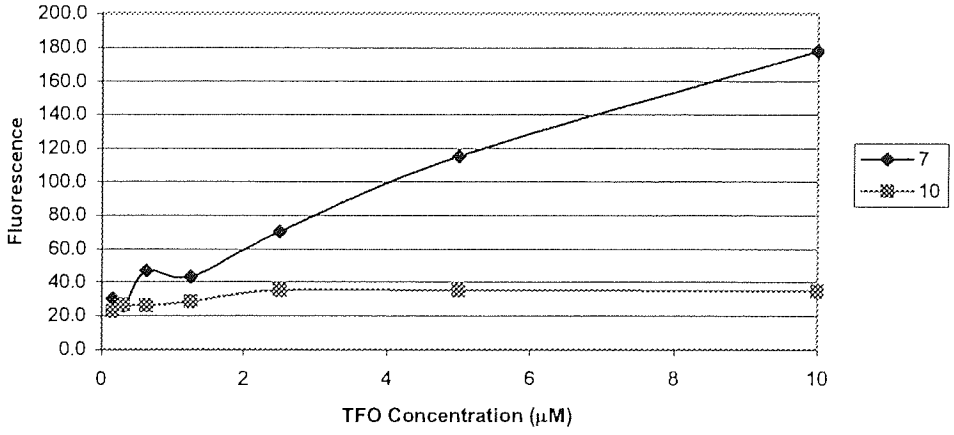

Figure 3.4 Comparison of fluorescence shown by **7** and **10** when in association with *E. coli* genomic DNA at a concentration of 580 μg/ml after plates were washed once in triplex buffer at pH 7.2.

The enhanced fluorescence depicted by **7** in comparison to **10**, shown in Figure 3.4, indicates sequence specific binding of the TFO to the target duplex. This also demonstrates an enhanced level of binding in comparison to the melting studies whereby **7** is able to associate with the target amongst the genomic DNA.

The K_d value produced from the association curve in Figure 3.5 is relatively high, and for a TFO with strong triplex binding affinity, it would need to be in the nanomolar range.

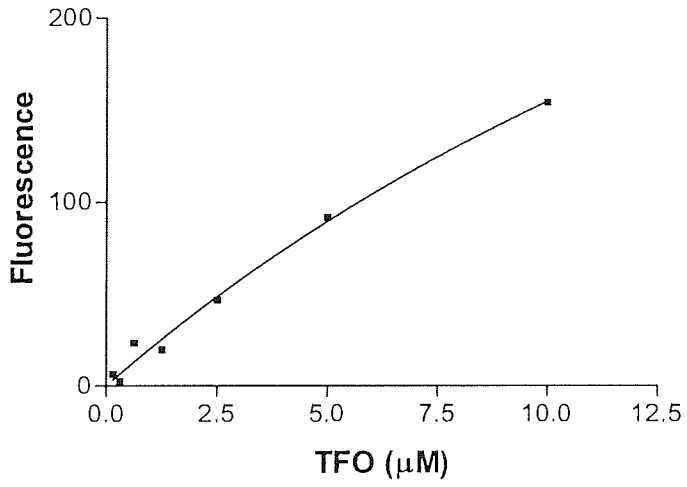

The calculated dissociation constant (K_d) = 26.5 μM

Figure 3.5 Association curve of **7**

The results illustrated in Figure 3.6 a) and b) demonstrate the binding of **20** in comparison to the same sequence with a reversed orientation of binding (**21**). Sequence **10** is used also as a control, as an absence of binding was observed in earlier assays. Sequence **20** clearly shows stronger binding in comparison to **21**, depicted by a heightened level of fluorescence, in both cases illustrated. The control sequences both illustrated very low levels of fluorescence indicating sequence-specific binding of **20**. The K_d value, demonstrated in Figure 3.7, is higher than that depicted for **6** and as a result would imply weaker binding of this TFO and therefore the production of a triplex with weaker stability.

a)

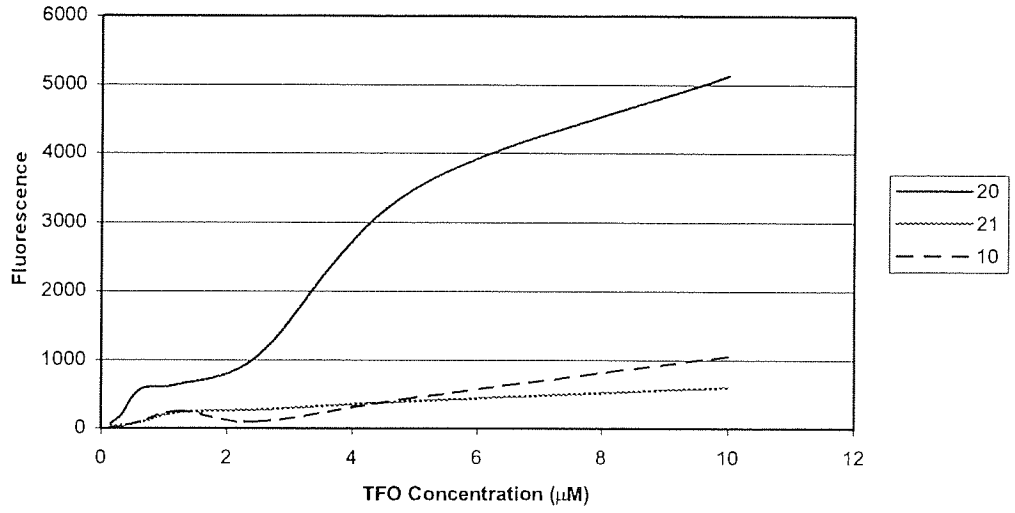

b)

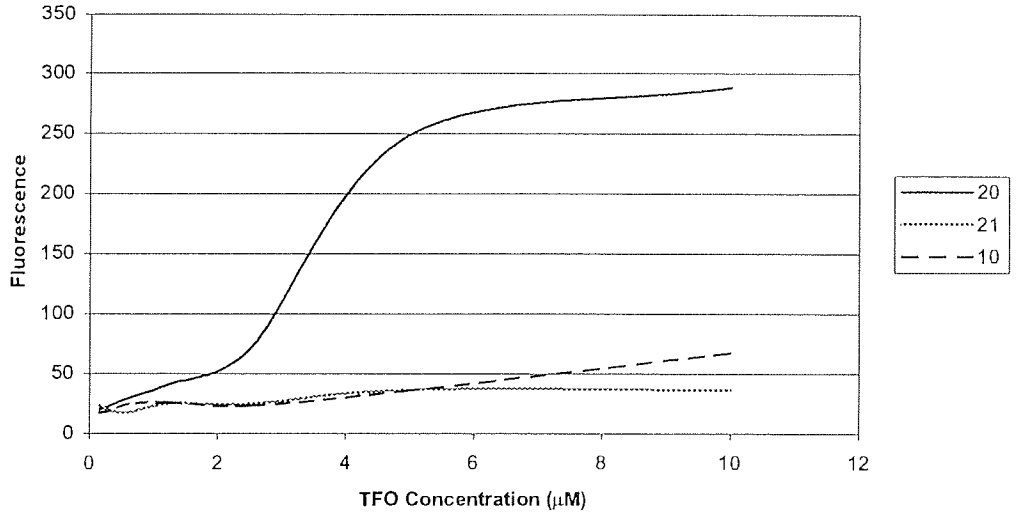

Figure 3.6 Comparison of the fluorescence produced by **20**, **21**, and **10** in association with a) 221.5 μg/ml of *E. coli* genomic DNA after washing once in triplex buffer, b) 443 μg/ml of *E. coli* genomic DNA after washing twice in triplex buffer at pH 7.2.

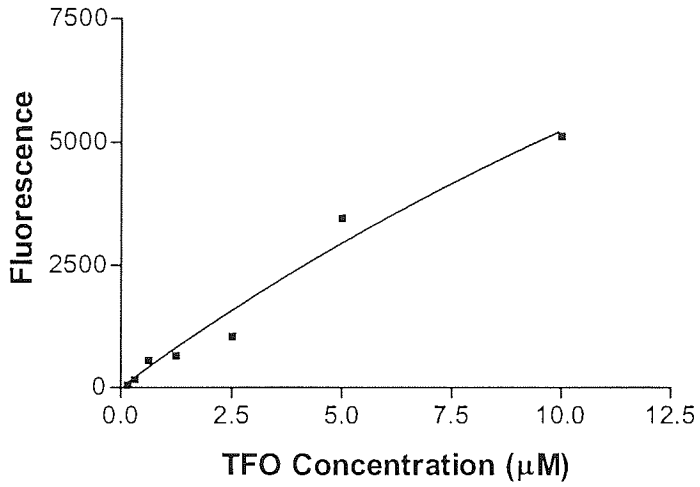

The Calculated dissociation constant (K_d) = 34.1 μM

Figure 3.7 Association curve of **20** to *E. coli* genomic DNA

The fluorescence emitted by **12** in comparison to **14** (Figure 3.8), is markedly greater implying stronger binding of this TFO to the genomic target. This is apparent for both the illustrated examples. Sequence **14** is composed of the same nucleobases as **12**, but has been produced to bind in an antiparallel manner, and the data presented here implies that these (T,G)-containing sequences have a preferred parallel orientation of binding in relation to the target purine strand. The results depicted in Figure 3.8 a) and b), indicate some degree of binding by **14**, but the lower fluorescence demonstrates a weaker affinity for the target and hence lower triplex stability.

a)

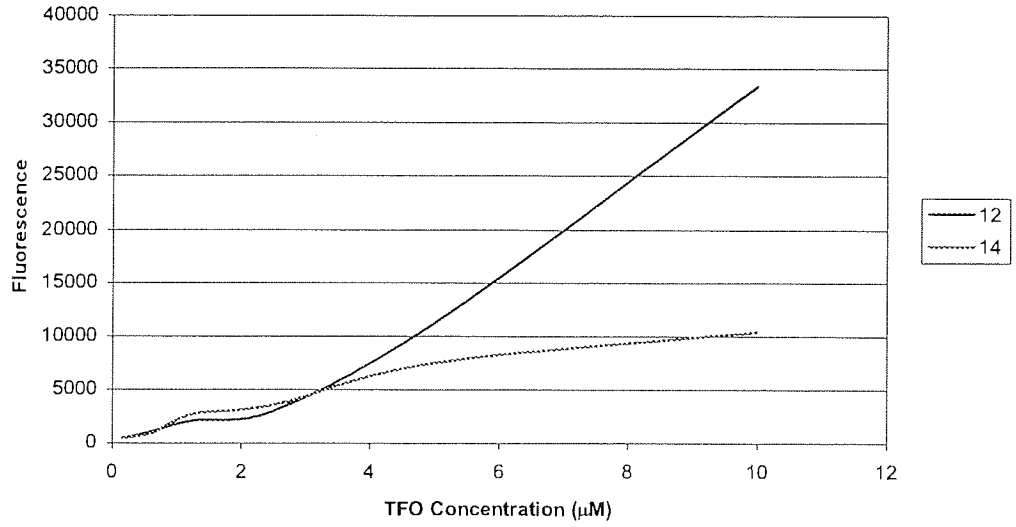

b)

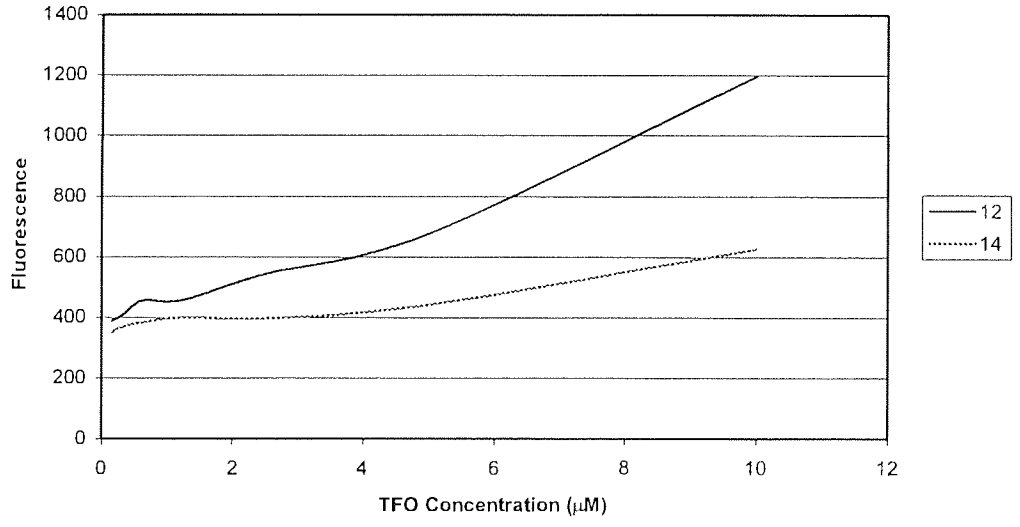

Figure 3.8 Comparison of the fluorescence produced by **12** and **14** in association with *E. coli* genomic DNA at a concentration of a) 580 μg/ml after a single plate wash and b) at 290 μg/ml after two plate washes in triplex buffer at pH 7.2.

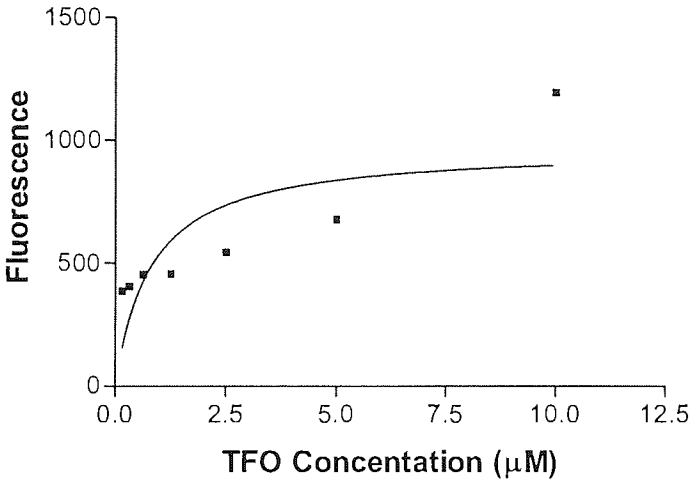

The calculated dissociation constant (K_d) = 800 nM

Figure 3.9 Association curve of **12** to *E. coli* genomic DNA

The association curve and the K_d value exhibited in Figure 3.9 implies **12** to have the strongest binding affinity in comparison to all the other TFOs assessed via this method. This would indicate this TFO to form the most stable triplexes, something that does not correlate with the triplex melting studies shown in this chapter where **11**, an analogue of **12**, failed to show a triplex transition. The curve illustrated here also shows a very poor line of best fit indicating the result to be questionable.

3.3 Discussion

3.3.1 Triplex Melting and Annealing Studies

Figure 3.1 shows two representative triplexation curves depicting the melting and annealing behaviour of **6** at pH 6.4 and 7.2. The curves are characteristically biphasic, with the first transition in the range of 20-40 °C (indicated T). This is the triplex transition, and it is over this range that the third strand oligonucleotide eventually becomes completely dissociated from the duplex target, hence the sharp rise in absorbance. It is during this transition that the T_m temperature value is reached; the temperature at which half of all the bound TFO is dissociated.

The second transition occurs between approximately 55-75 °C (indicated D), and represents the duplex transition. This is the temperature at which the DNA duplex dissociates resulting in single strand structures where absorbance is greatest. During duplex and triplex formation oligonucleotides are more compact and condensed, and as a result absorbance is lower.

Figure 3.2 indicates two further melting curves with **25** evaluated under the same pH conditions. Again, the duplex and triplex transitions are represented by D and T respectively. What is clear here is that this TFO is only able to form a triplex at pH 6.4 and not at pH 7.2, indicated by a lack of triplex transition. As a result this TFO would appear pH-dependent as opposed to **6**, which is pH-independent.

This is not only apparent for **25** but Table 3.1 shows that a number of the other designed TFOs show the same behaviour. Examples include **16**, **26**, and **27** and Table 3.1 shows that in these cases the triplexes are formed at pH 6.4 but not at 7.2. The reason for this would normally relate to the C content of the TFO. C bases in the third strand, are only able to form a single Hoogsteen bond with duplex G targets at neutral or higher pH. At acidic pH however, the N3 of C becomes protonated (C^+) and is consequently able to form a second Hoogsteen bond, hence stronger interactions are formed between C^+ on the TFO and G residues in the duplex target. This protonation also produces favourable electrostatic interactions between the triad, due to the positive charge of the protonated N3, and the anionic charge of the phosphate backbone of the target duplex (Chapter 1). Therefore in the case of triplexation, TFOs containing numerous C residues will only form stable triplexes at acidic pH. Above this pH triplexes are not formed due to the energy penalty being too great.

This explains the results obtained for **25** but not those obtained for the other TFOs in Table 3.1. Sequence **25** contains 5 C residues and as a result triplexation at pH 6.4 would have occurred due to protonation of these nucleotides. Sequences **26** and **27** however contained 5mC substituted for C. This is able to form two Hoogsteen bonds due to an additional methyl group at the 5 position which causes an increase in pK_a compared with the isolated base, and consequently a greater pH range over which the base is protonated (Chapter 1). These TFOs would therefore be expected to have more chance of forming stable triplexes at pH 7.2 and as a result show a transition. This is even more apparent with **27** which has an acridine unit covalently linked at the 5' end. This will further enhance triplexation due to intercalation with the duplex target. Acridine, when conjugated to the 5' end of the TFO, is well known when to enhance triplexation due to increased contact between the TFO and the target duplex. Consequently additional binding energy is provided when in the triplex formation (Chapter 1). These modifications do actually exhibit some degree of enhanced triplex stability here, but only at pH 6.4. Table 3.1 illustrates an increase in T_m (3.2 °C) with the addition of 5mC alone (**26**) and then a further increase (1.4 °C) with the addition of the 5' acridine (**27**). These increases in triplex stability are not entirely consistent with those demonstrated by other researchers who have shown marked increases with the same modifications. In one study (Leitner, *et al.*, 2000), it was actually shown that the addition of a single 5mC residue can increase the T_m of a given TFO by 2.1 °C, and in fact, the addition of further residues is actually additive in relation to the stability of a given TFO. Given this it would be expected that the addition of the five, 5mC residues would have shown a more profound increase in T_m. However, Leitner *et al* also state that neighbouring 5mC nucleotides can cause triplex destabilisation due to electrostatic repulsion, a trend that is more pronounced at neutral pH. At neutral pH a 12 °C drop in T_m by a TFO containing adjacent 5mC residues was documented.

Sequence **26** contains two neighbouring 5mC residues at the 3' end of the TFO, and it could be the repulsion produced by these that could have prevented successful triplexation at pH 7.2. This may also be true for **27**, and in fact, the destabilisation caused by the adjacent 5mC residues, may have been sufficient to prevent successful triplex binding even in the presence of the acridine moiety. This result would seem to be concurrent with the result presented by sequence **4** the acridine-tagged alternative of **6**. The T_m value demonstrated in Table 3.1 for **6** was almost 4.5 °C less than its

acridine-tagged counterpart. A similar situation would have been expected with **26** and **27**, however due to reasons discussed this was not observed.

This T_m increase demonstrated by **4** compared to **6**, would appear to be relatively small, however, in the context of other studies carried out on similar TFO sequences. Other research groups have shown that the addition of an acridine moiety at the 5' end can increase triplex stability by as much as 16 °C (Aubert, *et al.*, 2001; Kukreti, *et al.*, 1997). Again a similar degree of stability would have been expected here. Compound **4** only shows a T_m value at pH 7.2. Insufficient sample volume prevented study at the lower pH.

Sequence **6** exhibited a clear and consistent T_m value of 26 °C under both pH conditions. However, the T_m at pH 6.4 was far less compared to the polypyrimidine sequences (**25-27**). The difference ranged from 9 °C for **25** to 14 °C for **27**. What is interesting is that the difference between the unmodified polypyrimidine TFO, **25**, and the polypurine TFO **6**. This represents a modest increase simply by changing from a purine to a pyrimidine sequence. The reason for this is due to the more favourable stacking interactions that occur during pyrimidine TFO triplex formation, that result from the isomorphous base triplet structures (Chapter 1). These isomorphous pyrimidine triplets generally exhibit less backbone distortion and increased base stacking interactions, hence triplex stability is greatly enhanced.

The reason for the absence of a triplex T_m value for **16** measured at pH 7.2 is a little less clear. Sequence **16** does actually contain two central C residues and these could have been a major contributing factor to the TFOs inability to form a triplex at pH 7.2. It has been established in a number of studies that central mismatches such as these are more destabilising than terminal counterparts (Soyfer and Potaman, 1996). However, the ability of this sequence to form a triplex at all, albeit it only at pH 6.4, was unexpected. Sequence **16** is the phosphoramidate equivalent of **6**, and as a result will bind via an antiparallel manner by reverse Hoogsteen bonds. This conformation is strongly disfavoured during phosphoramidate triplexation, here a BI binding conformation is favoured, which promotes stronger triplexation, but does not support reverse Hoogsteen bonding (Escudé, *et al.*, 1996). As a result, no triple helix formation was expected for this sequence and was actually synthesised to test current thinking on this matter. The reversed sequence (**17**) was designed with a parallel orientation in relation to the target purine sequence and therefore would be expected

to have more chance of binding. This TFO, however, showed no triplex transition at either pH 6.4 or 7.2. Binding of this TFO would have to take place via Hoogsteen bonds, but due to the heavy A content of this sequence, which preferably form reverse Hoogsteen interactions (Chapter 1), triplexation is not possible.

Triplex formation by **16** was therefore surprising and may actually indicate some form of non-specific binding among this group of sequences. It is clear from HPLC and CE traces in chapter 2 that these phosphoramidate TFOs were not 100% pure, and may have contained other sequences of varying chain length and possible hyperstructures. As a result it is difficult to say here whether T_m values are produced by third strand dissociation or from some form of other structural change presented by the other constituents of the sequence sample. The data represented by **19** would seem to be consistent with this, as this TFO exhibited triplex transition at both pH 6.4 and 7.2. The reason this is unusual, is that this sequence has an antiparallel orientation in relation to the purine target, and as stated above, this binding is not tolerated by phosphoramidate sequences. Conversely, had this non-specific binding taken place it would have perhaps been expected across all sequences including **22**, which did not show any triplex melting transitions.

The absence of the triplex transition for sequences at pH 7.2 is particularly problematic because this is the pH found intracellularly. For the purpose of the biological evaluation, triplex formation at intracellular pH is fundamental in order for the TFOs to prevent *gyrA* transcription by steric blockade of gene transcription, and inevitably to exert an antibacterial action. Intracellular pH varies between pH 7.2-7.3, and is highly regulated in order to enable effective functioning of various intracellular pathways and biological mechanisms. Therefore if triplexes are unable to form *in vitro* at similar pH then chances of them forming *in vivo* (i.e. in the bacterial cell) are very unlikely hence no antibacterial activity will be observed.

A number of the TFOs synthesised did not produce a triplex transition at either pH, hence the absence of a T_m presented here (Table 3.1). The phosphorothioate sequence **8** was one of these TFOs. Characterisation of this sequence proved difficult (Chapter 2). The presence of multiple oligonucleotide species in this sample, and its failure to produce a molecular ion during MS analysis, would make it difficult to determine the nature of any triplex formed. A T_m value similar to that demonstrated by **6** would have been expected as the phosphorothioation was made really to test ability of the TFO to form triplexes *in vivo* and to assess their ability to evade nuclease activity.

Sequences **11**, **13** and **30-33** also showed no triplexation during the annealing and melting studies. These sequences are all (T,G)-containing analogues of **25**, and vary only slightly in their base composition (Chapter 8). Sequences **31** and **33** are also acridine-linked in order to increase triplex stability, which is clearly shown here to be ineffectual. Sequences **30-33** contain more GpT and TpG steps than **11** and **13**, and it is these, along with the length of contiguous G and T segments, that determine the orientation of TFO binding in relation to the purine target during triplexation. The number of GpT and TpG steps associated with **11** and **13**, and **30-33**, is five and seven respectively, which is perhaps relatively low considering the length of the sequences. The sequences contain a number of contiguous G and T bases, and **11** and **13** actually contain a run of 7 G residues incorporated in each oligonucleotide. It therefore could be predicted that these TFOs will bind in a parallel manner. As a result it would mean that **13**, **32** and **33**, would be unexpected to bind due to their antiparallel orientation, hence no triplex transition was observed during the melting studies. This does not explain the absence of triplexation demonstrated by **11**, **30** and **31**. A more favourable argument perhaps that encompasses all of these T, G sequences is linked to hyperstructure formation. It is possible that these actually hindered triplex formation. It is well known that sequences containing runs of contiguous G residues are able to self-associate and form intrastrand G quartets, as wells as interstrand quadruplexes where they associate with other like sequences (Chapter 1). It is clear from the HPLC purification techniques used in this work that these structures were able to form. It was necessary due to hyperstructure formation, to purify these sequences at 50 °C. If these structures were able to form in the sample diluent, then it is more than likely that they were able to form in the triplex buffer, during these triplexation experiments. The dissociation temperature of these structures is unknown, however from the HPLC work it is clear that a temperature of 50 °C is sufficient to separate these structures effectively. The HPLC purification run temperature of 50 °C, however, is well and above the expected T_m value of the TFOs represented here. As a result it is very possible that these structures would have formed between the third strand oligonucleotides reducing the concentration of single strands able to engage in triplex formation. Hence triplexation would be markedly reduced or even prevented. Although quadruplexes predominate in the presence of K^+, they are also able to form

in media containing Na^+ (Soyfer and Potaman, 1996), a principal constituent of the buffer used in these assays.

The reason for the inability of **39** to form triplexes is unclear here but is potentially a result of the two C residues that are found toward the 5' end of the TFO. These were substituted into the oligonucleotide due to the double T inversion that was found in the purine target (Chapter 2). These base substitutions could have been problematic to triplexation under both pH conditions. At pH 6.4, where conditions are slightly acidic, these residues may have become protonated where triplex formation would have usually been enhanced due to the availability of an additional Hoogsteen bond. However, because these two C^+ residues were neighbouring, positive charge resulting form the protonation, would have caused electrostatic repulsion between the pair. This may have produced sufficient triplex instability to prevent effective third strand binding. At pH 7.2, these residues may have hindered triplexation again, by each presenting single Hoogsteen bonds. Triplex stability would have been diminished to such a degree that triplex formation was undetectable.

Interestingly, **15** showed little indication of triplexation, again at either pH. It was expected that this RNA-type sequence would show enhanced triplex stability over DNA counterparts such as **6**. Third strand RNA molecules have been shown to bind as well as, or better than DNA molecules during triplex formation (Soyfer and Potaman, 1996). The substitution of standard RNA for 2'-*O*-methyl RNA has been shown to improve this stability further. Similar UV-annealing and melting studies depicted greater T_m values where 2'-*O*-methyl RNA TFOs were used in comparison to phosphodiester third strands (Beban and Miller, 2000). Therefore it is unusual here that 2'-*O*-methyl RNA sequence **15** showed no triplex transition.

The absence of a triplex transition in the otherwise characteristic biphasic curve is not always indicative of failed triplexation. As a result triplexes may still be formed but there melting behaviour is such that they do not produce this initial triplex melting transition. Such a result was in evidence here and is illustrated in Figure 3.3. These two curves represent annealing and melting behaviour of **20**, a) shows the two standard transitions clearly, and b) shows a single but very sharp transition. It seems feasible that triplexes were actually formed during experiment b), the ability of this TFO to do this, is clearly shown in the assay demonstrated in a). The different melting properties demonstrated by the transition in b), and the duplex transition in a), show that this single transition cannot simply result from duplex dissociation, had this been

so, then the two would be similar. The transition in b) is much more profound and shows a much greater increase in absorbance. The start of this transition is around 55 °C, where as the start of the duplex transition in a), starts much later at 65-70 °C and exhibits a much smaller rise in absorbance. The end of the transitions are also the same, at around 80 °C, indicating that the transition in a), is much longer. It is not unrealistic to expect therefore, that this single transition represents a mix of third strand and duplex dissociation, if the T_m of the triplex is closer to the T_m of the duplex, hence no separable triplex transition. This is further supported by the difference in absorbance from the start of the transition to the end of the transition. The single transition in b) shows a change in absorbance that is similar to that represented by the triplex and duplex transitions, represented in a), superimposed. These predictions are not unfounded and other researchers have observed triplexation due to differences in duplex melting and annealing curves compared with single transition triplex curves (Jetter and Hobbs, 1993; Parel and Leumann, 2001).

Although an important technique, the melting studies are by no means the only way of visualising triplexation. Gel retardation and band shift experiments are a widely used tool in this area of research. The techniques generally use radiolabelled double stranded DNA incubated in the presence of unlabelled oligonucleotide third strands, which are then loaded on to a non-denaturing polyacrylamide gel. Triplexes are identified by their retarded mobility on the gel compared with the duplex DNA. These techniques have actually shown clear evidence of DNA triplexes where melting studies have failed to do so (de Bizemont, *et al.*, 1996). Such studies were attempted here, using silver staining techniques to visualise the formation of duplex and triplex structures (data not shown). However, these staining techniques were not sensitive enough to determine retardation properties of the different structures. Unfortunately, radiolabelling was an unavailable resource here hence the absence of more supporting information. Optimisation of these procedures would be necessary to determine triplexation of TFOs that have failed to show a triplex transition by UV melting studies.

3.3.2 Fluorescence Spectrophotometry

The results in Figures 3.4 to 3.9 depict the binding of the TFOs **7**, **12**, **14**, **20**, and **21** to genomic DNA extracted from *E. coli* and adhered to microtitre plates. Their use

here is related to T_m values produced by their non-fluorescein labelled counterparts, illustrated in Table 3.1, where all except **20** and **21**, have no respective values. It was assumed therefore, for the purpose of this study, that the fluorescein has no influence in the binding ability during triplex formation.

The basis of these fluorescence studies, was that the designed TFOs would bind in a sequence-specific manner to their target within the DNA, and that the fluorescence produced was due to the fluorescein label attached at the 3' end of each oligonulceotide. It was assumed that the greater the fluorescence remaining after different numbers of washes, the stronger the binding stability of a given TFO. Plates were blocked with BSA to prevent any non-specific binding.

Figure 3.4 illustrates the binding of **7** to the genomic DNA in comparison to **10** (randomised **7**). The results indicate much higher fluorescence exhibited by **7** compared with **10**, a difference of approximately 140 fluorescent units (FU) at a TFO concentration of 10 μM. Sequence **10** actually exhibited a level of fluorescence similar to the blank, triplex-buffer containing wells, and therefore it can be presumed that binding to the genomic DNA did not occur. As a result the case for **7** (an analogue of **6**) binding by sequence specific means is strong. The ability of **6** has been shown above to form triplexes at pH 6.4 and 7.2, and thus binding has further been proven here with the enhancement of the TFO being able to bind to its target amongst all the other genomic DNA.

Figure 3.5 represents the association curve of **7** depicting it to have a K_d of 26.5 μM. This is relatively high according to current literature. Dissociation constants have been shown with polypyrimidine TFOs to have a value as low as 1-10 nM (Rougée, *et al.*, 1992). These values are very low and actually show a similar constant to DNA-binding proteins and as a result will exert strong competition for shared binding sites (Soyfer and Potaman, 1996). These agents will therefore be effective antigene agents, their only limiting factor is that triplex formation is slow. The lower the bonding constant the better, as this indicates stronger binding, and it is dependent on the nature of the sequence and the number of mismatches. The K_d in the example given was for a pyrimidine motif triplex, which is isomorphous unlike its purine counterpart. It is clear that the K_d of **7** should be higher due to the increased backbone distortion, during triplex formation. As a result triplex stability is diminished and the ability of the TFO to remain bound to the target is lessened. Regarding mismatches, this sequence

contains 3, two C-G inversions and one A-T inversion. Opposing these in the third strand are two C and one T bases respectively. These were not modified in any way, and perhaps to increase the binding avidity and hence decrease the K_d, base substitution, either with natural bases or base analogues, would be necessary along with the attachment of an intercalating agent. T is documented as the best natural substitute for C, and G the same for T (Gowers and Fox, 1999). However, G represented in this manner is only able to bind via a parallel orientation, in relation to the target purine, to the mismatched pyrimidine. Such a substitution would therefore be ineffectual here and C substitution has been demonstrated to be the least destabilising in such a situation. Base analogues and intercalating agents are numerous, for a short review see Chapter 1.

Figure 3.6 represents the binding of the phosphoramidate sequences **20** and **21**, along with **10** as a control. The latter of these was used because the previous study (involving **7**) had shown this TFO not to bind to the genomic DNA. Two association curves are shown here; one representing the binding of the TFOs after the microtitre plates were washed once a), and the second, after the plates had been washed twice b). The two different concentrations of DNA illustrated in these results were selected due to the clarity of separation of curves demonstrated by the different TFOs, after the subsequent washes. The results again show that the designated TFO, this time **20**, showed the highest level of fluorescence at every TFO concentration. What is interesting in these curves, is that **10** seems to show some low level fluorescence in both curves, where as **21** does in Figure 3.6 a), but in Figure 3.6 b), exhibits a level of fluorescence similar to the blank wells. It is clear that the designed TFO binds the strongest, but the fluorescence illustrated by the other sequences would seem to depict a level of non-specific binding. This is perhaps understandable, and should be considered in the context of Table 3.2. This table indicates the quality and quantity of the DNA extracted from the bacterial cells for the purpose of these studies. The DNA taken from the first extraction was used in the coating of microtitre plates utilised binding experiments of **7**, **12** and **14**. The DNA isolated during the second extraction, was utilised in the remaining assay. The DNA extracted second time around was not as pure as that during the first extraction. The Quality value of 1.33, is considerably lower than that of pure DNA (1.80), and therefore would indicate potential protein contamination. This could explain the low level of non-specific binding demonstrated by **21** and **10** during these experiments. It is possible that these sequences were able to

interact with the proteins, which too would have bound to the plate together with the DNA during coating, and hence the TFOs remained in place after washing. If this is the case however, questions could arise disputing the level of binding of **20**, and indeed how much of this is actually associated with specific and non-specific binding. The answer is not clear, but it can be assumed that a level similar to that demonstrated by **21** would consequent, due to the similar phosphoramidate structure of the oligonucleotides. Sequence **10** had a different sequence and backbone make up, and as a result will potentially have different binding properties under these conditions. It can therefore be postulated that the level of non-specific binding, if any, demonstrated by **20**, would be less than that depicted by **10**. The results demonstrated here correlate with those of the melting studies. A clear and defined T_m is illustrated for **20** at pH 7.2 where as one is absent for **21**. As a result it is expected that the former would bind more strongly.

Figure 3.7 shows the binding association curve of **20** with the genomic DNA. The K_d depicted here is even higher than that of **7** and shows a value of 34.1 μM. This would therefore indicate this TFO to have a lower binding affinity than **7** for the genomic DNA, and hence their target duplex. This however does not correlate with the results illustrated in the triplex melting and annealing studies, where the T_m of **20** is far higher than that depicted by **6**. Phosphoramidates are well documented for their improved triplex binding stability over phosphodiester sequences as discussed earlier. As a result, the K_d would have been expected to be appreciably lower. This may again be due to the low purity of these phosphoramidate sequences, where again the nature of the exact binding during these assays is unclear.

Figure 3.8 illustrates the binding of **12** and **14** under the same assay conditions as above. Curve 3.8 a), represents the binding of the two TFOs to the genomic DNA after washing once in triplex buffer, and 3.8 b) illustrates this same binding after the plate was washed twice in triplex buffer. The results demonstrate **12** to have a greater binding affinity for the target, as it demonstrated the highest level of florescence. Sequence **14** showed a reasonable level of fluorescence but this was still far less than for **12**. It is assumed that this fluorescence has not resulted from non-specific binding due to the purity of the DNA extracted for the purpose of this assay. Non-specific binding was also absent in earlier, similar studies (Figure 3.4, binding of **10**). Sequence **14** is the reverse sequence of **12**, and both are (T,G)-containing sequences.

The orientation of the binding of such TFOs, parallel vs antiparallel, is not fully predictable, but is dependant upon the number of TpG and GpT steps (Chapter 1). It is clearly shown here that this sequence has a preferred parallel orientation in relation to the purine target strand. However, it is also shown that alternative, weaker, antiparallel binding is still possible. This is evident in Figure 3.8 b), where after two washes, **14** is still bound to the target but too a lesser extent than its parallel counterpart. The difference between the levels of fluorescence demonstrated by the two oligonucleotides, particularly at the highest TFO concentration, has however narrowed. The parallel binding motif represented here, would seem to support the ideas put forward above, regarding the triplexation curves for the same sequences. Work carried out by de Bizemont *et al* (de Bizemont, *et al.*, 1996), however, seems to contradict this proposed manner of binding, and work carried out by them showed a 14mer (T,G)-containing oligonucleotide with 5 GpT and TpG steps to bind in an antiparallel manner. Further to this work, decreasing these steps to one, showed their TFO to take on a parallel orientation in relation to the polypurine target sequence. This latter work concurs with a similar study carried out by Giovannangéli *et al* (Giovannangéli, *et al.*, 1992). It would seem interesting here that a parallel orientation was preferred in these binding studies, and here consideration needs to be taken regarding the length of the sequence. The TFO used for the purpose of this study was a 21mer and as a result would perhaps tolerate more GpT and TpG steps before a change in orientation occurs. Also the G content is much higher in **12** and **6** (48%) than in those sequences used by de Bizemont *et al* (28%), which again would be another contributing factor. In fact it has been stated that a high G content is necessary for the detection of triplexes formed with such (T,G)-containing third strands.

Figure 3.9 represents the binding curve of this sequence in relation to its target. The K_d value represented is far lower than either of the other two sequences. This time it is in the nanomolar range at 800 nM, which would indicate this sequence to bind reasonably tightly to its target. Interestingly, this TFO did not produce a triplex transition during the melting and annealing studies, and hence would be unexpected to bind here, let alone produce the lowest k_d value. The sequence again has the potential to self-associate and perhaps structures formed were able to interact with genomic DNA more strongly than the TFO alone. As a result more oligonucleotide was present after washing. However such a phenomena would also be expected for the **20** as this too is a (T,G)-containing TFO of the same length.

The work detailed above gives a clear indication of the triplex stability of all TFOs synthesised for the purpose of this study. Results are generally mixed with many of the sequences showing a lack of triplexation by the melting studies. The T_m values represented support the use of phosphoramidate sequences as the most stable triplex formers, as these exhibited values above 40 °C. Such T_m values are required if these are to be used as therapeutic agents. High levels of triplex stability will be necessary at 37 °C and above, where these agents will have to be effective particularly in patients with raised basal temperatures resulting from infection and disease. No other TFOs studied were able to satisfy these criteria, **25-27** demonstrated reasonably good T_m values, but were only able to do so at pH 6.4, which is not directly relevant to intracellular conditions.

The phosphoramidate sequences (**16-22**) however lack proper, full characterisation so it is inappropriate to say that the results shown are due to sequence specific triplexation. Further characterisation is necessary before any true conclusions can be drawn.

The attachment of acridine at the 5' end of the oligonucleotides has shown little value with only small, if any, increase in T_m. Its attachment to phosphodiester sequences has been shown to be ineffectual. Of all the sequences analysed here **6** has shown the most reliable and consistent behaviour with a T_m of 26 °C at both pH conditions tested. Although this value is not completely desirable the sequence has shown clear binding to genomic DNA at a strength that would appear to be in agreement with the T_m value obtained, and it has been fully and appropriately characterised. It is for this reason that this TFO is the main focus of the uptake and biological evaluation work carried out. This work is documented in the following chapters.

4.0 BACTERIAL STRAINS, MAINTENANCE AND GROWTH CURVES

4.1 *Escherichia coli*

4.1.1 Bacterial Strains

The transformable strain of *E. coli*, *E. coli* DH5α (Aston University culture collection), was used for the purpose of the research carried out in this study. It was used to enhance the opportunity of triplex formation by each of the designed TFOs by avoiding unnecessary degradation of the oligonucleotides by endonucleases. This is a widely used organism particularly in transfection of plasmid and bacteriophage DNA, necessary for the purpose of cloning experiments. Genetic mutations predominant in the organism, enable maintenance of plasmid DNA inserts and the expression of genes carried by that DNA. The genotype of the organism is the same as that of the wild type K12 strain, but with the allelic mutations below:

Allelic Mutations of *E. coli* DH5α - ϕ80d*lacZ*ΔM15, *recA*1, *endA*1, *gyrA*96, *thi*-1, *hsdR*17(r_K^-, m_K^+), *supE*44, *relA*1, *deo*R, Δ(*lacZYA-argF*)U169.

Table 4.1 Explanation of allelic mutations in *E. coli* DH5α genome, adapted from Promega technical information (Promega, 1996).

Symbol	Description	Effect of Mutation
deoR	Regulatory gene mutation allowing constitutive expression of genes for deoxyribose synthesis	Allows efficient replication of large plasmids.
*end*A1	Endonuclease mutation	Improves quality of plasmid DNA isolations.
*gyrA*96	DNA gyrase mutation	Resistance to nalidixic acid.
hsdR(r_k-,m_k+)	Restriction negative, modification positive	Allows cloning without cleavage of transformed DNA by endogenous restriction endonucleases. DNA from this strain can be used to transform r_k+ *E. coli* strains.
*lacZ*ΔM15	Partial deletion of β-D-galactosidase gene	Allows blue/white selection for recombinant colonies when plated to X-Gal containing agar.
*recA*1	Mutation in recombination genes	Prevents recombination of introduced DNA with host DNA, ensuring stability of inserts.
*relA*1	Relaxed phenotype; mutation eliminating stringent factor	Allows RNA synthesis in the absence of protein synthesis.
SupE	Suppresser mutations	Suppress amber (UAG) mutations.
thi-1	Mutation in thiamine metabolism	Thiamine required for growth in minimal media.

Although many of the mutations presented in the Table 4.1 are of little benefit regarding triplex formation, two of particular interest are; *endA*1 and *gyrA*96. The former prevents the production of endonuclease that will degrade inserted DNA, and the latter is a mutation that confers resistance to nalidixic acid, the progenitor of the quinolone antibiotics. This latter mutation is of interest as it is the *gyrA* gene that the TFOs designed for the purpose of this study are targeted, however target sequences, as

stated, are found in both quinolone-susceptible and -resistant strains. The *end*A1 codes for specific endonuclease enzymes that form part of the restriction system within the cell. These are defence systems that prevent expression of foreign DNA by causing its degradation. With mutations in this gene, plasmids can be maintained within the cell and cellular machinery can be used to copy and express the genetic information. The advantage of the inactivation of such a system for this purpose is that it decreases chances of TFO degradation upon uptake into the cell.

4.1.2 Culturing and Maintenance

From frozen stocks (-70 °C) contained in the Aston University culture collection, the *E. coli* was sub-cultured to nutrient agar (NA) (Oxoid), and incubated overnight at 37 °C. This was subsequently stored at 4 °C for assay usage, where it was also sub-cultured to fresh NA plates every four to six weeks.

4.1.3 Growth Curves

Growth curves were recorded to determine the point at which the organism entered the log phase of growth. This was necessary for the antibacterial assay, where the organism was required to be in this phase to maximise uptake of exogenous compounds. This is due to more permeable membranes resulting from the higher levels of replication. Growth curve protocols can be found in Chapter 8. It is clear from Figure 4.1 that the organism enters log phase after 1.5 hours.

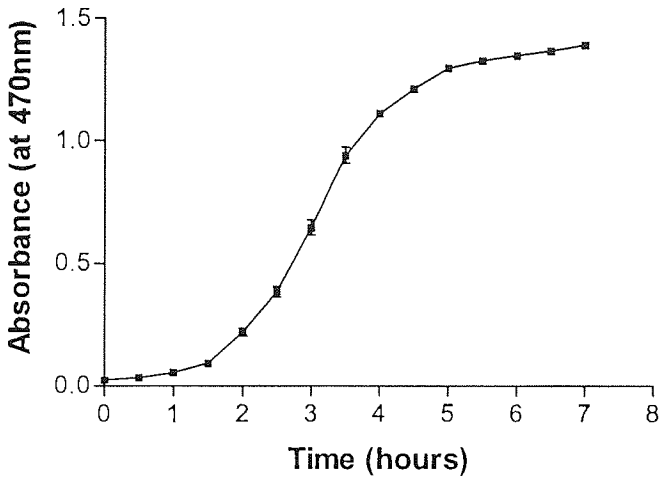

Figure 4.1 The growth curve of *E. coli* DH5α in LB broth measured at an absorbance of 470 nm.

4.1.4 Effect of Ciprofloxacin on Growth Curve

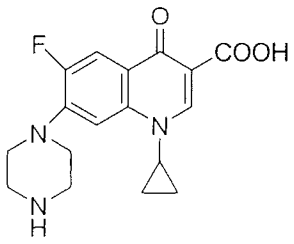

Figure 4.2 The structure of ciprofloxacin.

This assay was carried out to demonstrate the susceptibility of the organism to this antibiotic.

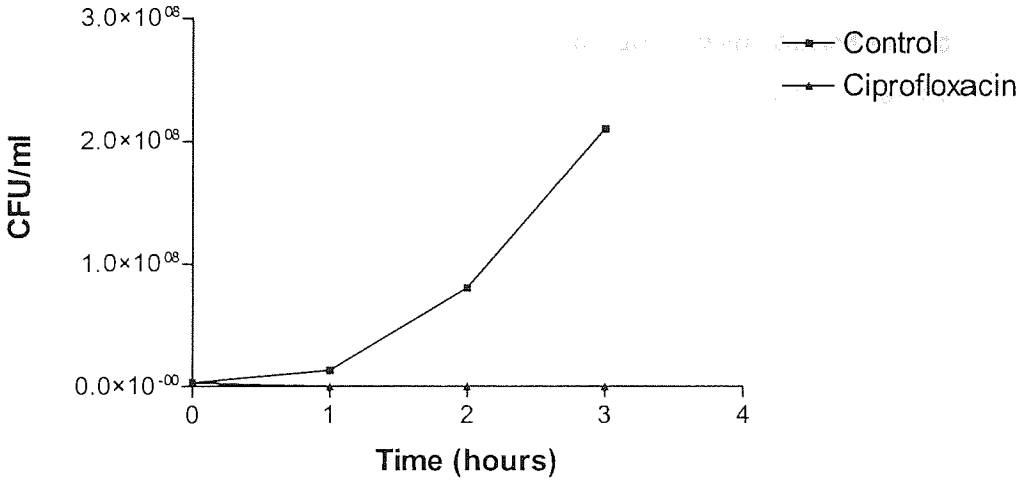

Figure 4.3 Growth curve in the presence and absence of ciprofloxacin at a concentration of 0.5 μg/ml at 37 °C.

Figure 4.3 indicates a very significant and sustained level of inhibition from time 0. Ciprofloxacin is currently one of the antibiotics of choice when patients present with infections caused by *E. coli* hence its inclusion here. It also has the same target as the TFO designed for the purpose of this study. Ciprofloxacin targets the gyrase enzyme and binds to the α subunits of the protein during the cutting process associated with the maintenance of DNA topology. The binding prevents resealing of the DNA and hence it remains fragmented (Chapter 1). The TFOs presented here were designed to bind at the gene that codes for this subunit of the gyrase enzyme and ultimately prevent protein synthesis. As a result of the successful binding of the TFO to the target comparable levels of kill demonstrated here might be achieved.

4.2 *Streptococcus pneumoniae*

4.2.1 Bacterial Maintenance and Culturing

S. pneumoniae (Aston University culture collection 8EIV) was sub-cultured on columbia blood agar plates (Oxoid) from stock samples stored at –70 °C and incubated under CO_2 enriched conditions for 24 hours at 37 °C. Cultured plates were then stored at 4 °C and subsequently sub-cultured to fresh blood agar plates once weekly in the same manner.

4.2.2 Growth Curves and Characteristics

The full methodology is given in Chapter 8. Growth curves were carried out to determine the growth pattern of *S. pneumoniae* and determine the length of culture time required to reach the log phase of growth.

a)

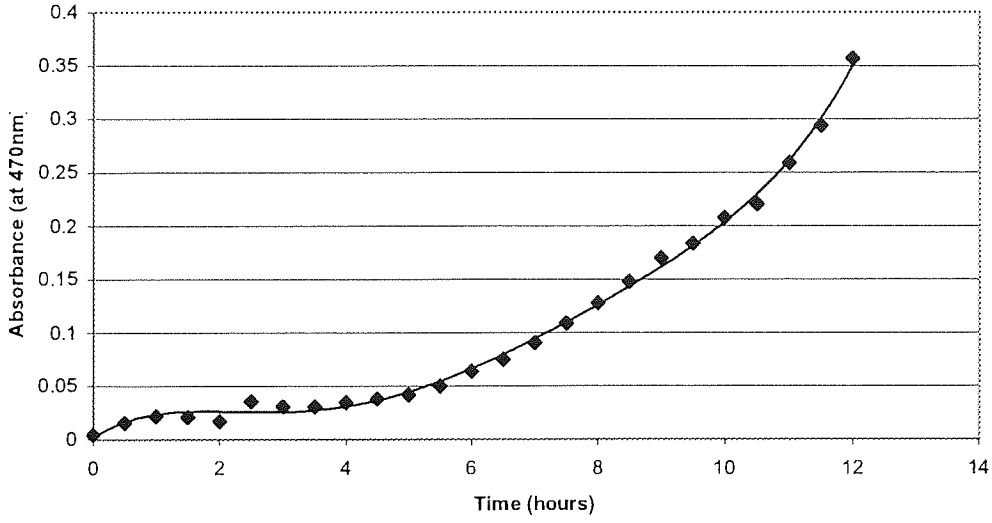

b)

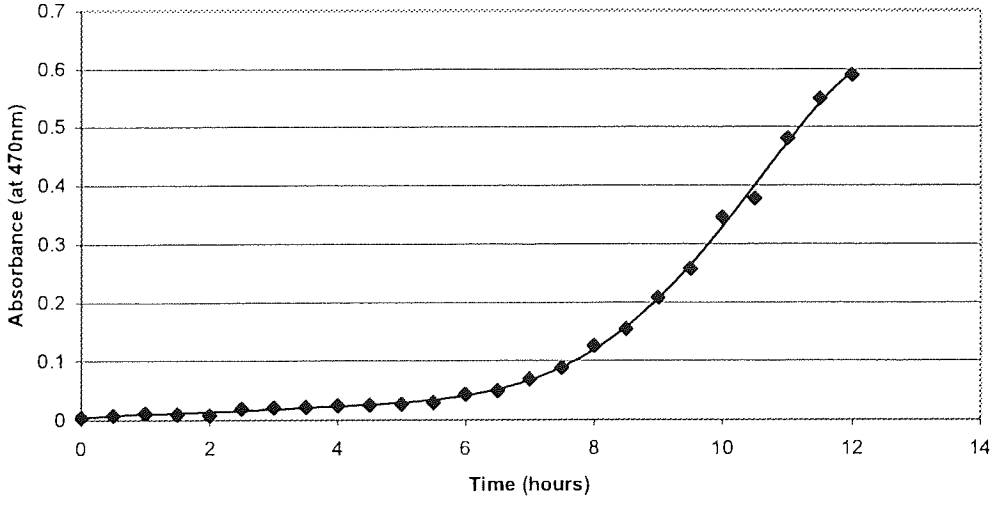

Figure 4.4 The growth curve of *S. pneumoniae* under a) aerobic and b) CO_2 enriched conditions at 37 °C.

Figure 4.4 shows that the length of time required for *S. pneumoniae* to reach the log phase of growth, is between 6-7 hours under aerobic conditions, and about 8 hours under CO_2 enriched conditions. This is considerably longer than *E. coli* and assay parameters were altered accordingly. However, the T_m values of the TFOs designed to bind within the *gyrA* gene of this organism dictated low assay temperatures. It was therefore necessary to determine the growth characteristics at temperatures lower than 37 °C. Initial culturing experiments proved that the culture was unable to grow at temperatures lower than 25 °C (data not shown), and as a result it was decided to run TFO kill assays at this temperature and therefore it was also necessary to ascertain growth patterns at this temperature.

Table 4.2 The growth of *S. pneumoniae* over 72 hours at 25 °C.

Culture	Time (hours)	Absorbance (at 470 nm)
1	24	-
	48	0.374
	72	0.478
2	24	0.105
	48	0.185
	72	0.372

The results indicated in Table 4.2 demonstrate very slow growth of the organism at 25 °C, and as a result, the kill assay using **36** and **39** had to be designed accordingly if cultures were to be grown to log phase prior to commencement of the assay. It would also mean that growth throughout the assay would be markedly slow and drastically diminished levels would perhaps be expected over the time course of the assay.

5.0 CHARACTERISATION AND ANALYSIS OF *IN VITRO* OLIGONUCLEOTIDE UPTAKE METHODS

5.1 Introduction

The aim of the following chapter is to assess the uptake methods that were employed to enhance TFO delivery during the antibacterial kill assays, which can be seen in chapter 6. Zeta potential and particle size analysis have been used to characterise the liposome in order to gain an insight into how the various liposome formulations interact with the bacterial cells. Results will provide indications to the possible interactions that take place between the two entities.

FACS analysis has been applied to ascertain the level of bacterial cell fluorescence produced by fluorescein-labelled TFOs when taken up into the cells via passive, cold shocking and liposome-mediated methods. This provided insight as to the most successful method of uptake and explaination to whether insufficient antibacterial kill was a result of poor cellular uptake. Table 5.1 highlights the composition of the sequences used in this chapter.

Table 5.1 The nucleotide sequences of the oligonucleotides used in this chapter.

Oligonucleotide	Sequence
6	3'-AAAAGAAAAACGCGTGGAAGG-5'
7	3'-Fl-AAAAGAAAAACGCGTGGAAGG-5'
10	3'-Fl-CGGAGAAAAGTGAAGAAGAAC-5'

5.2 Results

5.2.1 Lipid Characterisation and Analysis

All lipid formulations were exposed to zeta potential and particle size analysis in order to establish surface charge and diameter of the given lipid or liposome.

Figures 5.1 and 5.2 illustrate representative zeta and particle size plots of empty liposomes demonstrating single populations with a normal distribution and small population variation.

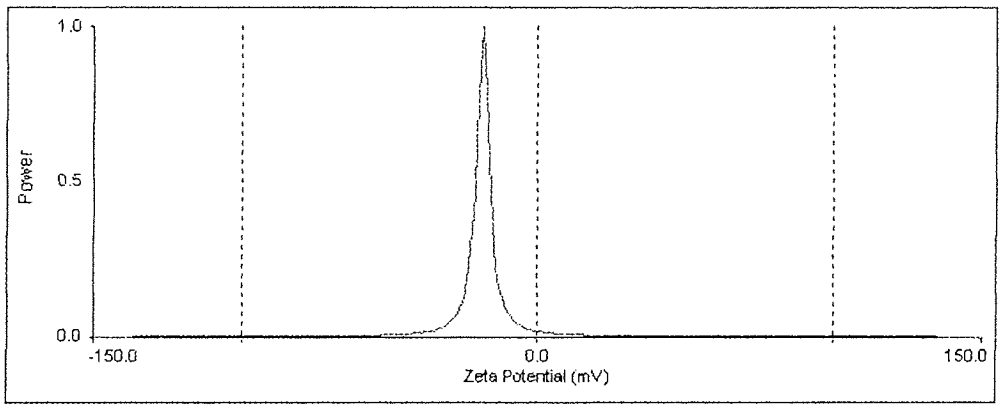

Figure 5.1 A representative zeta potential trace depicting the charge population of the empty liposomes formulated as stated (Chapter 8).

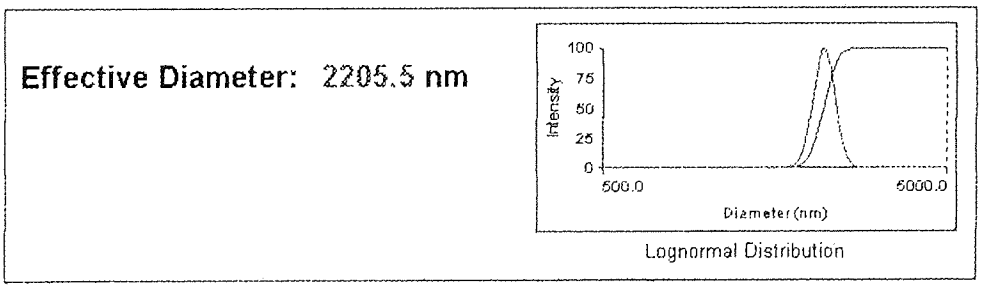

Figure 5.2 A representative trace of particle size analysis results for 1:20 (DMPG:DPPC) anionic liposome ratio where 'Effective Diameter' is the mean diameter of the liposomes in solution.

5.2.1.1 Cationic Lipids

Table 5.2 The charge interaction, measured by zeta potential, of the cationic lipids used for the purpose of the study with a) in phosphate buffered saline (PBS) to ascertain the charge of the lipids alone, b) in Luria Bertani broth (LB) to determine how the lipids interact with LB broth as would be the case under antibacterial assay conditions (Chapter 6), and c) with **6** in association with LB to gain an insight into charges of the three before interaction with the bacterial cells.

Sample Constituents	Zeta Potential (mV)
1. Lipofectin® + PBS	26.44 ± 1.28
2. Cellfectin® + PBS	29.68 ± 0.93
3. Lipofectamine™ + PBS	16.34 ± 2.61
4. DMRIE-C + PBS	20.64 ± 0.78
5. LB Broth	-12.92 ± 0.80
6. Lipofectin® + LB	-13.10 ± 0.58
7. Cellfectin® + LB	1.44 ± 0.60
8. Lipofectamine™ + LB	-1.62 ± 0.41
9. DMRIE-C + LB	-32.69 ± 1.33
10. 6 (0.5 μg) + Lipofectin® in LB	-6.47 ± 0.03
11. 6 (1.0 μg) + Lipofectin® in LB	-18.08 ± 0.79
12. 6 (1.5 μg) + Lipofectin® in LB	-12.34 ± 0.39
13. 6 (2.0 μg) + Lipofectin® in LB	-19.64 ± 0.56
14. 6 (2.5 μg) + Lipofectin® in LB	-12.86 ± 0.24
15. 6 (3.0 μg) + Lipofectin® in LB	-18.34 ± 0.68
16. *E. coli* in LB	-52.23 ± 0.14

Table 5.2 illustrates the zeta potentials obtained for the cationic lipids in PBS, LB broth and in association with **6** in LB broth. The results obtained for the lipids in PBS clearly indicate the cationic nature of the lipids. However, when added to the LB, the overall negative charge of the broth, indicated in 5, neutralises that of the lipids resulting in an overall negative zeta potential. The addition of the DNA only increases the negativity of the solution due to the anionic backbone, which could have implications on complexation.

5.2.1.2 Anionic Lipids

a)

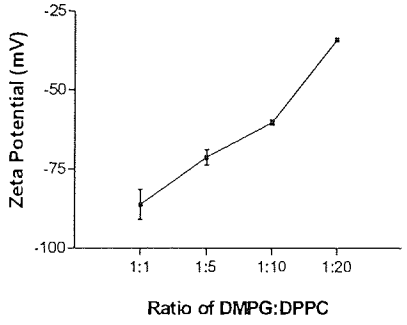

b)

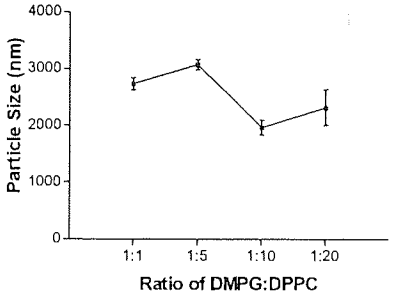

Figure 5.3 a) Zeta potential and b) particle size variation when different ratios of DMPG to DPPC are used.

Figure 5.3 highlights the effects on zeta potential and particle size when the ratio of DMPG:DPPC is varied. When the concentration of DPPC is increased and DMPG remains static, the liposomes are less negative, which is not unexpected. The effect on size is more variable and does not seem to show any pattern to the increase in DPPC concentration.

Table 5.3 Characterisation of formulated anionic liposomes used for the purpose of the study, using zeta potential and particle size analysis. (1) and (2) after 6 and 7 represent liposome formulated with the respective TFO during separate formulation cycles.

Sample	Zeta Potenial (mV)	Particle Size (nm)
Empty Liposomes	-65.03 ± 3.54	2293.4 ± 63.8
6 (1)	-36.55 ± 0.84	1504.5 ± 63.8
6 (2)	-79.80 ± 1.76	1986.8 ± 315.5
7 (1)	-73.10 ± 1.93	1721.7 ± 97.5
7 (2)	-72.42 ± 3.39	1934.7 ± 134.6
10	-47.06 ± 0.67	1620.1 ± 108.8

Table 5.3 Highlights the zeta potential and particle size of all the anionic liposome formulations produced for the purpose of this study.

5.2.2 FACS Analysis

Four representative traces produced during FACS analysis can be seen in Figure 5.4. In a) b) and c) a single population of cells is represented showing low-level fluorescence, whereas in d) two populations are highlighted. The first of these mimics those depicted in the other three traces, however, the second (indicated by the horizontal line) is not and although a smaller population has a higher level of fluorescence. The fourth trace, produced by anionic liposome-encapsulated **7** in association with *E. coli*, and in comparison to a) bacterial cells, b) empty liposomes and c) free **7**, shows the greatest fluorescence and hence potentially the greatest level of oligonucleotide delivery.

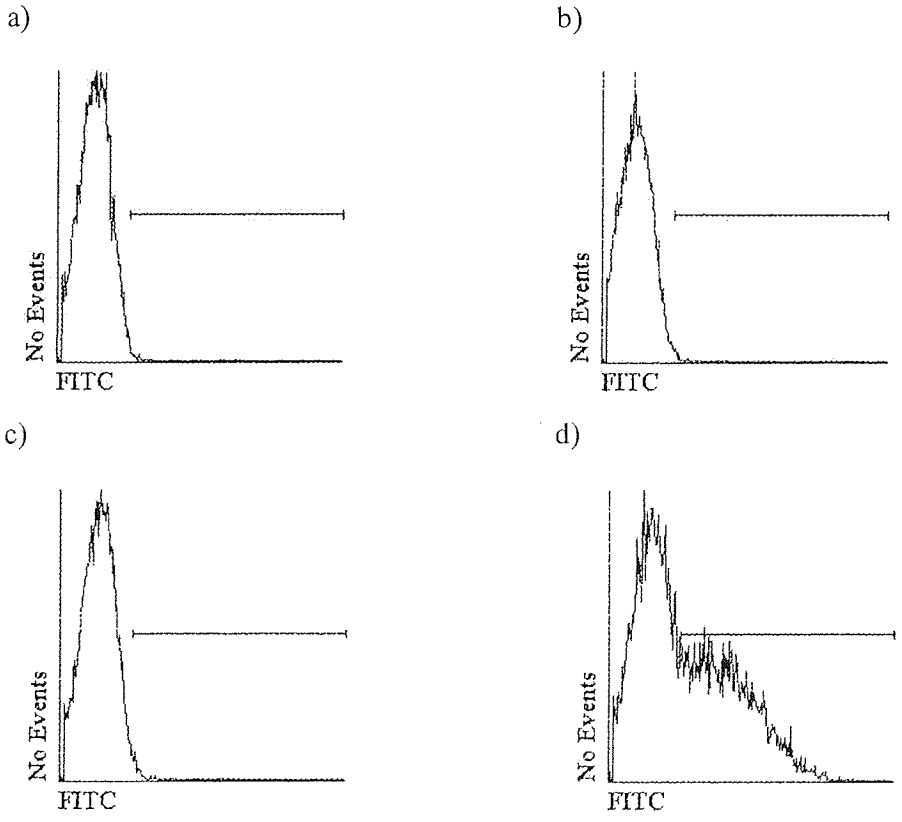

Figure 5.4 Representative FACS traces depicting the different populations of bacterial cells detected when cultures of *E. coli* DH5α were incubated with free **7** and negative liposome encapsulated **7**, with bacterial cultures and empty liposomes used as controls, where a) represents the bacterial culture, b) empty liposomes, c) free **7**, d) liposome-encapsulated **7**. The y-axis represents the number of cells counted and the x-axis illustrates the level of FITC fluorescence detected.

Figure 5.5 highlights the fluorescence produced by anionic liposome-encapsulated **7** when placed in solution with *E. coli* cells at 37 °C, in comparison to the fluorescence produced by bacterial cells alone, empty liposomes and free **7** when measured using FACS analysis. The fluorescence relates to the percentage of cells that fluoresce due to the uptake of the labelled oligonucleotide. The results clearly indicate a heightened level of fluorescence produced by the encapsulated TFO and a significant difference ($P < 0.01$) between this sample and the free **7**.

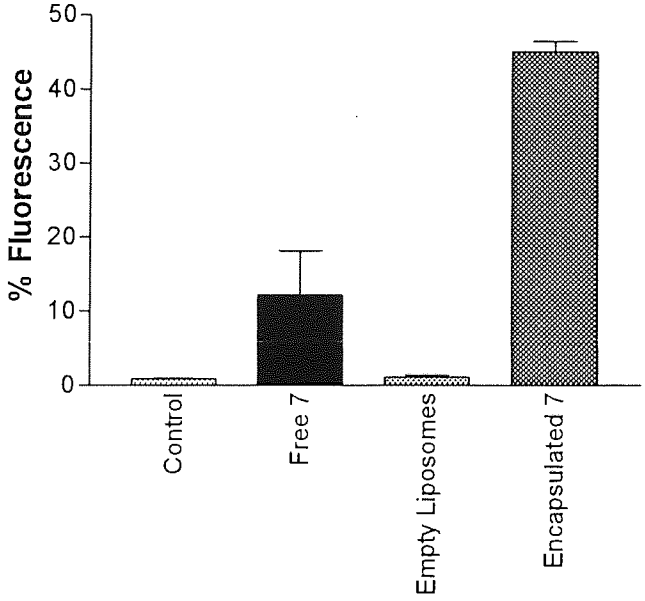

Figure 5.5 Uptake of liposome-encapsulated **7** into *E. coli* DH5α at 37 °C in comparison to free **7** with bacterial culture and empty liposomes used as controls.

Figure 5.6 highlights the results produced from the same analysis carried out for Figure 5.5, but this time the incubation of the agents with the bacterial cells took place at 20 °C instead of 37 °C. Again the level of fluorescence depicted by the culture treated with the encapsulated 7, was by and far the greatest. Statistical analysis used to compare the level of fluorescence exhibited by encapsulated 7 against that demonstrated where 7 was free in solution, showed a significant difference ($P < 0.01$) between the mean fluorescence values.

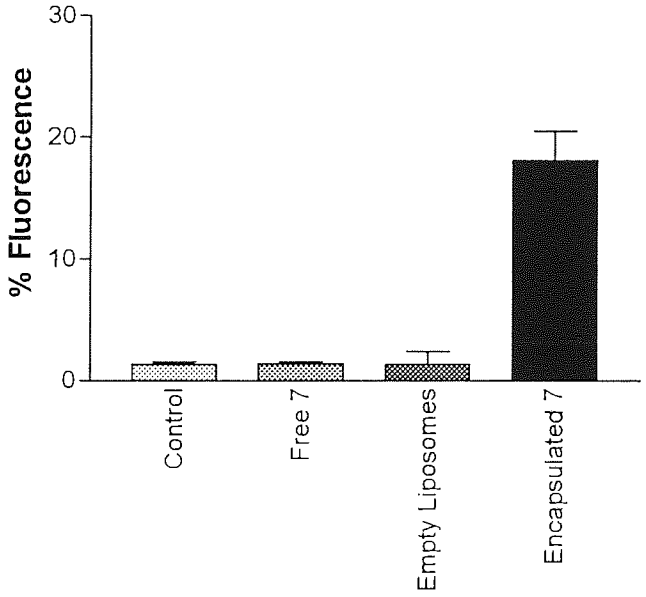

Figure 5.6 Uptake of liposome encapsulated 7 into *E. coli* DH5α at 20 °C in comparison to free 7 with bacterial culture and empty liposomes used as controls.

The level of fluorescence produced by free **7** when added to competent *E. coli* cells produced via the cold shocking procedure was also assessed by FACS analysis (Figure 5.7). A mean level of fluorescence of 13-14% was produced, which was also shown to be variable as depicted by the large error bar. As a result this would imply this delivery system to be less effective than anionic liposomes. Statistical analysis also illustrated the difference between the fluorescence emitted by the control culture and the **7** treated culture, to be insignificant (P = 0.26).

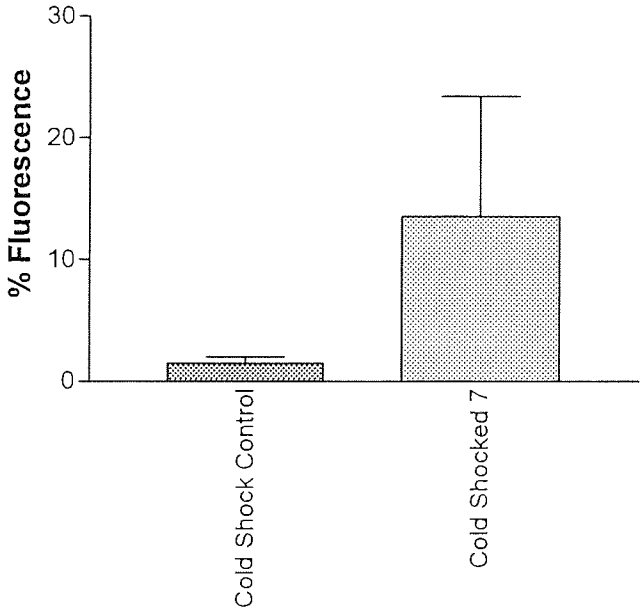

Figure 5.7 Uptake of liposome encapsulated **7** by *E. coli* DH5α after cells were exposed to the cold shocking procedure. Control samples consisted of cold shocked cells without the addition of TFO.

The results in Figure 5.8 illustrate the effect of varying the volume of anionic liposome-encapsulated **7** on fluorescence, measured by FACS analysis, of a static volume of *E. coli* culture. The results indicate that of all the volumes tested, a saturation point, at which further liposome associate with the bacterial cells was not possible, is not reached.

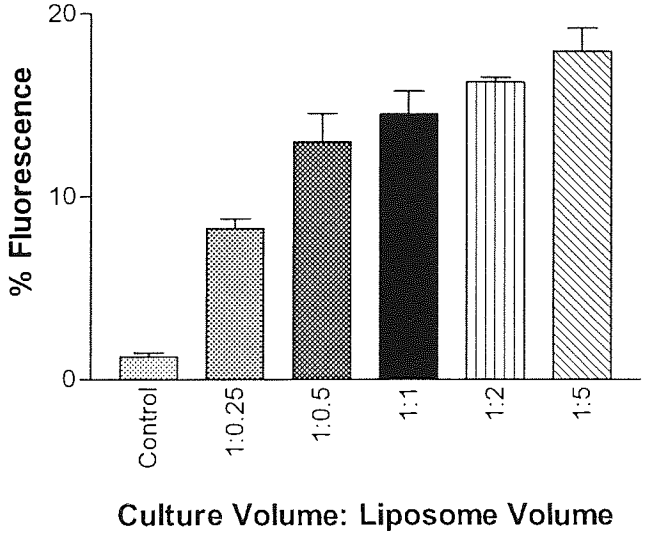

Figure 5.8 Uptake of liposome-encapsulated **7** by *E. coli* DH5α at 37 °C, using an increasing volume of liposome in comparison to a static volume of culture. The control in this case consisted of bacterial culture exposed to empty liposomes.

Figure 5.9 illustrates images of **7** (a) and **10** (b) in association with anionic liposomes viewed by fluorescence microscopy. The numerous small fluorescing vesicles indicate lipoosomes that have encapsulated the fluorescein labelled oligonucleotides, which also highlights the size variation in these samples.

a) b)

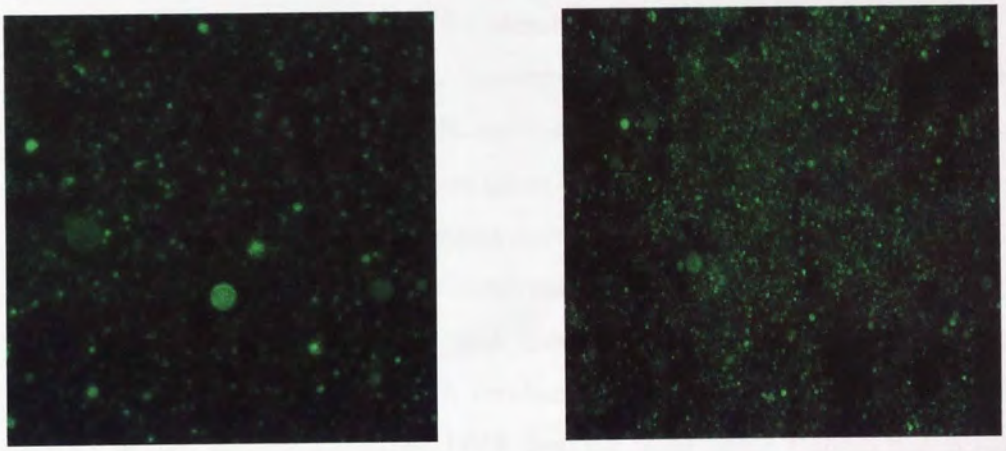

Figure 5.9 Images of fluorescein labelled oligonucleotides in association with anionic liposomes viewed via fluorescence microscopy at 40x magnification where a) represents encapsulated **7** and b) represents encapsulated **10**.

5.3 Discussion

5.3.1 Cationic Lipids

The use of cationic lipids as transfecting reagents is well documented as a means of transfecting cells with oligonucleotides as both antisense and antigene agents. The panel of four (Table 5.2) was chosen due to their strong literature precedents and depth of understanding (page 233 for chemical structures).

Lipofectin® was the first cationic liposome to be produced, back in 1987, and was shown to enhance uptake by 5-100 times in comparison to gene delivery systems at the time, such as calcium phosphate (Blau, *et al.*, 2000). The lipid is made up of the cationic lipid DOTMA, which contains a quaternary ammonium salt in the head group that is responsible for the lipids cationic nature. This is coupled with the neutral lipid DOPE. DOPE acts to stabilise and enhance liposome formulation due to the electrostatic repulsion of DOTMA residues. Cationic lipids containing DOPE have shown greater ability to transfect DNA than the same lipids without this group. It is thought that DOPE actually facilitates membrane fusion between the liposome and the cell membrane, and subsequent release of the DNA into the cytoplasm of the cell (Chapter 1). This is in fact one of the most widely used cationic lipids hence its usage here.

LipoFECTAMINE™ is made up of the cationic lipid DOSPA, an analogue of DOTMA, and again the neutral lipid DOPE. The head contains the polyamine spermine as well as a quaternary ammonium salt and it these that account for the cationic nature of the lipid that allow it to interact with DNA. The multivalent head, as opposed to the monovalent head demonstrated by the lipofectin reagent, make this a more powerful transfecting agent due to an increased ability to interact with DNA and the cell membrane. DNA condensation using this reagent is also more efficient.

CellFECTIN® is made up of the cationic lipid TMTPS in conjunction with the neutral lipid DOPE. In the case of this lipid it is a quaternary ammonium salt that produces the charged head group.

DMRIE-C is made up of the cationic lipid DMRIE coupled to cholesterol. DMRIE also has a quaternary ammonium salt pertaining to the cationic charge in the head group. The cholesterol replaces the DOPE in this lipid and serves to stabilise the lipid:DNA complexes when formed. Lipid containing cholesterol have been shown to

be slightly less efficient as transfecting reagents in comparison to those containing DOPE, but have shown greater biological activity when used *in vivo*.

DOTMA and DOSPA exhibit monounsaturated acyl chains, which show enhanced transfection ability in comparison to saturated anchoring units such as that demonstrated by DMRIE. This has been linked to enhance antisense activity of a given phosphorothioate oligonucleotide when delivered to cells via cationic lipids containing such aliphatic chains (Bennett, *et al.*, 1998). This structural variability, along with the others (i.e. single and multivalency, and DOPE and cholesterol co-lipids), among the agents here was necessary to test such a phenomenon in their transfection ability of bacterial cells (chapter 6).

5.3.1.1 Cationic Lipid Characterisation

Zeta potential analysis of the four cationic lipids, used for the purpose of this study, was carried out in order to gain insight into charge size of the lipids, and the interactions of the lipids with the LB broth used in the antibacterial studies (Chapter 6). Understanding these interactions was necessary to ascertain how TFO delivery would be affected by these delivery mechanisms. The cationic lipid zeta potentials can be seen in Table 5.2. The first section of this table – samples 1-4, shows the true cationic nature of the lipids and indeed the charge variation between the four candidates.

The LB broth, sample 5, shows a negative zeta potential of –12.92, which is unexpected. The reason being the opposing charge of this and cationic lipid creates potential for interaction between the two. This is further indicated by samples 6-9 which show the zeta potentials for the four cationic lipids in association with LB. All four samples with the exception of Cellfectin, sample 7 (which shows a mild positive zeta), show a negative zeta potential hence indicating some form of interaction between the lipids and the LB. This interaction could prevent efficient TFO-lipid interactions, a process that relies solely on opposing charge interactions for complexation. As a result, the negative charge repulsion encountered by the TFOs and the bacterial cell wall, will still remain a barrier to entry. The association process should produce a positively charged lipid-DNA complex. This is necessary for the charge attraction between the complex and the negatively charged teichoic acid or LPS units on the surface of the bacterial cell that mark the first step in the uptake process. Fusion with the cell membrane should then take place and the TFO is

subsequently released into the cytoplasm of the cell. Any interaction with the culture media will inhibit this encapsulation process.

Samples 10-15 enforce this and illustrate the addition of the oligonucleotides in increasing volumes in association with Lipofectin®. The addition of the increasing volumes increases solution negativity in the majority of cases, albeit in a rather unexpected manner. That is, increasing DNA amounts does not increase the zeta potential negatively in a uniform manner.

Sample 16 shows the zeta potential of *E. coli* in association with LB, this demonstrates quite a large negativity, one that the lipids would have to overcome in order to serve as an effective transfection agent.

The results overall indicate the use of the four cationic lipids in association with LB, as is the case under antibacterial assays conditions (Chapter 6), to potentially be a frivolous one. The interaction between the lipids and the LB could prevent efficient complexation with the oligonucleotides, hence diminishing the uptake efficiency.

LB is made up of tryptone, yeast extract, and NaCl in s.d.H_2O. The negative charge is likely to emanate from the proteins found in the tryptone and yeast extract, these two together present an overwhelming negative charge that by far neutralises the positive charge exerted by the Na^+ ions. The problem this poses is that the charge presented by the casein extract and the components of the yeast extract could lead to charge interactions with opposing charges of the cationic lipid heads rendering them neutral, hence effecting complexation efficiency with the oligonucleotide. Therefore, in such media, increased concentrations of lipid maybe necessary for effective complexes to be formed. This phenomenon was investigated by Son *et al* (Son, *et al.*, 2000) who investigated the effects of media on cationic lipid:DNA complexes. They found that although components of the media actually neutralised the charges of the cationic lipids and caused them to aggregate, as soon as the DNA was added liposome aggregation was prevented and stable lipid:DNA complexes formed. Furthermore, the interaction of the DNA with the lipid produced a negatively charged complex, which did not affect transfection efficiencies under optimum conditions. Therefore this would indicate the production of negative zeta potentials during this research, to be unproblematic due to the favourable complexation of the lipid and TFOs. However, to optimise lipid:DNA complexation, an alternative is to make up lipid:DNA complexes in neutral solutions before addition to the LB culture broth. Kim et al (Kim, *et al.*, 1999) actually carried out the delivery of vancomycin via lipid-mediated means for an

antibacterial kill assay in PBS, and then allowed subsequent growth to take place with the addition of nutrient broth, after varying lengths of incubation with the liposomes. Although this was due to the fact that biofilms were being targeted, it is a possibility here and may prevent interactions produced between the lipids and growth media used and hence improve complexation.

All cationic lipids should have been screened with **6**, however, due to the negative properties of the cationic lipids in the media, as indicated in samples 10-15, and the level of interaction shown with the LB broth in samples 6-9, it was decided that other avenues needed exploring in order to find a suitable vehicle for uptake. Hence anionic lipids were assessed for their potential as carriers of the TFOs.

When it comes to choice of cationic liposome, there tends to be few principles regarding structure in relation to uptake efficiency within a given cell line and between cell lines. It seems very much to be a case of trial and error (Miller, 1998). A number of studies have attempted to determine efficiency of a particular liposome measuring properties such as T_c (gel-liquid crystalline transition temperature), cytotoxicity and zeta potential. With the latter there was shown to be a direct correlation between zeta potential and efficiency of gene delivery. However, these rules will depend on the cell line that is being transfected and therefore it is very difficult to make predictions about the effects of structural variations particularly when it comes to biological activity (Ferrari, *et al.*, 2001).

The initial interaction between the lipid and the DNA is a rather complex one and involves massive structural change for both entities. There will be great structural variation determined by the head group of the lipid and the nucleic acids, in the latter this pertains to sequence length and strand nature, and as a result formulations will be to some extent heterogeneous. This is a problem as some formulations of the same lipids will be more successful transfecting agents than others. As a result current research is looking at controlling this initial interaction, which is very dependent on particle concentration, ionic strength of medium, temperature of the mixing medium, rate of mixing, sequence of addition of various components, charge ratio of the complex and the extent of complex formation (Woodle and Scaria, 2001). It is therefore clear that the uptake via this method is a multi-step process and as a result optimisation of all steps is necessary before any prediction regarding uptake behaviour can be determined.

The structure of the liposome complexes formed is also a restricting factor in the efficiency of uptake. Ideally a unilamellar structure is required as it is this that will fuse with the membrane more efficiently and as a result, more efficient release of the oligonucleotide will result. The reason for this is that large multilamellar vesicles (MLV) will contain different layers of lipid-DNA complexes and as a result release of the oligonucletide from this can be more difficult than from an small unilamellar (SUV). Studies have shown that most effective and efficient liposomes are formed when the charge ratio of DNA to lipid is slightly above 1 hence the overall charge is cationic (Hartmann, *et al.*, 1998). When the lipid charge greatly exceeds that of the DNA complex, MLV structures are produced which do not only transfect badly, but high concentrations of lipid are also cytotoxic (Felgner, *et al.*, 1987). Sakurai *et al* (Sakurai, *et al.*, 2000) showed that the zeta potential reaches zero at a ratio of 1:4.47 (DNA:lipid (w/w)) using DOTMA/DOPE (Lipofectin reagent) lipid complexes. However, it was demonstrated that such structures are not effectual in practice due to the ability of the lipids to aggregate forming large vesicles, a process that has been shown via atomic force microscopy.

The cytotoxicity of the lipid:DNA complexes occurs at higher lipid concentrations and has been stated that it should not exceed 20 μg/ml in the case of lipofectin (Felgner, *et al.*, 1993). Problems are caused where large amounts of the lipid are incorporated into the cell membrane resulting in a shift in the overall net charge of the membrane. The movement of this towards the positive changes the properties of the cell membrane and as a result activity of ion channels, membrane receptors and enzymes are affected (Felgner, *et al.*, 1994).

Taking all this into consideration it is clear that successful transfection using cationic lipids is very complex and in order to find a successful reagent, more thorough investigation than that illustrated here is needed. Each step of the uptake cycle requires optimisation with wide spread screening of lipids in association with growth media and the *E. coli* for transfection. As this was not the main focus of this research, time and resources were not available for such study, hence other agents were tested.

5.3.2 Anionic Liposomes

Anionic liposomes were tested as potential transfection reagents due again to strong literature precedents, particularly as uptake agents for bacterial cells.

5.3.2.1 Liposome Characterisation

The effect of increased DPPC content, in the formulation of DPPC and DMPG containing fluidosomes, was assessed via zeta potential and particle size analysis. Figure 5.3 illustrates the results where the concentration of DMPG is kept constant in relation to the DPPC concentration. The zeta potential results indicate a decrease in negative potential as the ratio of DPPC in respect to DMPG increases, something that is not unexpected due to the dilution of the negative charge emanating from the DMPG by the increased concentration of DPPC.

The particle size analysis of the same formulations shows no such pattern with the results and no consistent variation when the DPPC content is increased. This is perhaps not unexpected and indicates that the size is more affected by the level and intensity of sonication. During the process of lipid formulation, a key step in the formulation process is the sonication in order to disrupt MLV to form SUV. The extent of disruption would be dependent on the length and intensity of sonication, which would have varied slightly from one sample to the next. A clear indication of this is in the size variation of liposomes within the same samples, which can be seen in Figure 5.3 b). The error bars indicate variation in the average particle size taken for each of the replicate analyses. This is further indicated by the variation of particle size illustrated in Table 5.3. This table shows the zeta potential and particle size for each of the lipid formulations used for the purpose of this study. Attention is drawn to the particle size variation between liposomes containing the same oligonucleotides i.e. **6**(1) and (2), and **7**(1) and (2). To maintain particle size uniformity application of a size extruder is possible and perhaps necessary if further optimisation of liposomes was to be made. However, such techniques were not necessary here at this stage of the research.

The necessity for SUVs was to enhance encapsulation of the designated TFOs, and to produce vesicles small enough for the transfection of *E. coli*. *E. coli* are approximately 1-5 μM in length, and as a result, large vesicles would not fuse very efficiently due to an increased negative cell surface charge preventing bacterial cell interaction.

The formulation ratio chosen for the purpose of this study was 1:10, the reasons being two fold: A) this ratio has a literature precedent for being particularly efficient at oligonucleotide encapsulation, and also for the transfection of *E. coli* (Fillion, *et al.*, 2001). Fillion *et al* used a 1:10 ratio of DMPG:DPPC respectively and showed high levels of encapsulation of 15mer antisense oligonucleotides along with high levels of uptake into *E. coli*. B) The results in Figure 5.3 show the zeta potential at the same ratio to be more stable, that is the error bars are smallest, and the particle size is shown to be smallest at around 2000 nm.

The results in Table 5.3 show the zeta potential and particle size for each of the formulations used in FACS analysis and the antibacterial work (chapter 6). The methods were used in order to characterise each of the samples. These results indicate that generally, the greater the size of the liposome, the greater the zeta potential, which would correlate with that which is expected. The larger the liposome, the higher the amount of DMPG incorporated into the liposome, which would exert a greater overall negative charge. A larger vesicle could potentially mean a greater volume of oligonucleotide could be encapsulated, again increasing overall negative charge. These properties are likely to be important because they dictate the level of repulsion experienced between the bacterial cell and the oligonucleotide to be transfected. Liposomes with a smaller particle size, and hence slightly lower zeta potential, would be more efficient at internalising the TFO into the bacterial cell. The liposomes formulated containing the desired TFOs, i.e. **6** and **7**, range from ~1000-2000 nm, which in respect to *E. coli* with dimensions of 1-5 μM, is relatively large. It is argued that sizes greater than 500 nm are assumed too large to fuse (Fillion, *et al.*, 2001), sizes that are 3-4 times smaller than those demonstrated here. However, fusion does not necessarily imply complete incorporation of the liposome into the cell membrane, and partial incorporation may be sufficient to allow oligonucleotide release into the cytoplasm (Fillion, *et al.*, 2001). In addition to this, there is growing interest in giant or cell-size liposomes as more effective vehicles for the carriage and delivery of DNA molecules (Sato, *et al.*, 2003). These have the ability to take up larger quantities of DNA and therefore the potential to increase delivery efficiency.

5.3.2.2 FACS Analysis

The FACS analysis was carried out in order to gain insight into the levels of uptake of the fluorescent labelled TFO (**7**), targeted to the *gyrA* gene of *E. coli*. All methods

employed to enhance transfection in the antibacterial kill assays were assessed here in an attempt to determine the most efficient mode of uptake. Fluorescence of the various cell populations is represented in Figures 5.4 to 5.8 inclusive. For the purpose of these results the levels of fluorescence pertain to the level of uptake discussed here and throughout the thesis for simplicity. Although no analyses have been carried out to determine whether levels of fluorescence are a result of actual true cellular uptake, or whether they are simply due to surface binding, the latter is less likely due to the following reasons: the first of these is the fact that the liposomes and the cell surface are anionic in nature and as a result will repel one another, therefore cellular binding is electrostatically unfavourable. If the TFOs were able to escape the liposome by some means (potentially through liposomal leakage), cellular surface binding would again be unlikely due to the electrostatic repulsion emanating from the negatively charged phosphate groups of the TFO backbone. Although unfavourable, such interactions are possible. This has been observed more in eukaryotic cells where the surface binding forms the initial steps in the uptake process via endocytic pathways. However, it has been witnessed in bacterial cells, where studies have shown that exposure of mycobacteria to fluorescently-labelled oligonucleotides at 4 °C, produced fluorescence that resulted predominantly from surface bound DNA and not from internalisation (Attia, *et al.*, 1998). At these temperatures the biological membranes are more rigid and as a result pose more of a barrier to entry.

Had liposomal escape occurred, fluorescence resulting from passive uptake would neither produce levels of fluorescence depicted by the liposomally-encapsulated oligonucleotides, something that is clearly indicated in Figure 5.5 where free 7 indicates the level of uptake of the TFO via passive diffusion to be minimal. Non-specific porin channels are found throughout the cellular surface of *E. coli* and these allow uptake of extracellular particles. It is via these channels that the TFOs could potentially enter the cells during passive diffusion. However, these are approximately 10 times too small to permit entry of the oligonucleotides synthesised for the purpose of this study.

Figure 5.4 shows three representative traces from the FACS analysis, depicting fluorescence produced from the bacterial culture alone, bacterial culture incubated with empty liposomes, bacterial culture incubated with free 7 and bacterial culture incubated with liposome encapsulated 7. The y-axis represents the number of events

or cells counted; a usual run will count 10,000 events. The x-axis represents the level of FITC fluorescence, i.e. the amount of fluorescence emitted by the fluorescein. It is clear in the first three traces that there is a single population of cells that shows little fluorescence. In the fourth trace there are however two populations of cells, the first produced by the same populations demonstrated in the first three traces, and a second that does not appear on any of the other traces. This second population of cells also shows a greater level of fluorescence and is indicated by the horizontal line. This line is also represented in all of the other traces indicating where this second population falls. It is this population that contains those cells that have taken up the fluorescein-labelled oligonucleotides and hence are fluorescing. The simple basis of FACS analysis is that it will isolate populations of cells according to designated markers. Here only two cell populations are being isolated, those that emit the FITC label, and those that do not, however, the FACS has the power to isolate numerous populations in this same manner.

Figure 5.5 shows the level of uptake of free and encapsulated **7** when incubated with *E. coli* at 37 °C for 3 hours. Liposome-encapsulated **7** showed a significantly increased level of uptake ($P < 0.01$) in comparison to the free **7**. Levels of uptake are indicated at 43%, a result that was consistent on the three separate occasions the analysis was performed. Control and empty liposome samples represent fluorescence emitted by the bacteria alone and in the presence of PBS-containing liposomes respectively. These results clearly indicate that the size of the liposomes does not represent too great a problem as a reasonably high level of uptake was demonstrated. However, it may be the case that smaller liposomes would enhance this and perhaps increase the levels of uptake further. In fact Fillion *et al* showed uptake levels of 57% using liposomes that were 316-562 nm in size, which would seem to support this proposal.

The results shown in Figure 5.6 illustrate a repeat of the assay described above but with incubation of the samples at 20 °C. This temperature pertains to that at which the antibacterial assays were carried out in order to promote triplex binding of **6**, which has a T_m of 26 °C. An indication of uptake, at this temperature, was necessary to ascertain whether or not this was the limiting factor in these assays. Uptake via the liposomes is significantly greater ($P < 0.01$) at around 20%. However, both the encapsulated and free **7** showed greatly diminished fluorescence and hence uptake in

comparison to those assays carried out at 37 °C. The latter of these actually shows levels of fluorescence very similar to those demonstrated by the control and empty liposome samples, and hence it is actually questionable if any uptake took place at all. The reason for the difference between the two temperature results illustrated is potentially two fold. The first of these is linked to the cell population. *E. coli* has an optimal replication rate at 40 °C, and replicates, via binary fission, at this temperature at a rate of approximately once every 20 minutes. Below this temperature replication rates generally fall by approximately one replication cycle for every 10 °C. At 30 ° C replication will take place twice every hour instead of three times. As a result of this, bacterial numbers will be greatly diminished in the cultures grown at 20 °C. Therefore less cells are available for uptake of free and encapsulated **7**, the excess of which are lost during the centrifugation cycle, ultimately less fluorescence results. Although this maybe true to some extent this argument would tend to explain the uptake of free **7** more then that of the encapsulated TFO. Bacterial membranes are at their most permeable when the cells are dividing and indeed at their highest rate of division, during log phase. As a result it is not unexpected that the uptake of free **7** is greater at 37 °C than at 20 °C as replication would be more prolific hence allowing greater levels of passive uptake.

The uptake of liposome-encapsulated **7** may well suffer from this to an extent, but lower temperatures actually affect the liposome characteristics in that at such temperatures they become more rigid and less fusogenic; properties that are dependent on the T_c of the lipid. This is true of all biological lipid base membranes, which become less rigid and more fluid like as surrounding temperatures approach their T_c. As a result, fusion between the two membranes will be less efficient. This is concurrent with other investigations that have actually carried out kinetic studies to determine the effect of temperature on the fusion process. Lipid mixing assays, where *E. coli* was incubated with Dipalmitoylphosphatidylcholine (DPPC) and dimyristoylphosphotidylglycerol (DMPG) containing anionic liposomes, were carried out at 4 °C and 37 °C with fusion measured at 30, 60, 90 and 120 min. Fusion levels were less than 5% at 4 °C throughout the time course of the assay, where as at 37 °C (the phase transition temperature of these liposomes), fusion increased for the whole length of time of the assay (Desjardins, *et al.*, 2002). Furthermore, Desjardins *et al* showed, that rates of fusion were very low (0.2%/min for *E. coli*) at 25 °C and less,

with rates increasing dramatically between 28 °C and 31 °C from 0.39 to 0.66%/min, with a final rate of 1.26%/min observed at 37 °C. These correlate with the phase transition temperature of the liposome, which as quoted is 37 °C. It is this temperature at which the lipids in the liposome membrane become most unstable, and it is well known that the destabilisation of this membrane is necessary for the fusion process to take place (Fujii, 1999). As a result, the increased stability and hence rigidity of the liposome membrane encapsulating 7 during the 20 °C assay, is likely to account for the diminished cellular fluorescence and hence uptake.

Figure 5.7 shows the level of fluorescence of free 7 when in the presence of cold shocked cells. These cells were exposed to ice cold $CaCl_2$ with addition of the TFO in order to enhance uptake. This method is widely used in plasmid transfection, and cloning experiments. Its assessment here is based on the use of the protocol in the majority of the antibacterial experiments illustrated in chapter 6. The basis behind the method is not fully understood, and a number of ideas have been put forward from masking of backbone charges and opening of ion channels, to ion trafficking and the upregulation of heat shock proteins (Chapter 1), which all culminate in increased uptake of the oligonucleotide. The results in Figure 5.7 indicate 12-15% uptake of 7, which again is less than the encapsulated TFO at both 20 and 37 °C. However, also apparent is a large error bar, which indicates a degree of inconsistency and a lack of reproducibility in the results produced. Furthermore, statistical analysis of the cold shock results illustrates a non-significant ($P = 0.26$) difference between the level of fluorescence demonstrated by the control and 7 treated culture. This therefore implies this method of uptake to be a non-reproducible means of oligonucleotide delivery.

Finally the volume of liposome-encapsulated 7 added to the bacterial cell suspension was assessed via fluorescence, again using FACS analysis. Here the ratio of bacterial culture to liposome volume was assessed to establish whether the current 1:1 ratio was optimal and indeed to determine whether there was a saturation level. The results are illustrated in Figure 5.8, and indicate, as the volume of encapsulated TFO increases so too does the level of fluorescence, even at a ratio of 1:5, and in fact that during this assay no saturation point is achieved. Also as there are no sign of a plateau at all, it would suggest that to completely saturate the bacterial cells with the liposome-encapsulated fluorescently labelled TFO, the ratio will have to increase well in excess of 1:5. Further analysis is required here to assess this fully.

The results obtained through FACS analysis strongly support the use of anionic liposomes as potential means of TFO uptake into bacterial cells. However, a number of problems arise here, firstly, no experimentation has been carried out in order to determine whether or not the TFOs are actually encapsulated inside the liposome, something that would be necessary for efficient transfection. Secondly, if the TFO is encapsulated, what concentration of the oligonucleotide is indeed taken up by the liposomes during the formulation process.

In answer to the first of these problems, attempts were made to address the encapsulation via two methods. The first of these utilised fluorescence microscopy in order to visualise the liposomes. Figure 5.9 demonstrates one of the images produced by this method. Although the images indicate association of the liposomes with the fluorescein-labelled oligonucleotide, they do not show clear evidence that the oligonucleotides are actually encapsulated. As a result the second method of agarose gel electrophoresis was employed (data not shown). Intact lipid samples were run with lysed lipids through a gel containing ethidium bromide (EtBr). The basis of this was if TFOs were internalised by the liposome then intact samples would show no fluorescence under UV imaging and as a result would be unable to transcend the gel. If on the other hand they had associated to the exterior of the lipids then fluorescence would be observed in the wells. The lysed lipids were expected to show free movement of the DNA. Unfortunately no evidence of either of these phenomena was shown during gel imaging. This was perhaps due to the time span between the original formulation and the gel experiments. Exonucleases are ubiquitous throughout the environment and had samples been contaminated with these, either from instrumentation used during the formulation process or via human interaction, then degradation of the DNA would have been certain, hence it was not present in these studies. However, Fillion *et al* (Fillion, *et al.*, 2001) carried out the same set of gel analyses, after using the same formulation and reconstitution protocol as outlined here. They showed clearly that their antisense oligonucleotides were completely encapsulated within the liposomes. This is further supported by Perrie and Gregoriadis (Perrie and Gregoriadis, 2000). Their work investigating characteristics of anionic and cationic liposomes showed that lipids formed via the DRV method fully internalised the DNA, as opposed to those lipids that were allowed to simply associate with the DNA.

The second issue regarding the amount of encapsulated TFO, becomes significant in the next chapter where liposomes containing sequence **6** are used as antibacterial agents. The assumption made here, was that levels of encapsulation were similar to those demonstrated by Fillion and co-workers, who showed encapsulation efficiencies of 43.5% after lysis of liposomes, and UV-spectrophotometric analysis. Taking this into consideration 43% encapsulation efficiency was expected, indicating 8.6 μM of the initial 20 μM stock was, in fact, encapsulated.

Although both cationic and anionic lipids show potential as vehicles for uptake of oligonucleotides, currently the case is stronger for anionic lipids, particularly in bacterial cells. This is due to the lack of intracellular DNA release and the inefficiency of cationic lipid delivery as discussed above and in Chapter 1. This is also supported by work carried out by Robinson and co-workers who compared directly the antibacterial effect of triclosan delivered to bacterial biofilms by cationic and anionic liposomes (Robinson, *et al.*, 2001). They showed that a marked increase in bacterial inhibition when the triclosan (an antibacterial agent) was delivered via anionic liposomes. There is in fact a lack of studies in which cationic liposomes are used as effective transfection agents in bacterial cells for the delivery of antibacterial agents. Consequently, knowledge is lacking concerning the behaviour of such agents and hence content release into prokaryotic cells. Conclusions drawn here are done so from properties relating to uptake in mammalian cells and the lack of uptake pathways, such as the endosomal and lysosomal pathways, in bacterial cells. As a result it is presumed that the process of cationic lipid uptake is governed by fusion in bacterial cells as opposed to endocytosis in mammalian cells.

Encapsulation in anionic liposomes does not suffer from release problems, as with cationic lipid uptake, due to the absence of interaction between the DNA and the lipid. Here, uptake is reliant on fusion with the cell membrane, which is expected to expel the DNA into the cytoplasm of the cell. Such a mechanism has been demonstrated where liposome-encapsulated tobramycin was used to treat both sensitive and resistant strains of *Pseudomonas aeruginosa*. This is an interesting model as *P. aeruginosa* demonstrate their resistance through thickened cellular walls, which serve as permeability barriers to current therapeutics. Studies have shown anionic liposomes, with the same components as those demonstrated for the purpose of this study, to be able to fuse with these thickened membranes and exert strong levels of

bactericidal activity (Sachetelli, *et al.*, 2000). This was even possible at concentrations of the antibiotic lower than 50% of the MIC of the given agent (Beaulac, *et al.*, 1998). Sachetelli *et al* showed via negative staining techniques applied to electron microscopy, that fusion is the mechanism that takes place between the liposome and the bacterial outer membrane. Images actually revealed thickening of the outer membrane where fusion had taken place. As a result liposomal release does not hinder uptake efficiency. Although this is only one step in the uptake cycle it is one of the major limiting steps of the cationic lipid approach that has been the centre of a great deal of research.

What is perhaps surprising is the initial interaction of these liposomes and the bacterial cell wall that allows fusion to take place. The anionic nature of both the liposome and the cell wall would be expected to result in repulsion, hence preventing any interactions. Currently this initial interaction is not fully understood but it has been proposed that the interaction takes place potentially via hydrogen bonds between hydroxy-containing groups in the head of the liposome and polymers associated with the bacterium (Jones, *et al.*, 1994). In this study, where anionic liposomes containing triclosan were used to deliver the agent to bacterial biofilms, it was postulated that these hydroxy-containing head groups could hydrogen bond with polymers in the biofilm, providing a strong enough interaction to allow the fusion mechanism to take place. However, it is possible that similar interactions could take place between the liposome and components of the bacterial cell wall.

In conclusion, anionic liposomes would seem to be promising tools for the uptake into bacteria, including *E. coli* studied here. For use as a therapeutic agent an increase in uptake would be necessary and hence further optimisation of these liposomes is necessary. For cationic lipids to be a successful strategy, optimisation of every step of the uptake cycle, and applicability to bacterial uptake explored.

6.0 *IN VIVO* ANTIBACTERIAL EVALUATION

6.1 Introduction

This chapter outlines the antibacterial action of the pre-mentioned TFOs, and assesses their ability to form triplexes *in vitro*, under conditions that mimic those that exist *in vivo*. It has been shown in previous chapters that a number of the TFOs were able to form triplexes under triplex-promoting conditions, and it was now necessary to test this ability within the bacterial cell where intracellular conditions were not so favourable as those exhibited during the melting studies. These antibacterial assays were designed to test the uptake mechanisms explored to date, along with the ability of the TFO to find its molecular target, while avoiding non-specific binding sites, and bind with sufficient strength to cause cell death. It was for this purpose that the research was carried out, with the sole aim to produce antibacterial oligonucleotides. The sequences used for this section of the study are highlighted in Table 6.1.

Table 6.1 The sequences used for the purpose of work carried out in this chapter.

TFO	Sequence
3	5'-AAAAGAAAAACGCGTGGAAGG-3'
4	3'-AAAAGAAAAACGCGTGTAAGG-Acr-5'
5	3'-CGGAGAAAAGTGAAGAAGAAC-Acr-5'
6	3'-AAAAGAAAAACGCGTGGAAGG-5'
8	3'-AAAAGAAAAACGCGTGGAAGG-5'
9	3'-CGGAGAAAAGTGAAGAAGAAC-5'
11	5'-TTTTGTTTTTGGGGGGGTTGG-3'
13	3'-TTTTGTTTTTGGGGGGGTTGG-5'
15	5'-UUUUGUUUUUGGGGGGGUUGG-3'
16	3'-AAAAGAAAAACGCGTGGAAGG-5'
17	5'-AAAAGAAAAACGCGTGGAAGG-3'
18	5'-TTTTGTTTTTGGGGGGGTTGG-3'
19	3'-TTTTGTTTTTGGGGGGGTTGG-5'
20	5'-TTTTGTTTTTGGGGGGGTTGG-Fl-3'
21	3'-TTTTGTTTTTGGGGGGGTTGG-Fl-5'
22	5'-TTGGTGTGGGTTGGTGTGTTT-3'
25	5'-TTTTCTTTTTGCGCACCT-3'
26	5'-TTTTCTTTTTGCGCACCT-3'
27	5'-Acr-TTTTCTTTTTGCGCACCT-3'
30	5'-TTTTGTTTTTTGTGGGGTTGG-3'
31	5'-Acr-TTTTGTTTTTTGTGGGGTTGG-3'
32	3'-TTTTGTTTTTTGTGGGGTTGG-5'
33	3'-TTTTGTTTTTTGTGGGGTTGG-Acr-5'
36	3'-AAGGAAAAAGTGGAAGTG-5'
38	3'-TCTTTTTCTTCTTCAACCCT-5'
39	3'-AGAAAAAGAAGAAGCCGGGA-5'

6.2 Results

6.2.1 *E. coli* Kill Assays

Figures 6.1 to 6.14 illustrate the antibacterial activity of the stated TFOs, designed for the purpose of this study, against *E. coli* DH5α, using CFU/ml as a measure of their action in all cases except in Figures 6.8 and 6.9, where antibacterial activity is determine by BacLight™ stains.

6.2.1.1 The Passive Uptake Assay

a)

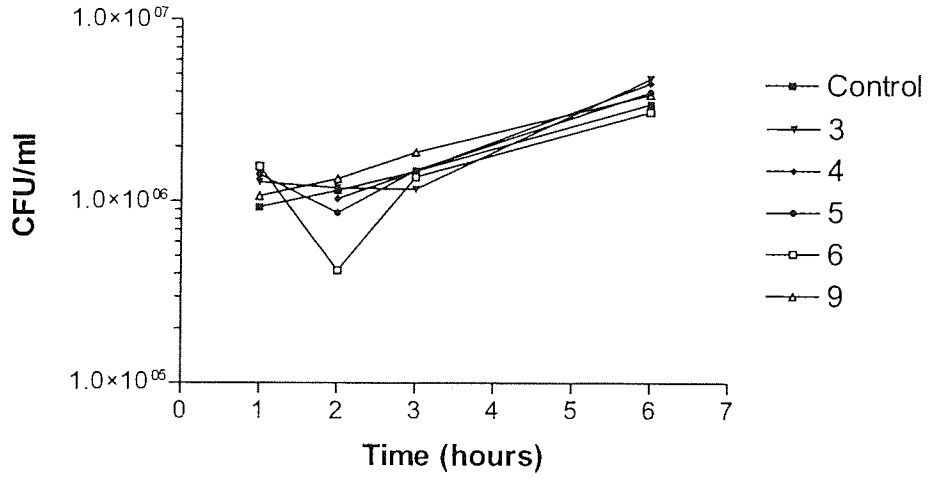

b)

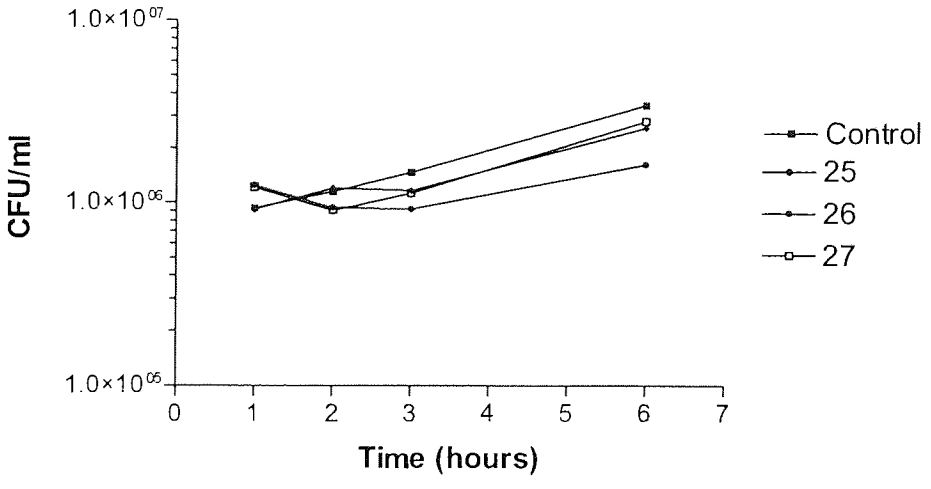

Figure 6.1 Antibacterial activity of TFOs vs *E. coli* DH5α, relying on passive uptake, of a) **3-6** and **9** b) **25-27**, where live cell numbers were determined by colony counts from which colony forming units (CFU) per millilitre were determined.

Figure 6.1 a) illustrates minimal and non-consistent antibacterial activity by the designed TFOs, where oligonucleotide delivery is reliant on passive uptake. Sequences **5** and **6** show diminished CFU/ml after 2 hours but this is followed by outgrowth of the organism. In Figure 6.1 b) all TFO-treated cultures demonstrate a pattern of growth similar to that of the control culture. The only culture to show a slight decline in bacterial numbers is that treated with **26** where CFU/ml are diminished in comparison to the other cultures.

6.2.1.2 The Cold Shock Assays

6.2.1.2.1 The Viable Count Assays

6.2.1.2.1.1 Compound **6**

The results obtained for the antibacterial activity of **6** under the cold shocking conditions (Figure 6.2) illustrate clear inhibition of the bacterial culture in Figures 6.2 a), b) and c). Here the TFO-treated cultures exhibit a marked decrease in the CFU/ml in comparison to non-TFO treated cultures. This is apparent with cultures containing high and low bacterial numbers and is consistent over 6 to 24 hours.

Figure 6.2 c) however, indicates a representative case where the TFO-treated culture exhibited a level of growth similar to the non-TFO treated control culture, and hence highlighting a case where **6** was inactive.

a)

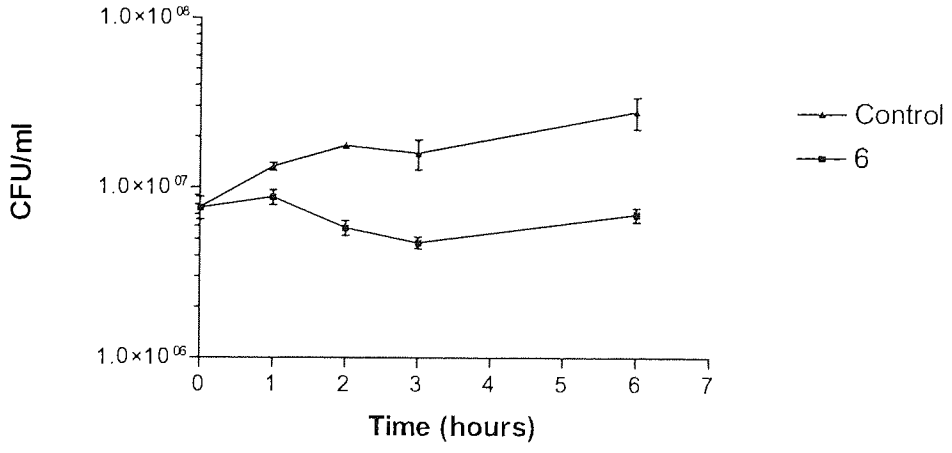

Figure 6.2 Continued over the page

b) (i)

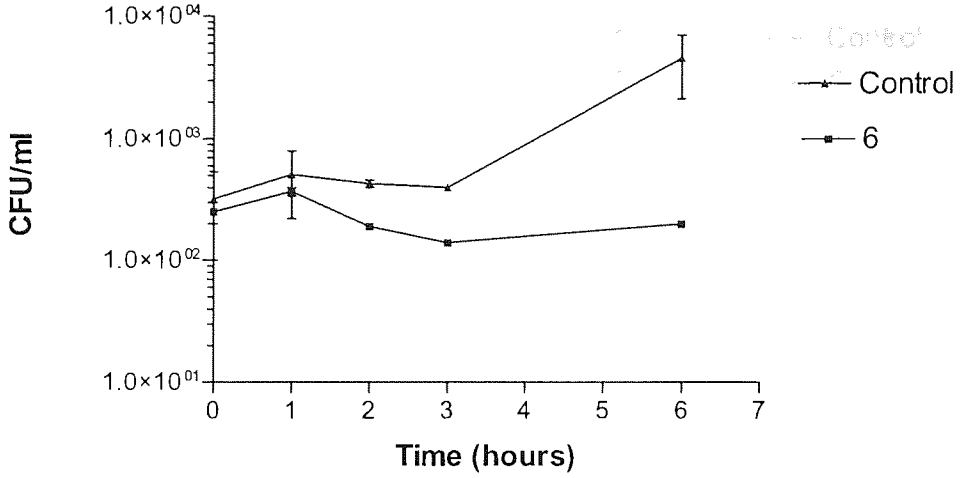

(ii)

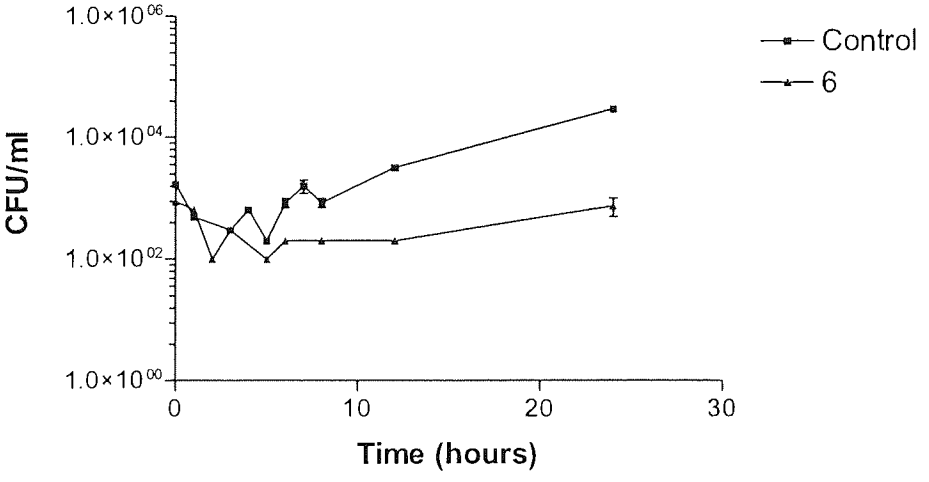

Figure 6.2 Continued over the page

c)

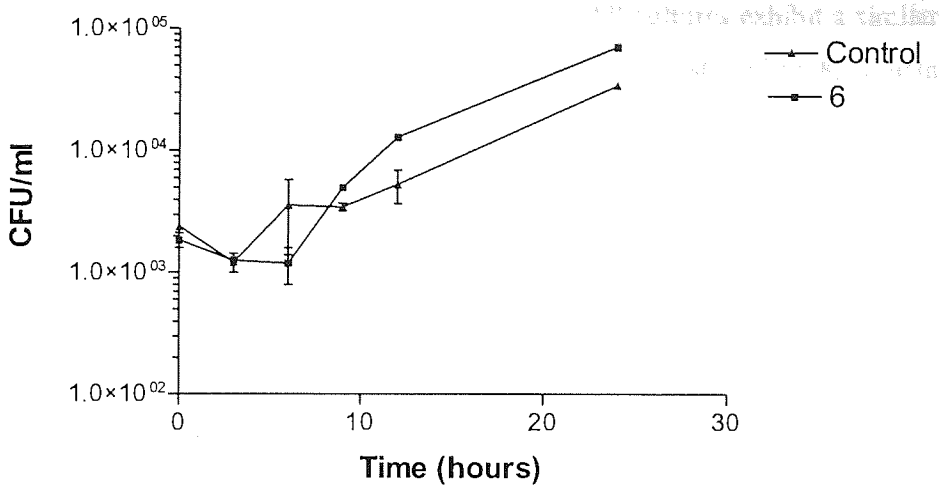

Figure 6.2 The antibacterial activity of **6** against *E. coli* DH5α after application of the cold shocking methodology to produce competent cells using: a) the initial cold shocking technique without the addition of LB broth; b) the modified cold shocking technique without the addition of LB, produced for low cell concentrations; and c) depicts a representative kill curve of **6** under the modified cold shock conditions as described in b).

6.2.1.2.1.2 Compound **8**

The results depicted in Figure 6.3 illustrate the antibacterial activity of **8** in comparison to **37** and a bacterial control culture. All cultures exhibit a similar pattern of growth and as a result no bacterial inhibition is demonstrated by **8**, something that is apparent over 7 and 24 hours.

a)

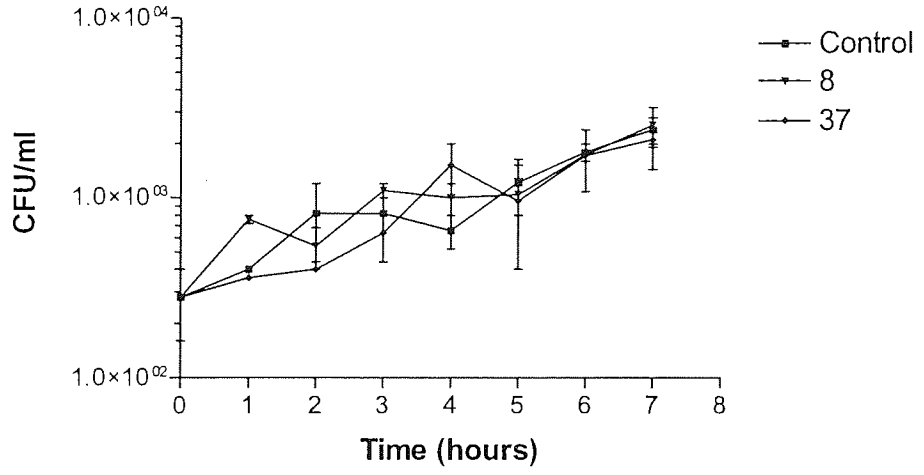

b)

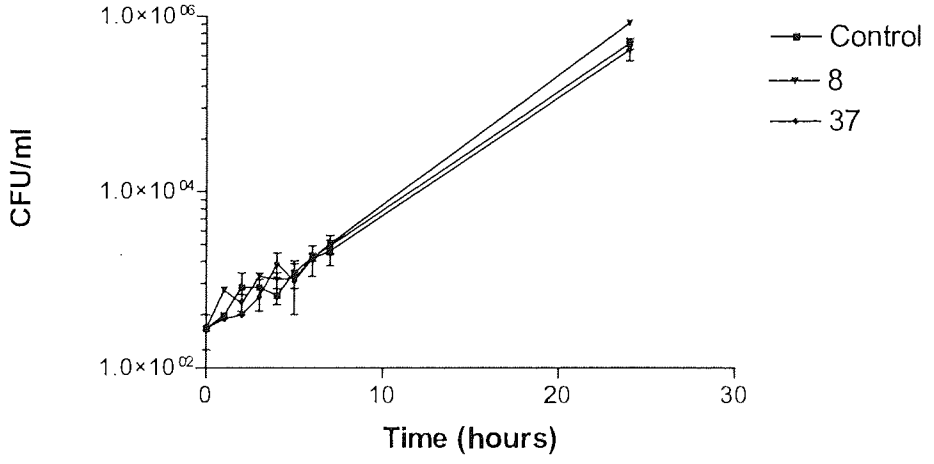

Figure 6.3 The antibacterial activity of **8**, with **37** used as a control sequence, utilising the modified cold shock technique, with oligonucleotides diluted in LB, after a) 7 hours and b) the same assay after 24 hours.

6.2.1.2.1.3 Compounds **25, 26 and 27**

The kill curve represented in Figure 6.4 demonstrates the antibacterial activity of **25-27** in comparison to a non-TFO treated bacterial culture under cold shock conditions. In this case, all TFO-treated cultures demonstrated a level of antibacterial activity, illustrated by the diminished CFU/ml in comparison to the control culture.

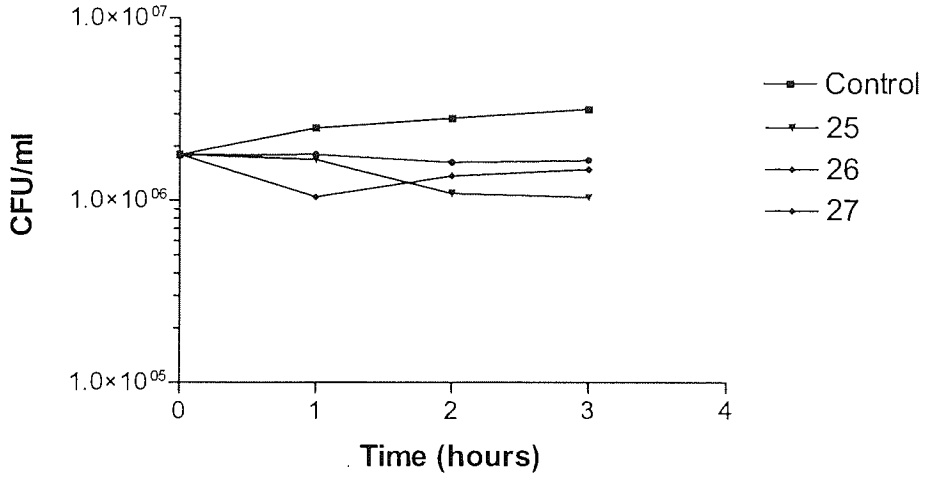

Figure 6.4 The antibacterial effect of **25-27** against *E. coli* DH5α utilising the initial cold shock protocol.

6.2.1.2.1.4 Compounds **11** and **15**

Figure 6.5 illustrates the antibacterial effect of **11** and **15** (the 2'-*O*-methyl modified oligonucleotide) against *E. coli* DH5α again under cold shocking conditions in comparison to **38** treated cultures and a bacterial control culture. The kill curve illustrates the outgrowth of the control culture by all of the TFO-treated cultures and hence the absence of an antigene effect.

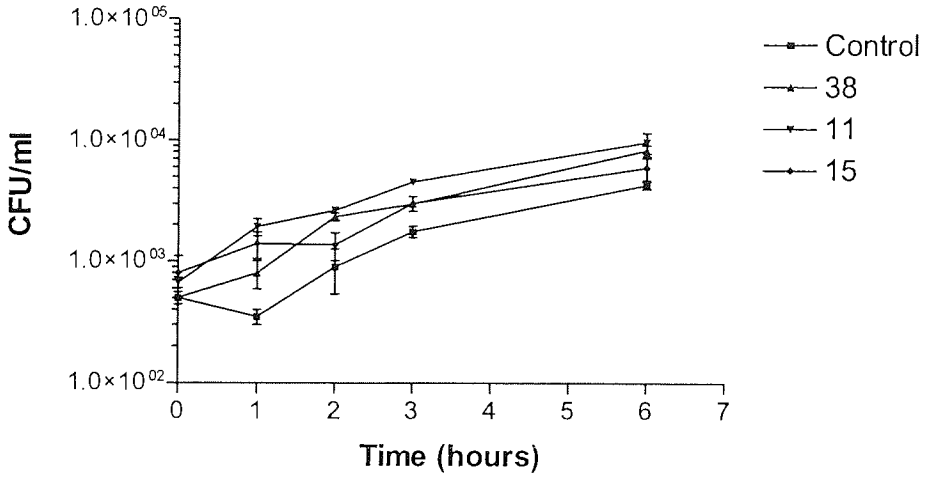

Figure 6.5 Antibacterial activities of **11** and **15** against *E. coli* DH5α utilising the modified cold shock protocol where **38** was used as a control sequence. TFOs were diluted in LB before addition to bacterial cultures.

6.2.1.2.1.5 The Phosphoramidate Sequences

Figure 6.6 demonstrates the antibacterial activity of the phosphoramidate sequences at 20 °C (Figure 6.6 a)) and 30 °C (Figure 6.6 b)). In both cases all the TFO-treated cultures outgrew the control culture indicating an absence of bacterial inhibition.

a)

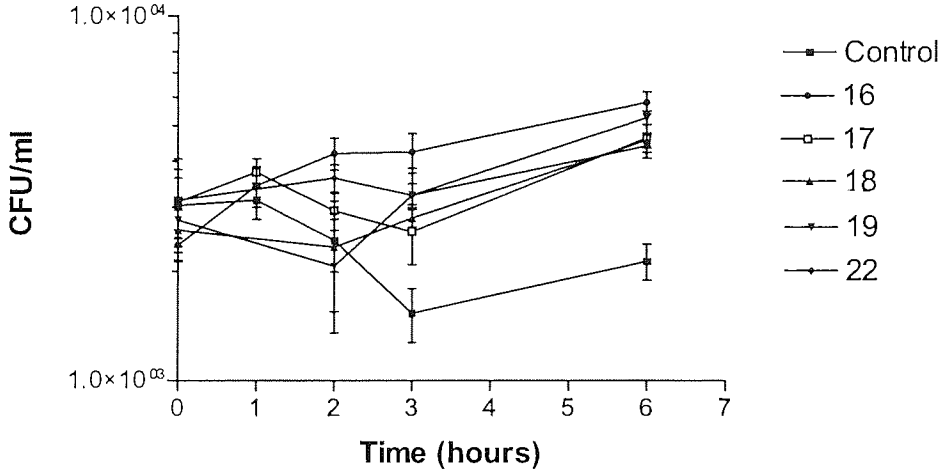

b)

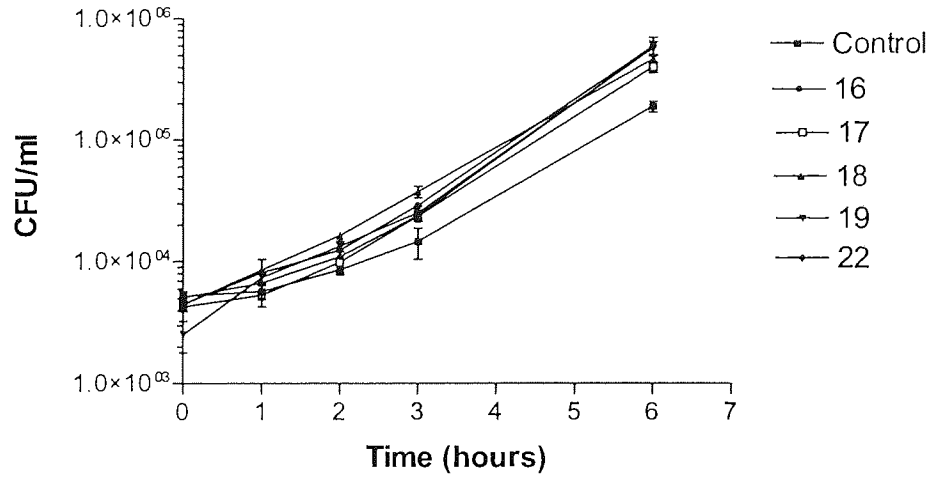

Figure 6.6 Antibacterial activity of the phosphoramidate sequences against *E. coli* DH5α using the modified cold shock protocol at a) 20 °C, and b) 30 °C.

6.2.1.2.1.6 Non-specific Antibacterial Activity

The results demonstrated in Figure 6.7 illustrate the antibacterial activity of **3** and **5** in comparison to a non-TFO treated control culture. Cultures treated with the TFOs exhibit diminished CFU/ml consistently for 24 hours. Figure 6.7 a) (i) and (ii) are representative of the same assay with a) (i) illustrating the level of bacterial suppression over 12 hours. The basis of the antibacterial activity is unfounded due to the non-sequence specific nature of the TFOs used.

a) (i)

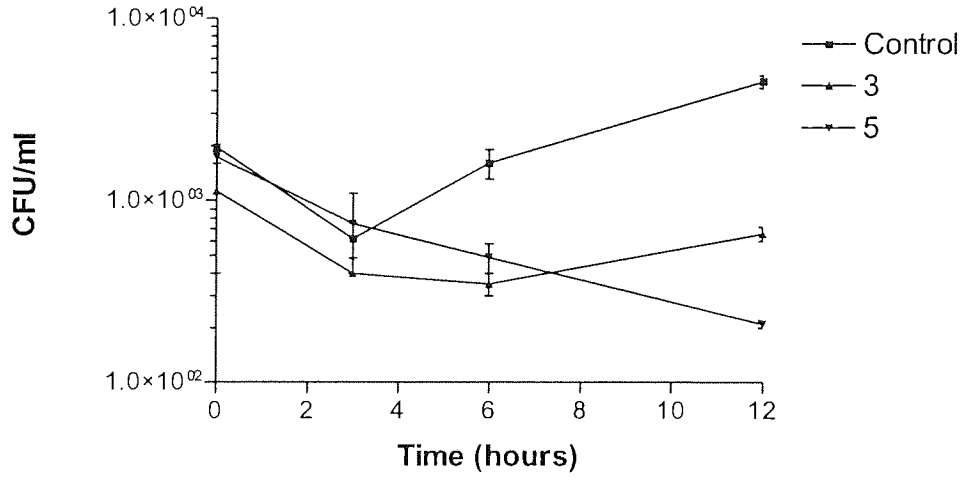

(ii)

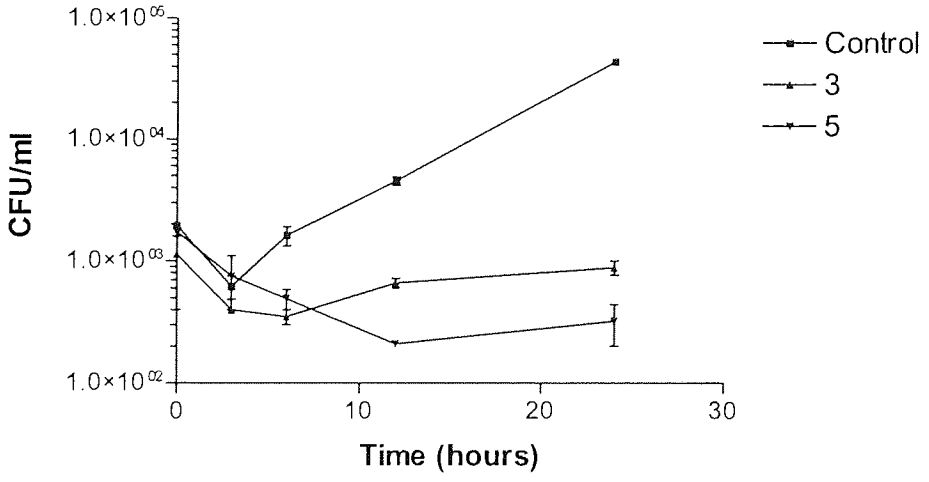

Figure 6.7 Continued over the page.

b)

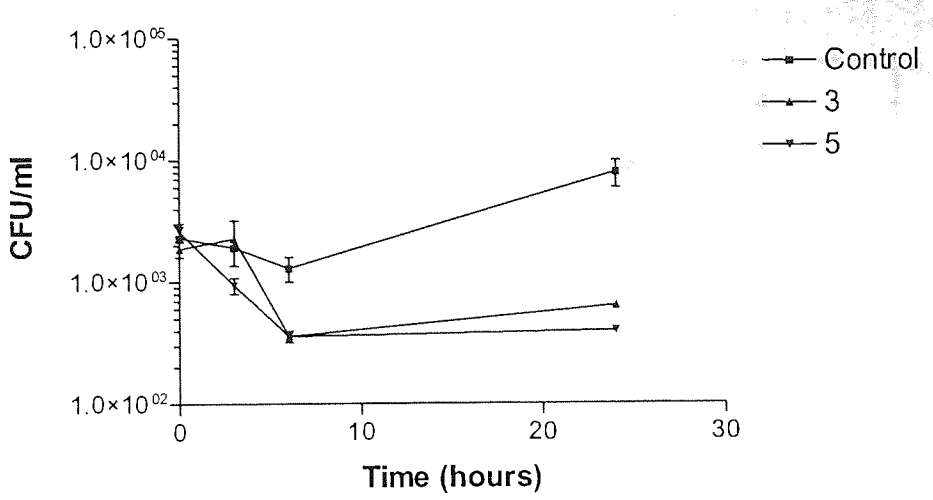

Figure 6.7 The antibacterial activity of **3** and **5** against *E. coli* DH5α via non-specific means after a) (i) 12 hours and (ii) the same assay after 24 hours, and b) a separate assay carried out under the same cold shocking conditions.

6.2.1.2.2 The BacLight™ Assay

The BacLight™ stains were used in order to determine antibacterial activity of the given TFOs, due to the potential failure of the viable count assays to fully demonstrate antibacterial kill. This was postulated to result from outgrowth of TFO-infected cells by those that had failed to take up the oligonucleotide. Data shown depict the green/red (G/R) ratio on the y-axis against time on the x-axis. The G/R ratio shows the concentration of live cells that take up Syto 9® stain and fluoresce green and the concentration of dead cells that take up the propidium iodide and fluoresce red. In a given population where dead cells predominate, the ratio will be small. Where live cells predominate and grow, the ratio will be higher and increase over time.

6.2.1.2.2.1 Compound **6**

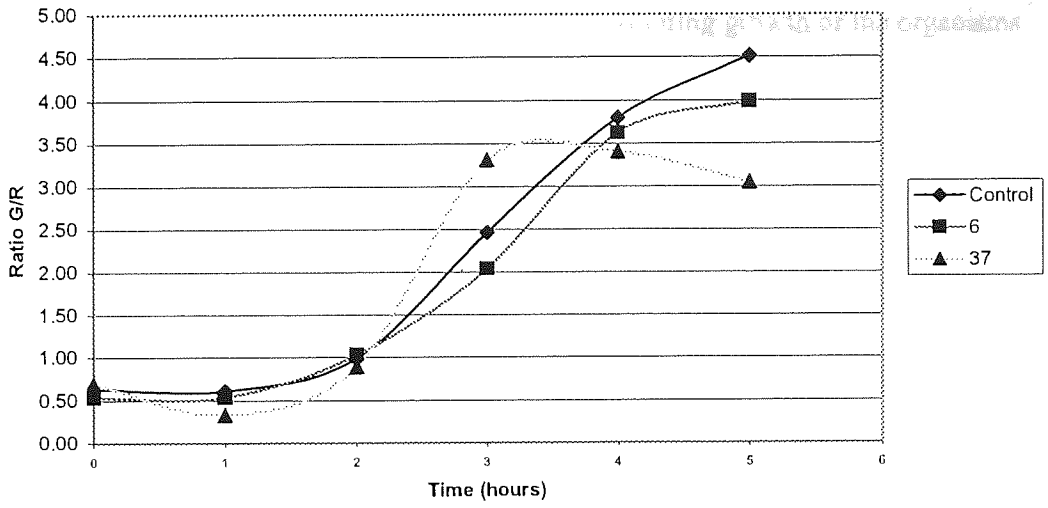

Figure 6.8 The antibacterial effect of **6** after employing the cold shock technique using the BacLight™ stains.

6.2.1.2.2.2 Compounds **11** and **15**

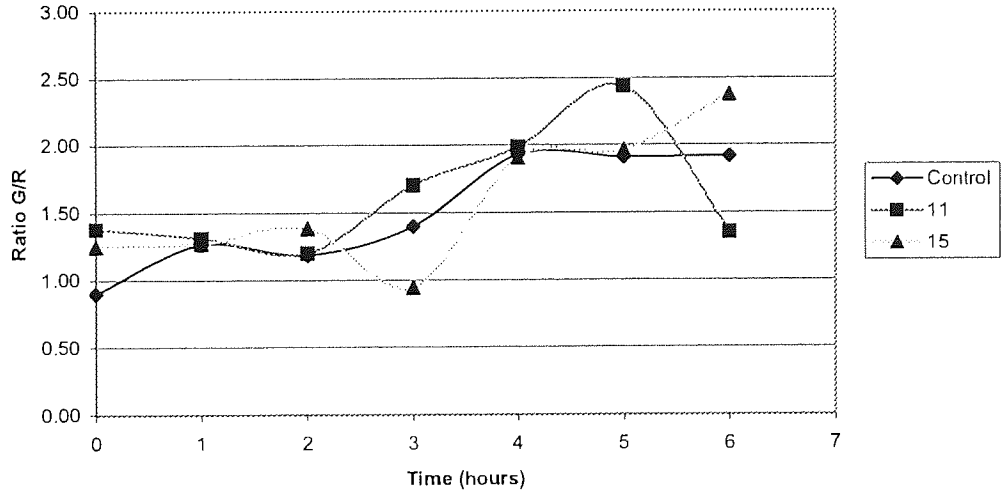

Figure 6.9 Antibacterial activity of **11** and **15**, assessed via the BacLight™ stains after cells were made competent using the cold shock technique.

Figures 6.8 and 6.9 indicate the antibacterial activity of **6**, **11** and **15** against *E. coli* DH5α using the baclight stains. Both curves indicate minimal antibacterial activity, exhibited by the gradual increase in G/R ratio, demonstrating growth of the organisms in the presence and absence of the TFOs.

6.2.1.3 CPZ Aided Uptake

Chlorpromazine (CPZ) was used in an attempt to enhance the uptake of the **6** via a means of chemical mediated uptake. A minimum inhibitory concentration (MIC) of CPZ had to be ascertained prior to commencement of the antibacterial assays due to its own antibacterial properties if administered at certain doses.

6.2.1.3.1 CPZ MIC

Table 6.2 The effect of CPZ concentration upon absorbance of *E. coli* DH5α. The MIC of CPZ = 55 μg/ml.

Chlorpromazine (μg/ml)	Absorbance (at 470 nm)
70	0.063
65	0.063
60	0.072
55	**0.075**
50	0.114
45	0.121
40	0.120
35	0.146
30	0.166
25	0.265
20	0.323
15	0.355

6.2.1.3.2 CPZ Kill Assay

The kill assay using **6** in conjunction with CPZ (Figure 6.10) showed no antibacterial activity, and the culture treated with both agents actually demonstrated the greatest level of growth over the 3 hour time course of the assay.

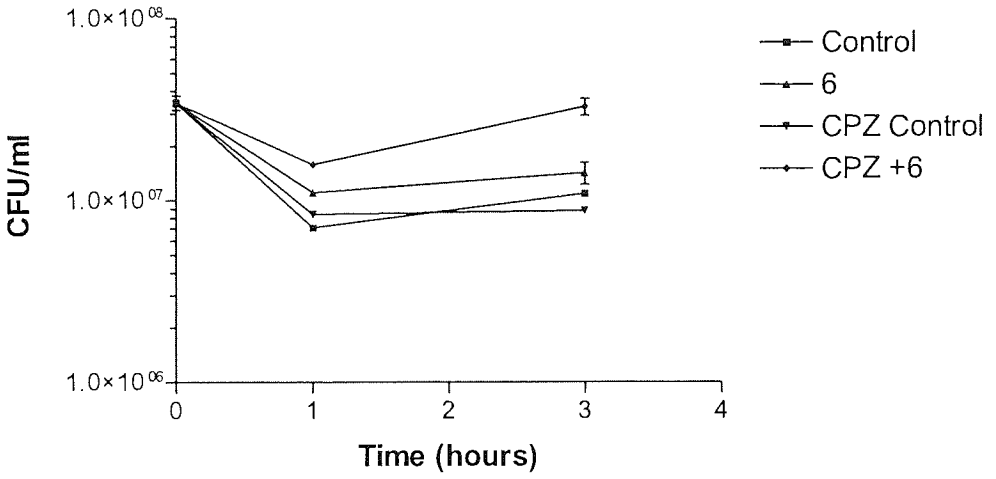

Figure 6.10 The antibacterial activity of **6** against *E. coli* DH5α in conjunction with CPZ.

6.2.1.4 Lipofection Aided Uptake

6.2.1.4.1 Cationic Lipid Kill Assays

Cationic lipids were used as a tool for delivery due to their ability to self-complex with the oligonucleotides producing positively charged complexes. These are able to interact with the outer membrane and release the oligonucleotide into the cytoplasm of the cell and hence increase oligonucleotide delivery efficiency. Figure 6.11 shows the antibacterial activity of **6** and **25** against *E. coli* DH5α when associated with the cationic lipids: Lipofectin®, Lipofectamine™, Cellfectin® and DMRIE-C. Antibacterial activity was only demonstrated by **25** in association with Cellfectin (Figure 6.11 c) (ii)) and DMRIE-C (Figure 6.11 d) (ii)) where it was more effective with the latter. The absence of any antibacterial activity demonstrated by **6** was clearly shown by the outgrowth of the control culture by the culture treated with sequence 6.

a) (i)

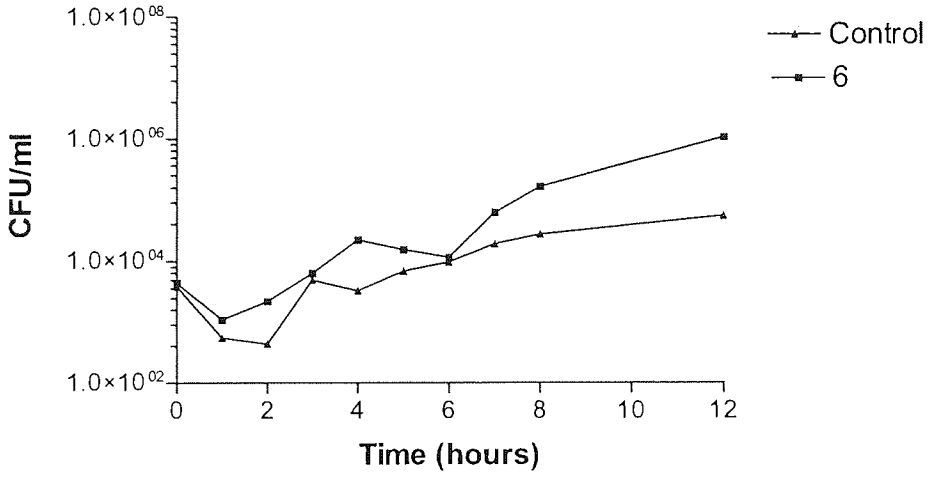

(ii)

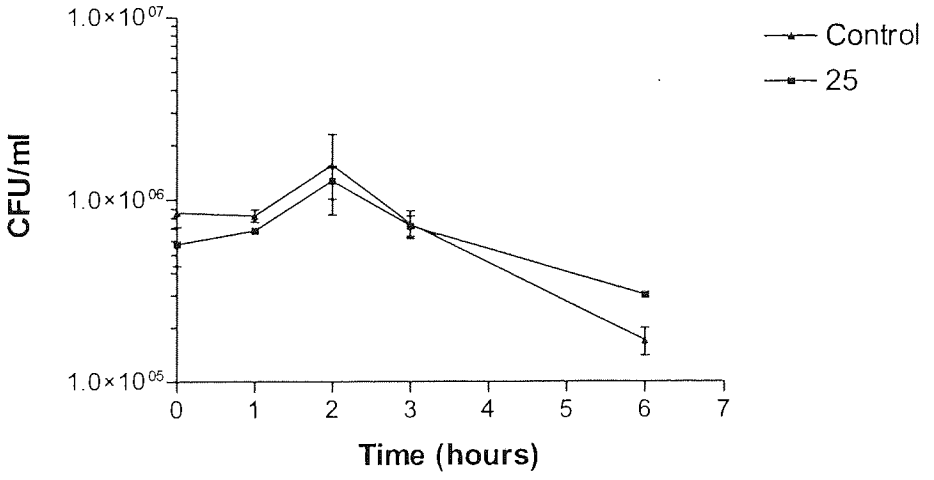

Figure 6.11 Continued over the page

b) (i)

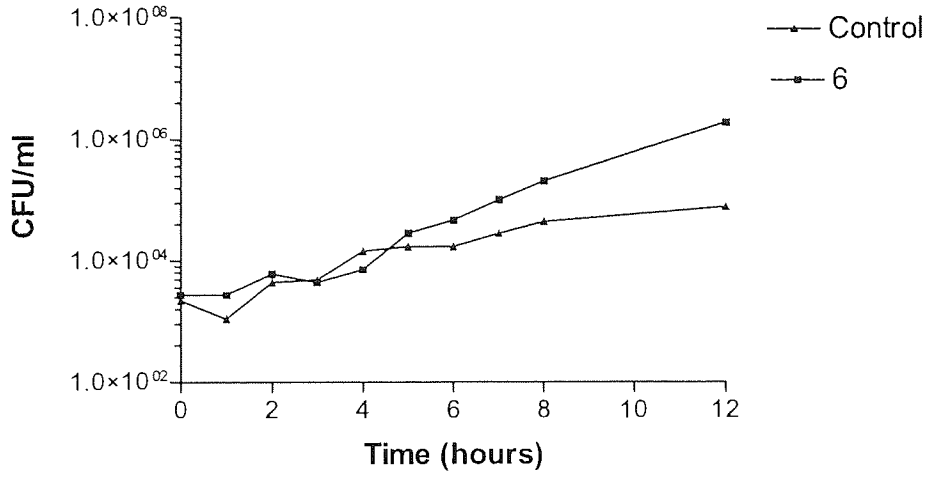

(ii)

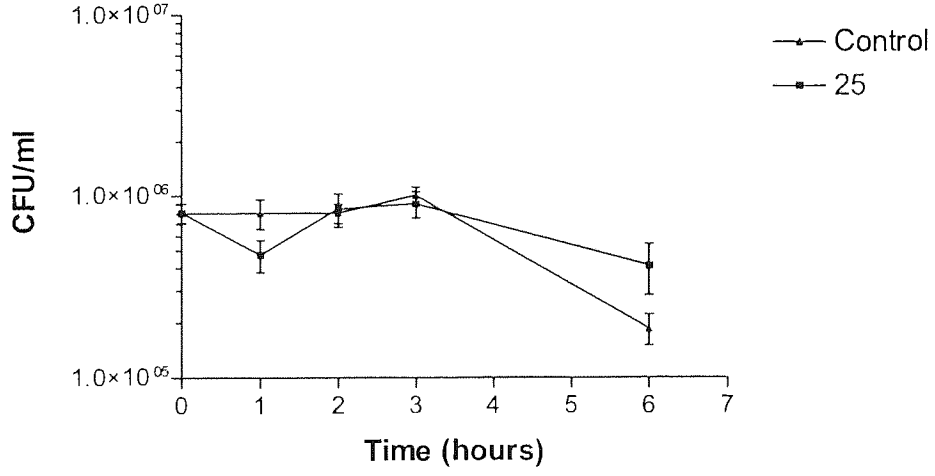

Figure 6.11 Continued over the page.

c) (i)

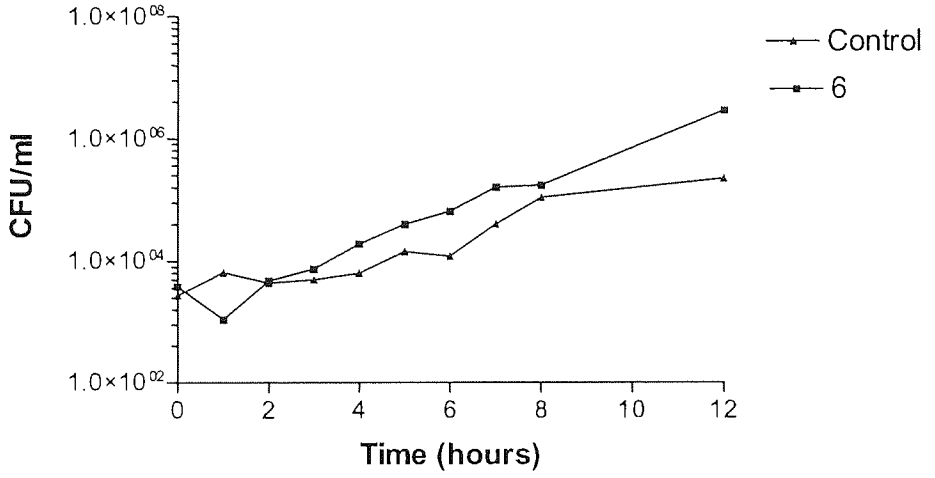

(ii)

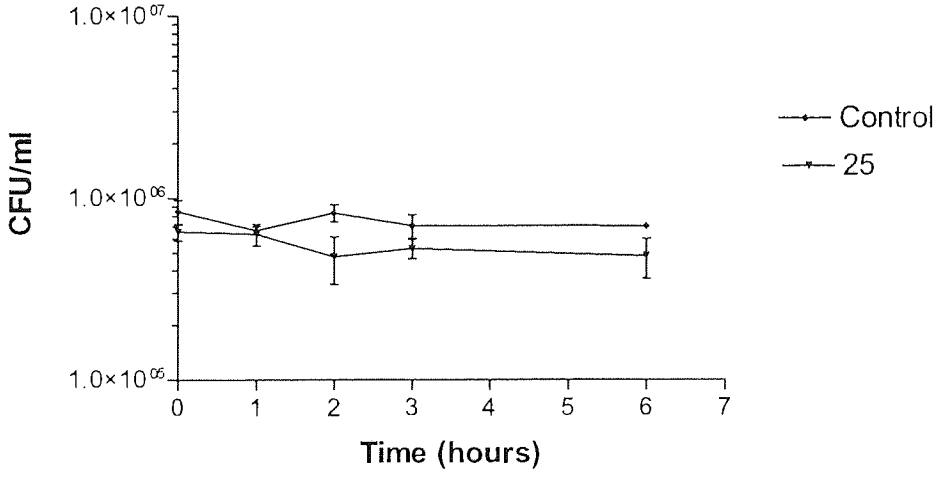

Figure 6.11 Continued over the page.

d) (i)

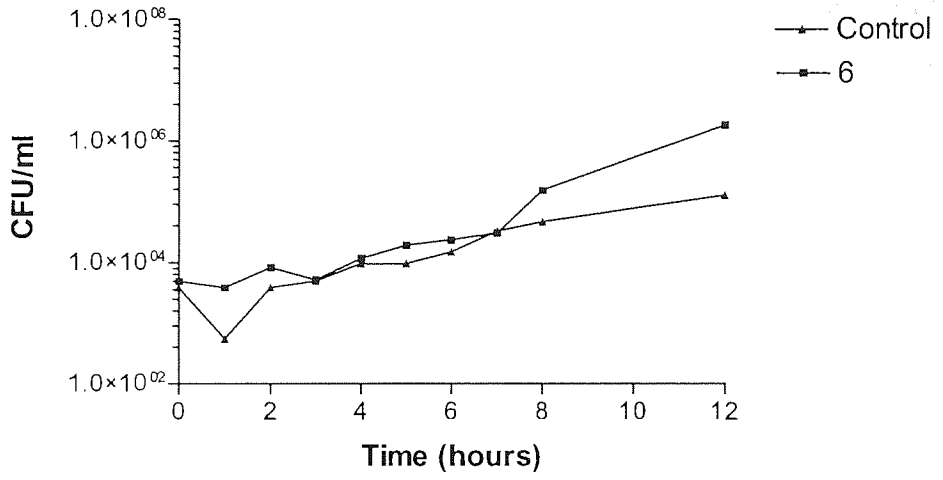

(ii)

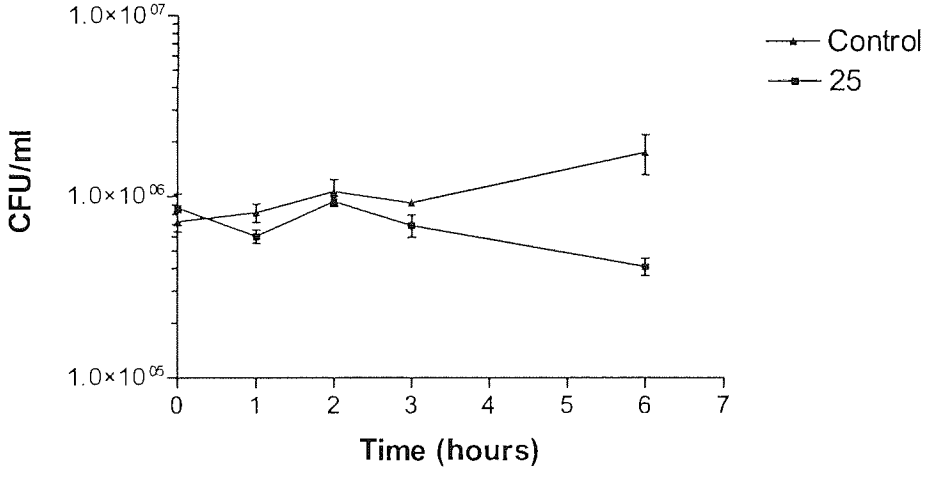

Figure 6.11 The antibacterial effect of **6** (i) and **25** (ii) with cationic lipid aided uptake using a) Lipofectin®, b) Lipofectamine™, c) Cellfectin®, d) DMRIE-C

6.2.1.4.2 Anionic Lipid Kill Assays

Anionic liposomes were used as an alternative to cationic lipids in a comparative model using **6**. The encapsulation of **6** appeared very effective with regards to the antibacterial activity against *E. coli* DH5α, as demonstrated in Figure 6.12 a) (i) and (ii). The encapsulated **6** showed a marked reduction in CFU/ml over the 3 hour time course of the assay in comparison to lipid and bacterial controls as well as liposomally-encapsulated **7**. This activity is more apparent in Figure 6.12 a) (ii) where the difference in CFU/ml between the encapsulated **6** and the other cultures was even more pronounced. However, this was not supported by the kill curves presented in Figure 6.12 b) and c) where antibacterial assays carried out over 3 and 6 hours respectively, using the encapsulated **6**, demonstrated outgrowth of the bacterial control culture by the culture treated with encapsulated sequence **6**.

a) (i)

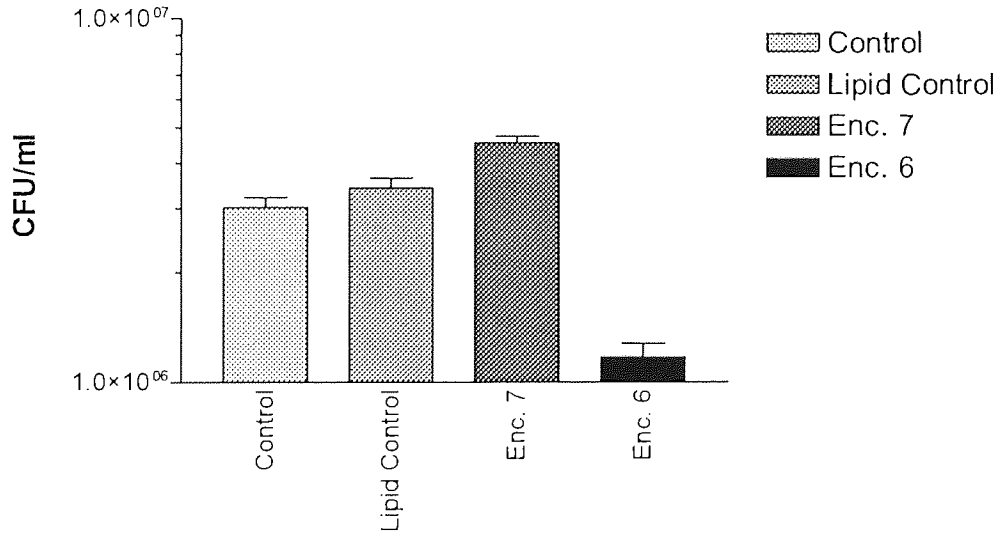

Figure 6.12 Continued over the page

(ii)

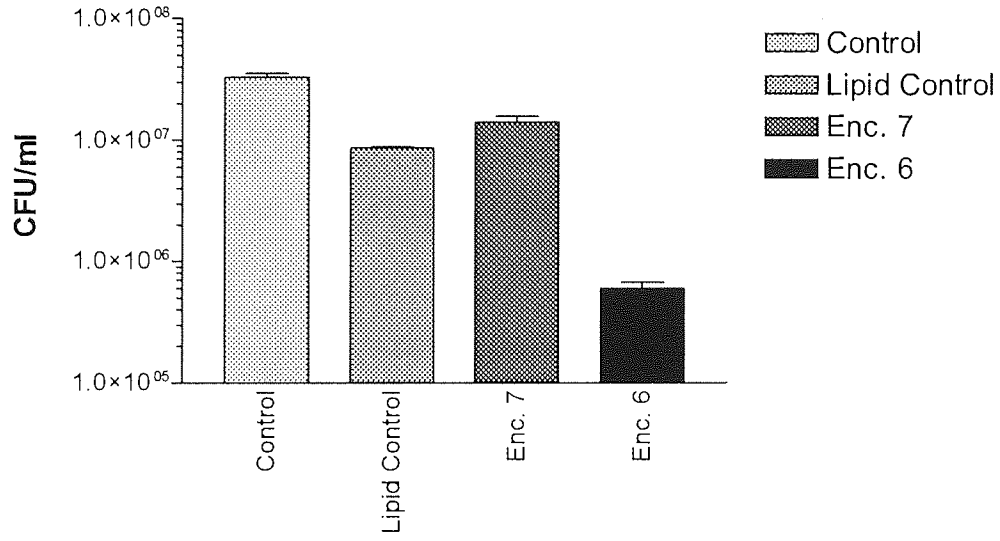

b)

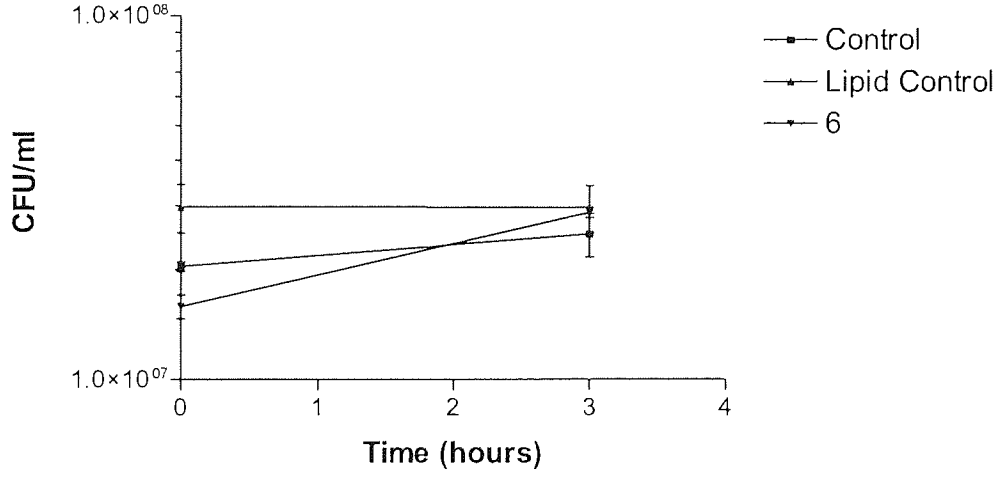

Figure 6.12 Continued over the page

c)

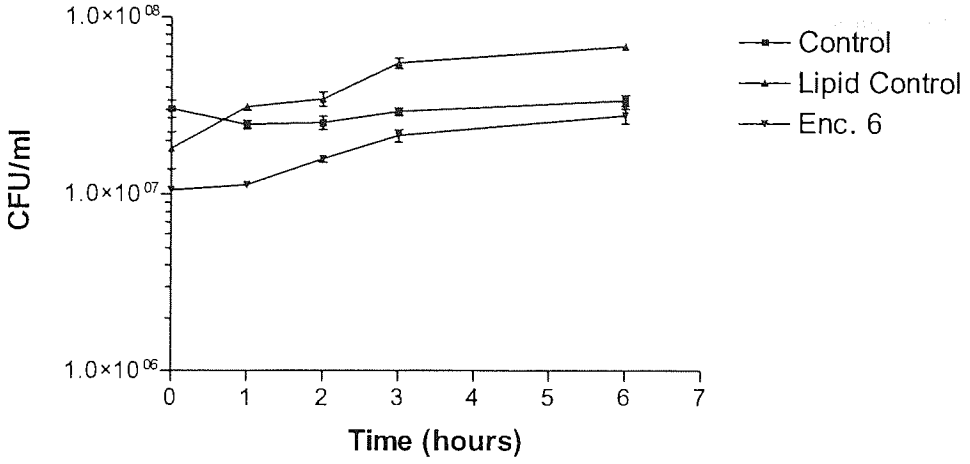

Figure 6.12 The antibacterial activity of anionic lipid-encapsulated **6**, where a) (i) and (ii), represent activity after a single time point of 3 hours, b) the kill after 3 hours with a time 0 count and c) a standard antibacterial kill assay carried out over 6 hours with a 1 hour preincubation period of the culture and anionic liposome encapsulated TFO.

6.2.2 *S. pneumoniae* Kill Assay

Figure 6.13 illustrates the antibacterial activity of the two anti-*S. pneumoniae* TFOs **36** and **39**, where passive uptake is relied upon for delivery of the oligonucleotides to the cells. The results indicate consistent growth by all bacterial cultures and hence a lack of antibacterial activity.

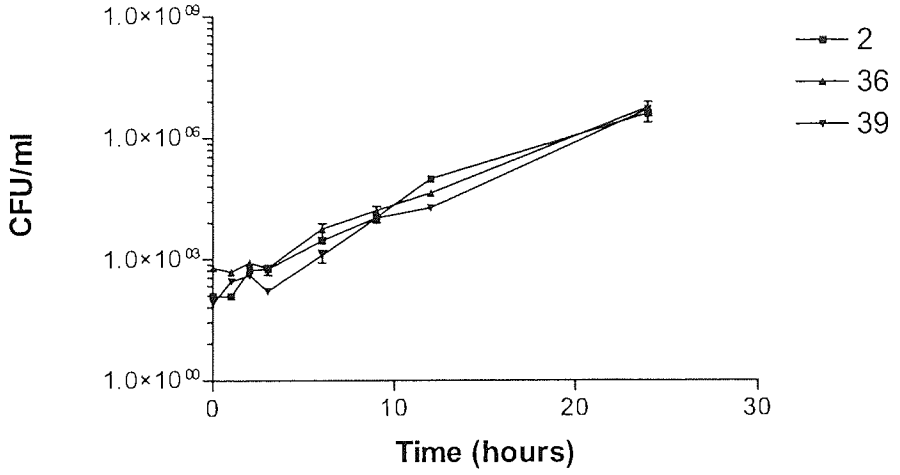

Figure 6.13 The antibacterial Activity of **36** and **39** against *S. pneumoniae* at 25 °C relying on passive uptake in BHI.

6.2.3 Theoretical Kill Model

The theoretical model was produced in order to illustrate the level of uptake required to demonstrate a clear level of inhibition while avoiding masking of TFO-infected cells by cells that had not taken up the TFO. The model indicates that a level greater than 50% and closer to 90%, would be required to establish a clear and definable level of bacterial inhibition via the viable count method.

a)

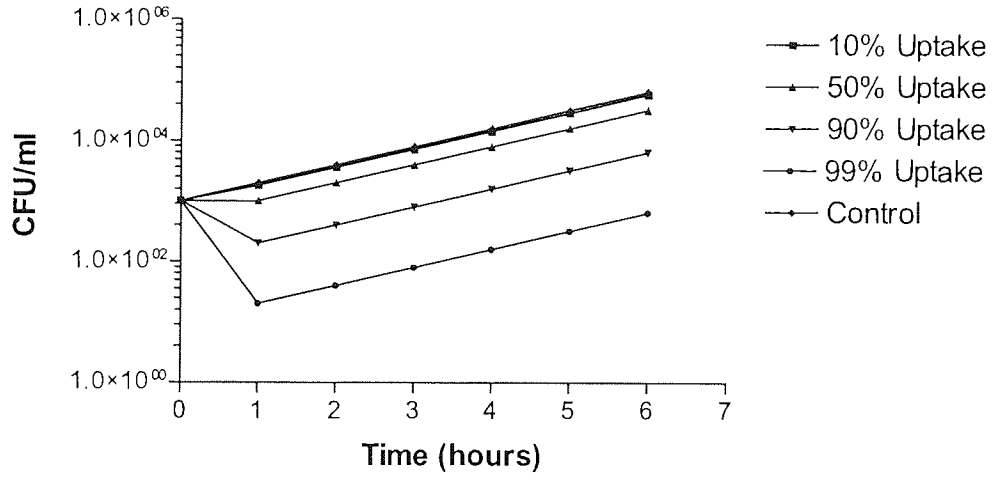

b)

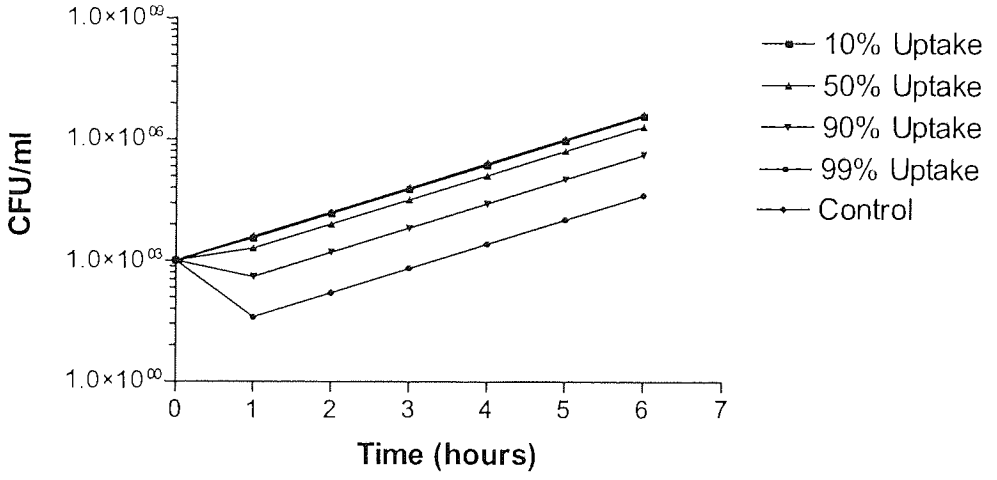

Figure 6.14 Theoretical models depicting the effect of different uptake efficiencies of a given TFO with an initial cell count of 10^3 CFU/ml and the organism replicating at a rate of a), once per hour and b), twice per hour. Calculation of CFU/ml is based on the assumption that uptake results in kill.

6.3 Discussion

6.3.1 Passive Uptake Assays

Figure 6.1 shows the results obtained when *E. coli* DH5α was exposed to sequences **3-6** and **9** (a) and **25-27** (b) at a concentration of 10 μM. The antibacterial activity of the oligonucleotides, determined via viable counts, was assumed to result from the oligonucleotides forming triplexes at the target site within the *gyrA* gene of the organism, after passive uptake. The results depicted in Figure 6.1 a), show that there is little in the way of sustained decline in the CFU/ml over the time course of the assay. However, a number of sequences show a decrease in colony numbers at the 2 hour time point. In particular, **5** and **6** show a marked decrease in CFU/ml at this point. This was perhaps expected of **6** due to the design of this TFO to bind to the target in an antiparallel manner in relation to the polypurine tract, a phenomenon that has been demonstrated in the melting studies (Chapter 3). The binding of **5** was not expected due to its randomised nature. Screening of this oligonucleotide against the *E. coli* genome has shown that it has no target site at which it is able to form a triplex (data not shown). In order for this sequence to exert an antibacterial activity it would have to do so via non-specific interactions. This is potentially possible due to the polyanionic nature of the backbone of the oligonucleotide, which once inside the cell, could bind non-specifically to any molecule bearing a cationic charge. Examples include proteins and intracellular salts, binding to which could upset pathways or solute concentrations to the extent that they prevent efficient functioning of fundamental processes, and hence viable counts are diminished. Such a process is possible and has been proven to be the source of antisense and antigene activity in a number of studies. The resultant gene inhibition was a product of non-sequence specific interactions, which has been so successful, that short chain oligonucleotides called aptamers have been used to inhibit proteins specifically. Examples include aptamers against throbin and HIV-1 integrases (Agrawal and Kandimalla, 2000).

However, if such an effect were apparent, the same level of antibacterial activity would be expected with all sequences and not just **5**. Although the other sequences demonstrated a slight decrease in CFU, none of them exhibited a level similar to that of **5** with the exception of **6**. The source therefore of the potential antibacterial activity demonstrated by these TFOs is not clear and may be a result of a slow growing culture, one that was slower than the others to respond after the lag phase of growth.

Figure 6.1 b) illustrates the antibacterial effect of **25-27** under the same passive uptake conditions. The results indicate little antibacterial activity presented by any of the sequences except potentially by **26** in comparison to the non-TFO treated culture. The culture containing **26**, showed a decrease in CFU/ml from time 0 to 3 hours, and then showed a slight increase over the remainder of the assay. The colony numbers were lower in comparison to the other samples even though this culture had the joint highest count at time 0. The difference is however nominal and if it were significant, a difference in CFU/ml of at least 1 log between this culture and the control culture would be expected.

The ability of **26** to exert a greater antibacterial action than **27** in particular, would however be unexpected due to the stronger binding of the latter resulting from the attachment of a 5' acridine moiety. This would be expected to have a greater binding affinity to the duplex target due to enhanced interactions at the duplex-triplex junction (Chapter 1). This enhanced binding was shown in Chapter 3 where **27** had a higher T_m than **26**. As a result a greater level of antibacterial kill would be expected with **27**. The 5' acridine could however have hindered **27** from exerting a full antibacterial activity by preventing efficient uptake. The overall size of **27** (6048.46 Da) is greater than **26** (5467.65 Da) and consequently could have prevented or decreased entry of the oligonucleotide to the cell. Uptake of the oligonucleotides via passive mechanisms is, however, not clear due to the electrostatic repulsion that would occur between the polyanionic backbone of the oligonucleotide and the cellular wall, which has a net negative charge conveyed by lipopolysaccharide (LPS) units in the outer membrane surface. Uptake of currently used drugs such as β-lactams, occurs via passage through non-specific porin channels that are present throughout the outer membrane. However, these admit molecules no larger than 600-700 Daltons in size, which is approximately 10-fold smaller than that of the TFOs used in this study. It is therefore possible that the size increase of **27** due to the addition of the acridine moiety was an issue in uptake, even though the mechanism of uptake is unclear. It is also possible that the positive charge of the acridine changed the overall properties in such a way, that uptake was slightly hindered. However, such an idea would be unfounded because the addition of the cationic unit would diminish overall anionic nature of the oligonucleotide and as a result should decrease the barrier to entry.

Overall it is surprising that **26** exerted any antibacterial activity due to its inability to form triplexes at pH 7.2 during the melting studies (Chapter 3). This would be

necessary because the intracellular pH at the duplex target, in the cytoplasm is strictly regulated at pH 7.2-7.3. It is possible to say therefore that the slight decrease in CFU/ml in the **26**-treated culture, is simply due to a slightly slower growing culture.

From the results depicted in Figure 6.1, it was presumed that the level of uptake of the TFOs was insufficient to exert an antigene effect. This idea was subsequently supported by the FACS analysis illustrated in Chapter 5, where it was shown that the level of fluorescence exhibited by cells exposed to **7** at 20 °C was similar to that demonstrated by the bacterial culture alone. This indicates that little or no uptake was present under these passive assay conditions during the FACS analysis, which indeed simulate those same conditions used in the antibacterial assays. As a result numerous methods were assessed for their ability to improve uptake and cold shocking, in the presence of $CaCl_2$ was the first of these methods to be investigated.

6.3.2 Cold Shocking Assays

6.3.2.1 Viable Count Assays

Cold shocking cells in the presence of $CaCl_2$ is a well-documented technique used to enhance plasmid and bacteriophage transfection during cloning experiments. The technique produces a transient state of competency in the bacterial cells, which allows enhanced uptake of DNA. It has been shown that the presence of divalent cations, particularly Ca^{2+}, is essential in the early stages of DNA uptake (Hanahan, 1983). The process however is not fully understood but a more in-depth discussion can be found in Chapter 1. The methodology was employed here in an attempt to improve the uptake of oligonucleotides by *E. coli.*

Figure 6.2 shows the antibacterial effect of **6** under cold shocking conditions where, a) represents the antibacterial kill utilising the initial cold shocking technique, and b) and c), represent results obtained where lower cell concentrations were used in order to maximise TFO activity. All assays were carried out under transient cold shocking conditions where no growth medium was added to the cultures. This was used in order to assess bacterial viability directly and preventing outgrowth of the organism. Without the addition of any growth medium it was assumed that the organism would not grow and would remain viable, unless antigene activity was present, until they were plated to NA plates where growth would recommence. Bacterial controls were present to determine any cytotoxicity of the $CaCl_2$.

The results in Figure 6.2 a) show a marked difference in the CFU/ml between the **6** infected culture and the bacterial control culture. The difference actually increases over time and was greater after 6 hours, this indicates a sustained level of antibacterial activity. **6** would however appear to be only active over 3 hours, because up to this point there was a consistent decline in organism numbers. After this time point however, and up to the 6 hour time point, there was an increase in CFU/ml. This increase in bacterial numbers is unexpected due to the lack of growth media.

The reasons that the TFO only appeared to be active for 3 hours could be numerous. It is possible that the TFO has a short half-life when inside the bacterial cell, and therefore triplex formation was only transient. The antigene strategy relies on the TFOs to bind to the duplex for long enough to prevent transcription of the *gyrA* gene and allow existing DNA gyrase levels to fall such that knotting of the DNA is problematic and cell death incurs. If the half-life is shorter than the time of these activities, then the bacterium will remain viable. Further research would be required to establish this value for **6** but triplexes with half lives of 10 hours have been demonstrated (Soyfer and Potaman, 1996). However, such triplex stability would require far higher T_m values than those demonstrated in this research, and those TFOs with half lives of 10 hours demonstrated K_d values between 1-10 nM. Therefore it is unlikely that **6** would have a similar half-life. Elsewhere half-lives in excess of 1 hour have been demonstrated (Fox, 1995), which would tend to fit more with the thinking here.

In Figure 6.2 b) the modified cold shocking technique was used to enable the use of lower organism numbers. Figure 6.2 b) (i) represents the results obtained for this assay carried out over 6 hours, and (ii) an assay utilising the same methodology but carried out over a prolonged time period of 24 hours. Figure 6.2 b) (i) again shows a consistent difference in the number of CFUs produced by the **6**-treated culture compared to the bacterial control culture, a difference that is greater than 1 log at 6 hours. Again with this assay there was a clear decline in the organism numbers up to 3 hours, and then from 3 to 6 hours, the bacterial numbers levelled off and increased slightly. The pattern was similar to that illustrated in Figure 6.2 a), suggesting that the antibacterial activity of **6** is transient. It is difficult to determine whether or not this same transient effect was present in Figure 6.2 b) (ii), because there was great variability in CFUs over the initial part of the assay. It would appear that there was a decline in the organism numbers up to 5 hours but as stated the numbers over this

period were quite variable. If this were the case, then it would indicate a greater binding ability of the TFO during this assay in comparison to the two previously mentioned experiments. After the 5 hours the culture stabilised and remained almost constant for the remainder of the assay, with only a slight increase in CFU/ml between 12 and 24 hours. A clear difference between the **6** infected culture, and the bacterial control culture, was demonstrated.

An interesting observation during these assays was the ability of the control organism to grow under the assay conditions. This is illustrated in Figure 6.2 b) (i) where there was a marked increase in bacterial numbers between 3 and 6 hours. This is surprising due to the lack of nutrients. It may be possible that minute traces of the LB broth remained after the dilution of the organism in the $CaCl_2$, and it was these traces that were able to sustain minimal growth for the time course of the assay. It is clear that the growth rates represented by this culture is by no means normal in comparison to that in growth media, even taking into consideration the low temperature at which the assay was performed.

Another possibility is that nutrients obtained and released from dying cells are sufficient to maintain a small amount of growth, this is a process known as cryptic growth. In any culture there will always be a population of cells that will be senescent and undergoing cell lysis, a population that will vary depending on the stage of the growth cycle the organism is at, and it is perhaps this that provides small levels of nutrients. If this is true for the control culture then the same would be reciprocated in the **6** infected culture, where the same growth would be expected. As a result it is possible that the antibacterial activity of **6** is more profound than originally thought, and while after 3 or 5 hours, a decline in bacterial numbers is not apparent, it is possible that the TFO is suppressing growth to a degree in a proportion of the cells throughout the time course of the assay.

Although the three results represented above indicate that **6** exerts antibacterial activity, when tested on some occasions no activity was observed. Figure 6.2 c) illustrates a case where the antibacterial activity of **6** was not apparent, showing the **6**-treated culture to actually outgrow the control culture. In a number of cases it was shown that TFO infected cultures, regardless of the oligonucleotide sequence, would outgrow the bacterial control culture. The reason for this is not clear, but may have resulted from cellular clumping in the control culture, reducing efficient cell replication or reducing apparent CFU numbers. Cellular clumping is possible due to

the interaction between the negatively charged cell wall and the Ca^{2+} ions. In TFO-containing samples, similar interactions took place between the polyanionic backbone of the oligonucleotide and the Ca^{2+}, diminishing such interactions between the bacterial cells, which in turn were able to grow more prolifically. Attempts were made to improve this by adding growth media to the cultures (this was done by diluting the TFOs in LB before addition to the bacterial culture), but to little avail (see discussion below). This, however, does not explain why, in some cases there was TFO activity and none was observed in others. If it were simply a case of cellular clumping this would be expected in all assays as the same concentration of $CaCl_2$ was used throughout.

Another explanation is the outgrowth of TFO-infected cells by those that had not taken up the oligonucleotide. If the number of cells that had taken up **6** was minimal, then the replication of the cells that had not taken up the TFO, could easily mask these cells out. If this were the case, then it would indicate that under these assay conditions, the level of uptake is variable. Support for this was obtained by the FACS analysis described in Chapter 5. Here the level of fluorescence demonstrated by *E. coli* cells exposed to **7** under the same cold shock assay conditions as depicted above, was presumed to demonstrate the level of uptake of the given TFO. These results demonstrated a level of uptake of ~13%, but also a large standard error was obtained, indicating a large degree of variability in the level of uptake. This perhaps suggests that the level of uptake is the key to the variable results obtained during the antibacterial assays. With a high degree of uptake, as is the case with those results illustrated in Figure 6.2 a) and b), TFO activity was observed, however, where these levels were low, the TFO infected cells were outgrown by those cells that have failed to take up the oligonucleotide. Hence antibacterial activity was not observed and presumed not to be present.

Figure 6.3 shows the antibacterial activity obtained by **8** under the modified cold shocking conditions in the presence of LB. Figure 6.3 a) and b) are representative of the same assay, with a) showing the result obtained over the initial 7 hours of the assay, and b) representing the results over the full time 24 hour time course, for clarity. Sequence **37** was used here as a control sequence to determine the presence of non-specific activity, its ability to bind within the *E. coli* genome had been ruled out through bacterial database BLAST searches (Biology Workbench - data not shown). The results clearly indicate consistent growth of all cultures throughout the time

course of the assay. Sequence **8** is a phosphorothioate analogue of **6**, and was tested here for its ability to evade nuclease degradation once inside the cell. It was postulated that phosphodiesterase-mediated degradation was perhaps a reason for the variability of the antibacterial activity demonstrated by **6**. This sequence was however not expected to produce an antibacterial effect, and if it did, the nature of the effect would be unknown due to the lack of purity of the sequence, and its inability to produce molecular ion during MS analysis (Chapter 2). In order to assess the true antibacterial activity of this sequence, further determination of the different species of sequence contained in the oligonucleotide sample would be required in order to isolate the correct sequence. This could then be utilised in the above assays. The problem faced during this research was the yields of each individual peak shown via HPLC analysis. These were deemed too small for antibacterial analysis and therefore resynthesis was the only logical step. However, after 2 further attempts at synthesis, purity was not improved and alteration of the synthesis protocol was required. As one of the main aims of the research was to increase the T_m of the given TFO, resources were directed elsewhere.

Figure 6.4 represents the antibacterial activity of **25**, **26**, and **27** using the initial cold shocking protocol with LB broth present in the cultures. As a result growth would be expected by all cultures that were not inhibited by TFO activity. This assay was carried out over 3 hours as opposed to the usual 6 hours or longer, and hence growth of the bacterial control culture was minimal but still clear. The greatest inhibition was shown by **25**, which deviated the greatest toward zero from the control culture, and showed a constant decline in the CFU/ml over the full 3 hours. Sequence **26** initially showed a sharp decrease in bacterial numbers between 0 and 1 hour, which was followed by a slow increase in these numbers for the rest of the assay. Sequence **27** also showed a diminished number of colonies in comparison to the control culture but the curve illustrated by this culture, was more characteristic of bacterial suppression rather than kill as no increase or decline in bacterial numbers is illustrated. It may just be a case that uptake of this oligonucleotide is such that bacterial suppression is similar to bacterial growth, and hence no sharp rise or fall in bacterial numbers is witnessed. However, such a phenomenon would not be expected as uptake of the TFO should take place during the cold shocking procedure, prior to the commencement of the assay, and not throughout. As a result suppression of growth would be expected to

be quite sharp initially, and then decline as non-TFO infected cells begin to outgrow those cells that had taken up the oligonucleotide.

Overall these curves would seem to indicate that all sequences exert some level of bacterial suppression. Of note is the fact that **25** exerted a greater antibacterial suppression than **26** and **27**, and **26** than **27**. It would be expected that **27** would produce the greatest level of antibacterial activity followed by **26** and then **25**. The reasons for these are similar to those discussed above for the antibacterial assays relying on passive uptake of the oligonucleotides. Sequence **27** had a greater binding avidity for the target duplex than **25** and **26**, due to the substitution of 5mC and the attachment of the acridine moiety. It is perhaps unusual that **25** actually exerted any antibacterial effect due to the nature of the sequence. This sequence contains five C residues, which under the pH conditions found intracellularly, would not be protonated, and as a result would only be able to form a single Hoogsteen hydrogen bond when bound in a triplex manner. As a result triplexation would not occur due to instability, a phenomenon that has been shown in the triplex melting data in Chapter 3 where this sequence was unable to produce a triplex at intracellular pH. The energy penalty for a third strand to bind with these 5 mismatch base pairs is too great for the triplex to form, hence the substitution of the 5mC residues in **26** and **27**. This would therefore indicate the antibacterial activity shown during this assay results from some other activity than an antigene effect. However, further investigation would be required to fully establish this.

Figure 6.5 depicts the antibacterial activity of **11** and **15** against *E. coli* after the modified cold shocking procedure was applied with the addition of LB broth. This assay was repeated a number of times initially without the addition of LB broth, but the control cultures, along with other cultures, were unable to sustain viability (data not shown). As a result the LB was added. The results showed considerable outgrowth of the control culture by the TFO-infected cultures. The reasons for this are not clear, but again it is possible that electrostatic interactions between the $CaCl_2$ and the TFOs prevented clumping of the cells, allowing them to replicate more efficiently. It was however, unlikely that these sequences would have produced any antibacterial activity via an antigene action, since they were unable to form triplexes during the melting studies depicted in Chapter 3. The buffer used during these studies provides an environment that promotes triplex formation; it contains divalent cations and the polyamine spermine, which while found intracellular, are so at different

concentrations. There are also other intracellular ions that will affect triplex formation, the predominant cation being K^+, which destabilises triplexes and prevents triplexation altogether. A problem manifest by (T,G)-containing oligonucleotides, particularly when they contain contiguous runs of G residues, is their ability to form G quartets and quadruplexes mediated by K^+ (Chapter 1). Because of the intracellular content of this ion, the formation of triplexes during these antibacterial assays could be markedly decreased due to the formation of such hyperstructures. This trend will be apparent for any of the (T,G)-containing TFOs including the phosphoramidate sequences discussed below. Potassium is an essential macronurient in bacterial cells where it is responsible for the activation of a number of enzymes, including those involved in protein synthesis. For effective triplexation inside the bacterial cell, triplexes must therefore be stable under these conditions. If they are unable to form under the artificial conditions presented in the melting studies, then it is unlikely that they will do so intracellularly.

Sequence **15** was expected to have greater antibacterial activity due to its increased theoretical stability, meaning it would be able to bind more strongly to the duplex target, and with the 2'-*O*-methyl backbone modification, be able to evade nuclease activity. However, this was clearly not the case.

The other (T,G)-containing sequences, **13** and **30-33**, displayed similar antibacterial behaviour as that demonstrated by **11** and **15** (data not shown). Sequence **13** was the reverse sequence of **11**, and as a result, it would be expected to bind via reverse Hoogsteen bonds in an antiparallel manner in relation to the target polypurine sequence, to form a triplex. However, triplexation was not observed during melting studies and as a result it was not expected here. Sequence **30** and **31** were parallel motif triplexes with **32** and **33** antiparallel, where **31** and **33** were acridine linked. None of these sequences showed a triplex transition during the melting studies and again it is unlikely that they would do so for reasons discussed above.

The antibacterial activity of the phosphoramidate sequences was assessed under the same assay conditions as those used for **11** and **15** but with additional assays carried out at 30 and 37 °C (results not shown). The results are illustrated in Figure 6.6. T_m values for **18** and **19** were shown to be in excess of 40 °C at pH 7.2, indicating that triplexes would be stable at 37 °C, the standard temperature used to culture many organisms. Antibacterial activity at such a temperature is important if this technology

is to be used to combat bacterial infections, hence the assay temperature used here. The assay results shown in Figure 6.6 a) indicate little antibacterial activity. The scenario presented in other assays with TFO-infected cultures outgrowing the bacterial control culture could also apply here. All of the phosphoramidate containing samples outgrew the control culture to varying degrees. The results illustrated in Figure 6.6 b) show the antibacterial effect of the TFOs at 30 °C and again a similar picture is exhibited with all cultures outgrowing the control culture, with the only difference being more linear growth amongst the different cultures. A similar pattern was shown when the assay was carried out at 37 °C but with increased bacterial replication and hence higher final organism counts. It was for this reason that the results were omitted. This was slightly disappointing due to the improved T_m of these oligonucleotides compared with the other sequences synthesised. An enhanced antibacterial activity was perhaps expected as consequence of the raised T_m. The reason this was not the case was potentially due to a lack of characterisation of the sequences during HPLC, CE and MS analysis. The presence of many peaks in the former two techniques indicates a sample containing many species of oligonucleotide sequence. The inability to produce a molecular ion during the latter technique would make it difficult to validate the nature of any antibacterial activity were it present but more importantly it makes it difficult to ascertain the basis of the binding that produced the raised T_m. As with **8**, the logical step would be to isolate separate peaks and characterise them accordingly, however, these were so numerous with the phosphoramidate sequences that yields would be too low for analysis. This would be particularly true for any antibacterial examination where a 10 μM concentration is required.

6.3.2.2 BacLight™ Assays

Taking into consideration the problem of uptake variability and the possibility of masking of TFO-infected cells by non-TFO infected cells under the cold shocking assay conditions, other cell viability detection methods were assessed. It has also been suggested that viable counts rely on cells that are able to initiate cell division at a rate that is sufficient to form colonies (Boulos, *et al.*, 1999). However, cell recovery rates are variable and can take longer than a week, indicating that after the three day incubation periods used in the viable count assays, cells may be still viable but have not yet recovered sufficiently to begin replication. Colony counts therefore may not

give a true indication of the TFO activity. The BacLight™ staining methodology was employed in order to assess TFO activity more effectively. It was thought that by using this technology, it would be possible to determine the true extent of TFO activity by distinguishing more accurately between those cells that had taken up the designated TFO, resulting in kill, and those that had not. This technique does not rely on the growth of cells it merely detects live and dead cells. The assay was performed in a similar vein to the above-mentioned cold shocking assays over a time period of 6 hours. At each time point however, cells were exposed to a stain solution containing two fluorescent nucleic acid stains, SYTO 9® and propidium iodide. SYTO 9® generally stains all cells green, both living and dead cells. Propidium iodide on the other hand, is only able to penetrate bacterial membranes that are damaged or compromised, a situation that is associated with dead cells. Live cells will therefore fluoresce green and dead cells will fluoresce red due to a combination of the two stains which results in different spectral characteristics that are detectable using a fluorescence plate reader. It is perhaps questionable whether or not the cold shocking method actually compromises the integrity of the cell membrane such that it will admit the propidium iodide. This was however tested using different ratios of dead and live cells that had, and had not been exposed to the cold shocking methodology. Calibration curves produced from these two cell populations were found to be similar (data not shown), and it was concluded that cold shocking did not compromise cells membranes to the degree that it allowed entry of the propidium iodide.

Figures 6.8 and 6.9 show the antibacterial effects of the TFOs **6**, **11** and **15** respectively. The two Figures show the ratio of G/R on the y-axis pertaining to the level of fluoresecence emitted by live/dead cells respectively, against time on the x-axis. It was expected that if there was any level of kill then the ratio value would decrease and hence a decline in the curve would be observed. It is clear from these results that this is not the case particularly with **6** where the curves represented are almost characteristic of standard growth curves. The curve representing **37** in Figure 6.8 shows tapering off after 3 hours, which is unexpected. **37** was used as a control sequence in this experiment to determine non-specific binding. It had been screened through databases and predicted not to bind in an antigene manner, and therefore its ability to exert antibacterial activity was only possible via non-specific means, as previously discussed.

The results illustrated in Figure 6.9 are a little less clear due to the erratic nature of the growth of the control culture. This curve fluctuates slightly when it would be expected to grow consistently, similar to the control in Figure 6.8. This makes it difficult to determine the activity of **11** and **15**. It would be surprising however if these two sequences were able to produce an antibacterial effect due to matters previously described with regard to their inability to form triplexes *in vitro*.

The application of this technique was not as effective as it was first thought. The T_m values of the TFOs determined an assay temperature of 20 °C, a temperature at which bacterial replication is slower due to rigidity of the cellular membranes and decreased metabolic activity. Lipids in the phospholipid bilayers could play a role here, as at such a temperature, they are more rigid and less fluid-like. This is due to the phase transition temperature (T_c), which denotes the temperature at which the lipids are most unstable and hence permeable (Chapter 1 and 5). For phospholipids, this temperature is around 37 °C, which is considerably higher than the assay temperature utilised here. As a result the permeability of lipids to exogenous agents will be relatively diminished, and therefore uptake of the Baclight™ stains could be hindered sufficiently to prevent effective measurements of live and dead cells. This is perhaps something that would need investigation if this means of detection were to be used in such antibacterial assays in the future.

6.3.3 CPZ Aided Uptake

CPZ is a phenothiazine that is able to alter the permeability of bacterial membranes by causing damage to cytoplasmic membranes (Chapter 1, page 61). The increase in permeability caused by this agent was the basis for its use here. It was postulated that by adding CPZ to the culture medium, prior to the addition of the designated TFO, would result in membrane damage rendering the cells more permeable to the oligonucleotide. CPZ is clearly an antibacterial agent alone and if administered in high enough doses will actually kill the bacteria directly. Therefore it was essential to determine a level that would merely increase membrane permeability but at the same time maintain viability of the organism. Hence the MIC had to be ascertained. Table 6.2 shows the MIC of CPZ against *E. coli* DH5α, the MIC is indicated by the bold text. Subsequent culturing of each tube, containing the different CPZ concentrations,

to NA demonstrated clear viability of the organisms. It was decided that half the MIC value would be used and hence a concentration of 27.5 μg/ml was utilised.

The results in Figure 6.10 demonstrate the antibacterial effect of **6** in association with CPZ. Bacterial cells were pre-incubated with the CPZ, 1 hour prior to the addition of the TFO. Control cultures of bacteria alone, bacteria and CPZ, and bacteria and 6 were run in unison with the test culture. The results clearly show increased growth of the culture containing the CPZ and **6**, over all of the control cultures, indicating the absence of any antibacterial activity. This increased growth suggests that the association of the two compounds is such that growth of the *E. coli* is promoted. It is possible that some form of interaction between the two took place, resulting in diminished antibacterial activity of both compounds. The control cultures were exposed to the full antibacterial activity of the two compounds, and as a result, CFU/ml are slightly lower. The interaction of CPZ and **6** would result form electrostatic attraction between the two due to the cationic nature of CPZ and the polyanionic nature of the oligonucleotide. It was for this reason that the cells were pre-incubated with the CPZ to prevent interaction with the TFO. This however seems to have been ineffectual, and even after interaction with the bacterial cells, further association with the TFO was still possible.

6.3.4 Lipofection Aided Uptake

6.3.4.1 Cationic Lipids

Cationic lipids were used to enhance the delivery of TFOs to the *E. coli* cells. The lipid:DNA complexes self associate due to opposing charges resulting in encapsulation of the DNA or the formation of lipoplexes, where the DNA aggregates around the lipid. The charge of the lipid, again via electrostatic attraction, interacts with the negative cell wall and releases the DNA in to the cytoplasm of the cell. The TFO is then able to bind to its target within the duplex genome. Further, more detailed discussion of the mechanism behind these interactions can be found in Chapter 1 and 5.

The results presented in Figure 6.11 illustrate the antibacterial effect of **6** and **25**, complexed with the four cationic lipids: Lipofectin®; Lipofectamine™; Cellfectin® and DMRIE-C. All four were screened for their ability to deliver the TFOs to the bacterial cells, determined through viable counts made on NA after incubation of the

lipid:DNA complexes with *E. coli* DH5α. Viable counts were taken over a 6 hour time period in the case of **25**, and over 24 hours in the case of **6**. Control bacterial cultures were run alongside the assay culture, containing each of the lipids to ascertain the antibacterial properties of them alone. The results pertaining to the antibacterial activity of **6** in association with the four lipids (Figure 6.11 a) (i), b) (i), c) (i) and d) (i)) show outgrowth of the control culture by the TFO-infected cultures. It is possible once again in this situation that the bacterial cells are subject to clumping due to the opposing charge of the lipids in respect to cell surface charges. It is possible that this not only affected bacterial growth but also could result in clumping after plating to nutrient agar. Here colonies will usually result from a single bacterium, however, where clumping takes place, colonies will result from a number of cells and hence diminished CFU/ml will be calculated. Such clumping is not apparent in the cultures containing the TFO due to interaction of the lipids with the oligonucleotides, hence replication is not hindered and colony counts are true to the bacterial numbers in culture. Another reason for the lack of antibacterial activity depicted by **6** is the potential interaction of the lipids with constituents of the LB broth. This idea is backed up by zeta potential results that were obtained for the work described in chapter 5. This preliminary research was carried out to try and understand the interactions that took place between the lipids and the other components of these lipid-mediated antibacterial assays. A full discussion of the results can be seen in Chapter 5, but briefly; the overall negative zeta potential of LB broth provides the potential for interaction with the cationic lipids thereby preventing efficient complexation with the oligonucleotides. If this were the case then uptake could be reliant on passive diffusion, which as previously discussed, culminates in very low levels of TFO uptake. While this is possible and such a phenomenon has been demonstrated in other studies, as stated in Chapter 5, the formation of lipid:DNA complexes is favoured more strongly over other media related interactions and these initial interactions do not impair transfection (Son, *et al.*, 2000). These studies however, are related to plasmid DNA, which will confer an overall greater anionic potential, and relate to the transfection of mammalian cells. Currently these interactions with single stranded oligonucleotides and bacterial cells relating to transfection efficiencies have not been studied.

The results for **25** in the case of Lipofectin® and Lipofectamine™ aided uptake (Figure 6.11 a) (ii) and b) (ii)), show a similar pattern to those depicted by **6**. Cultures

containing the TFOs out grew the control cultures, possibly for reasons similar to those for **6**. However, Figure 6.11 c) (ii) and d) (ii), where **25** was complexed with Cellfectin® and DMRIE-C, a degree of inhibition is observed, this is more apparent when the TFO was complexed with DMRIE-C. Here a large difference in bacterial numbers, between the control culture and the TFO-infected culture, is visible, particularly at 6 hours. This would indicate these two agents to be relatively effective at transfecting bacterial cells, DMRIE-C more so than Cellfectin®. Further study would be needed to determine the true source of this antibacterial activity and indeed optimisation of the uptake process would be needed. The effectiveness of lipofection is governed by a multitude of factors. Morphology along with size, zeta potential, efficacy of complexation with the DNA and stability, all affect the success of the technique and hence its biological activity both *in vivo* and *in vitro* (Pedrosa de Lima, *et al.*, 2001). These factors are essential in obtaining optimal uptake of given DNA and will differ from one oligonucleotide to another as a result of varying constituents. These factors would be key to this research to obtain optimal uptake of **6** and **25** to assess their full antibacterial action and it may be this that explains the poor results demonstrated by **6**. With little literature precedence for the use of cationic lipids as successful bacterial transfection agents, other more bacterial specific agents were assessed.

6.3.4.2 Anionic Liposomes

Anionic lipids were tested for their ability to overcome the uptake problems associated with oligonucleotide delivery. The assays were carried out in saline to prevent outgrowth of the organism and as a result static cultures should be obtained. Figures 6.12 a) (i), and (ii) illustrate the antibacterial activity of encapsulated **6** when the TFO and bacterial culture were incubated together at 20 °C for a 3 hour time period. Bacterial, empty lipid and encapsulated **7** controls were used. The last of these was used, as encapsulation **7** had previously been determined via fluorescence microscopy and FACS analysis (Chapter 5). Antibacterial activity was determined via a decrease in CFU/ml produced by the encapsulated **6** containing culture compared to the bacterial culture. The results in both Figure 6.12 a) (i) and (ii) show a clear difference in the bacterial numbers between the control culture and the **6** infected culture, this is more apparent in (ii) than (i) where a difference of almost two log cycles is represented. Interestingly the culture containing the encapsulated **7** showed

no decline in CFUs and bacterial numbers were similar to those of the control culture or greater. This is unusual and it could be postulated that the fluorescein label prevented efficient binding of the TFO to the target duplex. This would however, be unexpected due to previous studies carried out. It was shown via fluorescence spectrophotometry (Chapter 3), that **7** was able to bind to genomic DNA of *E. coli* when bound to microtitre plates. As a result it would be expected to bind here also and a decrease in the bacterial numbers represented by this culture would be expected. Conditions between the two assays were however different, and in the plate assay conditions under which triplexation took place were somewhat artificial. Triplex buffers were used to promote triplex formation. These buffers as previously stated, contain salts and polyamines at concentrations that are not found intracellularly, where triplex formation, as a result is less favoured. It is therefore possible that the fluorescein did in fact hinder triplex formation, and as a result antibacterial activity was not observed. A problem perhaps associated with these assays, is that the results are reliant on viable counts taken at a single time point, without bacterial counts taken at time zero. It is therefore unknown whether or not the results obtained for encapsulated **6** stemmed from a diminished initial bacterial inoculum, resulting from inefficient pipetting, or from true antibacterial kill. The former is perhaps questionable due to pipetting inaccuracies at worst summating to a 10% difference in colony counts, which is not sufficient to produce the effect shown here. However, because of this the assay was repeated but with counts made at time 0 and results are illustrated in Figure 6.12 b). These results show a different picture to those just discussed. The bacterial control culture and lipid control culture actually remain almost completely static throughout the assay as expected. This indicates the lipids alone to be non-cytotoxic. Encapsulated **6** however, showed an increased 3 hour count in comparison to its time 0 viable count. This is clearly unexpected and perhaps indicates growth of the organism, something that would not be deemed possible due to the lack of growth media. Had it been possible here the same would have been expected with the other cultures. Again the difference would appear to be too large to have emanated from pipetting errors, a view that is further supported by the similarity in replica counts, illustrated by a small standard error.

Figure 6.12 c) illustrates a further variation on this assay with the time course extended to 6 hours and bacterial cultures preincubated for 1 hour at 37 °C with the

addition of the varying liposome formulations. The samples were then incubated at 20 °C for the remainder of the assay to promote successful triplexation. The preincubation was carried out to increase uptake of the **6** by facilitating liposomal fusion. This was thought to be the limiting step in the previous assay. In order for the encapsulated TFO to enter the cell, fusion between the bacterial membrane and the liposomal bilayer is necessary, the efficiency of which is governed by the assay temperature, and the closeness of this to the T_c of the lipids used in the liposomal formulation. As discussed in Chapter 5, DPPC and DMPG in such a formulation have a T_c around 37 °C. At lower temperatures these membranes become more rigid and hence fusability decreases, markedly so at temperatures of 20 °C, the temperature of the assay (Chapter 5). It was therefore postulated that the preincubation of the liposomes with the bacterial cells at 37 °C would destabilise the membranes, enabling efficient fusion with the bacteria, and hence maximising oligonucletide uptake. Figure 6.12 c) however, does not support these claims and the encapsulated **6** did not show any antibacterial activity. In fact, quite the contrary is illustrated and growth ensued. The control culture appears to remain relatively static while the lipid control shows the greatest level of growth.

An explanation for the growth of the encapsulated **6** culture is not clear but a number of possibilities could have occurred. It is possible that insufficient liposomal fusion took place and as a result the levels of oligonucleotide release were minimal. FACS analysis, as previously reported, indicated uptake of **7** to be 43%. It would perhaps be expected that similar levels would be achieved here. However, the length of incubation of the liposomes with the bacterial cultures was greater during the FACS analysis and perhaps 1 hour is not sufficient to allow the fusion process to take place. A further prolonged incubation period of 3 hours prior to the commencement of the antibacterial assay could possibly be necessary. It is also possible that the temperature change from 37 °C to 20 °C had some effect on the ability of the TFO to form triplexes. It may be possible that the incubation period was sufficient to enable a good degree of uptake but triplexes were unable to form initially due to the culture slowly cooling from 37 °C. Triplex formation would not have been possible until temperatures of around 26 °C (the T_m of **6**), were reached, and in fact triplexes would only be stable at temperature well below this. It has been shown that it takes a 21mer third strand oligonucleotides 15 minutes to reach its target and form a triplex (Cheng,

et al., 2001). It is possible that culture cooling took longer than 15 minutes and as a result excess oligonucleotide would have accumulated within the cell. It is possible that these were then degraded by nuclease enzymes or, were expelled from the cell. Nuclease degradation is possible because *E. coli* contains numerous endo- and exonucleases that are present to protect the cell from exogenous DNA molecules such as phage DNA. Most of these systems have however been removed from *E. coli* DH5α as discussed in Chapter 4. *E. coli* however, contains one particular nuclease enzyme called exonuclease I, which could be particularly problematic in the context of this research. This enzyme will attack and digest single stranded DNA in the 3'-5' direction and will do so via the sole recognition of the 3'-hydroxyl groups (Lehman and Nussbaum, 1964). It cleaves mononucleotides step-wise leaving a terminal dinucleotide, which remains intact. Accumulation of the TFO within the cells could possibly result in this activity and therefore could explain the lack of activity exhibited by **6** under these assay conditions. Exonuclease activity would not only be a problem associated with this assay, but could also explain the failure of TFO activity through out the study. The gene associated with exonuclease I activity is *sbcB*. In mutants containing altered *sbcB* genes exonuclease I activity is absent (Kushner, *et al.*, 1971; Kushner, *et al.*, 1972) alterations that are not presented in *E. coli* DH5α. It would therefore be advantageous to compare antibacterial activity of the TFOs produced here against similar antibacterial activity in an *sbcB* mutant *E. coli* strain. One such example would be *E. coli* JM103, which contains a mutant form of this gene (Hanahan, 1983; Promega, 1996).

Cellular expulsion is possible due to passive diffusion, where solute pressures caused movement of the oligonucleotide out of the cell, or by active efflux mechanisms where the TFO was pumped out of the bacterial cells before stable triplexes could form. Bacterial cells have many control mechanisms in place that regulate the internal environment in relation to external culture conditions, in order to maintain the viability of the organism. It is possible that internal accumulation of the TFO could lead to the up regulation of mechanisms that result in the expulsion of the oligonucleotide from the cell. Examples include efflux pumps (translocases) that have a wide spectrum of substrates (Chapter 1). These have been recognised along with other efflux pumps as a major cause of drug resistance in bacteria. However, these have been tested for their ability to expel PNAs from *E. coli* (Good, *et al.*, 2000). Here, suppression of these translocases in wild type *E. coli* K12 (antibiotic susceptible

strain), has shown little attribution to increased PNA activity, and it was deemed that the major barrier to entry is the LPS layer associated to the outer membrane. PNAs are essentially peptides and as a result are structurally different to DNAs, so while these translocases do not necessarily expel PNAs to any extent, their ability to efflux DNA molecules may still be possible. Further research would be needed to clarify this.

6.3.5 *S. pneumoniae* Kill Assay

The antibacterial activity of oligonucleotides targeted to homopurine tracts within the duplex of *S. pneumoniae* as assessed via viable counts utilising passive uptake. Passive uptake within this organism would be deemed more effectual since its cell wall provides less of a barrier to small molecules than that of *E. coli* (Chapter 1). Gram positive bacteria are also more likely to interact with single stranded DNA than Gram negative organisms. Gram positive bacteria will interact with double stranded DNA but will only permit entry to one strand, where as Gram negative bacteria preferentially interact with and transfer double stranded DNA (Hanahan, 1983). This could be a further reason for the poor results obtained for the *E. coli* work but also would imply a potentially enhanced antibacterial activity of the *S. pneumoniae* TFOs here, particularly in relation to the passive uptake experiments.

Figure 6.13 illustrates the results of the antibacterial assay and show consistent growth represented by all cultures. **36** and **39** were the two TFOs designed to bind at two separate sites within the *S. pneumoniae* genome in an antigene manner. Compound **2** was a control sequence that would determine any non-specific binding due to its inability to form a triplex in the genome of *S. pneumoniae*. The assay conditions that were presented here were such that they were unlikely to promote triplexation. The assay temperature was set at 25 °C, the lowest temperature at which successful growth of the test organism was found possible. The T_m of **36** was determined at 20 °C at pH 7.2, which is far less than the assay temperature and as a result would be very unlikely to form triplexes under assay conditions. **39** actually failed to produce a triplex at either pH 6.4 or 7.2, so again its ability to do so under assay conditions and intracellularly would be unexpected. In order to assess the antibacterial activity of these TFOs in this organism successfully, the T_m would have to be increased greatly potentially by the 5' attachment of intercalating agents or

backbone modification. If phosphoramidate synthesis could be improved then this would be a particularly interesting path to follow. The increase in T_m would not only improve triplex stability but would also enable easier manipulations of the organism. It is for these reasons that this research was not pursued here and resources were concentrated into the development of the anti-*E. coli* TFOs where research was more successful.

6.3.6 Theoretical Model

There are perhaps two major problems that have prevented successful antibacterial activity by each of the designated TFOs. The first of these is the presumed poor level of uptake, and the second of these is the low T_m values of the oligonucleotides consistent with diminished triplex stability. These are by no means exclusive and a combination of the two was perhaps the cause of the poor and variable antibacterial activity witnessed here.

Theoretically for **6**, to be successful as an antibacterial agent via the antigene strategy, all that is required is one TFO to transfect the *E. coli* cell. The passage of **6** through the cell and subsequent binding to the duplex target within the *gyrA* gene with sufficient stability, will block transcription of the gene by steric blockade of RNA polymerase, preventing production of the A subunit of DNA gyrase. As levels of the gyrase enzyme fall within the cell, knotting of genomic DNA will occur eventually to such an extent that cell death will ensue. However, in reality it is much more complicated than this and levels of uptake necessary for an antigene effect would need to be far in excess of one TFO molecule.

The theoretical model was produced to establish the levels of uptake required to detect a definable level of inhibition during viable count assays. It was developed on the basis that antibacterial activity of the given TFOs was masked out by cells that did not take up the oligonucleotide sequence, as discussed above.

Figure 6.14 shows the results of the model where a) represents a replication or doubling time of once per hour and b) represents a rate of twice per hour. It is likely that during the antibacterial assays, when they were performed at 20 °C, that the division rate of the organisms was between once and twice each hour. It is assumed for the purpose of this model that any organism that takes up the TFO would be inhibited. It is clear from the results in a) that in excess of 50% uptake would be

required to determine a significant antibacterial effect, and in fact, 90% is necessary to obtain a log difference in growth (the benchmark for a significant level of inhibition), between the TFO-infected and the bacterial control cultures. This is only amplified in b), where a greater level of inhibition is required to achieve the same effect due to the increased doubling time. From these results it is clear as to the variability of the antibacterial results ascertained during the study. Where perhaps antibacterial activity was deemed not to be present, small levels were possible but went unnoticed due to outgrowth by cells that had not admitted the TFO. Support for this stems from the FACS analysis that showed at best uptake was only 43%, and from this model it would appear that this would not be sufficient to produce a significant level of antibacterial kill. This 43% was also produced at 37 °C when liposomal membranes were most fusable, T_m values dictate an assay temperature of 20 °C where uptake via liposomal encapsulation is less then half this value. This result was also only obtained with the anionic liposomes and not with other forms of uptake such as the cold shocking approach. This yielded even lower levels of uptake, which were also shown to be quite variable from one assay to the next. Therefore for true assessment of the antibacterial activity of the designed TFO a more sensitive mechanism of detection would be necessary. Examples include reporter systems where the down regulation of gene expression caused by triplex formation is determined by detectable product production. An example of such a system was used in the triplex inhibition of the *lac* operon gene of *E. coli* using a 21mer and 18mer TFO (Cheng, *et al.*, 2001). The *lac* operon gene codes for the β-galactosidase enzyme, the activity of which can be detected via the levels of ONPG substrate broken down. This can be detected spectrophotometrically, by the levels of a yellow colouration produced, which can then be interpreted as anitgene activity. The *lac* operon detection system is possible via a plasmid insert, binding to which by TFOs causes the down regulation of the β-galactosidase enzyme, and hence a decrease in the yellow colouration produced. Such plasmids are not available for the gyrase enzyme and hence it would have to be constructed, which was not feasible here. However, the true basis of this work was to determine the antibacterial activity of the designed TFOs.

Another point of interest in the work carried out by Cheng *et al* is the dose dependent nature of the TFO that they used to suppress the *lac* operon gene. They used TFO concentrations of 30 to 200 μM and observed an increase in β-galactosidase

suppression accordingly. These results are supported by those of other researchers such as Aggarwal *et al* (Aggarwal, *et al.*, 1996), who showed similar dose dependent TFO activity against tumour necrosis factor in glioblastoma cells. Similar dose response experiments utilising **6** were also pursued as part of this research but too little avail, except for the further highlighting of insufficient uptake as the barrier to TFO activity.

It is however possible that uptake was actually sufficient to induce an antibacterial effect and the problem may just result from a lack of target accessibility. The double helical DNA found predominantly in bacterial cells forms a circular structure, which is further supercoiled, and associated to basic proteins to form a highly organised and condensed complex. It is possible that target sites for the oligonucleotides will be concealed in this complex structure and as a result will be inaccessible to the TFOs. Promoter sites tend to be more accessible than whole genes to enable binding of DNA and RNA polymerase enzymes, which will then in turn cause the unwinding of the subsequent DNA for transcription or replication. The target site of the designed TFO is upstream of the promoter sequence and is found 1026 bp into the gene. As a result it will possibly remain inaccessible throughout the time course of the assays carried out above, except during transcription or replication of the *gyrA*, where the TFO will have to compete with the DNA binding proteins, i.e. DNA and RNA polymerases. Here they would most certainly be out-competed for binding sites by these proteins due to the low K_d that these demonstrate (1-10 nm). This is far lower than any of the K_d value demonstrated by the TFO designed for the purpose of this study. The lowest K_d presented during this research was 800 nM by **12**, a value that was perhaps questionable due to the lack of triplexation during the melting studies (Chapter 3). As a result it is clear that target binding by the oligonucleotides would not be possible under such conditions. Although binding to genomic DNA has been shown in the fluorescence plate assays in Chapter 3, here supercoiling would not be so problematic due to extraction of cellular proteins, which would imply the DNA would take on a more relaxed conformation and binding sites would perhaps be more accessible.

Throughout the course of this research all antibacterial activity has been presumed to result from antigene mechanisms and not through other non-sequence specific means. The problem here is that there is little evidence that these TFOs actually form triplexes intracellularly. The only support available for this notion is the production of

triplexes *in vitro* during the T_m studies. Here however, conditions promoted triplex formation and cation concentrations were such that electrostatic repulsion witnessed between the three backbones, one of the major problems of triplexation, was minimal. Therefore it is difficult to determine whether or not the inhibition demonstrated by **6** in particular was actually via this antigene mechanism. Non-specific binding is possible due to polyanionic nature of the oligonucleotide as discussed earlier in the chapter, and strong evidence for such a phenomenon has been demonstrated in this research.

Figure 6.7 illustrates the antibacterial activity of **3** and **5** under modified cold shocking conditions. In both a) and b), a marked difference between the control culture and the two TFO-infected cultures is observable, and is so after 12 hours in a), and after 24 hours in b). The difference in b) is very significant, particularly with **5** where there is almost 2 log cycles difference in growth between it and the control culture at 24 hours.

Sequence **3** is the reversed sequence of **6**, were it to form a triplex, it would do so via a parallel manner in relation to the target polypurine sequence via Hoogsteen hydrogen bonds. However, A residues predominate in this sequence quite heavily, which are only able to form triplets via reverse Hoogsteen bonds, due to the position of hydrogen bond donors and acceptors on this base. It is therefore not feasible for this sequence to form a triplex.

The sequence **5** is an acridine-linked analogue of **9**, and therefore the randomised version of **6** with an acridine moiety attached at the 5' end. It was specifically designed so that it would have no target within the *E. coli* genome and genomic database screening has proven this.

The basis of antibacterial activity represented here is therefore not understood but shows strong evidence for non-specific binding for these oligonucleotides and perhaps for the designed TFOs also. It would therefore be advantageous to determine the origin of the antibacterial activity associated with the various TFO and establish whether or not triplexation does actually occur intracellularly. This is a difficult phenomenon to prove, particularly in the case of endogenous DNA as opposed to plasmid DNA due to the overwhelming binding potential of the oligonucleotide to non-specific cellular constituents. Much current research has attempted to establish the origin of TFO mediated gene suppression only to find that observed inhibition resulted from non-sequence specific protein binding (Praseuth, *et al.*, 1999). One

potential mode of determining triplexation intracellularly is via radioprinting, which is a technique that uses ^{125}I-labelled TFOs that once bound to their target site cause duplex breakage. Extraction of cellular DNA and the application to agarose gel electrophoresis enables the determination of triplexation via increase gel retardation in comparison to duplex DNA (Sedelnikova, *et al.*, 1999). Such a technique would be useful here and would answer a lot of questions regarding the antibacterial behaviour of the TFOs presented here. A step further would be the ability to monitor TFO trafficking through the bacterial cell, from uptake through to triplexation. This would give a clearer understanding of the destination of the designated TFO. It is now becoming clearer that the reliance on cell viability as a means of determining the effectiveness of a given TFO is not realistic. Because uptake of these oligonucleotides and their intracellular trafficking is such a multifaceted event, antigene activity may not occur due to circumstances that occur long before the TFO reaches it target. Uptake has been answered to a degree with the use of FACS analysis where an idea of the levels of uptake, aided by each of the methods employed to improve antibacterial activity, was ascertained. Here an assumption was made that any fluorescence recorded resulted from cells that had actually taken up the oligonucleotide without taking into account potential surface binding (Chapter 5). However, in order to assess the true levels of oligonucleotide uptake, surface binding would have to be determined. Therefore the ability to understand the full process is paramount before the true antibacterial activity of the oligonucleotides presented here can be ascertained.

7.0 CONCLUSION AND FUTURE WORK

7.1 Conclusion

The research generally depicts **6** as the most successful antigene agent owing to its ability to form stable triplexes at pH 6.4 and 7.2, and also to produce the greatest level of bacterial suppression compared with all other agents tested.

In comparison to polypyrimidine counterparts (**25**, **26**, **27**), enhanced triplexation was demonstrated, particularly during the melting studies where polypurine third strands formed triplexes with the duplex target, with clear and definable T_m values obtained under both pH conditions tested. A consistent T_m value of 26 °C at both pH values evaluated demonstrated the pH independent nature of **6**. The T_m values obtained for **25**, **26** and **27** were 35, 38 and 39 °C respectively at pH 6.4, and far greater than those obtained for **6**. These sequences showed no triplex transitions at pH 7.2, which was a necessary prerequisite if the TFOs were to have an antigene effect. Poor binding at pH 7.2 was expected with **25**, where acidic pH was necessary for protonation of the C residues, but not so with **26** and **27**. Here C residues were substituted with 5mC in both sequences, and in addition **27** was further stabilised by covalent linkage with an acridine moiety, modifications that were expected to render the TFOs pH-independent.

Acridine intercalation was also disappointing throughout this research where direct stabilising comparisons of acridine linked TFOs, **4** and **27**, with unlinked counterparts, **6** and **26** respectively, yielded only a 4°C rise in triplex stability in the former and only 1 °C in the latter. This was unexpected according to related literature, where T_m values of TFOs containing an acridine residue were demonstrated to be substantially higher than unmodified counterparts. This would imply acridine as a weak triplex stabiliser and in order to increase stability further via intercalation, other agents would need to be investigated.

The only rival sequences to the PO sequences were the PNs. These out of all the sequences produced and tested had by far the greatest T_m values, and therefore would have the greatest potential as antigene agents. The use of these as therapeutic agents is a real possibility owing to them being stable at physiological temperature and being

nuclease resistant. The latter is an important issue particularly when considering **6**, which upon uptake into cells is likely to be degraded due to recognition by exonuclease I. Therefore, if the T_m value of **6** could be increased to such a degree that it was stable *in vivo* and hence an effective antigene therapeutic, its ability to exert this activity would be severely marked due to recognition by exonuclease enzymes. PNs remain 'invisible' to such enzymes, and hence degradation is not an issue.
This potential structural advantage was not however apparent in the antibacterial assays where these sequences failed to inhibit *E. coli* after application of the cold shocking procedure. In fact, **6** was the only agent that produced significant antibacterial activity during any of the assays, indicating a lack of degradation.

It is actually difficult to determine the activity of the PN sequences produced for this study due to inhomogeneity. It is therefore difficult to determine whether T_m values were produced by the designed TFO or another species of this sequence produced as a result of failed synthesis. Such an issue is further highlighted by the inability of these agents to produce a molecular ion under MS analysis despite use of a variety of conditions. These sequences are also complicated by their chemically 'sticky' nature compared with POs, which potentially could lead to hyperstructure formation, again producing misleading T_m values. In order for PNs to be successful in this research, further synthesis would be required coupled with a more discriminating purification procedure in an attempt to produce purer compounds for complete characterisation.

Surprisingly, the antibacterial activity produced by **6** under the cold shocking conditions, exhibited the greatest level of antibacterial activity in comparison to all other delivery methods employed. However FACS analysis demonstrated low and variable levels of uptake (determined as fluorescence produced by fluorescein labelled **6**) by this method, with anionic liposomes serving as far superior agents for this process. From these findings it was expected that antibacterial activity demonstrated by **6** would be greatly enhanced via this vehicle of uptake, and as a result it is could be postulated that antibacterial activity was due to a source other than antigene activity. This highlights a major downfall of this research. The origin of any antibacterial activity is unclear but assumed to result solely from antigene mechanisms. As a result it is difficult to say whether or not the antibacterial activity demonstrated in this research by **6**, is indeed via triplex formation, or via other mechanism such as binding

to other intracellular constituents due to the polyanionic nature of the backbone, or the production of cellular clumping. The former could disrupt fundamental intracellular pathways and hence lead to cellular death. This has been associated with antisense oligonucleotides which after being found as effective antisense agents were later discovered to exert their effect by binding to intracellular proteins (Chapter 1). Cellular clumping would result in inefficient growth of bacterial cells, culminating in diminished cellular counts. In order for the TFOs to produce such a response it would have to occur by repulsive mechanisms. The $CaCl_2$ used in the cold shocking procedure are more likely to cause such an effect due to the Ca^{2+} present in the medium surrounding the cells. In one of the mechanisms put forward for mode of action of the cold shocking procedure, the Cl ions were able to enter the cell inducing osmotic shift of water into the cell and subsequently the uptake of the oligonucleotides (Chapter 1). In this model, Ca^{2+} remained in the media surrounding the cells, potentially causing them to congregate around ions and collections of ions, and hence producing clumping. Further investigation would be required here to verify either of these ideas.

7.2 Future Work

7.2.1 Sequences and Modifications

Initially work needs to be carried out to determine the formation of hyperstructures with a number of sequences. This would be necessary for any of the (G,T) or (G,A)-containing sequences, which are able to form G quartets and homoduplexes respectively. Such structures would interfere with triplex formation *in vitro* but more so in vivo due to K^+ concentrations. Interference of this manner could form the basis of failed triplexation during melting studies, and the inability to produce any bacterial kill. G quartet formation would be possible for any of the polypurine sequences containing contiguous runs of G residues; this includes **6**. Homoduplex formation is an unlikely occurrence during this research as it requires runs of G, A repeats, which none of the synthesised sequences contain. Hyperstructure formation can be analysed by melting studies to see if absorbance varies during heating and cooling of the various TFOs in the absence of the duplex target. Another method of analysis is through gel electrophoresis where retardation properties of the individual TFOs can be determined to assess hyperstructure formation.

Such analysis would also be necessary for the PN sequences produced during this research, which have a natural tendency to form secondary structures. This formation again could affect triplex-forming capabilities. However, before this analysis, resynthesis of these sequences would be necessary in order to produce samples that were more pure and contained a higher yield of the designed TFO. In order to achieve this, the synthesis method would have to be adapted to increase the coupling efficiency at each step of the synthesis cycle. Because of the length of the sequences produced during this research, overall yields were expected to be, and were very low. Application of the amine exchange reaction, used in the synthesis of PNs, has demonstrated crude yields as low as 38% and therefore to produce concentrations of the designated TFOs sufficient to perform the melting studies and the antibacterial assays, this yield would need to be markedly increased. The successful synthesis of pure PNs would be hugely advantageous for this research as out of all the modifications made this would appear to hold the greatest potential. Although samples were not pure these sequences showed the largest increases in triplex stability, producing T_m values sufficient to produce stable triplexes at physiological temperatures enabling the potential use of these agents *in vivo*.

Due to the success of **6** throughout this research further work with this TFO could involve attempts to increase stability of the oligonucleotide on a triplex forming level and regarding exonuclease resistance. The low T_m value of **6** was one of the major limiting factors during this research and meant assays had to be carried out at 20 °C, which was particularly problematic in respect of bacterial replication and fusion of fluidosomes used to delivery **6**. One way of increasing triplex stability would be to replace the two C residues in the TFO with 5mC residues thereby reducing the pH dependence of these two residues. The substitution for 5mC should increase the T_m of **6** at pH 7.2. Other stabilising methods that can be employed are the conjugation to other intercalating agents. Acridine proved unsuccessful as a significant triplex stabiliser, but as illustrated in Chapter 1, there is a wealth of intercalating agents that has been developed and demonstrated as successful triplex stabilisers. Covalent attachment of these to the 5' end of **6** would be another way of increasing the stability of the related triplex.

Regarding exonuclease degradation it would be necessary to modify the backbone of the oligonucleotide so that it is unrecognised by these enzymes. Studies have shown that full backbone modification is not necessary to render TFOs unrecognisable, as it is the 3' hydroxyl that acts as the substrate for exonuclease activity. Substitution for a terminal PS residue is sufficient to decrease nuclease recognition while maintaining triplex stability. Synthesis of such hybrids might therefore discourage nuclease degradation of **6**.

7.2.2 Determination of TFO Activity

Future work regarding TFO activity is two fold; firstly it is necessary to determine true levels of uptake, and secondly to observe the fate of the oligonucleotide once internalised.

Levels of uptake were determined by FACS analysis, which showed delivery via anionic liposomes to be the most efficient method. The assumption was made here that the levels of fluorescence emitted by the fluorescein-labelled TFOs was due directly to the amount of oligonucleotide inside the cell. However, no experimentation was carried out to prove this or to demonstrate that fluorescence was not in fact produced by cell surface agglutination. Although such a phenomenon would be unexpected due to the repelling charges of the liposome and the bacterial surface, Fillion *et al* (Fillion, *et al.*, 2001) demonstrated 20% of the fluorescence exhibited by anionic liposomally-encapsulated fluorescein labelled antisense oligonucleotides, was produced by surface binding after 4 hours of incubation. It would therefore be important, as part of future work to determine what level of lipsomally-encapsulated **7** would share the same fate in this research.

Due to the success of anionic liposomes as bacterial delivery vehicles in this research and that of other groups, such liposomes would be the ideal candidate to pursue in the future. Necessary work here would involve the optimisation of these lipid formulations where work would include DPPC and DMPG ratio variations, to establish the best formulations for the delivery of the TFOs. Although some preliminary work has already been carried out (Chapter 5), further work would be necessary to determine how the levels of uptake vary by different formulations. It is very likely that the results obtained here will be very much sequence- or TFO-specific and as a result all TFO-liposome preparations will have to be screened.

One of the major drawbacks of this research is that the fate of the TFO once internalised is not fully known, as stated. It is not clear whether triplexes are actually formed within the bacterial cells, whether the TFO actually reaches its target, whether it binds to intracellular constituents or simply whether it is degraded upon entry. Before these TFOs can be proven as successful antigene agents these questions need answering.

The determination of intracellular triplexation has been covered in Chapter 6 where it was stated that techniques such as radioprinting using ^{125}I is a possible technique to ascertain this. Binding to intracellular constituents is quite difficult to determine but is perhaps possible via fluorescence of radiolabelling of oligonucleotides. Briefly and very simply, after incubation of the TFOs with the targeted cell line, cells can be lysed with DNA and protein components separated, which are then subsequently separated further using gel electrophoresis. The presence of the labelled oligonucleotide in either gels will enable determination of binding. For such a technique to be successful however, TFO binding either to the genome target or proteins would have to be strong and perhaps by covalent interactions. With triplex formation this is possible after near UV light activation of psoralen-conjugated TFOs.

An alternative approach is the use of confocal microscopy (Hu, *et al.*, 2002), or a mix of confocal microscopy and spectrofluorimetry (Kocisova, *et al.*, 2003). The former used FITC-labelled oligonucleotides and rhodamine-labelled PE to establish the fate of the oligonucleotide upon uptake. The latter was used to monitor antisense oligonucleotides within mammalian cells to determine their path of uptake and intracellular interactions. The method utilises the specific emission properties of labelled oligonucleotides during uptake and subsequent intracellular trafficking produced during incubation of the oligonucleotide with mammalian cells. Both techniques were successful in determining the passage of the oligonucleotide within the given cell lines.

In conclusion, this research shows potential for the use of TFOs as antibacterial agents, but there remains a great deal of unanswered questions that would need answers to promote these as successful therapeutics. Although such a stage is currently a long way off, the current research provides a starting point.

8.0 EXPERIMENTAL

This chapter details the experimental methods used for the purpose of this study and those that are referenced throughout the thesis. Materials and methods are laid out in accordance with the layout of the sections of the thesis.

8.1 Oligonucleotide Synthesis, Purification and Characterisation

8.1.1 Solid Supported Oligonucleotide Synthesis

8.1.1.1 Standard Synthesis Using Phosphoramidites

Oligonucleotides were prepared on a 1 μMol scale using a Beckman Oligo 1000 synthesizer with conventional phosphoramidites, and LCAA-CPG solid supports (Beckman Coultier). Phosphoramidites were purchased from Beckman Coultier as 0.5 g monopacks that were made up in 10 ml dry CH_3CN to yield a maximum of 54 couplings. Acridine and 5-methyl-cytosine (5mC) (Glen Research) for oligonucleotide substitutions were again made up in dry CH_3CN to the same concentration. Fluorescein columns (Glen Research) were attached during the oligomer synthesis to achieve 3' fluorescein labelling (Figure 8.1 for structures).

For all oligonucleotide sequences synthesised, the standard Beckman 'short oligo' method was used unless otherwise stated (Beckman Instruments inc., 1994). The synthesis process is outlined in Chapter 2.

Sequences **28-33** were synthesised by Siobhan Dunbar and sequences **12**, **13**, and **14** were synthesised by Katherine Chalmers, all under supervision. Custom synthesised oligonucleotide **15** was purchased from MWG-Biotech.

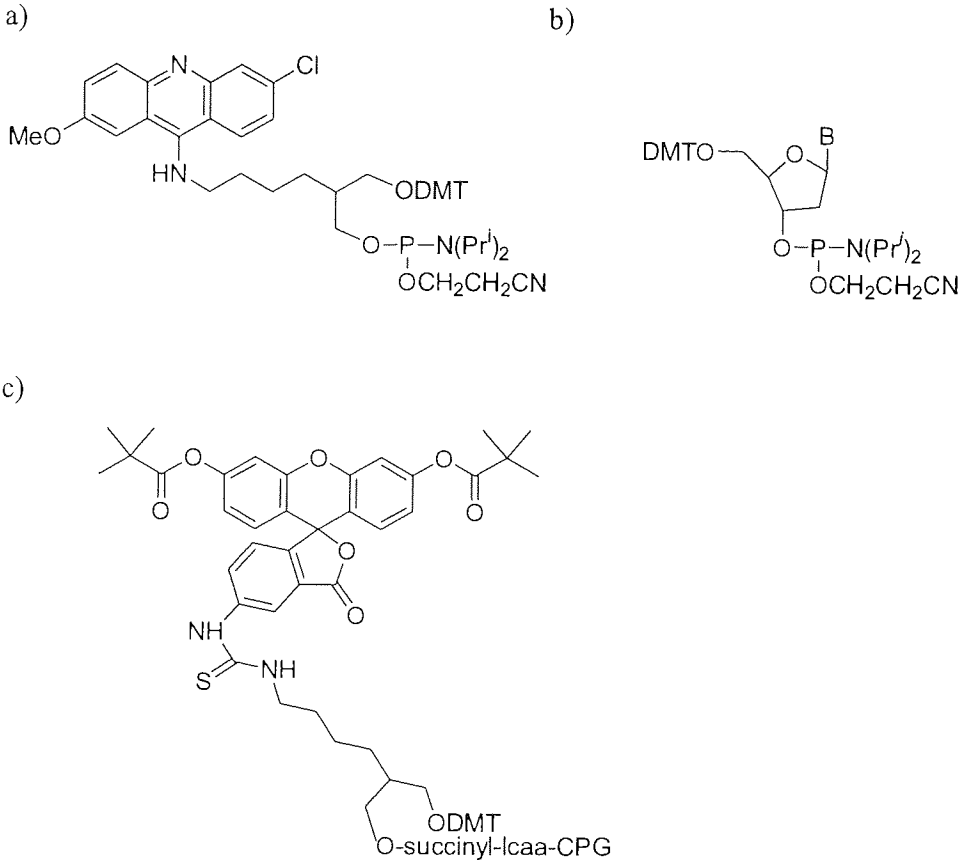

Figure 8.1 a) Acridine attached at the 5' end of the TFO to enhance triplex stability, b) phosphoramidites used in oligonucleotides synthesis where B = A^{BZ}, C^{BZ}, G^{iBu}, T or $5mC^{BZ}$, c) Fluorescein solid support used to label the 3' end of TFOs for their use in fluorescence studies (Chapter 3).

8.1.1.2 Phosphorothioate Synthesis

Phosphorothioates were produced in the same way as the phosphodiester oligonucleotides using the same reagents and the standard synthesis methodology as dictated by the Beckman Oligo 1000 synthesiser. The only alteration made was the replacement of the Oxidize reagent with sulfurising reagent (Glen Research).

8.1.1.3 Phosphoramidate Synthesis

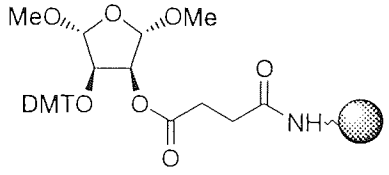

Figure 8.2 Structure of the universal support used in phosphoramidate synthesis.

Phosphoramidate synthesis took place on the Beckman Oligo 1000 Synthesiser using adapted reagents, universal support columns (Glen Research) (Figure 8.2). Phosphoramidate monomers were purchased from Transgenomic and were made up in dry CH_3CN. The synthesis took place in the 5'-3' direction due to the nature of the phosphoramidate amidites, which have a protective MMT group on the 3' amine group of the base.

The standard 'Deblock' solution was replaced with 3% dichloracetic acid in dichlormethane (Glen Research) with the detritylation step yielding a trityl cation and hence a yellow colouration. 'Cap1' solution was replaced with a solution of isobutyric anhydride-2,6-lutidine-THF made up under argon in a ratio of 1:1:8.

The method utilised the standard Beckman protocol for oligonucleotide synthesis. The only exception being the employment of 3 consecutive detritylation steps in order to completely remove the DMT group from the universal support. This was determined through the production of the DMT cation.

8.1.2 Sequences Designed and Synthesised

Table 8.1 – Oligonucleotide sequences produced for the purpose of the study where, **1-7, 9-14** and **23-39** represent phosphodiester sequences, **8** phosphorothioate, **15** 2'-*O*-methyl RNA, and **16-22** phosphoramidates. The table is continued over the page.

Oligonucleotide	Sequence
1	1026bp 1052bp 3'-TTTTCTTTTTGCGCACCTTCCGTAGTC-5'
2	1026bp 1052bp 5'-AAAAGAAAAACGCGTGGAAGGCATCAG-3'
3	5'-AAAAGAAAAACGCGTGGAAGG-3'
4	3'-AAAAGAAAAACGCGTGTAAGG-Acr-5'
5	3'-CGGAGAAAAGTGAAGAAGAAC-Acr-5'
6	3'-AAAAGAAAAACGCGTGGAAGG-5'
7	3'-Fl-AAAAGAAAAACGCGTGGAAGG-5'
8	3'-AAAAGAAAAACGCGTGGAAGG-5'
9	3'-CGGAGAAAAGTGAAGAAGAAC-5'
10	3'-Fl-CGGAGAAAAGTGAAGAAGAAC-5'
11	5'-TTTTGTTTTTGGGGGGGTTGG-3'
12	5'-TTTTGTTTTTGGGGGGGTTGG-Fl-3'
13	3'-TTTTGTTTTTGGGGGGGTTGG-5'
14	3'-Fl-TTTTGTTTTTGGGGGGGTTGG-5'
15	5'-UUUUGUUUUUGGGGGGGUUGG-3'
16	3'-AAAAGAAAAACGCGTGGAAGG-5'
17	5'-AAAAGAAAAACGCGTGGAAGG-3'
18	5'-TTTTGTTTTTGGGGGGGTTGG-3'
19	3'-TTTTGTTTTTGGGGGGGTTGG-5'
20	5'-TTTTGTTTTTGGGGGGGTTGG-Fl-3'
21	3'-TTTTGTTTTTGGGGGGGTTGG-Fl-5'
22	5'-TTGGTGTGGGTTGGTGTGTTT-3'

Table 8.1 Continued from over the page.

Oligoncleotide	Sequence
23	1020bp 1044bp
	5'-ACTGGTAAAAGAAAAACGCGTGGA-3'
24	1020bp 1044bp
	3'-TGACCATTTTCTTTTTGCGCACCT-5'
25	5'-TTTTCTTTTTGCGCACCT-3'
26	5'-TTTTCTTTTTGCGCACCT-3'
27	5'-Acr-TTTTCTTTTTGCGCACCT-3'
28	1021bp 1051bp
	3'-GACCATTTTCTTTTTGCGCACCTTCCGTAGT-5'
29	1021bp 1051bp
	5'-CTGGTAAAAGAAAAACGCGTGGAAGGCATCA-3'
30	5'-TTTTGTTTTTTGTGGGGTTGG-3'
31	5'-Acr-TTTTGTTTTTTGTGGGGTTGG-3'
32	3'-TTTTGTTTTTTGTGGGGTTGG-5'
33	3'-TTTTGTTTTTTGTGGGGTTGG-Acr-5'
34	1231bp 1248bp
	5'-AAGGAAAAAGCGGAAGCG-3'
35	1231bp 1248bp
	3'-TTCCTTTTTCGCCTTCGC-5'
36	3'-AAGGAAAAAG**T**GGAAG**T**G-5'
37	2553bp 2572bp
	5'-AGAAAAAGAAGAAGTTGGGA-3'
38	2553bp 2572bp
	3'-TCTTTTTCTTCTTCAACCCT-5'
39	3'-AGAAAAAGAAGAAG**CC**GGGA-5'

8.1.3 Deprotection

Removal from the solid support, and the removal of the protective group from the NH_2 group of the base, was achieved by treatment with concentrated ammonia (aq) at 55 °C for 16 hours, using a multi-compartmental heating block (Techne Dri-Block

DB.3A). Excess ammonia was evaporated under vacuum (Speedvac – Savant) post membrane filtration (0.45 μM pore size - Whatmann) of each individual oligonucleotide sample.

The pellet produced was resuspended in HPLC grade water, sonicated for 15 min, and membrane filtered again, ready for HPLC purification.

8.1.4 HPLC Purification

Samples were purified by reversed phase HPLC (Hewlett Packard Series 1100) and later purification clarified via a similar process using 20 μl samples post de-salting. Analytical runs were performed prior to purification runs in order to ascertain purity of the sample. Analytical runs required 20 μl sample injections with an absorbance wavelength of 260 nm. Purification runs were carried using 300 μl sample injections at an absorbance wavelength of 285 nm. The change in absorbance wavelength was to reduce the maximum absorbance value to prevent swamping of the sample signal.

Purification was carried out using a C18 reverse phase column (Techsphere) with gradient elution buffer A and increasing amounts of buffer B.

Buffer A consisted of 2% CH_3CN in 0.1 M triethylammonium acetate (TEAA) buffer at pH 7.0. Buffer B consisted of 80% CH_3CN in 0.1 M TEAA at pH 7.0. Table 8.2 illustrates the specific protocol employed for the purification of the oligonucleotides produced here.

Table 8.2 The HPLC buffer gradient employed for the purification of oligonucleotide samples.

Time (min)	Buffer A (%)	Buffer B (%)
0	100	0
20	60	40
30	0	100
40	0	100
45	100	0

The most abundant peaks from each purification run were collected with minor peaks discarded as impurities. Collected fractions were evaporated to dryness under vacuum

(Speedvac - Savant), and then resuspended in HPLC grade water ready for de-salting. Purification was normally carried out at an ambient column temperature. However, where hyperstructures were evident, as in the case of **11** and the phosphoramidate sequences, a column temperature of 50 °C was maintained in order to encourage single strand formation.

8.1.5 Desalting

The TFOs were desalted by a process of reversed phase silica chromatography using SepPak columns (Waters). The column was prepared via flushing with 10 ml CH_3CN, followed by 40 ml HPLC grade H_2O. Oligonucleotide samples, after addition to the column, were eluted by washing with 30:70, CH_3CN-water respectively. Eluted fractions were then subjected to UV-spectrophotometry and those exceeding the absorbance limit were retained and evaporated to dryness under vacuum (Speedvac - Savant).

Once evaporated the samples were resuspended in HPLC grade water and purification assessed via HPLC, MS and CE analysis.

Concentrations of the samples were then determined via UV-spectrophotometry using a 1 in 10 dilution of the oligonucleotide sample and calculated using absorbance and the relative extinction coefficient of the given bases (Table 8.3). Theoretical molecular weights (MW) were also calculated.

Table 8.3 Extinction coefficients and molecular weights of bases, modified bases and intercalating agents used in calculations for the purpose of this study.

Base, Modified Base or Intercalating Agent	**Extinction Coefficient (cm^{-1} M^{-1})**	**Molecular Weight**
A	15400	251.2447
C	7300	227.2187
5mC	7300	241.2455
G	11700	267.2437
T	8800	242.2296
Acridine	8845	558.1509
Fluorescein	72000	536.6022

8.1.6 Mass Spectrometry (MS)

Theoretical molecular weights of each individual oligonucleotide sample after purification were calculated. Each oligonucleotide was then characterised via negative-electrospray MS (Hewlett Packard Series 1100 coupled with Hewlett Packard 5989B Mass Spectrometer and Hewlett Packard 59987A Electrospray unit) to ascertain the practical molecular weight of the sample and to determine whether synthesis had been successful. The instrumental parameters can be seen below.

8.1.6.1 MS parameters

Table 8.4 Parameters for negative-electrospray MS. These parameters match those suggested by Greig *et al.* (Greig, *et al.*, 1995). Previous parameters for neat sample analysis utilised a fixed CapEx = 100V and a drying gas temperature of 300 °C.

ES Source Parameters	MS Acquisition Parameters
V_{cap} = 3500V	Scan range = 500 to 1800 amu
V_{end} = 3000V	Step size = 0.1 amu
V_{vcl} = 3500V	Integration = 100 μsec
EntLens = VAR (dynamically ramped)	Samples = 2-4 depending on sample
CapEx = VAR (dynamically ramped)	Averages = 3
Drying gas flow = 35	**Raw Data**
Gas 2 (oxygen) flow = 10	Mass filter = Gaussian 0.3 amu
Drying gas temperature = 185 °C	Time Filter = Gaussian 0.05 min
Nebulizing gas pressure = 70psi	Threshold = 50

Instrument tuning was carried out using known standard solutions (Electrospray Tuning Mix - Agilent), with tuning made at masses 112.99, 431.98, and 1305.95. Samples were injected into the mass spectrometer via the syringe pump utilising a flow rate of 10 μl/min in order to minimise the amount of sample required for an individual analysis.

8.1.6.2 Sample Preparation

Two sample methods were used in order to gain mass spectra. The first method involved the injection of neat oligonucleotides into the mass spectrometer. Out of all the samples injected no spectra were actually produced except for that of **6**. Failure of

the production of spectra of all other sequences lead to the application of a second method of sample preparation.

The second method required the dilution of oligonucleotide samples in 100 mM piperidine at a ratio of 1:1 to yield a final piperidine concentration of 50 mM (Greig, *et al.*, 1995).

8.1.7 Capillary Electrophoresis (CE)

Capillary electrophoresis was carried out to ascertain the purity of the synthesised oligonucleotides post purification, using the SpectraPHORESIS 100 CE system PC linked using tsp (thermo separation products) software. Polyacrylamide gel columns were used for the analysis (μPAGE fused silica capillary electrophoresis column filled with polyacrylamide (3% T, 3% C) 75μM I.D. x 50 cm – Agilent Technologies), with standard oligonucleotide samples (consisting of poly d(A) 25-30 nucleotide (0.01 mg/ml) and poly d(A) 40-60 nucleotides (0.02 mg/ml) – Agilent Technologies) used to assess column viability.

Synthesised samples were made up at a concentration of 0.01 mg/ml using distilled water as the diluent. CE was carried out at 12.5 kV with pre-run sample injections of 5 sec followed by 45 min running time. Samples migrated along the column in trisborate urea buffer (100 mM trisborate, 7 M urea at pH 8.3 - Agilent Technologies) and detected by UV-spectrophotometry at 260 nm.

8.2 *In Vitro* Triplexation

8.2.1 Triplex Annealing Studies

Triplex stability was assessed using a Varian-Cary E1 UV-visible spectrophotometer with a multi-compartmental Peltier heating block. Oligonucleotide samples were heated to 80 °C and then cooled at a rate of 0.5 °C min^{-1} to 0 °C to aid annealing before reheating to 80 °C with absorbance values recorded at a wavelength of 260 nm. The samples were then cooled to 0 °C before heating back to 20 °C. The block was flushed with N_2 below ambient temperature to avoid condensation on the cell walls.

The annealing studies were carried out under two separate pH conditions, pH 6.4 and pH 7.2. The samples containing the target strands (purine and pyrimidine) with the test TFO, were prepared in a total volume of 1.8 ml with an individual strand concentration of 1.5 μM and a total strand concentration of 4.5 μM. DNA strands were made up in buffer at pH 7.2 comprising 100 mM NaCl, 10 mM $MgCl_2$, 25 mM Tris.HCl and 0.5 mM spermine. Similarly the buffer at pH 6.4 containing additionally 10 mM PIPES in the place of Tris-HCl. Volumes of the individual strands used in the sample were dependent on individual oligonucleotide sample concentrations.

8.2.2 Fluorescence Spectrophotometry

8.2.2.1 Genomic DNA Extraction From *E. coli* DH5α

8.2.2.1.1 Cell Lysis

The *E. coli* was grown up overnight in 100 ml of LB broth at 37 °C with agitation (150 rpm). Cells were harvested via centrifugation at 10000 g for 10 min, and then washed in sterile, distilled water (s.d.H_2O). After centrifugation (10 min at 10000 g) the pellet was resuspended in 4.5 ml Tris-EDTA (TE) [10 mM Tris, 1 mM EDTA, pH 8.0]. Cells were then heated to 75 °C for 10 min to deactivate DNase enzymes.

The cells were then lysed by the addition of 500 μl SDS (0.1 g/ml) to yield a final concentration of 1% (w/v). Proteinase K (Sigma) was added to produce a final concentration of 10 mg/ml and cells incubated at 65 °C for 1 hour.

The lysed cell suspension was then aliquoted into separate tubes containing a small amount of silicone grease. The grease enabled easy separation of the phenol during phenol–chloroform–isoamyl alcohol extraction.

8.2.2.1.2 Phenol-Chloroform-Isoamyl Alcohol (P-C-I) Extraction

P-C-I (25:24:1) was added in equal volume to the lysed cell solution in each of the tubes. The mixture was then vortexed and centrifuged (4000 x g for 10 min). The top layer, containing the DNA, was then removed with care made not to disturb the white, precipitated protein layer on the surface of the grease. The DNA was then ethanol precipitated via addition of 0.1 volumes of 3 M sodium acetate (pH 5.2) and 2 volumes of ice-cold ethanol. This was placed at -20 °C for 15-20 min.

Post incubation, the suspension was centrifuged at 10000 x g for 5 min, the supernatant discarded, and the pellet washed in 70% ethanol. Centrifugation was again repeated at 10000 g for 5 min. The supernatant was again discarded and the pellet dried at 40 °C for 15-30 min.

The pellet was finally rehydrated in s.d.H_2O overnight at 4 °C. Quality and quantity of the DNA was determined by UV-spectrophotometry.

Optical densities (O.D.) taken at 260 and 280 nm allowed the purity of the DNA to be determined by dividing the former value by the latter. The extent of deviation below a value of 1.8 gave an indication of the extent of protein contamination. The O.D. value produced at 260 nm enabled quantities of the DNA in μg/μl to be ascertained (Sambrook, *et al.*, 1989).

8.2.2.2 Plate assay

96 well microtitre plates were coated using the *E. coli* DNA extract. This was applied neat in column one and then doubly diluted across the plate into subsequent wells containing s.d.H_2O.

After incubation the DNA solution was discarded and the plates washed 3 times in Tris-buffered saline containing Tween20 (Sigma) (TTBS) [0.01 M Tris-HCl pH 7.4, 0.9% (w/v) NaCl, 0.3% (v/v) Tween]. The plates were then blocked in 1% BSA (w/v) in TBS for 3 hours. The BSA was then discarded and the plates once again washed in TTBS. The fluorescein-labelled oligonucleotides (**7**, **10**, **20** and **21**) were then added at a concentration of 10 μM to the wells in row A (not including A12). They were then doubly diluted in triplex buffer [5 mM spermine, 1000 mM NaCl, 100 mM $MgCl_2$, pH 7.2] down the plate up to and including wells in row 7. Row 8 and column 12 were left as blank wells and were consequently filled with triplex buffer. The plates were incubated for 24 hours at 4 °C.

The plate was then washed in triplex buffer, and read (after 1, 2, and 3 washes) using a fluorescence plate reader (Molecular Devices, Spectra Max Gemini XS) with an excitation wavelength of 492 nm and an emission wavelength of 520 nm. Association curves and K_d values were calculated using GraphPad Prism®.

8.3 Bacterial Strains, Maintenance and growth Curves

8.3.1 *E. coli* DH5α

8.3.1.1 Growth Curve

E. coli DH5α was grown in Luria Bertani (LB) broth [1% (w/v) Tryptone (Oxoid), 0.5% (w/v) yeast extract (Oxoid), 0.5% (w/v) NaCl], overnight at 37 °C after inoculation with 2-3 colonies. Triplicate flasks containing fresh LB were inoculated using a 1% inoculum from the overnight culture and time 0 absorbances measured at a wavelength of 470 nm. The flasks were then placed at 37 °C with agitation (150 rpm) for the time course of the assay. Absorbance readings were taken every 30 min up to and including 7 hours and plotted.

Cultivation of *E. coli* DH5α for the purpose of all assay and kill assays was carried out in LB broth of the same constituents as those stated above unless otherwise stated.

8.3.1.2 Effect of Ciprofloxacin upon Growth Curve

The ciprofloxacin kill assay against *E. coli* was carried out using a concentration of 0.5μg/ml with an organism inoculum concentration of 10^6 CFU/ml. The organism was grown in LB broth at 37 °C overnight. Ciprofloxacin (Bayer) was dissolved in distilled water and then syringe filtered before addition to the culture. The samples were placed at 37 °C with agitation (150 rpm), throughout the time course of the assay after addition of the antibiotic. Viable counts were made at 0, 1, 2 and 3 hours via plating 0.1 ml of each sample to NA agar after sufficient serial dilutions were made. Ten fold serial dilutions were made in LB broth, which enabled replica counts to be made. Plates were incubated at 37 °C overnight after which CFU/ml were finally calculated.

8.3.2. *S. pneumoniae*

8.3.2.1 Growth Curve

Flasks containing brain heart infusion broth (BHI) (Oxoid) were inoculated with 2-3 colonies of *S. pneumoniae* (Aston culture collection 8EVI) taken from blood agar plates and incubated statically at 37 °C overnight under aerobic and CO_2 enriched conditions. After incubation separate flasks containing fresh BHI broth were inoculated with a 1% inoculum from each of the overnight cultures and time 0

absorbances were measured at a wavelength of 470 nm. Flasks were then placed under either aerobic conditions or under CO_2 enriched conditions, both at a temperature of 37 °C. Absorbance readings were taken every 30 min up to and including 12 hours.

8.3.2.2 Growth Characteristics at 25 °C

BHI broth was inoculated with a heavy inoculum of *S. pneumoniae* from blood agar plates. The cultures were then maintained at 37 °C under static aerobic conditions for 72 hours. The absorbance values were determined at 24, 48 and 72 hours at a wavelength of 470 nm.

8.4 Characterisation and Analysis of *In Vitro* Uptake Methods

8.4.1 Cationic Lipid Analysis

Zeta potential analysis (Brookhaven Instruments Corp.) was used to ascertain the charge of four cationic lipids alone and in association with LB bacterial culture broth, and designed TFOs. The four commercially available lipids used were Lipofectin®, LipofectAMINE™, CellFECTIN® and DMRIE-C (Gibco BRL - Life Technologies), chemical names and structures can be seen in Figure 8.3

a)

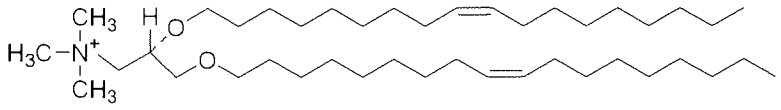

b)

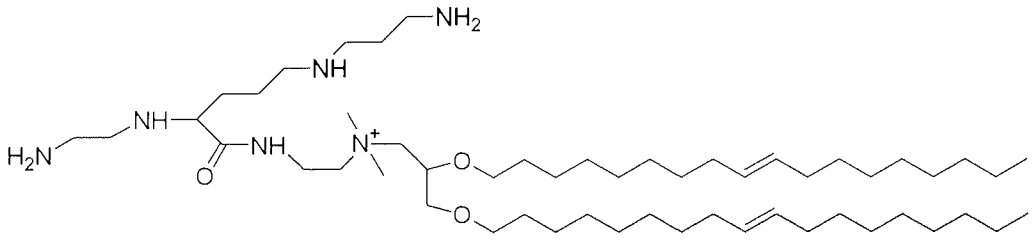

c)

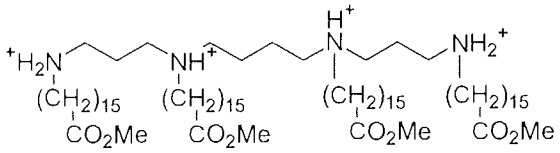

d)

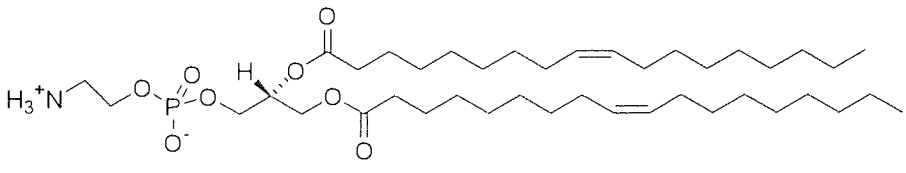

Figure 8.3 Continued over the page

e)

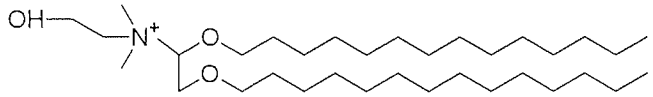

Figure 8.3 Structures of the four cationic lipids used for the purpose of the study, where;

a) = DOTMA (N-[1-(2,3-dioleyloxy)propyl]-N,N,N-trimethylammonium Chloride) the cationic lipid used in the Lipofectin® reagent in conjunction with DOPE (d) in a 1:1 formulation (Blau, *et al.*, 2000).

b) = DOSPA (2,3-dioleyloxy-N-[2(sperminecarboxamido)ethyl]-N,N-dimethyl-1-propanaminium trifluoroacetate) the polycationic lipid used in Lipofectamine™ reagent in conjunction with DOPE (d) in a 3:1 formulation (Blau, *et al.*, 2000).

c) = TMTPS (N,N^{I},N^{II},N^{III}-tetramethyl- N,N^{I},N^{II},N^{III}-tetrapalmitylspermine) the cationic lipid used in Cellfectin® reagent in conjunction with DOPE in a 1:1.5 formulation.

d) = DOPE (dioleoyl phosphotidylethanolamine) the neutral helper lipid used in conjunction with DOTMA, DOSPA and TMTPS (Miller, 1998).

e) = DMRIE (2 dimyristyloxypropyl-3-dimethyl-hydroxy ethyl ammonium bromide) the cationic lipid used in DMRIE-C reagent in conjunction with cholesterol (Blau, *et al.*, 2000).

Samples were made up in accordance with the literature supplied with the lipids, mimicking the same preparation protocol as that used for the antibacterial assay (Chapter 6). The constituents of each sample can be seen in Table 8.5.

Table 8.5 The constituents of the cationic lipid samples for zeta potential analysis where PBS = phosphate buffered saline, LB = Luria Bertani broth, **6** = the designed TFO targeted to *E. coli*.

	Volume (µl)							
Sample	Lipofectin	Lipofectamine	Cellfectin	DMRIE-C	PBS	LB Broth	6	*E. coli*
1	10				490			
2		10			490			
3			15		485			
4				5	495			
5						500		
6	10					490		
7		10				490		
8			15			485		
9				5		495		
10	10					487.80	2.20	
11	10					485.70	4.30	
12	10					483.55	6.45	
13	10					481.30	8.70	
14	10					479.20	10.80	
15	10					477.00	13.00	
16								500

8.4.2 Anionic Liposome Formulation

8.4.2.1 Liposome Formulation

Dipalmitoylphosphatidylcholine (DPPC) and dimyristoylphosphotidylglycerol (DMPG) (Avanti Polar lipids) were formulated at a molar ratio of 10:1 respectively via a dehydration-rehydration vesicle (DRV) method. The two lipids were dissolved in 2-5 ml of chloroform in a ratio of 10:1 respectively. Once dissolved the solution was evaporated to dryness via a rotary evaporator (Rotavapor REIII coupled to a Büchi 461 waterbath) at 65 °C, a temperature in excess of the T_c temperature (gel-liquid crystalline transition temperature).

After evaporation the flask was flushed with argon to eradicate any air. Two millilitres of prewarmed 1:20 PBS (55 °C) was added and the flask vortexed until the evaporate was fully resuspended. The flask was then incubated at 55 °C for 1-2 hours. After incubation the solution was sonicated (Soniprep 150 - Sanyo) at 15 amps under

argon using 30 sec on/off cycles. The purpose of the sonication is to break down large multilamellar vesicles (MLVs) (that are produced by stacking layers of liposome bilayers that form when the liposomes are first produced), to small unilamellar vesicles (SUVs) consisting of a single bilayer. 5 or 6 cycles were performed up to a maximum of 10 min per sample. During the process of sonication the solution became noticeably clearer. Post-sonication the lipid solution was left to rest for 1 hour at 55 °C.

Oligonucleotides were diluted to a concentration of 20 μM in 2 ml of PBS, prewarmed to 55 °C, and then added to the lipid solution. Upon addition, the solution was vortexed and rapidly frozen in liquid Nitrogen, after which it was freeze dried for ~ 12 hours (Virtis Advantage).

Liposomes containing **6**, **7** and **10** were prepared for the purpose of the study. Control liposomes, so-called 'empty liposomes', were made up containing the same volume of PBS.

8.4.2.2 Liposome Reconstitution

One hundred microlitres of pre-warmed s.d.H_2O (55 °C) was added to the freeze dried lipid-oligonucleotide, which was then vortexed vigorously until all H_2O absorbed. The lipid-oligonucleotide was then incubated at 55 °C for 30 min. A further 100 μl of H_2O was then added, the solution vortexed and then incubated again at 55 °C for 30 min. This process was finally repeated but with the addition of 800 μl of PBS. This is called controlled rehydration and has been reported to result in the internalisation of DNA (Perrie and Gregoriadis, 2000).

After the final 30 min incubation the lipid solution was centrifuged for 30 min at 10,000 x g. The supernatant was removed and retained, and the pellet resuspended in 1 ml s.d.H_2O. This procedure was repeated twice more with all 3 washes retained and the final resuspension carried out in 2 ml of H_2O.

8.4.3 Liposome Characterisation

8.4.3.1 Sample Analysis

All liposome samples after formulation were exposed to zeta potential and particle size analysis (Brookhaven Instruments Corp.). This was to establish average sizes and surface charge of the liposomes to determine how successful the formulation process had been, but also to gain an idea of how these would interact with the bacterial cells. Samples were diluted in saline (0.85%) and results presented are a mean of 5 readings.

8.4.3.2 DPPC and DMPG Ratio Analysis

A set of liposomes were formulated, made up of different ratios of DPPC and DMPG, and characterised to assess the favoured formulation for the oligonucleotides. These liposomes were formulated as stated above, but with different amounts of the DPPC and DMPG constituents used. Liposomes were made up in the following ratios; 1:1, 1:5, 1:10, 1:20 of DMPG:DPPC respectively.

After formulation and reconstitution, the liposomes were characterised using particle size and zeta potential analysis (Brookhaven Instruments Corp.). Sample readings were taken in triplicate and quintuplet respectively.

8.4.3.3 Fluorescence Microscopy

Encapsulation of fluorescein-labelled oligonucleotides was visualised using fluorescence microscopy. 5 µl samples of the liposomes were sandwiched between a microscope slide and cover slip, and imaged at x40 magnification using a Zeiss Axioskop microscope with an AxioCam HRc camera attached for imaging. The microscope and camera were PC interfaced where images were captured using Axio Vision 3.1 software.

8.4.4 FACS Analysis

FACS analysis was carried in order to ascertain the level of uptake of the oligonucleotides (7) into *E. coli*. This analysis enabled the quantitative measurement of oligonucleotide uptake as a measure of fluorescence emitted by the bacterial cells upon exposure to 7 where passive, cold shocking and lipid mediated methods of uptake were assessed for the most efficient.

Initial studies were carried out at 37 °C, followed by subsequent studies performed at ambient temperature due to the T_m value of **6**. Statistical analysis, in the form of unpaired t-tests, was performed to assess the differences between samples. In all cases autofluorescence produced by the bacterial culture was deducted.

8.4.4.1 Sample Preparation

8.4.4.1.1 Liposome-Encapsulated TFO Uptake Assay

E. coli DH5α was grown up overnight in LB, with fresh LB inoculated with a 1% inoculum and incubated for 1.5 hours. This was carried out in the same way as the *E. coli* manipulations were performed prior to the antibacterial kill assay (Chapter 6). The culture was then diluted to an absorbance of 0.05 at 600 nm and aliquoted into the desired number of Eppendorfs. Liposome-encapsulated TFOs, **7**, were added in an equal volume to the culture with empty (PBS-containing) liposomes added in the same way to separate Eppendorfs to be used as control samples. A bacterial control sample was also used containing only the diluted culture and s.d.H_2O. Samples were mixed and incubated for 3 hours in a shaking water-bath at 37 °C to allow uptake.

Post incubation samples were placed on to a sucrose cushion (sucrose solution (24% w/v) in buffer R (50 mM Tris, 10 mM $MgCl_2$, 150 mM KCl at pH 7.5)) and centrifuged at 4000 x g for 20 min. The cushion enables the separation of the bacterial cells, which form a pellet, from any unfused or excess liposomes, which accumulate as a surface layer.

The excess lipid was discarded along with the supernatant, the pellet washed in LB and then centrifuged at 10000 x g for 10 min. The cells were again placed on a sucrose cushion and recentrifuged at 4000 x g for 20 min as means of ridding the samples of any liposomes that were not discarded on the first cushion. Once the sucrose was discarded, cells were resuspended and fixed in 2% paraformaldehyde, and then placed at 4 °C before FACS analysis.

8.4.4.1.2 Concentration Assay

The above procedure was repeated but using different volumes of liposomes in comparison to the volume of culture. The basis behind this analysis was to ascertain how an increasing volume of liposomes to stationary cell volume, affects the level of uptake, and ultimately whether there is a point at which the uptake mechanisms become saturated and uptake reaches a plateau or declines.

The protocol above dictates a culture:liposome volume ratio of 1:1. In this assay the ratios were as follows; 1:0.25, 1:0.5, 1:1, 1:2, and 1:5 culture volume to liposome volume respectively. Incubation of the samples again took place at 37 °C for 3 hours in a shaking water-bath and the samples were processed as for the rest of the assay as stated above.

8.4.4.1.3 Analysis of Cold Shocked Cells

Cultures of *E. coli* were grown up overnight with fresh LB inoculated using a 1% inoculum, and incubated at 37 °C for 1.5 hours. The culture was then diluted 10^3 fold in cold $CaCl_2$ and placed on ice for 20 min.

An equal volume of 7 and 7F were then added at a strand concentration of 20 μM yielding an overall concentration of 10 μM. The solution was then vortexed and placed back on ice for 30 min. The cells were centrifuged at 10000 x g for 10 min, washed in LB, recentrifuged, and finally the pellet resuspended and fixed in 2% paraformaldehyde. Samples were again placed at 4 °C before FACS analysis.

The cold shocking procedure here, mimics that used in chapter 6 for the purpose of the antibacterial kill assays (Sambrook, *et al.*, 1989).

8.4.4.2 FACS Analysis

Bacterial cell fluorescence, from the various assays outlined, was determined via flow cytometry analysis using a Becton Dickinson FACS 440 with an argon laser (200 mW). FITC levels were detected with an excitation and emission wavelength of 488 and 530 nm (±15 nm) respectively. Fluorescence of 10,000 cells was measured per sample, post calibration of the flow cytometer with 1 μm fluorescent beads (Coulter). Samples were vortexed prior to injection to maintain a homogeneous distribution of cells.

8.5 Antibacterial Evaluation

8.5.1 Bacterial Kill Assays

8.5.1.1 *E. coli* Kill Assays

8.5.1.1.1 The Passive Uptake Assay

E. coli DH5α was grown in Luria Bertani (LB) broth for 18 hours at 37 °C to achieve ~10^8 CFU/ml. The culture was diluted in LB broth to achieve an ~10^6 CFU/ml test culture.

The oligonucleotide samples were diluted to a concentration of 20 μM in d. H_2O, and the samples then syringe filtered for sterility. The oligonucleotides were then added to an equal volume of bacterial culture to yield a final oligonucleotide concentration of 10 μM. Samples were then placed at 20 °C in a shaking water bath for the duration of the assay. Viable counts were made at 0, 1, 2, 3 and 6 hours after addition of the oligonucleotides to culture medium, through plating 50 μl onto nutrient agar (NA) after three, 10-fold serial dilutions in LB.

Plates were incubated at 20 °C, with counts and CFU/ml calculated after 3 days. This time span was necessary to allow adequate visualisation of the colonies.

8.5.1.1.2 The Cold Shock Assay

8.5.1.1.2.1 The Initial Cold Shocking Protocol (Sambrook, *et al.*, 1989)

E. coli was grown for 18 hours, and using a 1% inoculum, fresh LB broth was inoculated. This was incubated at 37 °C until an O.D. of 0.1 (approx. 10^{6-7} CFU/ml, at 470 nm) was achieved. 10 ml samples were then centrifuged at 4000 x g for 5 min, the supernatant was discarded and tubes inverted to drain any remaining media. The pellet was then resuspended in 6 ml cold $CaCl_2$ (50 mM) by gentle vortexing, and left on ice for 10-15 min.

The samples were then once again centrifuged (5 min at 4000 x g) and the whole wash step repeated. Resuspension took place this time in 1 ml $CaCl_2$ with samples left on ice for 20 min.

One hundred microlitre samples were aliquoted into precooled Eppendorf tubes, and 100 μl of designated TFO (at a concentration of 20 μM) was added. Samples were then left on ice for 30 min before incubation at 37 °C for 1 min, after which they were placed back on ice for further 2-5 min. The culture and TFO solution was then added

to 9.8 ml of LB broth, and the assay performed as previously described above, with viable counts made at the same time points. Antibacterial activity of the TFOs was also assessed in parallel, without the addition of the LB broth.

8.5.1.1.2.2 The Modified Cold Shocking Protocol for Low Cell Concentrations

The above protocol was not suitable for assays using low cell concentrations and hence was modified. After cells had been grown to an O.D. of 0.1 they were diluted down 10^3 fold in ice-cold $CaCl_2$ and placed on ice for 20 min. Designated volumes of *E. coli* culture were then aliquoted to separate sterile Eppendorf tubes, which had been pre-cooled. The oligonucleotides were then added in an equal volume, at a concentration of 20 μM. Two slight variations were made here, variation one involved the dilution of the oligonucleotides in s.d.H_2O, and two, involved the dilution of the sequences in LB broth. Once the oligonucleotides had been added to the culture the remainder of the assay proceeded as previously stated with the exception of a number of assays being carried out over 12 and 24 hours.

8.5.1.1.2.3 BacLight™ Staining

The Baclight™ stains (Molecular Probes) are another way of detecting both dead and live cells and were applied here to the cold shock assay. The assay was carried out predominantly in the same way as stated above using the low cell number protocol, but with a cell suspension measuring an O.D. of 0.06 at 670 nm. The initial culture was also split in two with one half used for a calibration curve to determine live cells, and the other half used as the assay culture. Both were subjected to cold shocking however. The protocol used was adapted from protocols published by Molecular Probes that accompanied the stains.

8.5.1.1.2.3.1 The Assay Culture

After the addition of the TFO and the final incubation on ice, the assay culture was assessed for live and dead cells.

Two hundred microlitres of each of the samples were taken and pelleted at 10,000 x g for 12 min. The supernatant was then discarded and the pellet washed in 200 μl of s.d.H_2O. After centrifugation the pellet was once again resuspended in 200 μl of s.d.H_2O. Two x 100 μl samples were then aliquoted to separate wells of a microtitre plate and 100 μl of stain solution added to each. The plate was then incubated in the dark for 15 min at ambient temperature.

The stain solution consisted of a 2 x solution comprising 6 µl of propidium iodide and 6 µl of Syto 9 stain, in a total volume of 2 ml of d.H_2O.

After 15 min the plate fluorescence was determined using a fluorescent plate reader (Molecular Devices, Spectra Max Gemini XS) at a wavelength of 530 nm (EM1) and 630 nm (EM2).

Samples were taken in the same manner after each hour up to and including 5 hours.

Finally the ratio of G/R was calculated:

$$G/R = EM1/EM2$$

Where; G represents green fluorescence that is emitted by live cells that take up the Syto 9 stain. All cells will take up this stain whether dead or alive, and R represents red fluorescence emitted by dead cells that take up propidium iodide in addition to the Syto 9 stain. The combination of the two stains, taken up by these cells causes them to fluoresce red.

8.5.1.1.2.3.2 The Calibration Culture

The calibration culture post cold shocking was pelleted, the supernatant discarded and the pellet resuspended in 1ml of s.d.H_2O. This culture was split between 2 separate tubes, with one tube made up to 10 ml with s.d.H_2O (live cells), and the other the same with 70% isopropyl alcohol (dead cells). These were incubated at ambient temperature for 1 h with shaking every 15 min. These were then centrifuged (10,000 x g for 10-15 min) and washed twice in s.d.H_2O, with the final resuspension made in 10 ml of s.d.H_2O.

The cells were then mixed together in 6 different proportions with a final volume of 2 ml (Table 8.6).

Table 8.6 - Volumes of live and dead cells used to yield the given proportions cells for the production of a calibration to determine the level of cell death during the above mentioned antibacterial assay.

Ratio of Live:Dead Cells	Volume of Live cell Suspension (ml)	Volume of Dead cell Suspension (ml)
0:100	0.0	2.0
10:90	0.2	1.8
30:70	0.6	1.4
70:30	1.4	0.6
90:10	1.8	0.2
100:0	2.0	0.0

100 µl of each of the cell suspensions was transferred to a single well in a 96-well microtitre plate in triplicate. Stain solution (at the same concentration as stated above) was added at an equal volume and the plate again incubated at ambient temperature, for 15 min, in the dark. After the incubation the plate was read and the ratio of G/R established in the same way as stated above. The ratio G/R was plotted (y-axis) against live cells (%) (x-axis). This curve enabled the determination of live cells in the assay samples.

8.5.1.1.3 Chlorpromazine (CPZ)-Aided Uptake

8.5.1.1.3.1 CPZ MIC

5 ml of double strength LB broth containing 100 µl of overnight *E. coli* culture was dispensed into glass test tubes and 5ml of CPZ added at a range of concentrations. The CPZ was diluted in s.d.H_2O and membrane filtered for sterility. Concentrations ranged from 70 µg/ml to 15 µg/ml in steps of 5 µg/ml and upon addition the tubes were incubated for 24 hours at 37 °C. Growth and hence the MIC was determined via spectrophotometry at 470 nm.

8.5.1.1.3.2 CPZ-Aided Antibacterial Action

E. coli DH5α was grown overnight at 37 °C, fresh LB was inoculated using a 1% inoculum and grown for a further 1.5 hours. The culture was then centrifuged at 10,000 x g for 10-15 min. The pellet was then washed in saline (0.85%) and re-centrifuged. This wash step was repeated and the final pellet again resuspended in saline. The culture was aliquoted to separate Eppendorfs where it was incubated for 1 h with CPZ prior to the addition of **6**. The CPZ was added at a concentration of 27.5 μg/ml (half the MIC), and the TFO at a concentration of 20 μM after 1 hour. Bacterial, CPZ and **6** control samples were run in unison and all samples incubated for 3 hours at 20 °C, after which, 50 μl was plated to NA in triplicate. The plates were incubated at 20 °C, and CFU/ml calculated after 3 days.

8.5.1.1.4 Antibacterial Activity Using Liposome-Aided Uptake

8.5.1.1.4.1 Cationic Lipid Kill Assays

Cultures were grown up overnight, and a 1% inoculum used to inoculate fresh LB broth, which subsequently was grown up to an O.D. of 0.1 (at 470nm).

A 250 μl sample of LB broth was added to 4 sterile Eppendorf tubes. A serum free medium was required to enable successful lipid/DNA complexation. The lipofection reagents (Life Technologies™) were added to the respective tubes in the following volumes stated in Table 8.7.

Table 8.7 The volumes of cationic lipids used in the cationic liposome assays.

Lipofection Reagent	Volume (μl)
Lipofectin®	10
Lipofectamine™	10
Cellfectin®	15
DMRIE-C	5

The Eppendorf tubes were then incubated at room temperature for 30 min, after which 250 μl of TFO, at a concentration of 1 μg/250 μl, was added to each tube and then incubated at room temperature for 15 min. 50 μl of culture was added to each of the tubes, which were in turn incubated at 20 °C for the time course of the assay. Viable counts were made at 0, 1, 2, 3 and 6 hours, plating 50 μl to NA after the required

serial dilutions. Controls containing each of the lipofection reagents were run in conjunction with the above-mentioned assay to assess the cytotoxicity of each lipid.

8.5.1.1.4.2 Anionic Lipid Kill Assay

E. coli DH5α was grown overnight at 37 °C, fresh LB was inoculated using a 1% inoculum and grown for a further 1.5 hours. The culture was then centrifuged at 10,000 x g for 10-15 min. The pellet was then washed in saline (0.85%) and re-centrifuged. This wash step was repeated and the final pellet again resuspended in saline. 200 µl of culture suspension was then added to sterile Eppendorfs, and then an equal volume of encapsulated **6**, empty liposomes and saline were subsequently added. The encapsulated **6** and empty liposomes had been pre-formulated using a 1:10 molar ratio of DMPG-DPPC as outlined in the section describing anionic liposome formulation. At this point three variations were made on the assay:

1. In the initial assay, samples were incubated at 20 °C for 3 hours, and then, 50 µl samples taken and plated to NA in triplicate. CFU/ml were calculated after a 3 day incubation period at 20 °C.

2. In the second variation, samples were incubated for total time of 3 hours, with samples taken in the same manner as stated above, at 0 and 3 hours.

3. In the third variation the assay was carried out over a period of 6 hours, with viable counts made at 0, 1, 2, 3, and 6 hours. Bacterial cultures were incubated for 1 hour at 37 °C, after the addition of the TFO, and prior to the commencement of the assay.

8.5.2. *S. pneumoniae* Kill Assays

Three colonies were used to inoculate 30 ml of brain heart infusion broth (BHI), which was incubated statically at 25 °C for 72 hours under aerobic conditions. 30 ml of fresh broth was inoculated with 0.3 ml of the 72 hour culture and the culture grown up for 48 hours at 25 °C to establish the organism in the log phase of growth. These cultures were again maintained under static aerobic conditions. After 48 hours the culture was diluted in BHI to establish 10^2 - 10^3 CFU/ml with the dilution factor

determined by absorbance values taken at a wavelength of 470 nm. The diluted culture was then aliquoted to sterile Eppendorfs and an equal volume of oligonucleotide added at a concentration of 20 μM, yielding a final oligonucleotide concentration of 10 μM. The Eppendorfs were then incubated statically at 25 °C in a water bath for 24 hours under aerobic conditions. Viable counts were taken at 0, 1, 2, 3, 6, 9, 12, and 24 hours, taking 50 μl samples from the Eppendorf tubes. Each sample was serially diluted in BHI and 50 μl of suitably diluted suspensions were plated on BHI to enable replica counts to be made. Plates were incubated at 25 °C for 2 days under aerobic conditions and colonies counted manually.

8.5.3 Theoretical Model

A theoretical model was produced in an attempt to simulate the effect of the TFO while depicting the outgrowth of the organism at different uptake efficiencies, during the course of the assays outline above. Replication rates (doubling times) were estimated to be 1-2 per hour due to the maintenance of a low incubation temperature through out the course of the assay. The results depict both situations. It was presumed for the purpose of this study that the uptake of the oligonucleotide would result in cellular death.

9.0 References

Agazie, Y. M., Burkholder, G. D. and Lee, J. S. 1996 'Triplex DNA in the Nucleus: Direct Binding of Triplex Specific Antibodies and Their Effect on Transcription, Replication, and Cell Growth', *Biochemistry* 316: 461-6.

Aggarwal, B., Schwarz, C. and Hogan, M. 1996 'Triple Helix-Forming Oligodeoxyribonucleotides Targeted to the Human Tumour Necrosis (TNF) Gene Inhibit TNF Production and Block the TNF-Dependent Growth of Human Glioblastoma Tumour Cells', *Cancer Research* 56: 5156-64.

Agrawal, S., Iadarola, P. L., Temsamani, J., Zhao, Q. and Shaw, D. R. 1996 'Effect of G-Rich Sequences on the Synthesis, Purification, Hybridization, Cell Uptake, and Haemolytic Activity of Oligonucleotides', *Bioorganic and Medicinal Chemistry Letters* 6(18): 2219-24.

Agrawal, S. and Iyer, R. P. 1997 'Perspectives in Antisense Therapeutics', *Pharmacological Therapy* 76: 151-60.

Agrawal, S. and Kandimalla, E. R. 2000 'Antisense Therapeutics: Is It as Simple as Complementary Base Recognition', *Molecular Medicine Today* 6 (February): 72-81.

Alberti, P., Arimondo, P. B., Mergny, J., Garestier, T., Hélène, C. and Sun, J. 2002 'A Directional Nucleation-Zipping Mechanism for Triple Helix Formation', *Nucleic Acids Research* 30(24): 5407-15.

Almofti, M. R., Harashima, H., Shinohara, Y., Almofti, A., Baba, Y. and Kiwada, H. 2003 'Cationic Liposome-Mediated Gene Delivery: Biophysical Study and Mechanism of Internalisation', *Archive of Biochemistry and Biophysics* 410: 246-53.

Amaral, L. and Kristiansen, J. E. 2000 'Phenothiazines: An Alternative to Conventional Therapy for the Initial Management of Suspected Multidrug Resistant Tuberculosis. A Call for Studies', *International Journal of Antimicrobial Agents* 14: 173-6.

Amaral, L., Kristiansen, J. and Lorian, V. 1992 'Synergic Effect of Chlorpromazine on the Activity of Some Antibiotics', *Journal of Antimicrobial Chemotherapy* 30: 556-8.

Amaral, L. and Lorian, V. 1991 'Effects of Chlorpromazine on the Cell Envelope Proteins of Escherichia Coli', *Antimicrobial Agents and Chemotherapy* 35(9): 1923-4.

Amaral, L., Viveiros, M. and Kristiansen, J. E. 2001 'Phenothiazines: Potential Alternatives for the Management of Antibiotic Resistant Infections of Tuberculosis

and Malaria in Developing Countries', *Tropical Medicine and International Health* 6(12): 1016.

Amosova, O. A. and Fresco, J. R. 1999 `A Search for Base Analogs to Enhace Third-Strand Binding to 'Inverted' Target Base Pairs of Triplexes in the Pyrimidine/Parallel Motif', *Nucleic Acids Research* 27(23): 4632-5.

Anon. 2002 `Staphlococcus Aureus Bacteraemia: England and Wales 2001', *CDR Weekly* 12(12): 1-17.

Arimondo, P. B., Garestier, T., Hélène, C. and Sun, J. 2001 `Detection of Competing DNA Structures by Thermal Gradient Gel Electrophoresis: From Self-Association to Triple Helix Formation by (G,A)-Containing Oligonucleotides', *Nucleic Acids Research* 29(4 e15, January): 1-5.

Asensio, J. L., Carr, R., Brown, T. and Lane, A. N. 1999 `Conformational and Thermodynamic Properties of Parallel Intramolecular Triple Helices Containing a DNA, RNA or 2'-OMe DNA Thid Strand', *Journal of the American Chemistry Society* 121: 11063-70.

Attia, S. A., Shepherd, V. E., Rosenblatt, M. N., Davidson M. K. and Hughes J. A. 1998 `Interaction of Oligodeoxynucleotides with Mycobacteria: Implications for New Therapeutic Strategies', *Antisense and Nucleic Acid Drug Development* 8: 207-14.

Aubert, Y., Perrouault, L., Hélène, C., Giovannangéli, C., Asseline, U. and. 2001 `Synthesis and Properties of Triple Helix-Formign Olideoxynucleotides Containing 7-Chlor-7-Deaza-2'-Deoxyguanosine', *Bioorganic and Medicinal Chemistry* 9: 1617-24.

Aviñó, A., Frieden, M., Morales, J. C., Torre, B. G., García, R. G., Azorín, F., Gelpí, J. L., Orozco, M., González, C. and Eritja, R. 2002 `Properties of Triple Helices Formed by Parallel-Stranded Hairpins Containing 8-Aminopurines', *Nucleic Acids Research* 30(12): 2609-19.

Baker, B. F. and Monia, B. P. 1999 `Novel Mechanisms for Antisense-Mediated Regulation of Gene Expression', *Biochimica et Biophysica Acta* 1489: 3-18.

Bakker-Woudenberg, I. A. J. M. 2002 `Long-Circulating Sterically Stablilised Liposomes as Carriers of Agents for Treatment of Infection or for Imaging Infectious Foci', *International Journal of Antimicrobial Agents* 19: 299-311.

Bakker-Woudenberg, I. A. J. M., Lokerse, A. F., Vink-Van Den Berg, J. C., Roerdink, F. H. and Michel, M. F. 1986 `Effect of Liposome-Entrapped Ampicillin

on Survival of Listeria Monocytogenes in Murine Peritoneal Macrophages', *Antimicrobial Agents and Chemotherapy* 30(2): 295-300.

Barawkar, D. A., Kumar, V. A. and Ganesh, K. N. 1994 'Triplex Formation at Physiological PH by Oligonucleotides Incorporating 5-Me-DC-(N4-Spermine)', *Biochemical and Biophysical Research Communications* 205(3): 1665-70.

Barawkar, D. A., Rajeev, K. G., Kumar V. A. and Ganesh, K. N. 1996 'Triplex Formation at Physiological PH by 5-Me-Dc-N4-(Spermine) [x] Oligodeoxynucleotides: Non Prontonation of N3 in X of X*G:C Triad and Effect of Base Mismatch/Ionic Strength of Triplex Stabilities', *Nucleic Acids Research* 24(7): 1229-37.

Beal, P. A. and Dervan, P. B. 1992 'The Influence of Single Base Triplet Changes on the Stability of a Pur-Pur-Pyr Triple Helix Determined by Affinity Cleaving', *Nucleic Acids Research* 20(11): 2773-6.

Beaulac, C., Clément-Major, S., Hawari, J. and Lagacé, J. 1996 'Eradication of Mucoid Pseudomonas Aeroginosa with Fluid Liposome-Encapsulated Tobramycin in an Animal Model of Chronic Pulmonary Infection', *Antimicrobial Agents and Chemotherapy* 40(3, March): 665-9.

Beaulac, C., Clément-Major, S., Hawari, J. and Lagacé, J. 1997 'In Vitro Kinetics of Drug Release and Pulmonary Retention of Microencapsulated Antibiotic in Liposomal Formulations in Relation to the Lipid Composition', *Journal of Microencapsulation* 14(3): 335-48.

Beaulac, C., Sachetelli, S. and Lagace, J. 1998 'In-Vitro Bactericidal Efficacy of Sub-MIC Concentrations of Liposom-Encapsulated Antibitotic Against Gram-Negative and Gram-Positive Bacteria', *Journal of Antimicrobial Chemotherapy* 41: 35-41.

Beban, M. and Miller, P. S. 2000 'Pyrimidine Motif Triplexes Containing Polypurine RNA or DNA with Oligo 2'-*O*-Methyl or DNA Triplex Forming Oligonucleotides', *Biochemica et Biophysica Acta (BBA) - Gene Structure and Expression* 1492(1, 21 June): 155-62.

Beckman Instruments inc. 1994 'Oligo 1000 DNA Synthesiser Operating Manual'.

Bennett, C. F., Mirejovsky, D., Crooke, R. M., Tsai, Y. J., Felgner, J., Sridhar, C. N., Wheeler, C. J. and Felgner, P. 1998 'Structural Requirements for Cationic Lipid Mediated Phosphorothioate Oligonucleotides Delivery to Cells in Culture', *Journal of Drug Targeting* 5(3): 149-62.

Blau, S., Jubeh, T. T., Haupt, S. M. and Rubinstein, A. 2000 'Drug Targeting by Surface Cationization', *Critical Reviews in Therapeutic Drug Carrier Systems* 17(5): 425-65.

Boulos, L., Prevost, M., Barbeau, B., Coallier, J. and Desjardins, R. 1999 'LIVE/DEAD Baclight: Application of a New Rapid Staining Method for Direct Enumeration of Viable and Total Bacteris in Drinking Water', *Journal of Microbiological Methods* 37: 77-86.

Brignole, C., Pagnan, G., Marimpietri, D., Cosimo, E., Allen, T. M., Ponzoni, M. and Pastorino, F. 2003 'Tareted Delivery System for Antisense Oligonucleotides: A Novel Experimental Strategy for Neuroblastoma Treatment', *Cancer Letters* 197(1-2, July): 231-5.

Brodin, P., Sun, J.-S., Mouscadet, J.-F. and Auclair, C. 1999 'Optimisation of Alternate-Strand Triplex Helix Formatiom at the 5'-TpA-3' and 5'ApT3' Junctions', *Nucleic Acids Research* 27: 3029-34.

Broskey, J., Coleman, K., Gwynn, M. N., McCloskey, L., Traini, C., Voelker, L. and Warren, R. 2000 'Efflux and Target Mutations as Quinolone Resistance Mechanisms in Clinical Isolates of Streptococcus Pneumoniae', *Journal of Antimicrobial Chemotherapy* 45(suppl. S1): 95-9.

Brown, D. A., Kang, S. H., Gryaznov, S. M., DeDionisio, L., Heidenreicht, O., Sullivan, S., Xu, X. and Nerenburg, M. I. 1994 'Effectof Phosphorothioate Modification of Oligodeoxynucleotides on Specific Protein Binding', *Journal of Biological Chemistry* 269(43, 28 October): 26801-5.

Brown, T. A. 1996 *Genetics; A Molecular Approach*, Chapman and Hall.

Campanhã, M. T. N., Mamizuka, E. M. and Carmona-Ribeiro, A. M. 1999 'Interactions Between Cationic Liposomes and Bacteria: The Physical-Chemistry of the Bactericidal Action', *Journal of Lipid Research* 40: 1495-500.

Cassidy, R. A., Puri N. and Miller, P. S. 2003 'Effect of Target Sequence on Triplex Formation by Oligo-2'-Deoxy and 2'-*O*-Methylribonucleotides', *Nucleic Acids Research* 31(14): 4099-108.

Chattopadhyay, D., Mukherjee, T., Pal, P., Saha, B. and Bhadra, R. 1998 'Altered Membrane Permeability as the Basis of Bactericidal Action of Methidilazine', *Journal of Antimicrobial Chemotherapy* 42: 83-6.

Chen, J. Y., Brunauer, L. S., Chu, F. C., Helsel, C. M., Gedde, M. M. and Huestis, W. H. 2003 'Selective Amphiphatic Nature of Chlorpromazine Binding to Plasma Membrane Bilayers', *Biochimica et Biophysica Acta* 1616: 95-105.

Cheng, B., Fournier, R. L., Relue, P. A. and Schisler, J. 2001 'An Experimental and Theoretical Study of the Inhibition of Escherichia Coli Lac Operon Gene Expression by Antigene Oligonucleotides', *Biotechnology and Bioengineering* 74(3, June): 220-9.

Corvo, M. L., Jorge, J. C. S., Hof, R. V., Cruz, M. E. M., Crommelin, D. J. A. and Storm, G. 2002 'Superoxide Dismutase Entrapped in Long-Circulating Liposomes: Formulation Design and Therapeutic Activity in Rat Adjuvant Arthritis', *Biochimica et Biophysica Acta* 1564: 227-36.

Critchley, I. A., Blosser-Middleton, R. S., Jones, M., Karlowsky, J. A., Karginova, E. A., Thornsberry, C. and Salım, D. F. 2002 'Phenotypic and Genotypic Analysis of Levofloxaxin-Resistant Clinical Isolates of Streptococcus Pneumoniae Collected in 13 Countries During 1999-2000', *International Journal of Antimicrobial Agents* 20: 100-7.

Cubbon, M. D., Masterton, R. G. and. 2000 'New Quinolones - a Fresh Answer to the Pneumococcus', *Journal of Antimicrobial Chemotherapy* 46: 869-72.

Đapić, V., Abdomerović, V., Marrington, R., Peberdy, J., Rodger, A., Trent, J. O. and Bates, P. J. 2003 'Biophysical and Biological Properties of Quadruplex Oligodeoxyribonucleotides', *Nucleic Acids Research* 31(8): 2097-107.

de Bizemont, T., Duval-valentin, G., Sun, J.-S., Bisagni, E., Garestier, T. and Hélène, C. 1996 'Alternate Stran Drecognition of Double-Helical DNA by (T,G)-Containing Oligonucleotides in the Presence of a Triple Helix-Specific Ligand', *Nucleic Acids Research* 24(6): 1136-43.

De Mola, N. J. and Posthumaa, R. M., Mohnb. 1983 'Chemico-Biological Interactions: Induction of Repairable DNA Damage in Escherichia Coli and Interaction with DNA in Vitro by the Radical Cation of Chlorpromazine', *Chemico-Biological Interaction* 47(2): 223-37.

De Oliveira, M. C., Boutet, V., Fattal, E., Bouqet, D., Grognet, J., Couvreur, P. and Deverre, J. 2000 'Improvement of in Vivo Stability of Phosphodiester Oligonucleotide Using Anionic Liposomes in Mice', *Life Sciences* 67: 1625-37.

Dean, D. A. 2000 'Peptide Nucleic Acids: Versatile Tools for Gene Therapy Strategies', *Advanced Drug Delivery Reviews* 44(2-3, November): 81-95.

Debin, A., Laboulais, C., Ouail, M., Malvy, C., Le Bret, M. and Svinarchuk, F. 1999 'Stability of G,A Triple Helices', *Nucleic Acids Research* 27(13): 2699-707.

Debin, A., Malvy, C. and Svinarchuk, F. 1997 'Investigation of the Formation and Intracellular Stability of Purine-(Purine/Pyrimidine) Triplexes', *Nucleic Acids Research* 25(10): 1965-74.

del Mar Tavío, M., Vila, J., Ruiz, J., Martín-Sánchez, A. M. and Jiménez de Anta, M. T. 1999 'Mechanism Involved in the Development of Resistance to Fluoroquinolones in Escherichia Coli Isolates', *Journal of Antimicrobial Chemotherapy* 44: 735-42.

Desiderio, J. V. and Campbell, S. G. 1983 'Intraphagocytic Killing of Salmonella Typhimurium by Liposome-Encapsulated Cepalothin', *The Journal of Infectious Diseases* 148(3): 563-70.

Desjardins, A., Chen, T., Khalil, H., Sayasith, K. and Legacé, J. 2002 'Differential Behaviour of Fluid Liposomes Toward Mammalian Epithelial Cells and Bacteria: Restriction of Fusion to Bacteria', *Journal of Drug Targeting* 10(1, August): 47-54.

Doronina, S. O. and Behr, O. 1997 'Towards a General Triple Helix Mediated DNA Recognition Scheme', *Chemical Society Reviews* 26(1): 63-71.

Duval -Valentin, G., Takasugi, M., Hélène, C. and Sage, E. 1998 'Triple Helix-Directed Psoralen Crosslinks Are Recognised by Uvr(A)BC Exinuclease', *Journal of Molecular Biology* 278: 815-25.

Eastman, S. J., Siegel, C., Tousignant J., Smith, A. E., Cheng, S. H. and Scheule, R. K. 1997 'Biophysical Characterization of Cationic Lipid:DNA Complexes', *Biochimica et Biophysica Acta* 1325: 41-62.

El-Aneed, A. 2004 'An Overview of Current Delivery Systems in Cancer Gene Therapy', *Journal of Controlled Release* 94: 1-14.

Escudé, C., Giovannangéli, C., Sun, J., Lloyd, D. H., Chen, J., Gryaznov, S. M., Garestier, T. and Hélène, C. 1996 'Stable Triple Helices Formed by Oligonucleotide N3'-P5' Phosphoramidates Inhibit Transcription Elongation', *Proceedings of the National Academy of Science USA* 93 (April): 4365-9.

Faucon, B., Mergny, J. and Hélène, C. 1996 'Effect of Third Strand Compostion on Triple Helix Formation: Purine Versus Pyrimidine Oligodeoxynucleotide', *Nucleic Acids Research* 24(16): 3181-8.

Fearon, K. L., Hirschbein, B. L., Nelson, J. S., Foy, M. F., Nyguyen, M. Q., Okruszek, A., McCurdy, S. N., Frediani, J. E., DeDionisio, L. A., Raible, A. M., Cagle, E. N. and Boyd, V. 1998 'An Improved Synthesis of Oligodeoxynucleotide N3'-P5' Phosphoramidates and Their Chimera Using Hindered Phosphoramidite Monomers and a Novel Handle for Reverse Phase Purification', *Nucleic Acids Research* 26(16): 3813-24.

Felgner, J. H., Kumar, R., Sridhar, C. N., Wheeler, C. J., Tsai, Y. J., Border, R., Ramsey, P., Martin, M. and Felgner, P. L. 1994 'Enahnced Gene Delivery and Mechanism with a Novel Series of Cationic Lipid Formulations', *Journal Biological Chemistry* 269(4): 2550-61.

Felgner, J., Bennett, F. and Felgner, P. L. 1993 'Cationic Lipid Mediated Delivery of Polynucleotides', *Methods* 5(1): 67-75.

Felgner, P. L., Gadek, T. R., Holm, M., Roman, R., Chan, H. W., Wenz, M., Northrop, J. P., Ringold, G. M. and Danielsen, M. 1987 'Lipofection: A Highly Efficient, Lipid-Mediated DNA-Transfection Procedure', *Proceedings for the National Academy of Science USA* 84 (November): 7413-7.

Felsenfeld, G. and Rich, A. 1957 'Studies on the Formation of Two and Three-Stranded Polyribonucleotides', *Biochimica et Biophysica Acta* 26: 457-68.

Ferrándiz, M. J., Fenoll, A., Liñares, J. and De La Campa, A. G. 2000 'Horizontal Transfer of ParC and GyrA in Fluoroquinolone-Resistant Clinical Isolates of Streptococcus Pneumoniae', *Antimicrobial Agents and Chemotherapy* 44(4, April): 840-7.

Ferrari, M. E., Rusalov, D., Enas, J. and Wheeler C. J. 2001 'Trends in Lipoplex Physical Properties Dependent on the Cationic Lipid Structure, Vehicle and Complexation Procedure Do not Correlate with Biological Activity', *Nucleic Acids Research* 29(7): 1539-48.

Felsenfeld, G., Davies, D. R., and Rich, A. 1957 'Formation of a three-stranded polynucleotide molecule', *Journal of the American Chemistry Society* 79: 2023-2024

Fillion, P., Desjardins, A., Sayasith, K., Legacé, J. and. 2001 'Encapsulation of DNA in Negatively Charged Liposomes and Inhibition of Bacterial Gene Expression with Fluid Liposome-Encapsulated Antisense Oligonucleoitdes', *Biochemica et Biophysica Acta* 1515: 44-54.

Fossella, J. A., Kim, Y. J., Shih, H. and Richards, E. G., Fresco. 1993 'Relative Specificities in Binding of Watson-Crick Base Pairs by Thrid Strand Residues in a DNA Pyrimidine Triplex Motif', *Nucleic Acids Research* 21(19): 4511-5.

Fox, K. R. 1995 'Kinetic Studies on the Formation of Acridine-Linked DNA Triple Helices', *FEBS Letters* 357: 312-6.

Fox, K. R. 2000 'Targeting DNA with Triplexes', *Current Medicinal Chemistry* 7: 17-37.

Fox, K. R., Polucci, P., Jenkins T. C. and Neidle S. 1995 'A Molecular Anchor for Stabilising Triple-Helical DNA', *Proceedings for the National Academy of Science of USA* 92 (August): 7887-91.

Frank-Kamenetskii, M. and Mirkin, S. 1995 'Triplex DNA Structures', *Annual Review of Biochemistry* 64: 65-95.

Fujii, G. 1999 'To Fuse or not to Fuse: The Effects of Electrostatic Interactions, Hydrophobic Forces, and Structural Amphiphilicity on Protein-Mediated Membrane Destabilisation', *Advanced Drug Delivery Reviews* 38: 257-77.

Gales, A. C., Gordon, K. A., Wilke, W. W., Pfaller, M. A. and Jones, R. N. 2000 'Occurence of Single-Point GyrA Mutations Among Ciprofloxacin-Susceptible Escherichia Coli Isolates Causing Urinary Tract Infections in Latin America', *Diagnostic Microbiology and Infectious Disease* 36: 61-4.

Garcia-Chaumont, C., Seksek, O., Grzybowska, J., Borowski, E. and Bolard, J. 2000 'Delivery Systems for Antisense Oligonucleotides', *Pharmacology and Therapeutics* 87: 255-77.

Giancola, C., Petraccone, L., Pieri, M., De Napoli, L., Montesarchio, D., Piccalli, G. and Barone, G. 2001 'Physico-Chemical Studies on DNA Triplexes Containing an Alternate Third Strand with a Non-Nucleotide Linker', *International Journal of Biological Macromolecules* 28: 387-94.

Gilar, M. and Bouvier, E. S. P. 2000 'Purification of Crude DNA Oligonucleotides by Solid-Phase Extraction and Reverse-Phase High-Performance Liquid Chromatography', *Journal of Chromatography A* 890: 167-77.

Giovannangéli, C., Rougée, M., Garestier, T., Thuong, N. T. and Hélène, C. 1992 'Triple-Helix Formation by Oligonucleotide Containing the Three Bases Thymine, Cytosine and Guanine', *Proceedings of the National Academy of Science USA* 89: 8631-5.

Goobes, R., Cohen, O. and Minsky, A. 2002 'Unique Conedensation Patterns of Triplex DNA: Physical Aspects and Physiological Implications', *Nucleic Acids Research* 30(10): 2154-61.

Good, L. and Nielsen, P. 1998 'Antisense Inhibition of Gene Expression in Bacteria by PNA Targeted to MRNA', *Nature Biotechnology* 16 (April): 355-8.

Good, L., Sandberg, R., Larsson, O., Nielsen, P. E. and Wahlestedt, C. 2000 'Antisense PNA Effects in Escherichia Coli Are Limited by the Outer-Membrane LPS Layer', *Microbiology* 146: 2665-70.

Gotfredsen, C. H., Schultze, P. and Fegion, J. 1998 'Solution Structure of an Intramolecular Pyrimidine.Purine.Pyrimidine Triplex Containing an RNA Third Strand', *Journal of the American Chemisty Society* 120: 4281-9.

Gottlieb, S. 1999 'Staphylococcus Resistant to Vancomycin Emerges', *British Medical Journal* 318 (February): 557.

Gowers, D. M. and Fox, K. 1999 'Towards Mixed Sequence Recognition by Triple Helix Formation', *Nucleic Acids Research* 27(7): 1569-77.

Greig, M., Klopchin, P., Griffey, R. and Hughes, J. 1995 'Desalting of Oligonucleotides for Electrospray Mass Spectroscopy', *Hewlett Packard Application Note.*

Grigoriev, M., Praseuth, D., Guieysse, A. L., Robin, P., Thuong, N. T., Hélène, C. and Harel-Bellan, A. 1993 'Inhibition of Gene Expression by Triple Helix-Directed DNA Cross-Linking at Specific Sites', *Protocol for the National Academy of Science USA* 90: 3501-5.

Gryaznov, S., Skorski, T., Cucco, C., Niebrowska-Skorska, M., Chiu, C. Y., Lloyd, D., Chen, J., Koziolkieicz, M. and Calabretta, B. 1996 'Oligonucleotide N3'-P5' Phosporamidate as Antisense Agents', *Nucleic Acids Research* 24(8): 1508-14.

Gryaznov, S. 1999 'Olgonucleotide N3'-P5' Phosphoramidates as Potential Therapeutic Agents', *Biochimica et Biophysica Acta* 1489: 131-40.

Guianvarc'h, D., Fourrey, J.-L., Maurisse, R., Sun, J. and Benhida, R. 2003 'Design of Artificial Nucleobases for the Recognition of the AT Inversion by Triple-Helix Forming Oligonucleotides: A Structure Stability Relationship Study and Neighbour Base Effect', *Bioorganic and Medicinal Chemistry* 11: 2751-9.

Guieysse, A.-L., Praseuth, D., Giovannangéli, C., Asseline, U. and Hélène, C. 2000 'Psoralen Adducts Induced by Triplex-Forming Oligonucleotides Are Refractory to Repair in HeLa Cells', *Journal of Molecular Biology* 296: 373-83.

Guntaka, R. A., Varma, B. R. and Weber, K. T. 2003 'Triplex-Forming Oligonucleotides as Modulators of Gene Expression', *The International Journal of Biochemistry and Cell Biology* 35: 22-31.

Hanahan, D. 1983 'Studies on Transformation of Escherichia Coli with Plasmids', *Journal of Molecular Biology* 166: 557-80.

Hari, Y., Obika, S., Sekiguchi, M. and Imanishi, T. 2003 'Selective Recognition of CG Interruption by 2',4'-BNA Having 1-Isoquinolone in a Pyrimidine Motif Triplex Formation', *Tetrahedron* 59(27): 5123-8.

Hartmann, G., Krug, A., Bidlingmaier, M., Hacker, U., Eigler, A., Albrecht, R., Strasburger, C. J., and Endres, S. 1998 'Spontaneous and Cationic Lipid-Mediated Uptake of Antisense Oligonucleotides in Human Monocytes and Lymphocytes', *The Journal of Pharmacolgy and Experimental Therapeutics* 285(2, January): 920-8.

Hélène, C., Thuong, N. T. and Harel-Bellan, A. 1992 'Control of Gene Expression by Triple Helix-Forming Oligonucleotide', *Annals of the New York Academy of Science* 660: 27-36.

Hocking, S. C. and Maxwell, A. 2002 'Identification of Four GyrA Residues Involved in DNA Breakage-Reunion Reaction of DNA Gyrase', *Journal of Molecular Biology* 318: 351-9.

Hong, K., Zheng, W., Baker, A. and Papahadjopoulos, D. 1997 'Stabilisation of Cationic Liposomplasmid DNA Complexes by Polyamines and Poly(Ethylene Glycol)-Phospholipid Conjugates for Efficient in Vivo Gene Delivery', *FEBS Letters* 400: 233-7.

Hoogkamp-Korstanje, J. A. A., Roelofs-Willemse, J. and The susceptiblity surveillance study group. 2003 'Antimicrobial Resistance in Gram-Negative Bacteria from Intensive Care Units and Urology Services. A Nationwide Study in the Netherlands 1995-2000', *International Journal of Antimicrobial Agents* 21: 547-56.

Hooper, D. C. 1998 'Clinical Applications of Quinolones', *Biochimica et Biophysica Acta* 1400: 45-61.

Hooper, D. C. 2002 'Fluoroquinolone Resistance Among Gram-Positive Cocci', *The Lancet Infectious Diseases* 2: 530-8.

Hoyne, P. R., Edwards, L. M., Viari, A. and Maher III, L. J. 2000 'Searching Genomes for Sequences with the Potential to Form Intrastrand Triple Helices', *Journal of Molecular Biology* 302: 797-809.

Hu, Q., Bally, M. B. and Madden, T. D. 2002 'Subcellular Trafficking of Antisense Oligonucleotides and Down Regulation of Bcl-2 Gene Expression in Human Melanoma Cells Using a Fusogenic Liposome Delivery System', *Nucleic Acids Research* 30(16, June): 3632-41.

Hu, Q., Shew, C. R., Bally, M. B. and Madden, T. D. 2001 'Programmable Fusogenic Vesicles for Intracellular Delivery of Antisense Oligodeoxynucleotides: Enhanced Cellular Uptake and Biological Effect', *Biochemica et Biophysica Acta* 1514 (February): 1-13.

Huang, C.-Y., Bi, G. and Miller, P. S. 1996 'Triplex Formation by Oligonucleotides Containing Novel Deoxycytidine Derivatives', *Nucleic Acids Research* 24(13): 2606-13.

Hughes, M. D., Hussain, M., Nawaz, Q., Sayyed P. and Akhtar S. 2001 'The Cellular Delivery of Antisense Oligonucleotides and Ribozymes', *Drug Discovery Today* 6(6, March): 303-15.

Hugo, W. B. and Russell, A. D. 1998 'Mechanisms of Action of Antibiotics', *Pharmaceutical Microbiology*: 173.

Hutvágner, G. and Zamore, P. D. 2002 'RNAi: Nature Abhors a Double-Strand', *Current Opinion in Genetics and Development* 12: 255-32.

Ito, T., Ueno, Y., Komatsu, Y. and Matsuda, A. 2003 'Synthesis, Thermal Stability and Resistance to Enzymatic Hydrolysis of the Oligonucleotides Containing 5-(N-Aminohexyl)Carbamoyl-2'-*O*-Methyluridines', *Nucleic Acids Research* 31(10): 2514-23.

James, P. L., Brown, T. and Fox, K. R. 2003 'Thermodynamic and Kinetic Stability of Intermolecular Triple Helices Containing Different Proportions of C+.GC and T.AT', *Nucleic Acids Research* 31(19): 5598-606.

Jetter, M. C. and Hobbs F. W. 1993 '7,8-Dihydro-8-Oxoadenine as a Replacement for Cytosine in the Third Strand of Triple Helices. Triplex Formation Without Hypochromicity', *Biochemistry* 32: 3249-54.

Jones, M. N. and Kaszuba, M. 1994 'Polyhydroxy-Mediated Interactions Between Liposomes and Bacterial Biofilms', *Biochimica et Biophysica Acta* 1193: 48-54.

Jones, M. N., Kaszuba, M., Reboiras, M. D., Lyle, I. G., Hill, K. J., Song, Y., Wilmot, S. W., and Creeth, J. E. 1994 'The Targeting of Phospholipid Liposomes to Bacteria', *Biochemica et Biophysica Acta* 1196: 57-64.

Jones, M. N., Song, Y., Kaszuba, M. and Reboiras, M. D. 1997 'The Interaction of Phospholipid Liposomes with Bacteria and Their Use in the Delivery of Bactericides', *Journal of Drug Targeting* 5(1): 25-34.

Jones, R. N. 2002 'Microbiology of Newer Fluoroquinolones: Focus on Respiratory Pathogens', *Diagnostic Microbiology and Infectious Disease* 44: 213-20.

Kaszuba, M., Robinson, A. M., Song, Y., Creeth, J. E. and Jones, M. N. 1997 'The Visualisation of the Targeting of Phospholipid Liposomes to Bacteria', *Colloids and Surfaces B: Biointerfaces* 8 (January): 321-32.

Keppler, M. D., Neidle, S. and Fox, K. R. 2001 'Stabilisation of TG- and AG-Containing Antiparallel DNA Triplexes by Triplex-Binding Ligands', *Nucleic Acids Research* 29(9): 1935-42.

Keppler, M., Zegrocka, O., Strekowski, L. and Fox, K. 1999 'DNA Triple Helix Stabilisation by a Naphthyloquinolone Dimer', *FEBS Letters* 447: 223-6.

Kim, H.-J., Gias, E. L. M. and Jones, M. 1999 'The Adsorption of Cationic Liposomes to Staphylococcus Aureus Biofilms', *Colloids and Surfaces A: Physicochemical and Engineering Aspects* 149: 561-70.

Kim, O. K., Barrett, J. F. and Ohemeng, K. 2001 'Advances in DNA Gyrase Inhibitors', *Expert Opinion on Investigational Drugs* 10(2): 199-212.

Klysik, J., Kinsey, B. N., Hua, P., Glass, G. A., and Orson, F. M. 1997 'A 15-Base Acridine-Conjugated Oligodeoxynucleotide Forms Triplex DNA with Its IL-2Ra Promoter Target with Greatly Improved Avidity', *Bioconjugate Chemistry* 8(3): 318-26.

Kocisova, E., Sureau, F., Praus, P., Rosenberg, I., Stepanek, J. and Turpin, P.-Y. 2003 'Monitoring of Labeled Antisense Oligonucleotides Within Living Cells by Using a Multifrequency Phase/Modulation Approach for Fluorescence Lifetime Measurements', *Journal of Molecular Structure* 651-653: 115-22.

Koizumi, K., Morita, K., Tsutsumi, S., Abe, K., Obika, S. and Imanishi, T. 2003 'Triplex Formation with 2'-O, 4'-C-Ethylen Bridged Nucleic Acids (ENA) Having C3'-Endo Conformation at Physiological PH', *Nucleic Acids Research* 31(12): 3267-73.

Koppelhus, U. and Nielsen, P. E. 2003 'Cellular Delivery of Peptide Nucleic Acid (PNA)', *Advanced Drug Delivery Reviews* 55: 267-80.

Kristiansen, M. M., Leandro, C., Ordway, D., Martins, M., Viveiros, M., Pacheco, T., Kristiansen, J. E. and Amaral, L. 2003 'Phenothiazines Alter Resistance of Methiciliin-Resistant Strains of Staphylococcus Aureus (MRSA) to Oxacillin in Vitro', *International Journal of Antimicrobial Agents* 22: 250-3.

Kukreti, S., Sun, J., Garestier, T. and Hélène, C. 1997 'Extension of the Range of DNA Sequences Available for Triple Helix Formation: Stabilization of Mismatched Triplexes by Acridine-Containing Oligonucleotides', *Nucleic Acids Research* 25(21): 4264-70.

Kushner, S. D., Nagaishi, H., Templin, A. and Clark, A. J. 1971 'Genetic Recombination in Escherichia Coli: The Role of Exonuclease I', *Proceedings of the National Academy of Science USA* 68(4): 824-7.

Kushner, S. D., Nagaishi, H., Templin, A. and Clark, A. J. 1972 'Indirect Suppression of RecB and RecC Mutations by Exonuclease I Deficiency', *Proceedings of the National Academy of Science USA* 69(6): 1366-70.

Lacoste, J., François, J. and Hélène, C. 1997 'Triple Helix Formation with Purine-Rich Phosphorothioate-Containing Oligonucleotides Covalently Linked to an Acridine Derivative', *Nucleic Acids Research* 25(10): 1991-8.

Le Doan, T., Perrouault, L., Praseuth, D., Habhoub, N., Decout, J. L., Thuong, N. T., Lhomme, J. and Hélène, C. 1987 'Sequence-Specific Recognition, Photocrosslinking and Cleavage of the DNA Double Helix by an Oligo-[Alpha]-Thymidylate Covalently Linked to an Azidoproflavine Derivative', *Nucleic Acids Research* 15(19): 7749-60.

Lebedeva, I., Benimetskaya, L., Stein, C. A., and Vilenchik, M. 2000 'Cellular Delivery of Antisense Oligonucleotides', *European Journal of Pharmaceutics and Biopharmaceutics* 50 (February): 101-19.

Lehman, I. R. and Nussbaum, A. L. 1964 'The Deoxyribonucleases of Escherichia Coli', *Journal of Biological Chemistry* 239(8): 2628-36.

Leitner, D., Schröder, W. and Weisz, K. 2000 'Influence of Sequence-Dependent Cytosine Protonation and Methylation on DNA Triplex Stability', *Biochemistry* 39: 5886-92.

Levin, A. A. 1999 'A Review in the Pharmacokinetics and Toxicology of Phosphorothioate Antisense Oligonucleotides', *Biochimica et Biophysica Acta* 1489: 69-84.

Lugtenberg, E. J. J. and Peters, R. 1976 'Distribution of Lipids in Cytoplasmic and Outer Membranes of Escherichia Coli', *Biochimica et Biophysica Acta* 441: 38-47.

Lundemose, A. 2001 'Pantheco Takes up Challenge to Develop Peptide Nucleic Acid (PNA) Based Drugs', *Biosystems Solutions* 2: 30-1.

Macaulay, V. M., Bates, P. J., McLean, M. J., Rowlands, M. G., Jenkins, T. C., Ashworth, A. and Neidle, S. 1995 'Inhibition of Aromatase Expression by a Psoralen-Linked Triplex-Forming Oligonucleotide Targeted to a Coding Sequence', *FEBS Letters* 372: 222-8.

Marchand, C., Sun, J.-S., Bailly, C., Waring, M. J., Garestier, T. and Hélène, C. 1998 'Optimisation of Alternate-Strand Triple Helix Formation at the 5'CpG3' and 5'GpC3' Junction Steps', *Biochemistry* 37: 13322-9.

Martínez, J. L., Alonso, A., Gomez-Gomez, J. M. and Baquero, F. 1998 'Quinolone Resistance by Mutations in Chromosomal Gyrase Genes. Just the Tip of the Iceberg', *Journal of Antimicrobial Chemotherapy* 42: 683-8.

Mas, T., Susperregui, J., Berké, B., Chèze, C., Moreau, S., Nuhrich, A. and Vercauteren, J. 2000 'DNA Triplex Stabilization Property of Natural Anthocyanins', *Phytochemistry* 53: 679-87.

McCurdy, S. N., Nelson, J. S., Hirschbein, B. L. and Fearon, K. L. 1997 'An Improved Method for the Synthesis of N3'-P5' Phosphoramidiate Oligonucleotides', *Tetrahedron Letters* 38(2): 207-10.

McEachern, F. and Fisher, L. M. 1989 'Regulation of DNA Supercoiling in Escherichia Coli: Genetic Basis of a Compensatory Mutation in DNA Gyrase', *FEBS Letters* 253(1,2): 67-70.

McGuffie, E. M. and Catapano, C. V. 2002 'Design of a Novel Triple Helix-Forming Oligodeoxyribonucleotide Directed to the Major Promoter of the c-Myc Gene', *Nucleic Acids Research* 30(12): 2701-9.

McMahon, B. M., Stewart, J. A., Bitner, M. D., Fauq, A., McCormick, D. J. and Richelson, E. 2002 'Peptide Nucleic Acids Specifically Cause Antugene Effects in Vivo by Systemic Injection', *Life Sciences* 71: 325-37.

McMurry, J. 2004 *Organic Chemistry*, Thomas, Brooks/Cole.

Micklefield, J. 2001 `Backbone Modification of Nucleic Acids: Synthesis, Structure and Therapeutic Applications', *Current Medicinal Chemistry* 8: 1157-79.

Miller, A. D. 1998 `Cationic Liposomes for Gene Therapy', *Angew. Chem. Int. Ed.* 37: 1768-85.

Miyoshi, D., Nakao, A. and Sugimoto, N. 2003 `Structural Transition from Antiparallel to Parallel G-Quadruplex of d(G4T4G4) Induced by Ca2+', *Nucleic Acids Research* 31(4): 1156-63.

Muñoz, R. and De La Campa, A. G. 1996 `ParC Subunit of DNA Topoisomerase IV of Streptococcus Pneumoniae is a Primary Target of Fluoroquinolones and Cooperates with DNA Gyrase A Subunit in Forming Resistance Phenotype', *Antimicrobial Agents and Chemotherapy* 40(10, October): 2252-7.

Muratovska, A., Lightowlers, R. N., Taylor, R. W., Turnbull, D. M., Smith, R. A. J., Wilce, J. A., Martin, S. W. and Murphy, M. P. 2001 `Targeting Peptide Nucleic Acid (PNA) Oligomers to Mitochondria Within Cells by Conjugation to Lipophilic Cations: Impliactions for Mitochondrial DNA Replication, Expression and Disease', *Nucleic Acids Research* 29(9): 1852-63.

Neidle. S. 1997 `Recent Developments in Triple-Helix Regulation of Gene Expression', *Anti-Cancer Drug Design* 12: 433-42.

Nielsen, P. E. 2001 `Peptide Nucleic Acid: A Versatile Tool in Genetic Diagnostics and Molecular Biolgy', *Current Opinion in Biotechnology* 12: 16-20.

Nielsen, P. E. and Egholm, M. 2001 `Strand Displacement Recognition of Mixed Adenine-Cytosine Sequences in Double Stranded DNA by Thmine-Guanine PNA(Peptide Nucleic Acid)', *Bioorganic and Medicinal Chemistry* 9(2, May): 2429-34.

Nikaido, H. 1994 `Prevention of Drug Access to Bacterial Targets: Permeabiltiy Barriers and Active Efflux', *Science* 264 (15 April): 382-8.

Noguchi, A., Furuno, T., Kawaura, C. and Nakanishi, M. 1998 `Membrane Fusion Plays an Important Role in Gene Transfection Mediated by Cationic Liposomes', *FEBS Letters* 433: 169-73.

Noonberg, S. B., François, J. C., Garestier, T. and Hélène, C. 1995a `Effect of Competing Self-Structure on Triplex Formation with Purine-Rich Oligodeoxynucleotides Containing G,A Repeats', *Nucleic Acids Research* 23(11): 1956-63.

Noonberg, S. B., François, J. C., Praseuth, D., Guieysse-Peugeot, A. L., Lacoste, J., Garestier, T. and Hélène, C. 1995b 'Triplex Formation with Alpha Anomers of Purine-Rich and Pyrimidine-Rich Oligodeoxynucleotides', *Nucleic Acids Research* 23(20): 4042-9.

Oberie, V., Bakowsky, U., Zuhorn, I. S. and Hoekstra, D. 2000 'Lipoplex Formation Under Equilibrium Conditions Reveals a Three-Step Mechanism', *Biophysical Journal* 79: 1447-54.

Olavarrieta, L., Martínez-Robles, M. L., Hernández, P., Krimer, D. B. and Schvartzman, J. B. 2002 'Knotting Dynamics During DNA Replication', *Molecular Microbiology* 46(3): 699-707.

Omri, A., Ravaoarinoro, M. and Poisson, M. 1995 'Incorporation, Release and in-Vitro Antibacterial Activity of Liposomal Aminoglycosides Against Pseudomanas Aeruginosa', *Journal of Antimicrobial Chemotherapy* 36: 631-9.

Ono, A., Chen, C. N. and Kan, L. 1991 'DNA Triplex Formation of Oligonucleotide Analogues Consisting of Linker Groups and Octamer Segments That Have Opposite Sugar-Phosphate Backbone Polarities', *Biochemistry* 30: 9914-21.

Paes, H. M. and Fox, K. R. 1997 'Kinetic Studies on the Formation of Intermolecular Triple Helices', *Nucleic Acids Research* 25(16): 3269-74.

Parel, S. and Leumann, C. 2001 'Triple-Helix Formation in the Antiparallel Binding Motif of Oligodeoxynucleotides Containing N9- and N7-2-Aminopurine Deoxynucleosides', *Nucleic Acids Research* 29(11): 2260-7.

Pedrosa de Lima, M. C., Simões, S., Pires, P., Faneca, H. and Düzgünes, N. 2001 'Cationic Lipid-DNA Complexes in Gene Delivery: From Biophysics to Biological Applications', *Advanced Drug Delivery Reviews* 47: 277-94.

Perkins, B. D., Wilson, J., Wensel, T. and Vasquez, K. M. 1998 'Triplex Targets in the Human Rhopopsin Gene', *Biochemistry* 37: 11315-22.

Perrie, Y. and Gregoriadis, G. 2000 'Liposome-Entrapped Plasmid DNA: Characterisation Studies', *Biochimica et Biophysica Acta* 1475: 125-32.

Petraccone, L., Erra, E., Messere, A., Montesarchio, D., Piccialli, G., Barone, G. and Giancola, C. 2003 'Physico-Chemical Studies of a DNA Triplex Containing a New Ferrocenemethyl-Thymidine Residue in the Third Strand', *Biophysical Chemistry*.

Pilch, D. S., Levenson, C. and Shafer, R. H. 1991 'Structure, Stability, and Thermodynamics of a Short Intermolecular Purine-Purine-Pyrimidine Triple Helix', *Biochemistry* 30(25): 1991.

Pooga, M., Land, T., Bartfai, T. and Langel, U. 2001 'PNA Oligomers as Tools for Specific Modulation of Gene Expression', *Biomolecular Engineering* 17: 183-92.

Praseuth, D., Guieysse, A. L. and Hélène, C. 1999 'Triple Helix Formation and the Antigene Strategy for Sequence-Specific Control of Gene Expression', *Biochimica et Biophysica Acta (BBA) - Gene Structure* 1489(1, December): 181-206.

Prescott, L. M., Harley, J. P. and Klein D. A. 2002 *Microbiology*, McGraw-Hill.

Promega. 1996 'Protocols and Applications Guide', *Biological Research Products* 3: 380.

Protozanova, E. and Macgregor, J. R. B. 1996 'Kinetic Footprinting of DNA Triplex Formation', *Analytical Biochemistry* 243: 92-9.

Rädler, J., Koltover, I., Salditt, T. and Safinya, C. R. 1997 'Structure of DNA-Cationic Liposome Complexes: DNA Intercalation in Multilamellar Membranes in Distinct Interhelical Packing Regimes', *Science* 275: 810-4.

Ramzaeva, N. and Seela, F. 1995 '7-Substituted 7-Deaza-2'-Deoxyguanosines: Regioselective Halogenation of Pyrrolo[2,3-d]Pyrimidine Nucleosides', *Helvetica Chimica Acta* 78: 1083-90.

Ramzaeva, N. and Seela, F. 1996 'Duplex Stability of 7-Deazapurine DNA: Oligonucleotides Containing 7-Bromo- or 7-Iodo-7-Deazaguanine', *Helvetica Chimica Acta* 79: 1549-58.

Robinson, A., Bannister, M., Creeth, J. E. and Jones, M. N. 2001 'The Interaction of Phospholipid Liposomes with Mixed Bacterial Biofilms and Their Use in the Delivery of Bactericide', *Colloids Adn Surfaces A: Physicochemical and Engineering Aspects 186* 186: 43-54.

Rougée, M., Faucon, B., Mergny, J., Barcello, F., Giovannangéli, C. and Hélène, C. 1992 'Kinetics and Thermodynamics of Triple-Helix Formation: Effects Ionic Strength and Mismatches', *Biochemistry* 31: 9269-78.

Sachetelli, S., Beaulac, C., Riffon, R. and Lagace, J. 1999 'Evaluation of the Pulmonary and Systemic Immunogenecity of Fluidosomes, a Fluid Liposomal-Tobramycin Formulation for the Treatment of Chronic Infections in Lungs', *Biochimica et Biophysica Acta* 1428: 334-40.

Sachetelli, S., Khalil, H., Chen, T., Beaulac, C., Sénéchal, S. and Legacé, J. 2000 'Demonstration of a Fusion Mechanism Between a Fluid Bactericidal Liposomal Formulation and Bacterial Cells', *Biochimica et Biophysica Acta* 1463 (November): 254-66.

Sakurai, F., Inoue, R., Nishino, Y., Okuda, A., Matsumoto, O., Taga, T., Yamashita, F., Takakura, Y. and Hashida, M. 2000 'Effect of DNA/Lipid Mixing Ratio on the Physicochemical Characteristics, Cellular Uptake and Intracellular Trafficking of Plasmid DNA/Cationic Liposome Complexes and Subsequent Gene Expression', *Journal of Controlled Release* 66: 255-69.

Sambrook, J., Fritsch, E. F. and Maniatis, T. 1989 *Molecular Cloning: A Laboratory Manual*, New York, Cold Spring Harbour Laboratory Press.

Sandström, K., Wärmländer, S., Gräslund, A. and Leijon, M. 2002 'A-Tract DNA Disfavours Triplex Formation', *Journal of Molecular Biology* 315: 737-48.

Sasaki, M., Hayashi, J., Fujii, M., Koizumi, K., Fujita, H., Kobayashi, M., Kawakubo, Y. and Ito, A. 2001 'Neutral Liposome-Mediated Delivery Process of Fluorescein-Modified Oligonucleotides in Cultured Human Keratinocytes', *Journal of Photochemistry and Photobiology B: Biology* 60 (May): 120-8.

Sato, Y., Normura, S.-I. M. and Yoshikawa, K. 2003 'Enhanced Uptake of Giant DNA in Cell-Sized Liposomes', *Chemical Physics Letters* 380: 279-85.

Schiffelers, R. M., Storm, G., Kate, M. T. and Bakker-Woudenberg, I. A. J. M. 2001 'Therapeutic Efficacy of Liposome-Encapsulated Gentamicin in Rat Kleibsiella Pneumoniae Pneumonia in Relation to Impaired Host Defence and Low Bacterial Susceptibility to Gentamicin', *Antimicrobial Agents and Chemotherapy* 45(2): 464-70.

Schou, C., Hansen, H. F., Nielsen, Beck, F., Ravin, B. T., Kristensen, E., Giwercman, B. and Frimodt-Møller, N. 2000 'Antibiotic Effects of PNA (Peptide Nucleic Acid) Antisense. Compounds Against Multiresistant Escherichia Coli', *ICAAC Abstracts* 40 (17-20 September).

Sedelnikova, O. A., Panyutin, I. G., Luu, A. N. and Neumann, R. D. 1999 'The Stability of DNA Triplexes Inside Cells as Studied by Iodine-125 Radioprinting', *Nucleic Acids Research* 27(19): 3844-50.

Senior, K. 2000 'Pseudocomplementary Strategy Strengthens PNA Therapeutic Potential', *Drug Discovery Today* 5(12, December): 538-40.

Shaw, D. R., Rustagi, P. K., Kandimalla, E. R., Manning, A. N., Jiang, Z. and Agrawal, S. 1997 'Effects of Synthetic Oligonucleotides on Human Complement and Coagulation', *Biochemical Pharmacology* 53: 1123-32.

Singleton, S. and Dervan, P. 1993 'Equilibrium Association Constants for Oligonucleotide-Directed Triplex Helix Formation at Single DNA Sites: Linkages to Cation Valence and Concentration', *Biochemistry* 32: 13171-9.

Son, K. K., Patel, D. H., Tkach, D. and Park, A. 2000 'Cationic Liposome and Plasmid DNA Complexes Formed in Serum-Free Medium Under Optimum Transfection Conditions Are Negatively Charged', *Biochimica et Biophysica Acta* 1466: 11-5.

Song, Y. and Liu, D. 1998 'Free Liposomes Enhance the Transfection Activity of DNA/Lipid Complexes in Vivo by Intravenous Administration', *Biochimica et Biophysica Acta* 1372: 141-50.

Soyfer, V. N. and Potaman, V. N. 1996 'Triplex DNA-Drug Interactions', *Triple Helical Nucleic Acids*: 191-2.

Stein, C. A. 1999 'Two Problems in Antisense Biotechnology: In Vitro Delivery and the Design of Antisense Experiments', *Biochemica et Biophysica Acta* 1489 (May): 45-52.

Stewart, B. A., Johnson, A. P. and Woodford, N. 1999 'Relationship Between Mutations in ParC and GyrA of Clinical Isolates of Streptococcus Pneumoniae and Resistance to Ciprofloxacin and Grepafloxacin', *Journal of Medical Microbiology* 48: 1103-6.

Stilz, H. U. and Dervan, P. B. 1993 'Specific Recognition of CG Base Pairs by 2-Deoxynebularine Within the Purine.Purine.Pyrimidine Triple-Helix Motif', *Biochemistry* 32: 2177-85.

Strekowski, L., Say, M., Zegrocka, O., Tanious, F. A., Wilson, W. D., Manzel, L. and Macfarlane, D. E. 2003 'Bis-4-Aminoquinolones: Noevl Triplex-Helix DNA Intercalators and Antagonists of Immunostimulatory CpG-Oligodeoxynucleotides', *Bioorganic and Medicinal Chemistry* 11: 1079-85.

Stuart, D. D. and Allen, T. M. 2000 'A New Liposomal Formulation for Antisense Oligodeoxynucleotides with Small Size, High Incorporation Efficiency and Good Stability', *Biochimica et Biophysica Acta* 1463: 219-29.

Stuger, R., Woldringh, C. L., Weijden, C. C., Vischer, N. O. E., Bakker, B. M., Spanning, R. J. M., Snoep, J. L. and Westerhoff, H. V. 2002 'DNA Supercoiling by Gyrase is Linked to Nucleoid Compaction', *Molecualr Biology Reports* 29(1-2): 79-82.

Sun, J. S. and Hélène, C. 1993 'Oligonucleotide-Directed Triplex Helix Formation', *Current Opinion in Structural Biology* 3: 345-56.

Svinarchuk, F., Cherny, D., Debin, A., Delain, E. and Malvy, C. 1996 'A New Approach to Overcome Potassium-Mediated Inhibition of Triplex Formation', *Nucleic Acids Research* 24(19): 3858-65.

Tackett, A. J., Corey, D. R. and Raney, K. D. 2002 'Non-Watson-Crick Interactions Between PNA and DNA Inhibit the ATPase Activity of Bacteriophage T4 Dda Helicase', *Nucleic Acids Research* 30(4): 950-7.

Tarasi, A., Capone, A., Tarasi, D., Cassone, M., Bianco, G. and Venditti, M. 1999 'Comparative in-Vitro Activity of Moxifloxacin, Penicillin, Ceftriaxone and Ciprofloxacin Against Pneumococci Isolated from Meningitis', *Journal of Antimicrobial Chemotherapy* 43: 833-5.

Thomas, T. and Thomas, T. J. 1993 'Selectivity of Polyamines in Triplex DNA Stabilization', *Biochemistry* 32: 14068-74.

Thuong, N. T. and Hélène, C. 1993 'Sequence-Specific Recognition and Modification of Double-Helical DNA by Oligonucleotides', *Angewandte Chemie International Edition in English* 32: 666-90.

Times. 2003 'Hospitals Loosing Fight Against Antibiotic Resistant Superbugs', *Times*, 6 December, 4, 2W.

Tiner Sr, W. J., Potaman, V. N., Sinden, R. R. and Lyubchenko, Y. L. 2001 'The Structure of Intramolecular Triplex DNA: Atomic Force Microscopy Study', *Journal of Molecular Biology* 314: 353-7.

Torigoe, H. 2001 'Thermodynamic and Kinetic Effects of N3'-P5' Phosphoramidate Modification on Pyrimidine Motif Triplex DNA Formation', *Biochemistry* 40: 163-1069.

Torigoe, H., Hari, Y., Sekiguchi, M., Obika, S. and Imanishi, T. 2001 '2'-O, 4'-C-Methylene Bridged Nucleic Acid Modification Promotes Pyrimidine Motif Triplex DNA Formation at Physiological PH', *Journal of Biological Chemistry* 26(4): 2354-60.

Travers, A., Schneider, R. and Muskhelishvili, G. 2001 'DNA Supercoiling and Transcription in Escherichia Coli: The Fis Connection', *Biochimie* 83: 213-7.

Tros de Ilarduya, C., Arangoa, M. A., Moreno-Aliaga, M. J. and Düzgünes, N. 2002 'Enhanced Gene Delivery in Vitro and in Vivo by Improved Transferrin-Lipoplexes', *Biochimica et Biophysica Acta* 1561 (January): 209-21.

Tung, C. H. B., K. J. and Stein, S. 1993 'Polyamine-Linked Oligonucleotides for DNA Triple Helix Formation', *Nucleic Acids Research* 21(23): 5489-94.

Urban, E. and Noe, C. R. 2003 'Structural Modifications of Antisense Oligonucleitdes', *Il Farmaco* 58(3, March): 243-58.

Walberer, B. J., Cheng, A. C. and Frankel, A. D. 2003 'Structural Diversity and Isomorphism of Hydrogen Bonded Interactions in Nucleic Acids', *Journal of Molecular Biology* 327: 767-80.

Wickens, H. J. and Pinney, R. J. 2001 'Investigation of Smith's Quinolone Killing Mechanisms During PAE of Ciprofloxacin on Escherichia Coli', *International Journal of Pharmaceutics* 227: 149-56.

Willmott, C. R., Critchlow, S. E., Eperon, I. C. and Maxwell, A. 1994 'The Complex of DNA Gyrase and Quinolone Drugs with DNA Forms a Barrier to Transcription by RNA Polymerase', *Journal of Molecular Biology* 242: 351-63.

Woodle, M. C. and Scaria, P. 2001 'Cationic Liposomes and Nucleic Acids', *Current Opinion in Colloid and Interface Science* 6: 78-84.

Xiang, G., Bogacki, R. and McLaughlin, L. W. 1996 'Use of Pyrimidine Nucleosides That Function as a Bidentate Hydrogen Bond Donor for the Recognition of Isolated or Contiguous G-C Base Pairs by Oligonucleotide-Directed Triplex Formation', *Nucleic Acids Research* 24(10): 1963-70.

Xodo, L. E. 1995 'Characterization of the DNA Triplex Formed by d(TGGGTGGGTGGTTGGGTGGG) and a Critical R.Y Sequence Located in the Promoter of the Murine Ki-Ras Proto-Oncogene', *FEBS Letters* 370: 153-7.

Xu, Y. and Szoka Jr, F. C. 1996 'Mechanism of DNA Release from Liposome/DNA Complexes Used in Cell Transfection', *Biochemistry* 35: 5616-22.

Yuan, X., Ma, Z., Zhou, W., Niidome, T., Alber, S., Huang, L., Watkins, S. and Li, S. 2003 'Lipid Mediated Delivery of Peptide Nucleic Acids to Pulmonary Endothelium', *Biochemical and Biophysical Research Communications* 302: 6-11.

Zamaratski, E., Pradeepkumar, P. I. and Chattopadhyaya, J. 2001 `A Critical Survey of the Structure-Function of the Antisense Oligo/RNA Heteroduplex as Substrate for RNase H', *Journal of Biochemical and Biophysical Methods* 48: 189-208.

Zelphati, O. and Szoka Jr, F. C. 1996 `Mechanisms of Oligonucleotide Release from Cationic Liposomes', *Proceedings of the National Academy of Science USA* 93: 11493-8.

Zhanel, G. G., Walkty, A., Nichol, K., Smith, H., Noredin, A. and Hoban, D. J. 2003 `Molecular Characterization of Fluoroquinolones Resistant Streptococcus Pneumoniae Clinical Isolates Obtained from Across Canada', *Diagnostic Microbiology and Infectious Disease* 45: 63-7.